5. SHIELDING EVALUATION

The shielding analysis of the NUHOMS®-MP187 Cask is described in this chapter. During shipment, the NUHOMS®-MP187 Cask contains one of the three DSC designs described in Chapter 1. The FO-DSC and the FC-DSC each contain 24 intact PWR spent fuel assemblies. The FF-DSC contains 13 potentially failed PWR spent fuel assemblies. The design basis fuel parameters evaluated herein include a maximum burnup of 40,000 megawatt days per metric ton uranium (MWd/MTU), initial ^{235}U enrichments ranging from 2.38% to 3.19% by weight (w/o), a minimum post-irradiation cooling time of at least five years, a maximum assembly decay heat of 0.764 kW, and a maximum cask decay heat of 13.5 kW. Fuel assemblies with initial enrichments greater than those used for this analysis, up to the maximum allowable initial enrichment of 3.43 w/o ^{235}U, will have source terms bounded by those used herein. Other fuel having varied characteristics will be licensed by amendment to the certificate of compliance for this package.

The packaging is shown in the following sections to provide adequate shielding to ensure compliance with the external dose rate requirements specified in 10 CFR Part 71.47, 10 CFR Part 71.51 [5.1], and 49 CFR Part 173.441 [5.2] for the fuel parameters stated above. As stated in Chapter 7, the dose rates surrounding the package are measured prior to each shipment and verified to be in compliance with 10 CFR Part 71.47 and 49 CFR 173.441. The MP187 shielding evaluation results presented in Table 5.1-1 show that the predicted dose rates with the least margin relative to the regulatory limits are those for normal conditions of transport. A package that meets the dose rate limits of 10 CFR Part 71.47 and 49 CFR 173.441 for normal conditions of transport will also, therefore, meet the limits of 10 CFR 71.51 after sustaining damage from the hypothetical accident conditions. The shielding evaluation presented herein is thus intended to describe the expected shielding performance of the packaging and to show that the dose rates observed during normal conditions of transport represent the bounding case.

5.1 Discussion and Results

The packaging provides neutron and gamma-ray radiation shielding for up to 24 PWR spent fuel assemblies. Gamma-ray shielding is provided by lead and stainless steel shells that make up the cask wall. Neutron shielding is provided by a cementitious castable material contained within a stainless steel jacket surrounding the cylindrical portion of the cask body. Gamma shielding in the cask ends is provided by stainless steel and the top and bottom end assemblies of the DSC.

The FO-DSC and FC-DSC transported in the cask contain 24 intact PWR fuel assemblies. The FC-DSC also contains 24 PWR control components and therefore represents the design basis source term. The design basis payload neutron and gamma-ray sources, based on the FC-DSC, are $4.640\text{x}10^{9}$ neutrons/sec and $3.162\text{x}10^{16}$ MeV(γ)/sec, respectively as derived in Sections 5.2.2 (neutron) and 5.2.1.5 (gamma). The FF-DSC contains 13 PWR fuel assemblies that may have experienced gross cladding failure prior to shipment.

The NUHOMS®-MP187 package will be transported by exclusive use shipment, inside a closed transport vehicle (enclosure provided by the personnel barrier). The applicable 10 CFR Part 71.47 external radiation requirements for normal conditions during shipment include [5.1]:

1. Radiation levels must not exceed 10 mSv/hr (1000 mrem/hr) on the external surface of the package.

2. Radiation levels must not exceed 2 mSv/hr (200 mrem/hr) at any point on the outer surface of the transport vehicle.

3. Radiation levels must not exceed 0.1 mSv/hr (10 mrem/hr) at any point two meters from the outer lateral surfaces of the vehicle or, in the case of a flat-bed style vehicle, at any point two meters from the vertical planes projected by the outer edges of the vehicle and on the lower external surface of the vehicle.

4. Radiation levels must not exceed 0.02 mSv/hr (2 mrem/hr) in any normally occupied space.

In the shielding evaluations, the external surface of the packaging is defined as the radial surface of the cask neutron shield panel and the surfaces of the impact limiters. The outer surface of the vehicle is bounded by the impact limiters and the personnel barrier, which is mounted on the skid and extends to the same radius as the impact limiters as shown on the drawings provided in Section 1.3.2. The 10 CFR Part 71.51 external radiation requirements after the 10 CFR Part 71.73 hypothetical accident conditions are that there shall be [5.1],

> "... no external radiation dose rate exceeding 10 mSv/h (1 rem/hr) at one meter from the external surface of the package."

During the hypothetical accident conditions defined in 10 CFR Part 71.73, the cask is assumed to be separated from the skid. The cask neutron shield and neutron shield jacket are assumed to be lost during the accident, as are the impact limiters. The cask lead shielding is assumed to have slumped, producing relatively unshielded gaps in the cask wall. The suitability of the cask cavity closure during the hypothetical accident conditions is documented in Chapters 2 and 4.

The results of the shielding evaluation performed for the NUHOMS®-MP187 Cask are summarized in Table 5.1-1. The values in Table 5.1-1 are described in detail in Section 5.4.2. The bounding dose rate for the MP187 Package is the two meter dose rate along the package side. The reported value of 9.94 mrem per hour is just below the 10CFR71.47 limit. This result is acceptable because:

(1) The methodology used to calculate the package dose rates is based on a series of conservative assumptions which provide assurance that the actual package dose rates will be below the applicable limits. Conservative assumptions in the analysis include:

- Impact limiter thickness assumed equal to the minimum thickness with no credit taken for the actual rectangular cross-section.
- Worst case nuclear data used for source term calculations.

- Source terms used in shielding analysis based on total cask heat load of 14.3 kW, which exceeds maximum allowable heat load by 6%.

- No credit taken for shielding of control components by fuel rods (worth about 14% of the total dose rate for the FC-DSC).

- Conservative neutron shield properties used including a 10% reduction in hydrogen and a 50% reduction in boron

- The methodology used to perform the shielding calculations has been thoroughly benchmarked against measured data and shown to provide significantly conservative (factor of two or more) results as documented in Reference [5.15].

(2) All package dose rates are measured immediately prior to shipment and the package will not be shipped if the 10CFR71 limits are exceeded.

Because the dose rates at the top and bottom ends of the package are less than two mrem/hr, the radiation level in occupied positions of the vehicle will also be less than two mrem/hr. The cask meets all of the applicable external radiation criteria as documented in the remainder of this chapter.

Table 5.1-1

Summary of Maximum Dose Rates

(mrem/hr)

	Package Surface		
	Side (mrem/hr)	Top (mrem/hr)	Bottom (mrem/hr)
Normal Conditions			
Gamma	1.87E+1	2.18E-1	6.40E-1
Neutron	2.37E+2	6.79E-1	1.31E+0
Total	2.37E+2	8.47E-1	1.62E+0
10 CFR 71.47 Limit	1.00E+3	1.00E+3	1.00E+3
	Vehicle Outer Surface		
	Side (mrem/hr)	Top (mrem/hr)	Bottom (mrem/hr)
Normal Conditions			
Gamma	1.07E+1	2.18E-1	6.40E-1
Neutron	5.13E+1	6.79E-1	1.31E+0
Total	5.56E+1	8.47E-1	1.62E+0
10 CFR 71.47 Limit	2.00E+2	2.00E+2	2.00E+2
	2 Meters from Vehicle Outer Surface		
	Side (mrem/hr)	Top (mrem/hr)	Bottom (mrem/hr)
Normal Conditions			
Gamma	3.14E+0	6.46E-2	2.16E-1
Neutron	7.04E+0	3.02E-1	5.39E-1
Total	9.94E+0	3.37E-1	6.72E-1
10 CFR 71.47 Limit	1.00E+1	1.00E+1	1.00E+1
	1 Meter from Surface of Package		
	Side (mrem/hr)	Top (mrem/hr)	Bottom (mrem/hr)
Hypothetical Accident Conditions			
Gamma	1.8E+2	1.7E+0	1.8E+0
Neutron	4.4E+2	3.6E+1	5.8E+1
Total	4.8E+2	3.6E+1	5.9E+1
10 CFR 71.51 Limit	1.00E+3	1.00E+3	1.00E+3

5.2 Source Specification

The NUHOMS®-MP187 Cask is designed to transport any one of the three DSCs described in Chapter 1. Each DSC can hold 24 PWR fuel assemblies (13 in the FF-DSC). The neutron and gamma-ray radiological source strengths and the gamma-ray source spectrum for the design basis fuel assembly are determined using the ORIGEN2 computer code [5.3]. Section 1.2.3 defines two sets of fuel assembly parameters (described below) which are suitable for transportation in the MP187 Cask. Selection and placement of assemblies are controlled by the specifications in Section 1.2.3 and the procedures in Section 7 of this SAR. Type I assemblies, which have the larger sources, may be placed only in an FF-DSC (any fuel cell) or in the interior four fuel cells of an FO-DSC or FC-DSC. Type II assemblies, which have the smaller sources, may be placed in any fuel cell of any DSC type. Design basis sources for both Type I and Type II assemblies are developed in this section. Gamma-ray source strengths are also developed for the design basis control components that will be shipped with the fuel assemblies in the FC-DSC.

The design basis payload neutron and gamma-ray sources are 4.640×10^9 neutrons/sec and 3.162×10^{16} MeV(γ)/sec, respectively. The fuel parameters used to develop the design basis source are taken from Section 1.2.3. These parameters include a maximum burnup of 40,000 MWd/MTU and a minimum cooling time of five years. Type I assemblies are limited to a maximum decay heat of 0.764 kW. Type II assemblies are limited to 0.563 kW, with a total cask maximum decay heat not to exceed 13.5 kW. The PWR fuel assembly chosen as the design basis radiological source is a Babcock and Wilcox (B&W) 15x15 assembly, with its associated B&W control components. The control component with the largest gamma source is an axial power shaping rod assembly (APSRA). Other fuel having varied radiological characteristics will be licensed by amendment to the certificate of compliance for this package.

The ORIGEN2 computer code [5.3] is used to calculate the gamma and neutron sources for the Type I and Type II assemblies described above. The design basis source term for the NUHOMS®-MP187 Cask shielding analysis is represented by 4 Type I assemblies and 20 Type II assemblies, including control components, with the design basis neutron and gamma source terms described below. The ORIGEN2 results were then mapped from the ORIGEN2 energy structure to the CASK-81 [5.4] energy structure for the external dose rate calculations.

For the acceptable fuel parameters defined in Section 1.2.3, the source calculations described below determine bounding neutron and gamma-ray sources. The process used to develop the design basis source is shown in Figure 5.2-1. The bounding sources are calculated by preparing several ORIGEN models of the design basis assembly and, for each case, calculating the required cooling times to meet the Type I and Type II allowable decay heats per assembly. The neutron and gamma sources that correspond to the burnup, enrichment, and cooling time for each case are then input to 1-D cask shielding calculations to determine which case maximizes the cask surface dose rates.

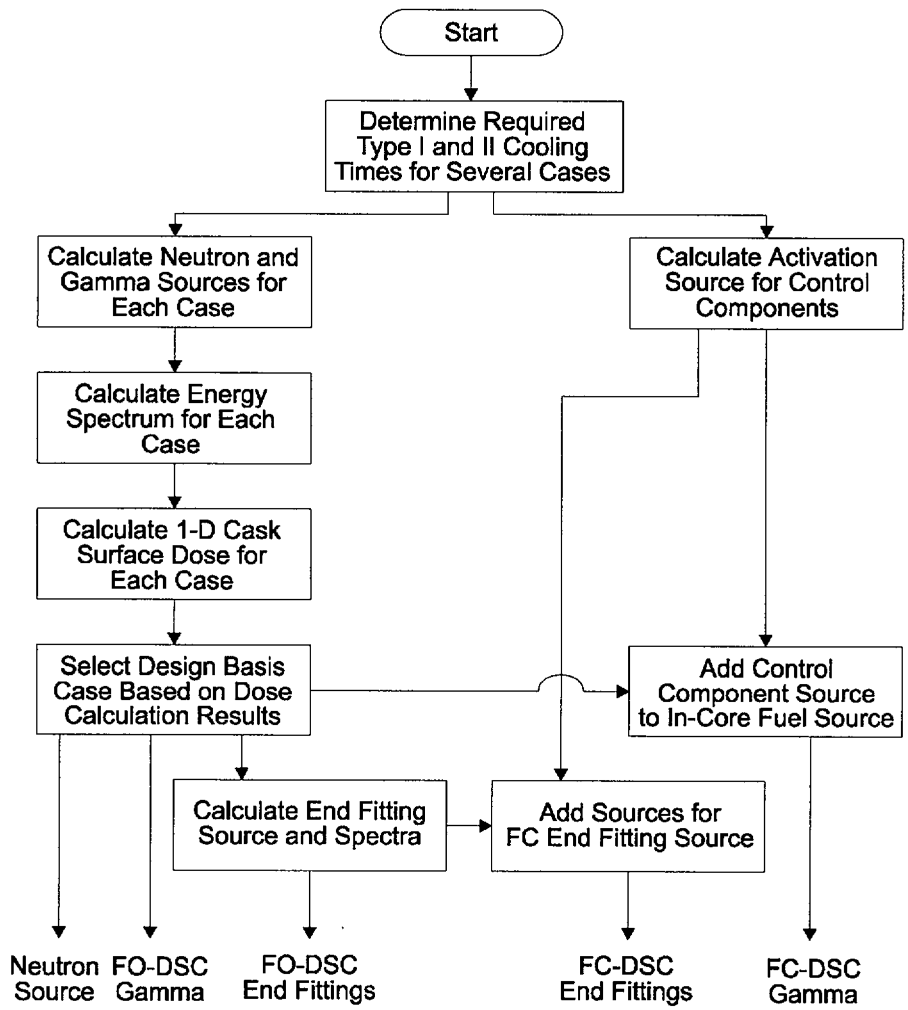

Figure 5.2-1

Source Term Calculation Flow Chart

Acceptable fuel burnups range from 0 MWd/MTU to 40,000 MWd/MTU. Acceptable fuel cooling times are greater than or equal to five years, such that the decay heat criteria are met. The initial enrichments of the fuel assemblies vary according to the burnup of the assembly. The choice of initial enrichment for each case has a significant effect on the neutron source (lower enrichments produce greater sources). To select an appropriate enrichment for a given burnup, a statistical evaluation was performed for 2615 B&W 15x15 fuel assemblies from five reactors. The average enrichment and standard deviation were calculated as a function of burnup and the design basis initial enrichment is then defined as the average enrichment minus one standard deviation. This choice of enrichment will result in bounding sources for about 84% of the fuel inventory. This is considered a reasonable design value for shielding calculations because actual dose rates are measured and must meet 10CFR71.47 and 49CFR173.441 prior to each shipment.

Five ORIGEN cases are run to bound the minimum cooling time and maximum burnup specifications listed above. For each ORIGEN case, the cooling time required to meet the assembly decay heat limits of 0.764 kW (Type I) and 0.563 kW (Type II) is calculated. The gamma and neutron sources for each case are extracted from the ORIGEN output and used to develop the design basis sources discussed below. A summary of the ORIGEN cases is provided in Table 5.2-1. As will be shown below, the case that results in the largest dose rates around the cask, for both Type I and Type II assemblies is a burnup of 40,000 MWd/MTU and an initial enrichment of 3.19 w/o ^{235}U. The corresponding cooling time for Type I assemblies is 9 years and for Type II assemblies is 17 years.

Table 5.2-1

ORIGEN2 Input Cases for Shielding Evaluation

Case	Burnup (MWd/MTU)	Initial Enrichment (w/o ^{235}U)	Type I Required Cooling Time (years)	Type II Required Cooling Time (years)	Type II Decay Heat (kW/assy)
I	23,200	2.38	5	5	0.5600
II	25,000	2.49	5	6	0.5206
III	30,000	2.76	5	8	0.5329
IV	35,000	2.99	7	11	0.5590
V	40,000	3.19	9	17	0.5536

5.2.1 Gamma Source

ORIGEN2 [5.3] is used to calculate both the neutron and gamma-ray source terms for the NUHOMS®-MP187 Cask. A description of the fuel assembly models and data reduction is provided in this section. Data reduction that applies specifically to the neutron source is described in Section 5.2.2. The ORIGEN2 code computes the radioactivity of fuel assemblies that have undergone irradiation in a nuclear reactor and subsequent decay after removal from the reactor core. It has the ability to compute the isotopic fractions, radioactivity, decay thermal power, toxicity, neutron absorption, neutron emission, and photon emission for various isotopes in the fuel assembly. ORIGEN2 results are used in spent fuel shipping package analyses to develop neutron and gamma ray radioactive decay source strengths and to develop decay thermal powers. ORIGEN2 is an industry standard code that is distributed by Oak Ridge National Laboratory's Radiation Shielding Information Center (ORNL/RSIC).

5.2.1.1 Description of Fuel Assembly ORIGEN Models

The assumed fuel assembly material weights used in the ORIGEN2 models are shown in Table 5.2-2. The detailed material compositions and impurities are given in the sample input files reproduced in Section 5.5.2. The fuel assembly ORIGEN2 model is split into four distinct regions: in-core, plenum, top nozzle, and bottom nozzle. Additional ORIGEN2 runs are made to calculate the activation source term in the design basis control components.

The power irradiation in ORIGEN2 is performed for the fuel assembly materials in the active fuel region. A flux irradiation is then performed on the top nozzle, plenum, bottom nozzle, and control component regions. The assumed operating histories are listed in the ORIGEN2 input files. The fractions of the in-core flux that are applied to the top nozzle, plenum, and bottom nozzle zones for the calculation of activation products in these zones are taken from Reference 5.5.

Table 5.2-2

Summary of Fuel Assembly Material Weights Used in Source Term Calculations

Region	Component(s)	Material	Weight (kg) [5.6]
In-Core	Fuel	UO_2	525.9
	Cladding	Zircaloy-4	107.14
	Guide/Inst. Tubes	Zircaloy-4	7.972
	Grid Spacers	Inconel-718	4.90
	Grid Supports	Zircaloy-4	0.64
	APSRA (FC)	SS-304	9.009
	APSRA Poison (FC)	Inconel-718	15.36
Gas Plenum	Cladding	Zircaloy-4	8.976
	Guide/Inst. Tubes	Zircaloy-4	0.668
	Grid Spacer	Inconel-718	1.04
	Support Spacers	Zircaloy-4	3.925
	APSRA (FC)	SS-304	0.764
Top Nozzle	Top Nozzle	SS-304	8.96
	Holddown Spring	Inconel-718	1.80
	APSRA (FC)	SS-304	2.50
Above Top Nozzle	APSRA (FC)	SS-304	1.136
Bottom Nozzle	Bottom Nozzle	SS-304	8.31
	Grid Spacer	Inconel-718	1.30
	Support Spacers	Zircaloy-4	3.925

A sample ORIGEN2 input file for the design basis fuel assembly is reproduced in Section 5.5.2. After the assembly is irradiated in the manner described above, the materials in the assembly are decayed for 5 to 17 years, depending on the irradiation parameters assumed, until the assembly decay heat reaches the cask average decay heat of 0.563 kW/assy. The ORIGEN2 33,000 MWd/MTU burnup, PWR data library is used in this calculation for burnup cases less than 33,000 MWd/MTU (Cases I through III). The ORIGEN2 50,000 MWd/MTU burnup, PWR data library is used for burnup cases greater than 33,000 MWd/MTU (Cases IV and V). In this way, the most conservative library is used for actual burnups between those used to generate the libraries.

5.2.1.2 Description of Control Component ORIGEN Models

The B&W axial power shaping rod assembly was selected as the design basis control component. The APSRA was selected due to its significant mass, which increases the amount of activated material, and its presence in the core during reactor operation. Control rod assemblies, while more massive than the APSRAs, are withdrawn from the core during full power operation. Orifice rods and burnable poison rods contain significantly less material than the APSRAs.

Both black and gray APSRAs are modeled using the ORIGEN code. The black and gray APSRAs differ primarily in the poison material used. The black APSRA uses a silver-indium-cadmium poison while the gray APSRA uses Inconel. The APSRA materials used in the ORIGEN runs are listed in Table 5.2-3. Each APSRA is assumed to be irradiated for five cycles. Each irradiation cycle is identical to those used for the fuel assembly source calculation. Each control component is assumed to have cooled for at least 8 years prior to placement in the cask.

As discussed in detail in Section 5.2.1.5, the gray APSRA will result in larger dose rates on the surface of the cask. This was determined using a 1-D shielding model of the MP187 Cask with both of the calculated control component source terms. The derivation of the cask source term is discussed in detail below.

Table 5.2-3

Control Component Regional Weights

Region	Material	Black APSRA (kg)	Gray APSRA (kg)
Above Top	SS304	1.182	1.136
Top Nozzle	SS304	2.632	2.500
Gas Plenum	SS304	0.891	0.764
In-Core	SS304	10.57	9.009
In-Core	Poison(1)	10.64	15.36

1) Black APSRA poison material is Ag-In-Cd, Gray poison material is Inconel.

5.2.1.3 Selection of Design Basis Fuel Parameters

As stated in Section 5.2, five burnup/enrichment/cooling time cases were modeled for both Type I and Type II fuel assemblies in order to determine the case that will result in the largest cask surface dose rates. This determination was made by performing one-dimensional shielding calculations using the neutron and gamma-ray sources taken from the five ORIGEN runs. The discrete-ordinates code ANISN [5.13] was used for this calculation. The ANISN models are similar to the shielding models described in Section 5.4. The results of the ANISN runs are used only to compare the dose rates due to each of the five source cases and are not used in the final shielding calculations. The two-dimensional code DORT-PC is used to perform the final shielding calculations for the design basis source term as described in Section 5.4.

The 1-D ANISN dose rate results are multiplied by peaking factors (PF for gammas and $(PF)^4$ for neutrons) to account for axial peaking in the assemblies. The peaking factor for an assembly (equal to the peak axial burnup divided by the assembly average burnup) decreases as the burnup is increased. Previous revisions of this SAR conservatively used a peaking factor of 1.2 for all fuel burnups. However, because this section of the SAR determines which combination of fuel parameters results in the highest cask surface dose rates, it is a relatively simple matter to incorporate the variation in axial peaking factors. Figure 4-4 of Reference [5.14], portions of which are included as an Appendix to this Chapter, provides the normalized axial burnup profile as a function of burnup for PWR fuel assemblies. Based on this data, an appropriate peaking factor for the 23.2 GWd/MTU case is 1.17 and for the remaining cases is 1.12.

The results of the 1-D dose rate comparison for the five source cases are shown in Figure 5.2-2 (assuming 24 Type I assemblies) and in Figure 5.2-3 (assuming 24 Type II assemblies). The total cask gamma source strength and spectrum are shown in Table 5.2-4 and Table 5.2-5 for each of the five burnup cases, assuming the presence of 24 Type I and Type II assemblies, respectively. These tables provide sources for 24 assemblies because the 1-D dose rate comparisons are performed for both Type I and Type II assemblies to verify that the same assembly parameters are bounding for each case. In both cases, for a given decay heat, the cask surface dose rate increases as a function of burnup. Case V, the 40,000 MWd/MTU model, represents the worst case for the shielding evaluation. The ORIGEN results from Case V are used to develop the design basis source terms in the next section and in Section 5.2.2.

5.2.1.4 Design Basis Gamma Source for FO-DSC

The gamma source strengths and energy spectra for the top nozzle (including the top nozzle and plenum sources), in-core, and bottom nozzle regions and for the whole assembly are shown in Table 5.2-6 and Table 5.2-7 for the design basis Type I and Type II sources, respectively. The maximum source in an FO-DSC, as discussed above, is based on 4 Type I and 20 Type II assemblies. Table 5.2-8 and Table 5.2-9 provide the total FO-DSC source. The energy structure is that used by the CASK-81 cross-section library. The total design basis gamma source strength in the package containing 24 PWR fuel assemblies (4 Type I and 20 Type II) in an FO-DSC is

8.429×10^{16} photons per second (2.723×10^{16} MeV/sec). This design basis source, when used with the design basis neutron source described below, bounds that of B&W 15x15 assemblies that meet the acceptance criteria listed in Section 1.2.3.

The 18 group gamma ray energy spectra shown in Table 5.2-4 through Table 5.2-9 have been converted from that used by the ORIGEN2 code. The energy spectrum used in the shielding calculations is that of the CASK-81 22 neutron group, 18 gamma ray group cross section set [5.4]. To map the ORIGEN2 energy structure into the CASK-81 energy structure, the particles in each group are assumed to be evenly distributed in logarithmic energy space. The total number of particles and the total gamma power (MeV/sec) are conserved. Logarithmic mapping is a common practice and is considered reasonable for this application. The formulae used to map the ORIGEN2 energy structure into the CASK-81 gamma-ray energy group structure are shown in Table 5.2-10.

Table 5.2-4

In-Core FO-DSC Gamma Source Strength and Energy Spectrum for Each Burnup Case for Type I Fuel

Upper Energy (MeV)	Case I 23.2 GWd/MTU (γ/sec/cask)	Case II 25 GWd/MTU (γ/sec/cask)	Case III 30 GWd/MTU (γ/sec/cask)	Case IV 35 GWd/MTU (γ/sec/cask)	Case V 40 GWd/MTU (γ/sec/cask)
10.000	6.370E+05	7.978E+05	1.401E+06	2.340E+06	3.365E+06
8.000	4.003E+06	5.015E+06	8.808E+06	1.470E+07	2.114E+07
6.500	2.318E+07	2.904E+07	5.101E+07	8.514E+07	1.224E+08
5.000	2.645E+07	3.313E+07	5.820E+07	9.714E+07	1.397E+08
4.000	1.452E+11	1.573E+11	1.924E+11	6.065E+10	1.842E+10
3.000	1.137E+12	1.232E+12	1.505E+12	4.716E+11	1.439E+11
2.500	3.599E+13	3.882E+13	4.662E+13	1.025E+13	2.300E+12
2.000	3.843E+13	4.237E+13	5.405E+13	3.963E+13	3.588E+13
1.660	1.064E+15	1.152E+15	1.415E+15	1.222E+15	1.102E+15
1.330	2.468E+15	2.672E+15	3.280E+15	2.842E+15	2.562E+15
1.000	4.343E+15	4.901E+15	6.636E+15	4.951E+15	3.552E+15
0.800	1.569E+16	1.720E+16	2.165E+16	1.996E+16	1.894E+16
0.600	2.490E+16	2.715E+16	3.361E+16	3.216E+16	3.175E+16
0.400	1.176E+15	1.266E+15	1.518E+15	1.086E+15	9.348E+14
0.300	1.563E+15	1.690E+15	2.046E+15	1.568E+15	1.497E+15
0.200	4.208E+15	4.580E+15	5.638E+15	4.440E+15	4.277E+15
0.100	6.864E+15	7.419E+15	8.964E+15	7.266E+15	7.097E+15
0.050	3.765E+16	4.066E+16	4.907E+16	4.068E+16	3.995E+16
Total	1.000E+17	1.088E+17	1.339E+17	1.162E+17	1.117E+17
Mean Energy (MeV)	**Case I 23.2 GWd/MTU (MeV/sec/cask)**	**Case II 25 GWd/MTU (MeV/sec/cask)**	**Case III 30 GWd/MTU (MeV/sec/cask)**	**Case IV 35 GWd/MTU (MeV/sec/cask)**	**Case V 40 GWd/MTU (MeV/sec/cask)**
8.944	5.697E+06	7.135E+06	1.253E+07	2.092E+07	3.009E+07
7.211	2.886E+07	3.616E+07	6.351E+07	1.060E+08	1.524E+08
5.701	1.322E+08	1.656E+08	2.908E+08	4.854E+08	6.978E+08
4.472	1.183E+08	1.482E+08	2.603E+08	4.344E+08	6.245E+08
3.464	5.031E+11	5.449E+11	6.664E+11	2.101E+11	6.382E+10
2.739	3.115E+12	3.373E+12	4.123E+12	1.292E+12	3.941E+11
2.236	8.047E+13	8.680E+13	1.042E+14	2.292E+13	5.143E+12
1.822	7.002E+13	7.719E+13	9.847E+13	7.220E+13	6.537E+13
1.486	1.581E+15	1.712E+15	2.103E+15	1.816E+15	1.637E+15
1.153	2.846E+15	3.081E+15	3.782E+15	3.277E+15	2.954E+15
0.894	3.883E+15	4.381E+15	5.933E+15	4.426E+15	3.176E+15
0.693	1.087E+16	1.192E+16	1.501E+16	1.383E+16	1.313E+16
0.490	1.220E+16	1.330E+16	1.647E+16	1.576E+16	1.556E+16
0.346	4.070E+14	4.381E+14	5.251E+14	3.758E+14	3.234E+14
0.245	3.830E+14	4.141E+14	5.012E+14	3.842E+14	3.669E+14
0.141	5.933E+14	6.457E+14	7.950E+14	6.261E+14	6.031E+14
0.071	4.874E+14	5.267E+14	6.364E+14	5.159E+14	5.039E+14
0.022	8.283E+14	8.946E+14	1.079E+15	8.949E+14	8.789E+14
Total	3.424E+16	3.748E+16	4.704E+16	4.200E+16	3.920E+16

Case	Burnup (MWd/MTU)	ANISN Neutron (mrem/hr)	ANISN Gamma (mrem/hr)	Peaked Neutron (mrem/hr)	Peaked Gamma (mrem/hr)	Total Dose Rate (mrem/hr)
I	23,200	4.70	21.80	8.81	25.51	34.31
II	25,000	5.87	23.70	9.24	26.54	35.78
III	30,000	10.30	29.40	16.21	32.93	49.14
IV	35,000	17.10	22.60	26.91	25.31	52.22
V	40,000	24.60	20.40	38.71	22.85	61.56

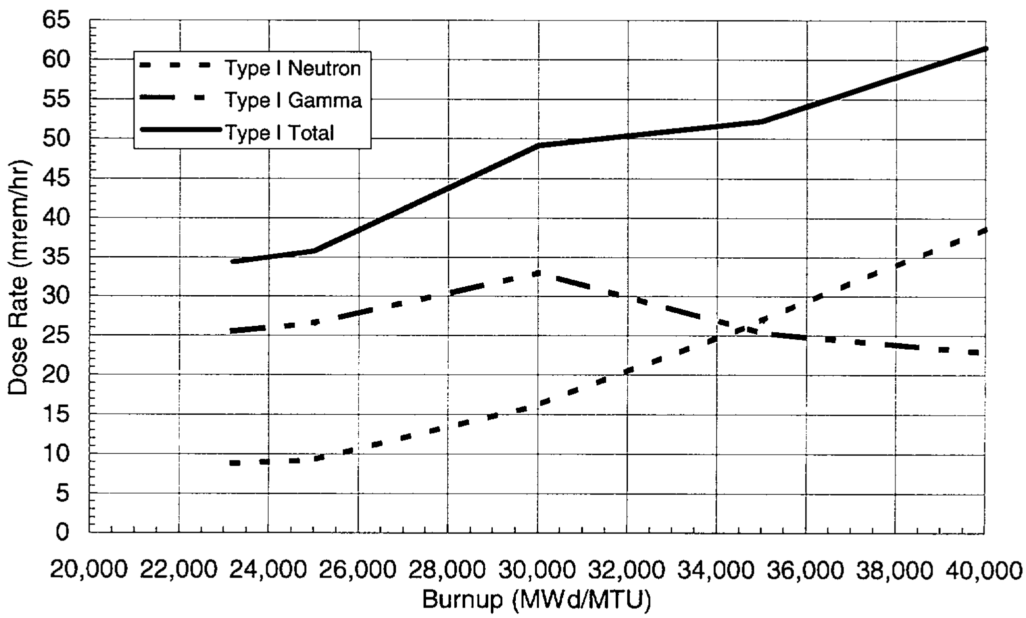

Figure 5.2-2

Determination of Bounding Type I Assembly Source

Table 5.2-5

In-Core FO-DSC Gamma Source Strength and Energy Spectrum for Each Burnup Case for Type II Fuel

Upper Energy (MeV)	Case I 23.2 GWd/MTU (γ/sec/cask)	Case II 25 GWd/MTU (γ/sec/cask)	Case III 30 GWd/MTU (γ/sec/cask)	Case IV 35 GWd/MTU (γ/sec/cask)	Case V 40 GWd/MTU (γ/sec/cask)
10.000	6.370E+05	7.682E+05	1.252E+06	2.013E+06	2.491E+06
8.000	4.003E+06	4.828E+06	7.869E+06	1.265E+07	1.566E+07
6.500	2.318E+07	2.796E+07	4.557E+07	7.328E+07	9.069E+07
5.000	2.645E+07	3.190E+07	5.199E+07	8.361E+07	1.035E+08
4.000	1.452E+11	7.914E+10	2.463E+10	4.203E+09	5.127E+08
3.000	1.137E+12	6.178E+11	1.923E+11	3.472E+10	7.427E+09
2.500	3.599E+13	1.669E+13	3.813E+12	4.096E+11	9.215E+09
2.000	3.843E+13	3.028E+13	2.604E+13	2.423E+13	1.845E+13
1.660	1.064E+15	9.795E+14	9.064E+14	7.372E+14	4.547E+14
1.330	2.468E+15	2.280E+15	2.112E+15	1.714E+15	1.053E+15
1.000	4.343E+15	3.616E+15	2.762E+15	1.743E+15	7.272E+14
0.800	1.569E+16	1.483E+16	1.472E+16	1.411E+16	1.266E+16
0.600	2.490E+16	2.402E+16	2.470E+16	2.466E+16	2.303E+16
0.400	1.176E+15	9.578E+14	8.010E+14	6.888E+14	5.744E+14
0.300	1.563E+15	1.312E+15	1.217E+15	1.188E+15	1.116E+15
0.200	4.208E+15	3.529E+15	3.314E+15	3.252E+15	2.881E+15
0.100	6.864E+15	5.928E+15	5.689E+15	5.736E+15	5.515E+15
0.050	3.765E+16	3.312E+16	3.215E+16	3.207E+16	3.056E+16
Total	1.000E+17	9.062E+16	8.840E+16	8.592E+16	7.859E+16
Mean Energy (MeV)	**Case I 23.2 GWd/MTU (MeV/sec/cask)**	**Case II 25 GWd/MTU (MeV/sec/cask)**	**Case III 30 GWd/MTU (MeV/sec/cask)**	**Case IV 35 GWd/MTU (MeV/sec/cask)**	**Case V 40 GWd/MTU (MeV/sec/cask)**
8.944	5.697E+06	6.871E+06	1.120E+07	1.801E+07	2.228E+07
7.211	2.886E+07	3.481E+07	5.674E+07	9.124E+07	1.129E+08
5.701	1.322E+08	1.594E+08	2.598E+08	4.178E+08	5.170E+08
4.472	1.183E+08	1.427E+08	2.325E+08	3.739E+08	4.627E+08
3.464	5.031E+11	2.742E+11	8.532E+10	1.456E+10	1.776E+09
2.739	3.115E+12	1.692E+12	5.267E+11	9.509E+10	2.034E+10
2.236	8.047E+13	3.733E+13	8.526E+12	9.158E+11	2.060E+10
1.822	7.002E+13	5.517E+13	4.744E+13	4.415E+13	3.361E+13
1.486	1.581E+15	1.456E+15	1.347E+15	1.096E+15	6.757E+14
1.153	2.846E+15	2.628E+15	2.435E+15	1.976E+15	1.214E+15
0.894	3.883E+15	3.232E+15	2.469E+15	1.559E+15	6.502E+14
0.693	1.087E+16	1.028E+16	1.020E+16	9.777E+15	8.771E+15
0.490	1.220E+16	1.177E+16	1.210E+16	1.208E+16	1.129E+16
0.346	4.070E+14	3.314E+14	2.771E+14	2.383E+14	1.987E+14
0.245	3.830E+14	3.214E+14	2.981E+14	2.912E+14	2.734E+14
0.141	5.933E+14	4.975E+14	4.672E+14	4.585E+14	4.062E+14
0.071	4.874E+14	4.209E+14	4.039E+14	4.072E+14	3.916E+14
0.022	8.283E+14	7.287E+14	7.074E+14	7.056E+14	6.722E+14
Total	3.424E+16	3.176E+16	3.076E+16	2.863E+16	2.457E+16

Case	Burnup (MWd/MTU)	ANISN Neutron (mrem/hr)	ANISN Gamma (mrem/hr)	Peaked Neutron (mrem/hr)	Peaked Gamma (mrem/hr)	Total Dose Rate (mrem/hr)
I	23,200	4.70	21.80	8.81	25.51	34.31
II	25,000	5.66	18.20	8.91	20.38	29.29
III	30,000	9.20	15.80	14.48	17.70	32.17
IV	35,000	14.80	13.40	23.29	15.01	38.30
V	40,000	18.30	9.21	28.80	10.32	39.11

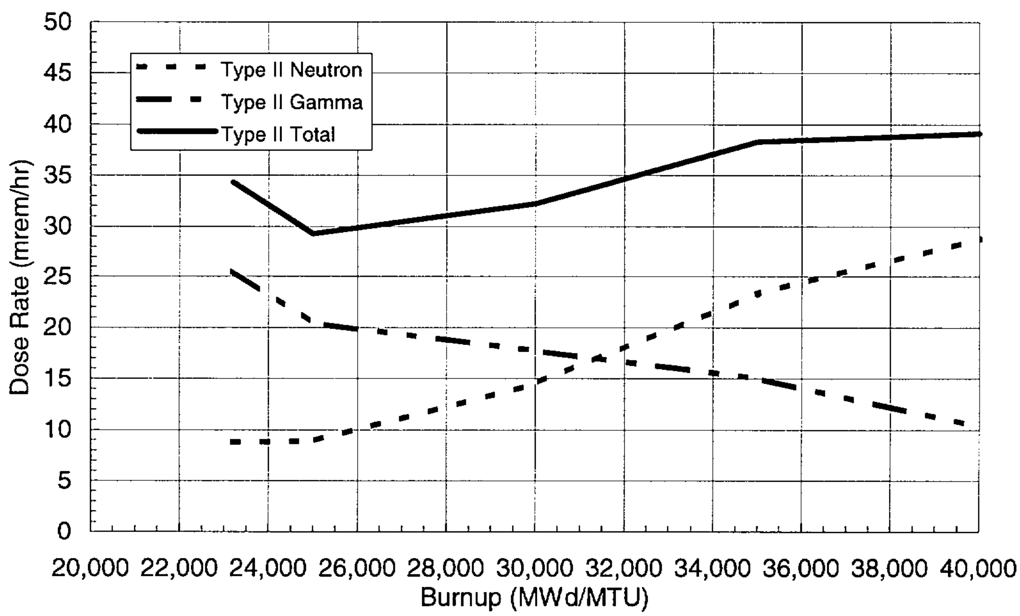

Figure 5.2-3

Determination of Bounding Type II Assembly Source

Table 5.2-6

Type I Assembly Design Basis Gamma Source Strength and Energy Spectrum

Upper Energy (MeV)	In-Core (γ/sec/assy)	Top Nozzle (γ/sec/assy)	Bottom Nozzle (γ/sec/assy)	Total (γ/sec/assy)
10.000	1.402E+05	1.525E-06	4.451E-07	1.402E+05
8.000	8.808E+05	9.646E-06	2.815E-06	8.808E+05
6.500	5.100E+06	5.663E-05	1.651E-05	5.100E+06
5.000	5.819E+06	6.468E-05	1.885E-05	5.819E+06
4.000	7.676E+08	4.050E-01	2.175E-01	7.676E+08
3.000	5.995E+09	1.277E+05	1.427E+05	5.996E+09
2.500	9.584E+10	4.125E+07	4.612E+07	9.593E+10
2.000	1.495E+12	2.782E+02	9.659E+01	1.495E+12
1.660	4.591E+13	2.312E+12	2.584E+12	5.081E+13
1.330	1.068E+14	5.473E+12	6.117E+12	1.183E+14
1.000	1.480E+14	3.740E+09	6.273E+09	1.480E+14
0.800	7.892E+14	1.834E+10	9.586E+09	7.892E+14
0.600	1.323E+15	4.054E+10	1.477E+10	1.323E+15
0.400	3.895E+13	2.571E+10	9.486E+09	3.898E+13
0.300	6.240E+13	4.205E+09	2.028E+09	6.240E+13
0.200	1.782E+14	6.951E+09	5.499E+09	1.782E+14
0.100	2.957E+14	2.724E+10	2.993E+10	2.957E+14
0.050	1.665E+15	3.658E+11	3.391E+11	1.665E+15
Total	4.654E+15	8.278E+12	9.119E+12	4.672E+15

Table 5.2-7

Type II Assembly Design Basis Gamma Source Strength and Energy Spectrum

Upper Energy (MeV)	In-Core (γ/sec/assy)	Top Nozzle (γ/sec/assy)	Bottom Nozzle (γ/sec/assy)	Total (γ/sec/assy)
10.000	1.038E+05	1.423E-06	4.115E-07	1.038E+05
8.000	6.525E+05	9.018E-06	2.609E-06	6.525E+05
6.500	3.779E+06	5.311E-05	1.536E-05	3.779E+06
5.000	4.311E+06	6.066E-05	1.755E-05	4.311E+06
4.000	2.136E+07	1.913E-03	5.534E-04	2.136E+07
3.000	3.094E+08	4.458E+04	4.426E+04	3.095E+08
2.500	3.839E+08	1.440E+07	1.430E+07	4.126E+08
2.000	7.686E+11	1.416E+02	4.096E+01	7.686E+11
1.660	1.895E+13	8.072E+11	8.016E+11	2.056E+13
1.330	4.386E+13	1.911E+12	1.897E+12	4.767E+13
1.000	3.030E+13	2.356E+09	1.596E+09	3.031E+13
0.800	5.274E+14	3.584E+09	1.585E+09	5.274E+14
0.600	9.598E+14	5.499E+09	1.617E+09	9.598E+14
0.400	2.393E+13	3.521E+09	1.074E+09	2.394E+13
0.300	4.650E+13	7.124E+08	3.707E+08	4.650E+13
0.200	1.200E+14	1.788E+09	1.488E+09	1.200E+14
0.100	2.298E+14	9.387E+09	9.249E+09	2.298E+14
0.050	1.273E+15	1.108E+11	1.013E+11	1.273E+15
Total	3.274E+15	2.856E+12	2.817E+12	3.280E+15

Table 5.2-8

FO-DSC Design Basis Gamma Source Strength and Energy Spectrum

Upper Energy (MeV)	In-Core (γ/sec/cask)	Top Nozzle (γ/sec/cask)	Bottom Nozzle (γ/sec/cask)	Total (γ/sec/cask)
10.000	2.637E+06	3.456E-05	1.001E-05	2.637E+06
8.000	1.657E+07	2.189E-04	6.343E-05	1.657E+07
6.500	9.598E+07	1.289E-03	3.733E-04	9.598E+07
5.000	1.095E+08	1.472E-03	4.264E-04	1.095E+08
4.000	3.498E+09	1.658E+00	8.810E-01	3.498E+09
3.000	3.017E+10	1.402E+06	1.456E+06	3.017E+10
2.500	3.910E+11	4.531E+08	4.705E+08	3.920E+11
2.000	2.135E+13	3.945E+03	1.205E+03	2.135E+13
1.660	5.626E+14	2.539E+13	2.637E+13	6.144E+14
1.330	1.304E+15	6.011E+13	6.242E+13	1.427E+15
1.000	1.198E+15	6.207E+10	5.702E+10	1.198E+15
0.800	1.370E+16	1.451E+11	7.005E+10	1.370E+16
0.600	2.449E+16	2.722E+11	9.139E+10	2.449E+16
0.400	6.345E+14	1.732E+11	5.943E+10	6.347E+14
0.300	1.180E+15	3.107E+10	1.553E+10	1.180E+15
0.200	3.114E+15	6.357E+10	5.176E+10	3.114E+15
0.100	5.779E+15	2.967E+11	3.047E+11	5.780E+15
0.050	3.212E+16	3.680E+12	3.382E+12	3.213E+16
Total	8.411E+16	9.022E+13	9.282E+13	8.429E+16

Table 5.2-9

FO-DSC Design Basis Gamma Power and Energy Spectrum

Mean Energy (MeV)	In-Core (MeV/sec/cask)	Top Nozzle (MeV/sec/cask)	Bottom Nozzle (MeV/sec/cask)	Total (MeV/sec/cask)
8.944	2.358E+07	3.091E-04	8.953E-05	2.358E+07
7.211	1.195E+08	1.579E-03	4.574E-04	1.195E+08
5.701	5.472E+08	7.347E-03	2.128E-03	5.472E+08
4.472	4.897E+08	6.583E-03	1.907E-03	4.897E+08
3.464	1.212E+10	5.744E+00	3.052E+00	1.212E+10
2.739	8.264E+10	3.841E+06	3.988E+06	8.264E+10
2.236	8.744E+11	1.013E+09	1.052E+09	8.764E+11
1.822	3.890E+13	7.187E+03	2.196E+03	3.890E+13
1.486	8.360E+14	3.773E+13	3.919E+13	9.129E+14
1.153	1.504E+15	6.930E+13	7.197E+13	1.645E+15
0.894	1.071E+15	5.549E+10	5.097E+10	1.071E+15
0.693	9.497E+15	1.005E+11	4.854E+10	9.497E+15
0.490	1.200E+16	1.334E+11	4.478E+10	1.200E+16
0.346	2.195E+14	5.994E+10	2.056E+10	2.196E+14
0.245	2.890E+14	7.612E+09	3.804E+09	2.890E+14
0.141	4.390E+14	8.963E+09	7.297E+09	4.390E+14
0.071	4.103E+14	2.107E+10	2.163E+10	4.103E+14
0.022	7.067E+14	8.096E+10	7.440E+10	7.068E+14
Total	2.701E+16	1.075E+14	1.114E+14	2.723E+16

Table 5.2-10

Formulae for Mapping Gamma Source from ORIGEN2 to CASK-81 Energy Groups

ORIGEN2 Group	ORIGEN2 E_{mean} (MeV)	CASK-81 Group	CASK-81 E_{upper} (MeV)	Formula ORIGEN2 → CASK-81
a	9.500	23	10.000	a
b	7.000	24	8.000	0.722b
c	5.000	25	6.500	0.278b + 0.450c
d	3.500	26	5.000	0.550c
e	2.750	27	4.000	d
f	2.250	28	3.000	e
g	1.750	29	2.500	f
h	1.250	30	2.000	0.648g
i	0.850	31	1.660	0.352g + 0.297h
j	0.575	32	1.330	0.703h
k	0.375	33	1.000	0.626i
l	0.225	34	0.800	0.374i + 0.349j
m	0.125	35	0.600	0.651j + 0.290k
n	0.085	36	0.400	0.710k
o	0.058	37	0.300	0.585l
p	0.038	38	0.200	0.415l + m
q	0.025	39	0.100	n + 0.762o
r	0.010	40	0.050	0.238o + p + q + r

5.2.1.5 Design Basis Gamma Source for FC-DSC

The payload of the FC-DSC differs from that of the FO-DSC only by the addition of control components. As discussed in Section 5.2.1.2, ORIGEN2 was used to calculate sources for both black and gray APSRAs, which represent the bounding control components, after 8-years cooling. The calculated source per component for both the in-core and top nozzle regions is provided in Table 5.2-11 (energy group mapping per Table 5.2-10). As shown in Table 5.2-11, it is not obvious which control component would produce the greatest cask dose rates. The black APSRA has the highest total source while the gray APSRA has the highest source in the specific energy groups that contribute the most to the cask dose rates. The effect of the two types of APSRA on the cask dose rates is assessed using two additional ANISN runs. The Type I assembly, Case V ANISN runs described in Section 5.2.1.3 were modified to include the control component sources from Table 5.2-11. The calculated gamma dose rates with the black and gray APSRAs (neglecting axial peaking) are 25.4 mrem/hr and 35.6 mrem/hr, respectively. Based on these results, the gray APSRA is considered the design basis control component.

The gamma source strengths and energy spectra for the top nozzle (including the top nozzle and plenum sources), in-core, and bottom nozzle regions and for the whole assembly are shown in Table 5.2-12 and Table 5.2-13 for the design basis Type I and Type II sources, respectively, with control components. These sources were calculated by summing the contributions from the design basis FO sources and control components, group-by-group, for the in-core and top-nozzle regions. Because the APSRA does not extend into the bottom nozzle region, the bottom nozzle source for the FO-DSC and FC-DSC are identical.

The maximum source in an FC-DSC, as discussed above, is based on 4 Type I and 20 Type II assemblies. Table 5.2-14 and Table 5.2-15 provide the total FC-DSC source. The energy spectrum is that used by the CASK-81 cross-section library. The total design basis gamma source strength in the package containing 24 PWR fuel assemblies (4 Type I and 20 Type II) in an FC-DSC is 8.794×10^{16} photons per second (3.162×10^{16} MeV/sec). This design basis source, when used with the design basis neutron source described below, bounds that of B&W 15x15 assemblies with control components that meet the acceptance criteria listed in Section 1.2.3.

Table 5.2-11

Design Basis Control Component Source Terms

Upper energy (MeV)	Black Top (γ/sec/assy)	Black Core (γ/sec/assy)	Gray Top (γ/sec/assy)	Gray Core (γ/sec/assy)
10.000	0.000E+00	0.000E+00	0.000E+00	0.000E+00
8.000	0.000E+00	0.000E+00	0.000E+00	0.000E+00
6.500	0.000E+00	0.000E+00	0.000E+00	0.000E+00
5.000	0.000E+00	0.000E+00	0.000E+00	0.000E+00
4.000	4.117E-20	1.724E-03	3.590E-20	2.169E-07
3.000	3.416E+04	7.606E+05	3.123E+04	2.362E+06
2.500	1.104E+07	2.532E+08	1.009E+07	7.632E+08
2.000	4.372E-03	1.203E+11	4.010E-03	1.205E+01
1.660	6.187E+11	1.352E+13	5.655E+11	4.277E+13
1.330	1.464E+12	3.184E+13	1.339E+12	1.012E+14
1.000	2.194E+09	3.608E+13	1.996E+09	1.989E+11
0.800	1.313E+09	4.648E+13	1.194E+09	1.189E+11
0.600	2.803E+07	6.807E+13	2.562E+07	1.940E+09
0.400	6.078E+07	5.284E+13	5.556E+07	4.208E+09
0.300	1.785E+08	1.381E+11	1.632E+08	1.245E+10
0.200	1.055E+09	2.945E+11	9.641E+08	7.329E+10
0.100	7.100E+09	5.582E+12	6.491E+09	4.926E+11
0.050	7.331E+10	5.167E+13	6.701E+10	5.220E+12
Total	2.168E+12	3.066E+14	1.982E+12	1.501E+14

Table 5.2-12

Type I Assembly w/ Control Component

Design Basis Gamma Source Strength and Energy Spectrum

Upper Energy (MeV)	In-Core (γ/sec/assy)	Top Nozzle (γ/sec/assy)	Bottom Nozzle (γ/sec/assy)	Total (γ/sec/assy)
10.000	1.402E+05	1.525E-06	4.451E-07	1.402E+05
8.000	8.808E+05	9.646E-06	2.815E-06	8.808E+05
6.500	5.100E+06	5.663E-05	1.651E-05	5.100E+06
5.000	5.819E+06	6.468E-05	1.885E-05	5.819E+06
4.000	7.676E+08	4.050E-01	2.175E-01	7.676E+08
3.000	5.998E+09	1.589E+05	1.427E+05	5.998E+09
2.500	9.660E+10	5.134E+07	4.612E+07	9.670E+10
2.000	1.495E+12	2.782E+02	9.659E+01	1.495E+12
1.660	8.868E+13	2.878E+12	2.584E+12	9.414E+13
1.330	2.080E+14	6.811E+12	6.117E+12	2.209E+14
1.000	1.482E+14	5.736E+09	6.273E+09	1.482E+14
0.800	7.893E+14	1.954E+10	9.586E+09	7.894E+14
0.600	1.323E+15	4.057E+10	1.477E+10	1.323E+15
0.400	3.895E+13	2.576E+10	9.486E+09	3.899E+13
0.300	6.241E+13	4.368E+09	2.028E+09	6.241E+13
0.200	1.783E+14	7.915E+09	5.499E+09	1.783E+14
0.100	2.962E+14	3.373E+10	2.993E+10	2.962E+14
0.050	1.670E+15	4.328E+11	3.391E+11	1.671E+15
Total	4.804E+15	1.026E+13	9.119E+12	4.824E+15

Table 5.2-13

Type II Assembly w/ Control Component

Design Basis Gamma Source Strength and Energy Spectrum

Upper Energy (MeV)	In-Core (γ/sec/assy)	Top Nozzle (γ/sec/assy)	Bottom Nozzle (γ/sec/assy)	Total (γ/sec/assy)
10.000	1.038E+05	1.423E-06	4.115E-07	1.038E+05
8.000	6.525E+05	9.018E-06	2.609E-06	6.525E+05
6.500	3.779E+06	5.311E-05	1.536E-05	3.779E+06
5.000	4.311E+06	6.066E-05	1.755E-05	4.311E+06
4.000	2.136E+07	1.913E-03	5.534E-04	2.136E+07
3.000	3.118E+08	7.581E+04	4.426E+04	3.119E+08
2.500	1.147E+09	2.449E+07	1.430E+07	1.186E+09
2.000	7.686E+11	1.416E+02	4.096E+01	7.686E+11
1.660	6.172E+13	1.373E+12	8.016E+11	6.389E+13
1.330	1.451E+14	3.249E+12	1.897E+12	1.502E+14
1.000	3.050E+13	4.352E+09	1.596E+09	3.051E+13
0.800	5.275E+14	4.779E+09	1.585E+09	5.275E+14
0.600	9.598E+14	5.525E+09	1.617E+09	9.598E+14
0.400	2.394E+13	3.577E+09	1.074E+09	2.394E+13
0.300	4.651E+13	8.756E+08	3.707E+08	4.651E+13
0.200	1.201E+14	2.752E+09	1.488E+09	1.201E+14
0.100	2.303E+14	1.588E+10	9.249E+09	2.303E+14
0.050	1.278E+15	1.779E+11	1.013E+11	1.279E+15
Total	3.425E+15	4.838E+12	2.817E+12	3.432E+15

Table 5.2-14

FC-DSC Design Basis Gamma Source Strength and Energy Spectrum

Upper Energy (MeV)	In-Core (γ/sec/cask)	Top Nozzle (γ/sec/cask)	Bottom Nozzle (γ/sec/cask)	Total (γ/sec/cask)
10.000	2.637E+06	3.456E-05	1.001E-05	2.637E+06
8.000	1.657E+07	2.189E-04	6.343E-05	1.657E+07
6.500	9.598E+07	1.289E-03	3.733E-04	9.598E+07
5.000	1.095E+08	1.472E-03	4.264E-04	1.095E+08
4.000	3.498E+09	1.658E+00	8.810E-01	3.498E+09
3.000	3.023E+10	2.152E+06	1.456E+06	3.023E+10
2.500	4.094E+11	6.953E+08	4.705E+08	4.105E+11
2.000	2.135E+13	3.945E+03	1.205E+03	2.135E+13
1.660	1.589E+15	3.897E+13	2.637E+13	1.654E+15
1.330	3.734E+15	9.223E+13	6.242E+13	3.888E+15
1.000	1.203E+15	1.100E+11	5.702E+10	1.203E+15
0.800	1.371E+16	1.737E+11	7.005E+10	1.371E+16
0.600	2.449E+16	2.728E+11	9.139E+10	2.449E+16
0.400	6.346E+14	1.746E+11	5.943E+10	6.348E+14
0.300	1.180E+15	3.499E+10	1.553E+10	1.180E+15
0.200	3.115E+15	8.671E+10	5.176E+10	3.115E+15
0.100	5.791E+15	4.525E+11	3.047E+11	5.792E+15
0.050	3.225E+16	5.288E+12	3.382E+12	3.226E+16
Total	8.771E+16	1.378E+14	9.282E+13	8.794E+16

Table 5.2-15

FC-DSC Design Basis Gamma Power and Energy Spectrum

Mean Energy (MeV)	In-Core (MeV/sec/cask)	Top Nozzle (MeV/sec/cask)	Bottom Nozzle (MeV/sec/cask)	Total (MeV/sec/cask)
8.944	2.358E+07	3.091E-04	8.953E-05	2.358E+07
7.211	1.195E+08	1.579E-03	4.574E-04	1.195E+08
5.701	5.472E+08	7.347E-03	2.128E-03	5.472E+08
4.472	4.897E+08	6.583E-03	1.907E-03	4.897E+08
3.464	1.212E+10	5.744E+00	3.052E+00	1.212E+10
2.739	8.279E+10	5.894E+06	3.988E+06	8.280E+10
2.236	9.153E+11	1.555E+09	1.052E+09	9.179E+11
1.822	3.890E+13	7.187E+03	2.196E+03	3.890E+13
1.486	2.361E+15	5.790E+13	3.919E+13	2.458E+15
1.153	4.305E+15	1.063E+14	7.197E+13	4.483E+15
0.894	1.075E+15	9.833E+10	5.097E+10	1.076E+15
0.693	9.499E+15	1.204E+11	4.854E+10	9.499E+15
0.490	1.200E+16	1.337E+11	4.478E+10	1.200E+16
0.346	2.196E+14	6.040E+10	2.056E+10	2.196E+14
0.245	2.891E+14	8.571E+09	3.804E+09	2.891E+14
0.141	4.393E+14	1.223E+10	7.297E+09	4.393E+14
0.071	4.111E+14	3.213E+10	2.163E+10	4.112E+14
0.022	7.094E+14	1.163E+11	7.440E+10	7.096E+14
Total	3.135E+16	1.648E+14	1.114E+14	3.162E+16

Table 5.2-16

FC-DSC Gamma Source Strength and Energy Spectrum for Each Burnup Case for Type I Fuel

Upper Energy (MeV)	Case I 23.2 GWd/MTU (γ/sec/cask)	Case II 25 GWd/MTU (γ/sec/cask)	Case III 30 GWd/MTU (γ/sec/cask)	Case IV 35 GWd/MTU (γ/sec/cask)	Case V 40 GWd/MTU (γ/sec/cask)
10.000	6.370E+05	7.978E+05	1.401E+06	2.340E+06	3.365E+06
8.000	4.003E+06	5.015E+06	8.808E+06	1.470E+07	2.114E+07
6.500	2.318E+07	2.904E+07	5.101E+07	8.514E+07	1.224E+08
5.000	2.645E+07	3.313E+07	5.820E+07	9.714E+07	1.397E+08
4.000	1.452E+11	1.573E+11	1.924E+11	6.065E+10	1.842E+10
3.000	1.137E+12	1.232E+12	1.505E+12	4.717E+11	1.439E+11
2.500	3.601E+13	3.884E+13	4.664E+13	1.027E+13	2.319E+12
2.000	3.843E+13	4.237E+13	5.405E+13	3.963E+13	3.588E+13
1.660	2.090E+15	2.178E+15	2.442E+15	2.249E+15	2.128E+15
1.330	4.898E+15	5.102E+15	5.710E+15	5.272E+15	4.992E+15
1.000	4.348E+15	4.905E+15	6.641E+15	4.956E+15	3.557E+15
0.800	1.569E+16	1.721E+16	2.166E+16	1.996E+16	1.894E+16
0.600	2.490E+16	2.715E+16	3.361E+16	3.216E+16	3.175E+16
0.400	1.176E+15	1.266E+15	1.518E+15	1.086E+15	9.349E+14
0.300	1.564E+15	1.691E+15	2.046E+15	1.568E+15	1.498E+15
0.200	4.210E+15	4.581E+15	5.640E+15	4.442E+15	4.279E+15
0.100	6.876E+15	7.430E+15	8.975E+15	7.278E+15	7.108E+15
0.050	3.777E+16	4.079E+16	4.919E+16	4.080E+16	4.007E+16
Total	1.036E+17	1.124E+17	1.375E+17	1.198E+17	1.153E+17
Mean Energy (MeV)	**Case I 23.2 GWd/MTU (MeV/sec/cask)**	**Case II 25 GWd/MTU (MeV/sec/cask)**	**Case III 30 GWd/MTU (MeV/sec/cask)**	**Case IV 35 GWd/MTU (MeV/sec/cask)**	**Case V 40 GWd/MTU (MeV/sec/cask)**
8.944	5.697E+06	7.135E+06	1.253E+07	2.092E+07	3.009E+07
7.211	2.886E+07	3.616E+07	6.351E+07	1.060E+08	1.524E+08
5.701	1.322E+08	1.656E+08	2.908E+08	4.854E+08	6.978E+08
4.472	1.183E+08	1.482E+08	2.603E+08	4.344E+08	6.245E+08
3.464	5.031E+11	5.449E+11	6.664E+11	2.101E+11	6.382E+10
2.739	3.115E+12	3.373E+12	4.123E+12	1.292E+12	3.943E+11
2.236	8.051E+13	8.684E+13	1.043E+14	2.296E+13	5.184E+12
1.822	7.002E+13	7.719E+13	9.847E+13	7.220E+13	6.537E+13
1.486	3.106E+15	3.237E+15	3.628E+15	3.342E+15	3.163E+15
1.153	5.647E+15	5.883E+15	6.584E+15	6.078E+15	5.755E+15
0.894	3.887E+15	4.385E+15	5.937E+15	4.431E+15	3.180E+15
0.693	1.087E+16	1.192E+16	1.501E+16	1.383E+16	1.313E+16
0.490	1.220E+16	1.330E+16	1.647E+16	1.576E+16	1.556E+16
0.346	4.071E+14	4.381E+14	5.251E+14	3.758E+14	3.235E+14
0.245	3.831E+14	4.142E+14	5.013E+14	3.843E+14	3.670E+14
0.141	5.936E+14	6.460E+14	7.952E+14	6.263E+14	6.033E+14
0.071	4.882E+14	5.276E+14	6.373E+14	5.167E+14	5.047E+14
0.022	8.310E+14	8.974E+14	1.082E+15	8.977E+14	8.816E+14
Total	3.857E+16	4.182E+16	5.138E+16	4.634E+16	4.354E+16

Table 5.2-17

FC-DSC Gamma Source Strength and Energy Spectrum for Each Burnup Case for Type II Fuel

Upper Energy (MeV)	Case I 23.2 GWd/MTU (γ/sec/cask)	Case II 25 GWd/MTU (γ/sec/cask)	Case III 30 GWd/MTU (γ/sec/cask)	Case IV 35 GWd/MTU (γ/sec/cask)	Case V 40 GWd/MTU (γ/sec/cask)
10.000	6.370E+05	7.682E+05	1.252E+06	2.013E+06	2.491E+06
8.000	4.003E+06	4.828E+06	7.869E+06	1.265E+07	1.566E+07
6.500	2.318E+07	2.796E+07	4.557E+07	7.328E+07	9.069E+07
5.000	2.645E+07	3.190E+07	5.199E+07	8.361E+07	1.035E+08
4.000	1.452E+11	7.914E+10	2.463E+10	4.203E+09	5.127E+08
3.000	1.137E+12	6.179E+11	1.924E+11	3.477E+10	7.483E+09
2.500	3.601E+13	1.671E+13	3.831E+12	4.279E+11	2.753E+10
2.000	3.843E+13	3.028E+13	2.604E+13	2.423E+13	1.845E+13
1.660	2.090E+15	2.006E+15	1.933E+15	1.764E+15	1.481E+15
1.330	4.898E+15	4.709E+15	4.541E+15	4.143E+15	3.482E+15
1.000	4.348E+15	3.620E+15	2.767E+15	1.748E+15	7.320E+14
0.800	1.569E+16	1.483E+16	1.472E+16	1.411E+16	1.266E+16
0.600	2.490E+16	2.402E+16	2.470E+16	2.466E+16	2.303E+16
0.400	1.176E+15	9.579E+14	8.011E+14	6.889E+14	5.745E+14
0.300	1.564E+15	1.312E+15	1.217E+15	1.189E+15	1.116E+15
0.200	4.210E+15	3.530E+15	3.315E+15	3.254E+15	2.883E+15
0.100	6.876E+15	5.940E+15	5.701E+15	5.748E+15	5.527E+15
0.050	3.777E+16	3.325E+16	3.228E+16	3.220E+16	3.068E+16
Total	1.036E+17	9.423E+16	9.200E+16	8.952E+16	8.219E+16
Mean Energy (MeV)	Case I 23.2 GWd/MTU (MeV/sec/cask)	Case II 25 GWd/MTU (MeV/sec/cask)	Case III 30 GWd/MTU (MeV/sec/cask)	Case IV 35 GWd/MTU (MeV/sec/cask)	Case V 40 GWd/MTU (MeV/sec/cask)
8.944	5.697E+06	6.871E+06	1.120E+07	1.801E+07	2.228E+07
7.211	2.886E+07	3.481E+07	5.674E+07	9.124E+07	1.129E+08
5.701	1.322E+08	1.594E+08	2.598E+08	4.178E+08	5.170E+08
4.472	1.183E+08	1.427E+08	2.325E+08	3.739E+08	4.627E+08
3.464	5.031E+11	2.742E+11	8.532E+10	1.456E+10	1.776E+09
2.739	3.115E+12	1.692E+12	5.269E+11	9.525E+10	2.050E+10
2.236	8.051E+13	3.737E+13	8.567E+12	9.568E+11	6.156E+10
1.822	7.002E+13	5.517E+13	4.744E+13	4.415E+13	3.361E+13
1.486	3.106E+15	2.981E+15	2.872E+15	2.621E+15	2.201E+15
1.153	5.647E+15	5.430E+15	5.236E+15	4.777E+15	4.015E+15
0.894	3.887E+15	3.237E+15	2.474E+15	1.563E+15	6.544E+14
0.693	1.087E+16	1.028E+16	1.020E+16	9.779E+15	8.773E+15
0.490	1.220E+16	1.177E+16	1.210E+16	1.208E+16	1.129E+16
0.346	4.071E+14	3.314E+14	2.772E+14	2.384E+14	1.988E+14
0.245	3.831E+14	3.215E+14	2.982E+14	2.912E+14	2.735E+14
0.141	5.936E+14	4.978E+14	4.675E+14	4.588E+14	4.065E+14
0.071	4.882E+14	4.218E+14	4.047E+14	4.081E+14	3.924E+14
0.022	8.310E+14	7.314E+14	7.101E+14	7.084E+14	6.750E+14
Total	3.857E+16	3.610E+16	3.510E+16	3.297E+16	2.891E+16

5.2.2 Neutron Source

The neutron source strength for the design basis fuel assembly is calculated using the same ORIGEN2 runs as were used to calculate the gamma source. All input parameters and assumptions are the same as those used for the gamma ray calculations described above.

The neutron source results from spontaneous fission and (α,n) reactions in the active fuel region. The total neutron sources for the design basis case are 2.455×10^8 neutrons/sec per Type I assembly and 1.829×10^8 neutrons/sec per Type II assembly (4.640×10^9 neutrons/sec/cask assuming 4 Type I assemblies and 20 Type II assemblies) as calculated by the ORIGEN2 code.

The spectrum for spontaneous fission neutrons from ^{244}Cm is assumed for the neutron source in this analysis [5.7]. The ^{244}Cm spontaneous fission spectrum was chosen because it represents more than 90% of the total neutron source in the package. The ^{244}Cm spectrum group fractions for the CASK-81 energy structure are then multiplied by the total source strength to determine the groupwise source strengths for the cask to be used in the shielding calculations. The total neutron source strength and energy spectrum for each of the five burnup cases is shown in Table 5.2-18 and Table 5.2-19 for Type I and Type II assemblies, respectively.

Table 5.2-18

Design Basis Neutron Source Strength and Energy Spectrum for Type I Fuel

Upper Energy (MeV)	Case I 23.2 GWd/MTU (n/sec/cask)	Case II 25 GWd/MTU (n/sec/cask)	Case III 30 GWd/MTU (n/sec/cask)	Case IV 35 GWd/MTU (n/sec/cask)	Case V 40 GWd/MTU (n/sec/cask)
1.492E+01	2.274E+05	2.840E+05	4.964E+05	8.277E+05	1.189E+06
1.220E+01	1.291E+06	1.613E+06	2.819E+06	4.700E+06	6.752E+06
1.000E+01	5.038E+06	6.292E+06	1.100E+07	1.834E+07	2.634E+07
8.180E+00	1.992E+07	2.488E+07	4.349E+07	7.252E+07	1.042E+08
6.360E+00	4.695E+07	5.864E+07	1.025E+08	1.709E+08	2.455E+08
4.960E+00	6.356E+07	7.939E+07	1.388E+08	2.314E+08	3.324E+08
4.060E+00	1.349E+08	1.685E+08	2.945E+08	4.910E+08	7.053E+08
3.010E+00	1.084E+08	1.353E+08	2.366E+08	3.944E+08	5.666E+08
2.460E+00	2.542E+07	3.175E+07	5.550E+07	9.253E+07	1.329E+08
2.350E+00	1.383E+08	1.727E+08	3.018E+08	5.033E+08	7.229E+08
1.830E+00	2.378E+08	2.970E+08	5.191E+08	8.654E+08	1.243E+09
1.110E+00	2.021E+08	2.525E+08	4.413E+08	7.358E+08	1.057E+09
5.500E-01	1.282E+08	1.602E+08	2.799E+08	4.668E+08	6.705E+08
1.110E-01	1.466E+07	1.831E+07	3.200E+07	5.336E+07	7.665E+07
3.350E-03	7.386E+04	9.225E+04	1.613E+05	2.689E+05	3.862E+05
5.830E-04	5.369E+03	6.706E+03	1.172E+04	1.954E+04	2.808E+04
1.010E-04	3.531E+02	4.411E+02	7.710E+02	1.285E+03	1.847E+03
2.900E-05	5.101E+01	6.371E+01	1.114E+02	1.857E+02	2.667E+02
1.010E-05	1.100E+01	1.373E+01	2.401E+01	4.003E+01	5.750E+01
3.060E-06	1.714E+00	2.141E+00	3.742E+00	6.239E+00	8.962E+00
1.120E-06	3.778E-01	4.719E-01	8.248E-01	1.375E+00	1.976E+00
4.140E-07	1.091E-01	1.363E-01	2.382E-01	3.972E-01	5.705E-01
Total	1.127E+09	1.407E+09	2.460E+09	4.102E+09	5.892E+09

Table 5.2-19

Design Basis Neutron Source Strength and Energy Spectrum for Type II Fuel

Upper Energy (MeV)	Case I 23.2 GWd/MTU (n/sec/cask)	Case II 25 GWd/MTU (n/sec/cask)	Case III 30 GWd/MTU (n/sec/cask)	Case IV 35 GWd/MTU (n/sec/cask)	Case V 40 GWd/MTU (n/sec/cask)
1.492E+01	2.274E+05	2.739E+05	4.450E+05	7.149E+05	8.858E+05
1.220E+01	1.291E+06	1.556E+06	2.527E+06	4.060E+06	5.030E+06
1.000E+01	5.038E+06	6.069E+06	9.860E+06	1.584E+07	1.963E+07
8.180E+00	1.992E+07	2.400E+07	3.899E+07	6.263E+07	7.761E+07
6.360E+00	4.695E+07	5.656E+07	9.190E+07	1.476E+08	1.829E+08
4.960E+00	6.356E+07	7.657E+07	1.244E+08	1.998E+08	2.476E+08
4.060E+00	1.349E+08	1.625E+08	2.640E+08	4.240E+08	5.254E+08
3.010E+00	1.084E+08	1.305E+08	2.121E+08	3.406E+08	4.221E+08
2.460E+00	2.542E+07	3.062E+07	4.975E+07	7.992E+07	9.903E+07
2.350E+00	1.383E+08	1.666E+08	2.706E+08	4.347E+08	5.386E+08
1.830E+00	2.378E+08	2.864E+08	4.653E+08	7.474E+08	9.262E+08
1.110E+00	2.021E+08	2.435E+08	3.956E+08	6.355E+08	7.875E+08
5.500E-01	1.282E+08	1.545E+08	2.510E+08	4.031E+08	4.995E+08
1.110E-01	1.466E+07	1.766E+07	2.869E+07	4.609E+07	5.711E+07
3.350E-03	7.386E+04	8.898E+04	1.446E+05	2.322E+05	2.877E+05
5.830E-04	5.369E+03	6.468E+03	1.051E+04	1.688E+04	2.092E+04
1.010E-04	3.531E+02	4.254E+02	6.912E+02	1.110E+03	1.376E+03
2.900E-05	5.101E+01	6.145E+01	9.984E+01	1.604E+02	1.987E+02
1.010E-05	1.100E+01	1.325E+01	2.152E+01	3.457E+01	4.284E+01
3.060E-06	1.714E+00	2.065E+00	3.354E+00	5.388E+00	6.677E+00
1.120E-06	3.778E-01	4.551E-01	7.395E-01	1.188E+00	1.472E+00
4.140E-07	1.091E-01	1.314E-01	2.135E-01	3.430E-01	4.250E-01
Total	1.127E+09	1.357E+09	2.205E+09	3.542E+09	4.390E+09

5.3 Model Specification

The shielding analysis described below was performed to verify that the packaging containing 24 PWR fuel assemblies meets the shielding criteria specified in 10 CFR Part 71 [5.1] and 49 CFR Part 173 [5.2]. Analytical models of the package were developed to determine the dose rates around the package for both normal and hypothetical accident conditions. The 2-D discrete ordinates code DORT-PC [5.9] was used to calculate the neutron and gamma-ray dose rates as described in Section 5.4.

5.3.1 Description of the Radial and Axial Shielding Configuration

The radial and axial shielding configuration of the package is shown in Figure 5.3-1, and Figure 5.3-2 through Figure 5.3-5. Figure 5.3-1 is a scale drawing of the package that shows the overall package dimensions for both the FO-DSC and the FC-DSC. The FF-DSC shielding configuration is identical to that of the FC-DSC. The DORT-PC model for the FC-DSC is shown in Figure 5.3-2 and Figure 5.3-3 (not to scale). The model for the FO-DSC is similar and is shown in Figure 5.3-4 and Figure 5.3-5. The cask is modeled symmetrically in cylindrical coordinates and nominal dimensions were used to generate the model. A single model is used to calculate radial and axial, neutron and gamma-ray dose rates around the NUHOMS®-MP187 Cask containing an FC-DSC as defined in Chapter 1. A separate model is used to calculate dose rates around the cask containing an FO-DSC. The FF-DSC contains only 13 fuel assemblies and its source is therefore bounded by that of the FC-DSC.

The DORT-PC model of the package includes irregularities in the lead shielding to represent the tapered ends of the lead column. Minor discontinuities in the cask components due to fabrication details which do not significantly affect the cask shielding performance have been neglected in the models. Significant penetrations are addressed as described below. The impact limiters have a square cross-section that cannot be modeled accurately in cylindrical coordinates. The impact limiter geometry is therefore approximated using cylinders with radii such that they would be completely enclosed by the actual impact limiter geometry. The trunnions and the drain, vent, and test ports have been neglected. Because the upper trunnions extend through the neutron shield, the dose rates around these trunnions are evaluated separately as described in Section 5.4.1.8. The cask drain, vent and test ports contain steel plugs during shipment and do not represent a shine path. The support rods in the DSC have also been neglected. The spacer discs are neglected in the homogenized fuel region, but are explicitly modeled in the gap between the fuel region and the DSC shell. A gap is modeled in the cask bottom cover. This gap is not currently shown on the cask drawings, but represents a conservatism in the shielding calculations. The package shielding normal operation materials are shown for the FC-DSC in Figure 5.3-6. The FO-DSC materials are identical except for the use of carbon steel shield plugs rather than lead.

The neutron shielding and neutron shield jacket are assumed to be lost during the hypothetical accident conditions due to the postulated cask drop and subsequent fire. This assumption is made purely for conservatism as the neutron shield is expected to at least partially survive the hypothetical accident. The impact limiters are assumed to be lost during the hypothetical accident as well, even though there is no physical mechanism that could remove the impact limiter inner shells. The cask lead shielding is assumed to slump 2.5 inches at each end during the postulated drop, producing air gaps in the cask shielding. The suitability of the cask cavity closure during the hypothetical accident conditions is documented in Chapters 2 and 4. During the accident, the DSC is assumed to slide to the top of the cask cavity, and the fuel is assumed to slide to the top of the DSC cavity. These assumptions are made to maximize the streaming through the lead slump gap at the top of the DSC. The package shielding materials for the hypothetical accident conditions are shown in Figure 5.3-7.

Neutron and gamma ray dose rates were calculated in various locations, radially and axially, around the package. These locations include the package surface, the surface of the transport vehicle, and two meters from the surface of the transport vehicle along its top, bottom, and sides. The maximum dose rates reported in Table 5.1-1 are the maximum dose rates observed at any location, radially and axially, along the surface, for any of the three DSC designs. The package surface is defined by the surface of the impact limiters and the neutron shield during normal conditions of transport. The package surface is defined by the cask structural shell after the hypothetical accident. The outer surface of the vehicle is defined by the impact limiters and the personnel barrier, which is mounted on the skid and extends to the same radius as the impact limiters as shown on the drawings provided in Section 1.3.2.

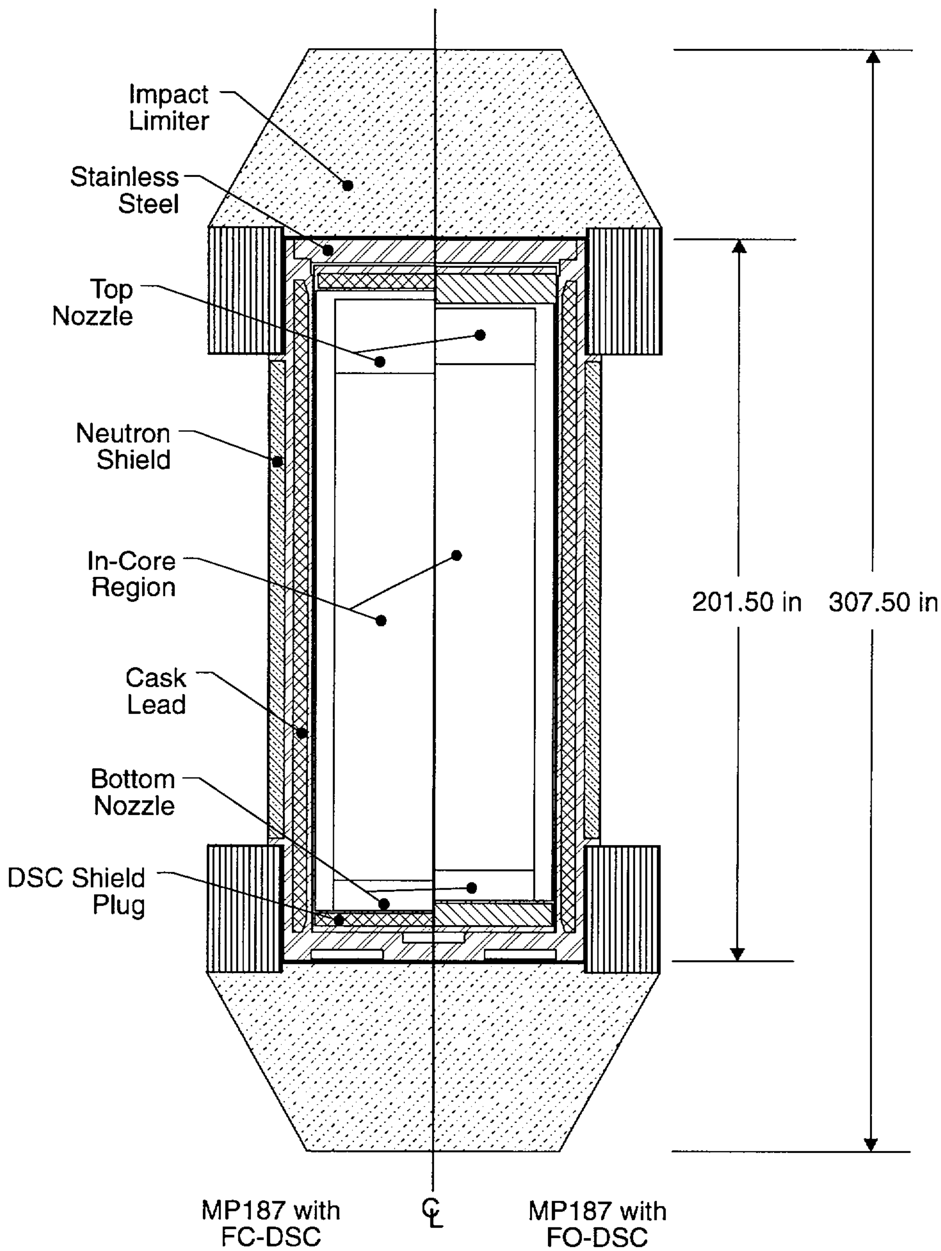

Figure 5.3-1

NUHOMS®-MP187 Cask Configuration

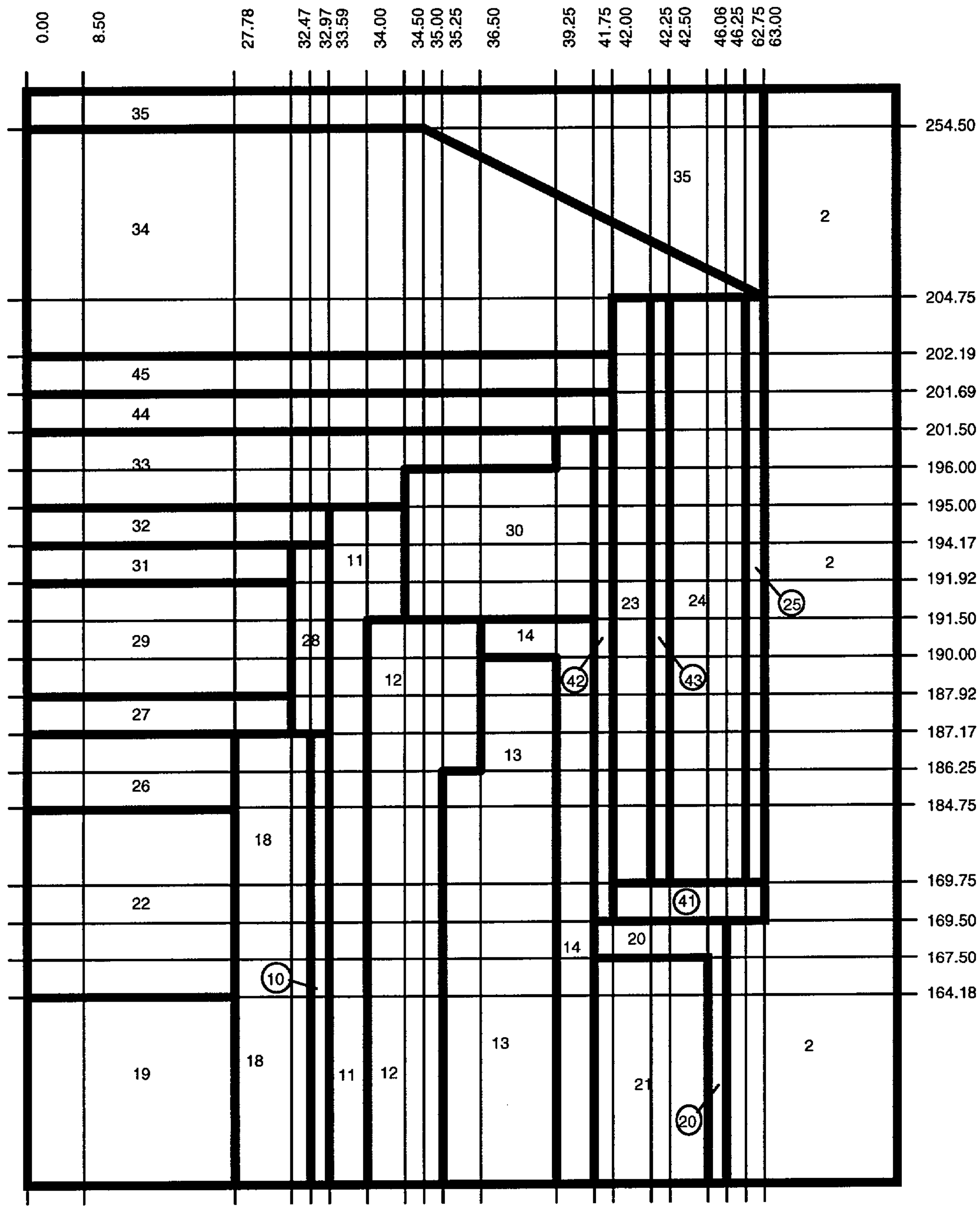

Figure 5.3-2

NUHOMS®-MP187 Normal Operations DORT-PC FC-DSC Top End Model

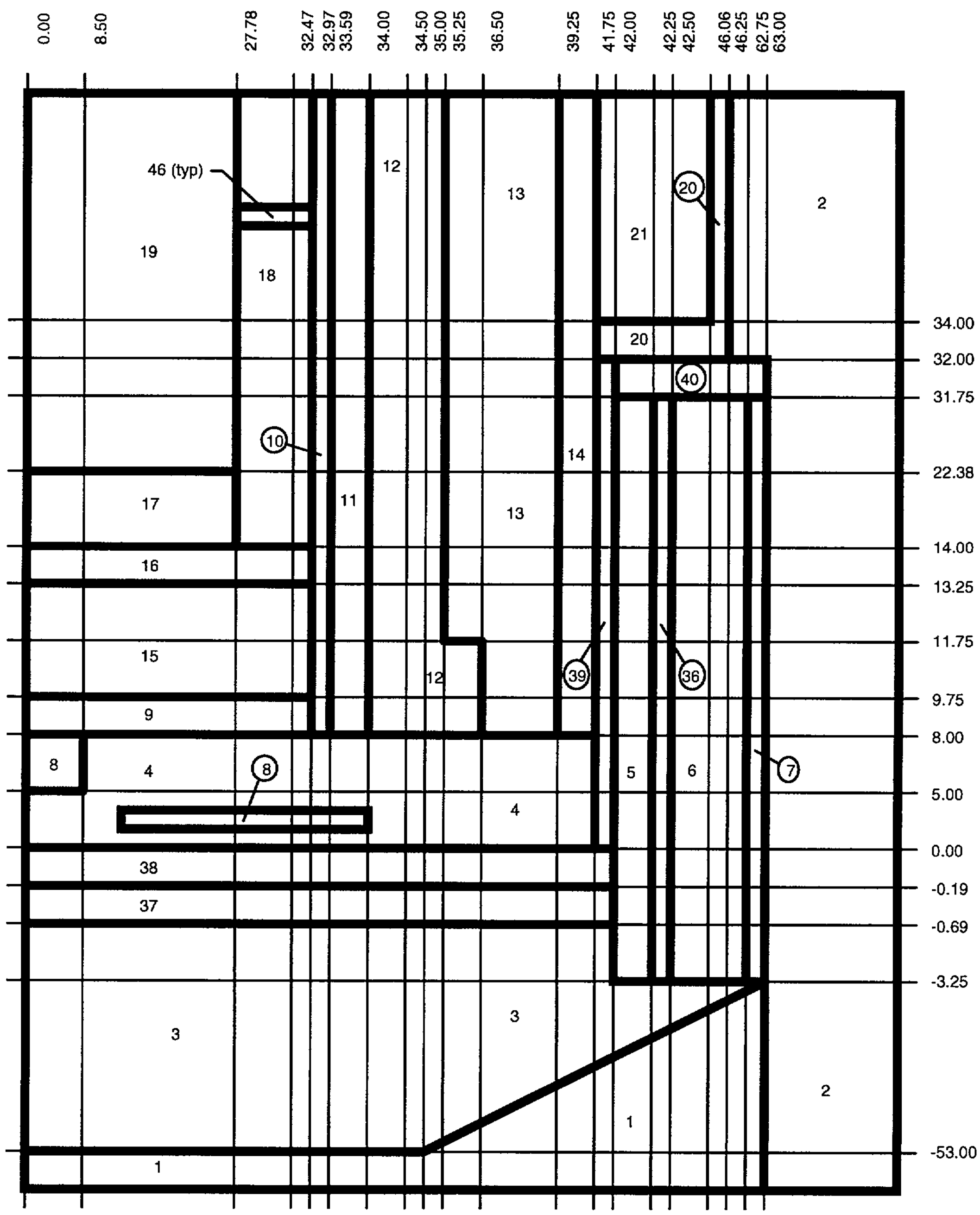

Figure 5.3-3

NUHOMS®-MP187 Normal Operations DORT-PC FC-DSC Bottom End Model

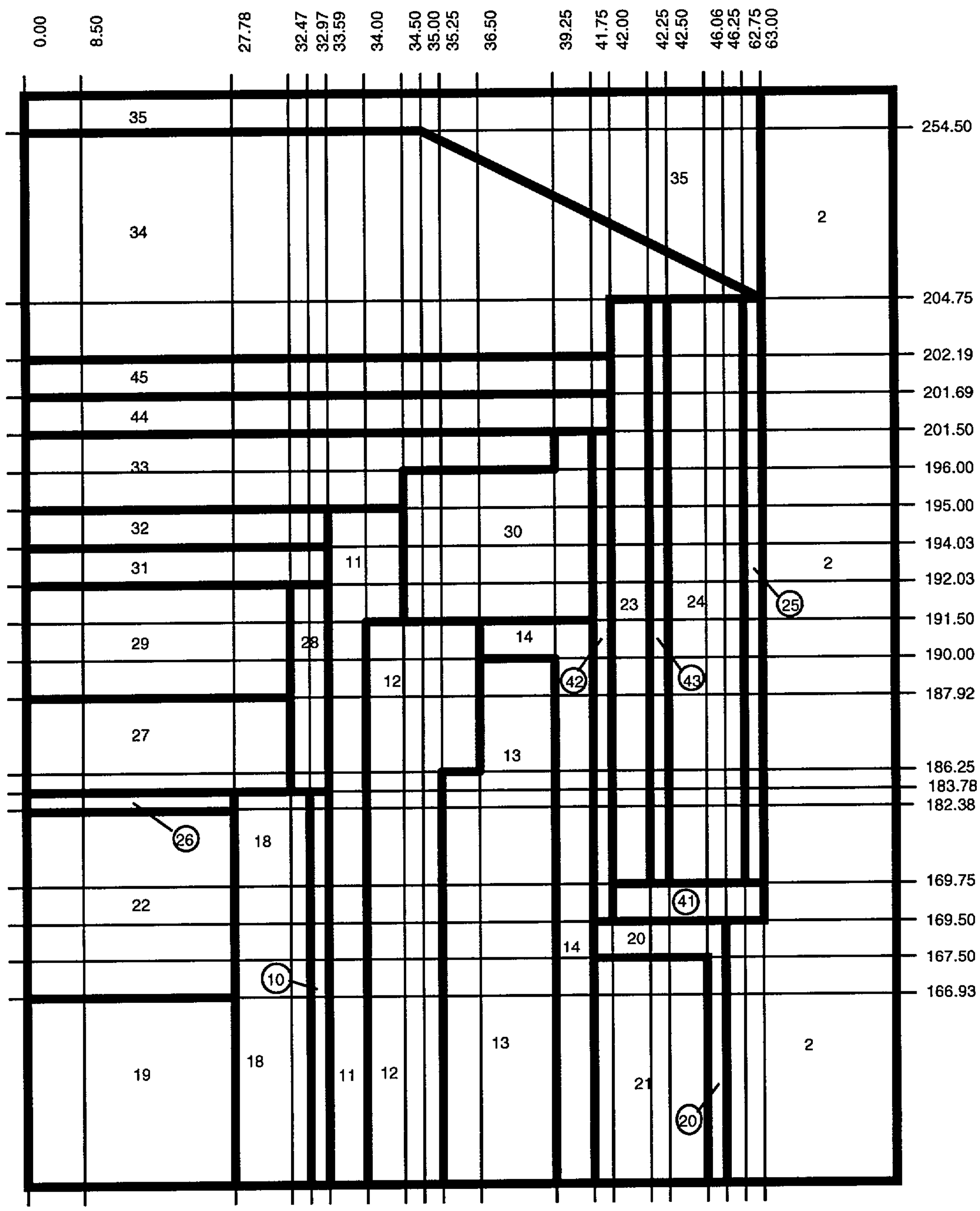

Figure 5.3-4

NUHOMS®-MP187 Normal Operations DORT-PC FO-DSC Top End Model

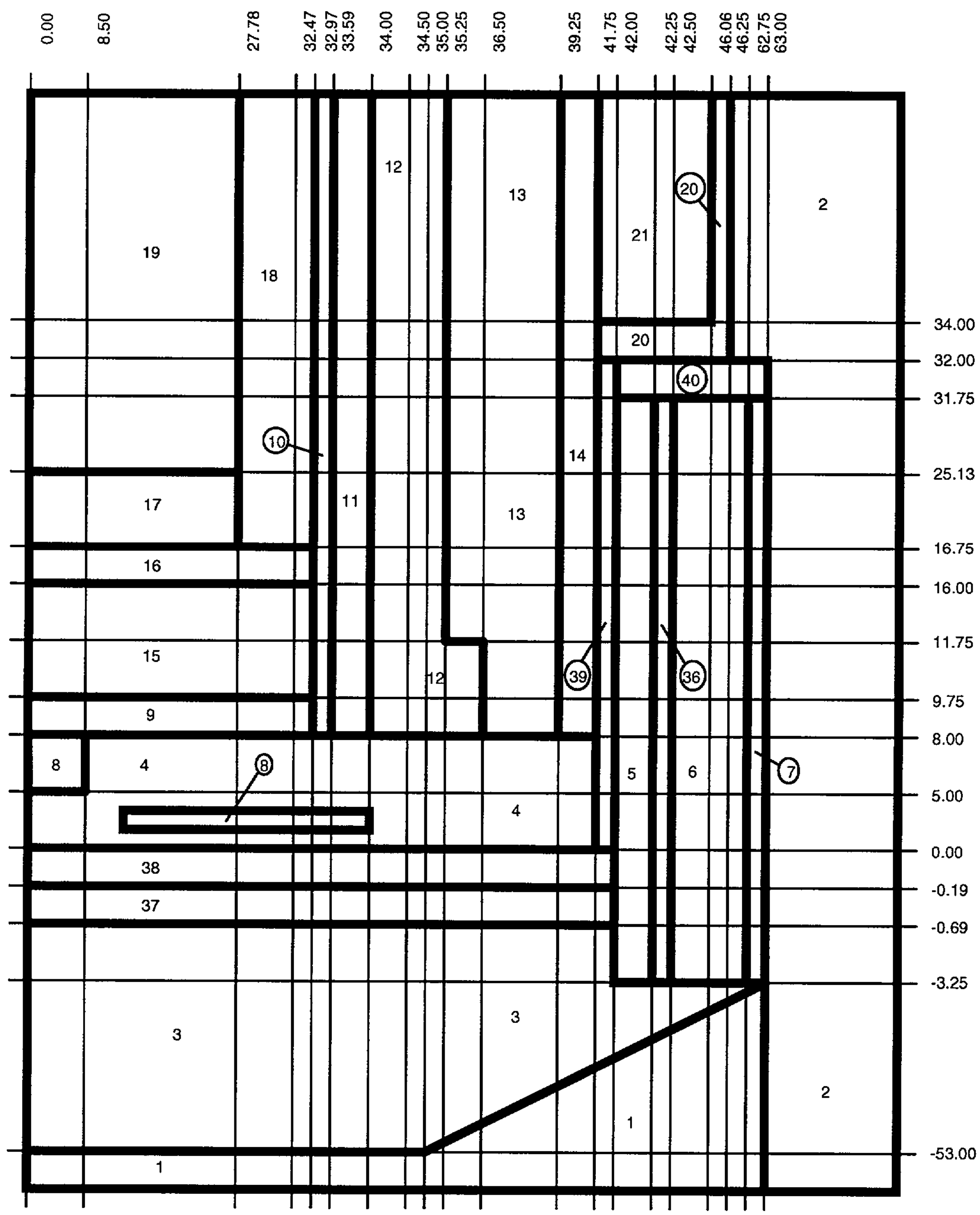

Figure 5.3-5

NUHOMS®-MP187 Normal Operations DORT-PC FO-DSC Bottom End Model

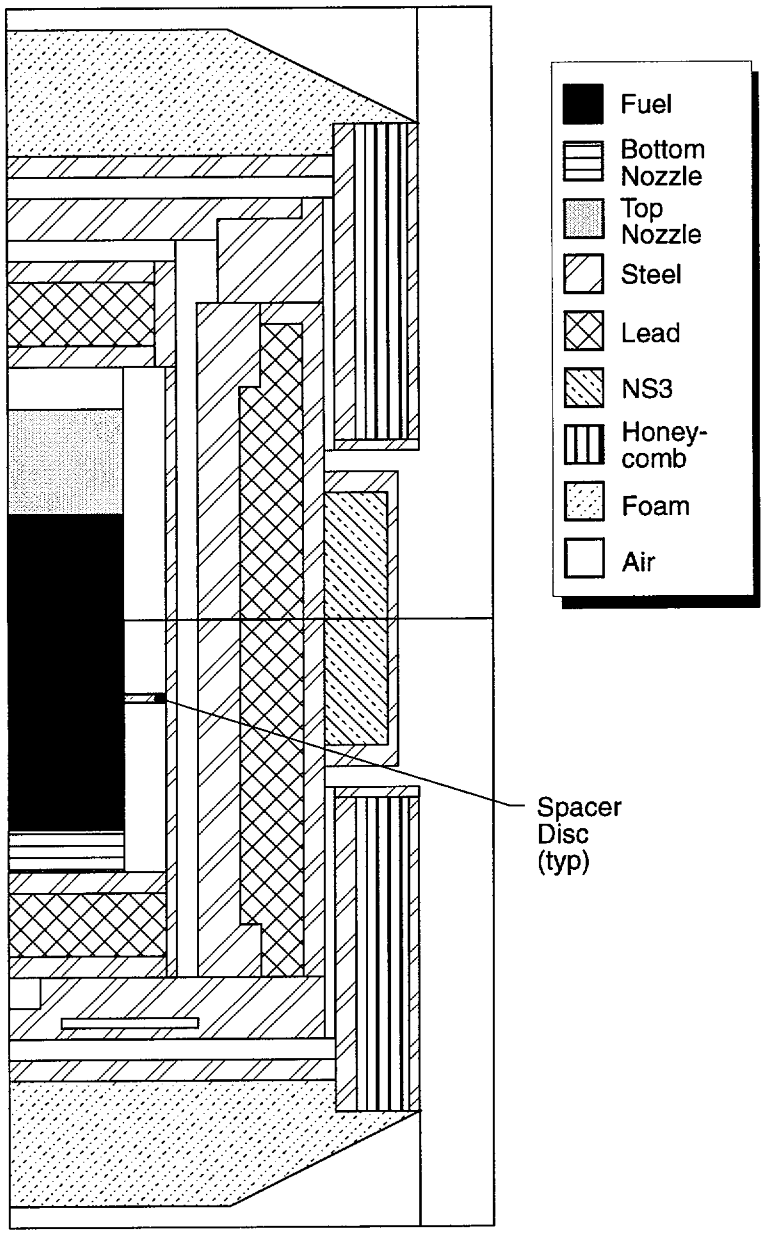

Figure 5.3-6

NUHOMS®-MP187 Normal Operation Shielding Materials

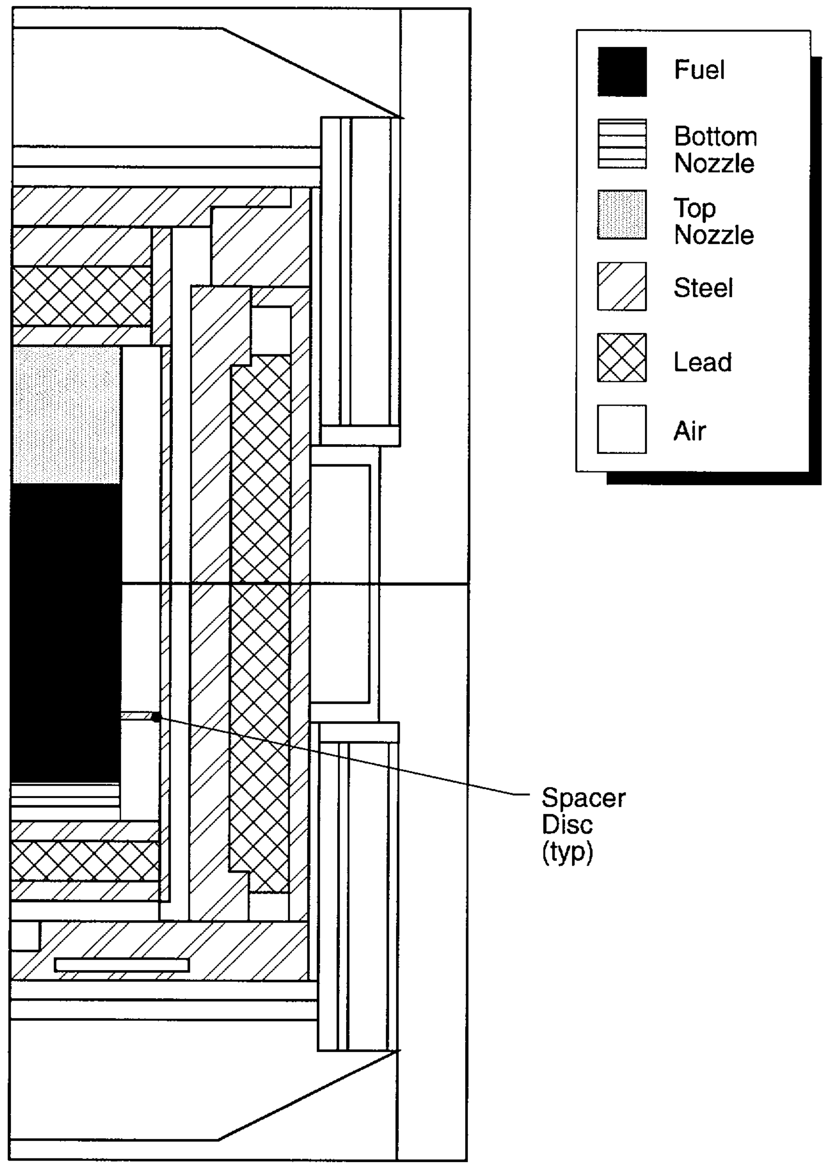

Figure 5.3-7

NUHOMS®-MP187 Hypothetical Accident Condition Shielding Materials

5.3.2 Shield Regional Densities

The mass densities (grams/cc) and atomic number densities (atoms/barn·cm) for all of the constituent nuclides in the materials used in the analytical models of the package are given in this section. Shield regional densities for the in-core, top nozzle, and bottom nozzle regions are calculated using the material weights given in Table 5.2-2. The materials in these regions are assumed to be evenly distributed over the entire volume of the region (smeared). This is a common modeling technique for shielding calculations.

The basket assembly support rods are not assumed to provide any shielding. The DSC guide sleeves and neutron absorber plates are assumed to completely cover the active fuel region in the model. The top nozzle and bottom nozzle regions are assumed to be uncovered. Minor impurities in the fuel, DSC, and the cask materials have been neglected.

The fissile nuclides present in significant quantities in the fuel, ^{235}U, ^{239}Pu, and ^{241}Pu, are included in the homogenized fuel region to provide a source for subcritical multiplication. Subcritical multiplication accounts for only about 5% of the total cask surface dose rates reported in Table 5.1-1. Because the fixed neutron source (spontaneous fission and (α,n) reactions) produces the majority of the neutron dose rate on the package surface, the overall neutron dose rates are thus maximized by using the largest possible fixed neutron source. This occurs at the greatest fuel burnup allowed by the package design. The fissile content in the fuel is significantly depleted at these high burnups and use of the initial enrichment for subcritical multiplication is, therefore, unnecessarily conservative.

The ORIGEN2 runs described above calculate fuel weight fractions of 0.635% ^{235}U, 0.579% ^{239}Pu, and 0.111% ^{241}Pu for the design basis, 40 GWd/MTU case. For simplicity, the quantities of the two Pu isotopes are summed and modeled as ^{239}Pu. An extra margin of safety is included to account for uncertainties in the quantities calculated by ORIGEN2 such that a weight fraction of 0.75% is used for both ^{235}U and ^{239}Pu. Additional margin is provided by: (1) Not taking credit for the buildup of other actinides which would serve as neutron poisons; and (2) Not taking credit for the buildup of fission products which would serve as neutron poisons. It is therefore concluded that using the burned fuel enrichment, including fissile plutonium, represents a more realistic while still conservative methodology to account for subcritical multiplication in the MP187 Cask than using the initial enrichment.

The neutron shield density and material composition are shown in Table 5.3-1. Variations in the composition of the neutron shield over the life of the package are accounted for by neglecting 10% of the hydrogen weight and 50% of the boron weight. Variations in the actual neutron shield boron loading have only a small impact on the cask dose rates. A 50% reduction in the boron weight conservatively bounds any depletion that may occur during the life of the package.

The neutron shield is completely encased in a sealed, stainless-steel annulus. When the neutron shield is exposed to high temperatures, some steam can be evolved from the material. Because the neutron shield is completely encased in a sealed, stainless-steel annulus, none of this steam is released from the cask and the total neutron shield weight remains constant. A 10% loss of hydrogen is assumed, however, to account for stratification of steam released by the solid material. Long term thermal testing of the neutron shield has been performed as discussed in Reference 5.8. Blocks of neutron shield material were held at a constant temperature of 250°F for an extended period of time. The test results show that the neutron shield material weight stabilized after a two month period and that the total reduction in hydrogen weight is less than 9.3 percent. The maximum neutron shield temperature during normal operation in the NUHOMS®-MP187 Cask is less than 250°F as documented in Chapter 3. The assumed hydrogen loss of 10 weight percent, therefore, results in conservative material properties for the shielding calculations.

The mass and atom densities of the remaining materials used in the shielding calculations are given in Table 5.3-1.

Table 5.3-1

Summary of NUHOMS®-MP187 Cask Shielding Material Densities

(atoms/b·cm, g/cc)

Element	Stainless Steel	Carbon Steel	Lead	Neutron Shield[(1)]	Aluminum Honeycomb	Foam	Air
H	-	-	-	4.180×10^{-2} (0.070)	-	1.004×10^{-2} (0.017)	-
B	-	-	-	7.131×10^{-4} (0.013)	-	-	-
C	-	-	-	7.871×10^{-3} (0.157)	-	7.220×10^{-3} (0.144)	-
N	-	-	-	-	-	8.255×10^{-4} (0.019)	3.587×10^{-5} (8.343×10^{-4})
O	-	-	-	3.442×10^{-2} (0.915)	-	2.168×10^{-3} (0.058)	9.534×10^{-6} (2.533×10^{-4})
Al	-	-	-	8.528×10^{-3} (0.382)	6.428×10^{-3} (0.288)	-	-
Si	-	-	-	1.155×10^{-3} (0.054)	-	-	-
Ca	-	-	-	1.351×10^{-3} (0.090)	-	-	-
Cr	1.728×10^{-2} (1.492)	-	-	6.104×10^{-4} (0.053)	-	-	-
Fe	6.073×10^{-2} (5.632)	8.465×10^{-2} (7.85)	-	2.242×10^{-3} (0.208)	-	-	-
Ni	7.447×10^{-3} (0.726)	-	-	2.631×10^{-4} (0.026)	-	-	-
Pb	-	-	3.296×10^{-2} (11.34)	-	-	-	-

(1) Neutron shield material densities include an assumed 10% hydrogen loss and a 50% reduction in boron. Neutron shield material densities include the stainless steel and aluminum stiffeners present in the neutron shield annulus.

Table 5.3-1

Summary of NUHOMS®-MP187 Cask Shielding Material Densities

(atoms/b·cm, g/cc)

(concluded)

Element	FO Top Nozzle	FC Top Nozzle	FO Active Fuel	FC Active Fuel	Bottom Nozzle
B	-	-	8.137×10^{-4} (1.461×10^{-2})	8.137×10^{-4} (1.461×10^{-2})	-
C	-	-	2.033×10^{-4} (4.055×10^{-3})	2.033×10^{-4} (4.055×10^{-3})	-
O	-	-	9.992×10^{-3} (2.655×10^{-1})	9.992×10^{-3} (2.655×10^{-1})	-
Al	-	-	8.656×10^{-4} (3.878×10^{-2})	8.656×10^{-4} (3.878×10^{-2})	-
Cr	1.412×10^{-3} (1.219×10^{-1})	1.344×10^{-3} (1.161×10^{-1})	8.658×10^{-4} (7.476×10^{-2})	1.094×10^{-3} (9.449×10^{-2})	2.244×10^{-3} (1.937×10^{-1})
Fe	4.731×10^{-3} (4.387×10^{-1})	4.552×10^{-3} (4.221×10^{-1})	2.923×10^{-3} (2.711×10^{-1})	3.347×10^{-3} (3.104×10^{-1})	7.345×10^{-3} (6.812×10^{-1})
Ni	7.873×10^{-4} (7.676×10^{-2})	7.138×10^{-4} (6.959×10^{-2})	4.648×10^{-4} (4.532×10^{-2})	8.504×10^{-4} (8.290×10^{-2})	1.379×10^{-3} (1.344×10^{-1})
Zr	2.489×10^{-3} (3.770×10^{-1})	1.869×10^{-3} (2.831×10^{-1})	3.255×10^{-3} (4.931×10^{-1})	3.255×10^{-3} (4.931×10^{-1})	-
^{235}U	-	-	3.795×10^{-5} (1.481×10^{-2})	3.795×10^{-5} (1.481×10^{-2})	-
^{238}U	-	-	4.921×10^{-3} (1.945×10^{-0})	4.921×10^{-3} (1.945×10^{-0})	
^{239}Pu	-	-	3.731×10^{-5} (1.481×10^{-2})	3.731×10^{-5} (1.481×10^{-2})	-

5.4 Shielding Evaluation

The neutron and gamma-ray dose rates for the package are estimated using the DORT-PC computer code [5.9]. The DORT-PC input parameters and results are discussed in the following sections.

5.4.1 DORT-PC Input Parameters

5.4.1.1 The DORT-PC Computer Code

DORT-PC determines the fluence of particles throughout one-dimensional or two-dimensional geometric systems by solving the Boltzmann transport equation using either the method of discrete ordinates or a diffusion theory approximation. Particles can be generated by either particle interaction with the transport medium or extraneous sources incident upon the system. Anisotropic cross-sections can be expressed in a Legendre expansion of arbitrary order. DORT-PC is an industry standard code distributed by ORNL/RSIC.

The DORT-PC code implements the discrete ordinates method as its primary mode of operation. Balance equations are solved for the flow of particles moving in a set of discrete directions in each cell of a space mesh and in each group of a multigroup energy structure. Iterations are performed until all implicitness in the coupling of cells, directions, groups, and source regeneration has been resolved.

DORT-PC was chosen for this application because of its ability to solve two dimensional, cylindrical, deep penetration, radiation transport problems. The package has thick multilayered shields which are difficult to analyze with point-kernel codes. The cask geometry is too complicated to be treated adequately with a one-dimensional discrete ordinates code.

5.4.1.2 Source Distribution

Four DORT-PC runs were made for each case, normal operating and hypothetical accident, to account for the contributions from the three different source regions and for neutron and gamma sources. In the first two runs, the gamma and neutron sources were placed throughout the active fuel region of the DORT-PC model. The remaining runs accounted for the gamma contributions from the top nozzle and bottom nozzle regions. The results of these four runs were then summed to determine the total neutron and gamma-ray dose rates around the package.

Figure 5.4-1 shows the arrangement of the Type I and Type II assemblies in an FO-DSC or FC-DSC. Type I assemblies are placed only in the interior four fuel cells and are radially shielded by the remaining 20 Type II assemblies. The Type II source, therefore, will dominate the cask surface dose rates. The DORT-PC models described in this calculation use cylindrical source regions with volumetric Type II assembly sources from Table 5.2-7 (FO gamma), Table 5.2-13 (FC gamma), and Table 5.2-19 (neutron). Volumetric sources are calculated by multiplying the assembly sources by 24 (assemblies) and dividing by the regional volumes. The volume of the active fuel region assumed in this analysis is 5,633,674 cm^3, the volume of the top nozzle region is 817,439 cm^3 (FC) and the volume of the bottom nozzle region is 332,736 cm^3.

In order to conservatively account for the effect of the four Type I assemblies on the cask dose rates, including streaming effects, two 3-D MCNP [5.7] models of the DSC were generated. MCNP is a multi-purpose neutron, photon, and electron monte-carlo transport code. Each model includes a 1/8 symmetric (on the x, y, and z-axes), pin-by-pin representation of the fuel assemblies in the basket including the cladding, fuel, and guide sleeves as shown in Figure 5.4-1. The first model calculates the dose rate on the DSC surface as a function of angle assuming all 24 fuel cells contain a Type II fuel assembly. The second model includes the Type I assemblies in the four innermost fuel cells. The MCNP input files are provided in Appendix 5.5.3.

The purpose of the MCNP models is to calculate a conservative factor by which the dose rates calculated using only the Type II assembly sources can be multiplied to account for the presence of the Type I assemblies. As shown in Figure 5.4-1, dose rate ratios from the two MCNP models are calculated for both neutrons and gammas in 10° increments along the DSC surface. The maximum ratio is 1.029, calculated for neutrons in the 40°-50° segment. All dose rates, neutron and gamma, calculated by the DORT-PC models are then multiplied by 1.03 to bound any source/streaming from the Type I assemblies.

Dose rates are calculated on the DSC surface instead of the cask surface to improve the statistics of the monte-carlo simulation. This is expected to produce a conservative result since scattering in the cask layers will tend to "smooth" the dose rate ratios. The resulting DORT-PC dose rate calculations will be conservative because the worst case ratio (as a function of angle) is applied over the entire DSC/cask. An additional conservatism is introduced by using a single bounding factor for both neutron and gamma dose rate calculations. This represents a 2% conservatism in the gamma dose rate calculations. Although this method will slightly underpredict the cask top and bottom dose rates, the dose rates at these locations are well below the limits for transportation (see Table 5.1-1).

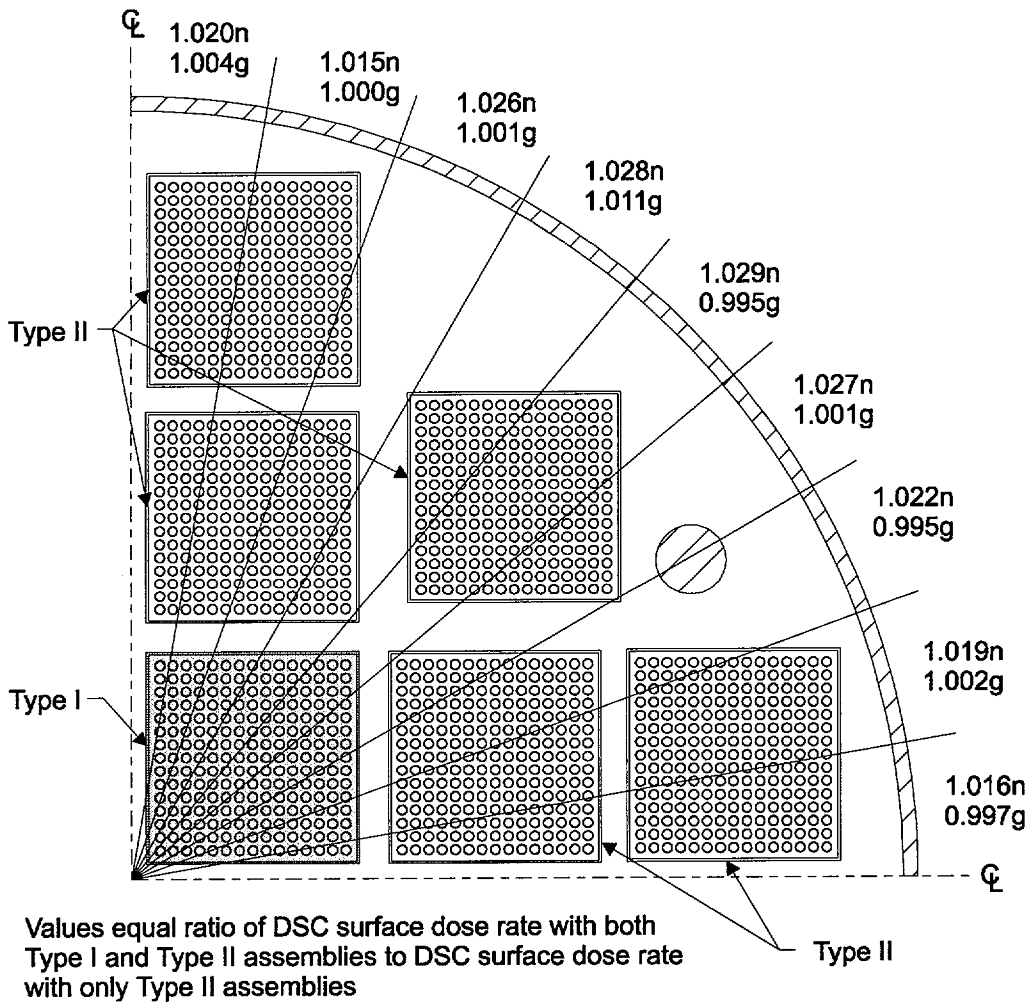

Figure 5.4-1

DSC Dose Rate Ratios as a Function of Angle

The Watt ^{235}U fission spectrum [5.10] is input into the 1* array of the DORT-PC input file to account for subcritical multiplication, increasing the neutron source in the active fuel region. Axial peaking is accounted for in the active fuel region by inputting a relative flux factor at each node in the 97* array. As discussed in Section 5.2.1.3, the flux factor data is taken from Figure 4-4 of Reference [5.14] for PWR fuel. The appropriate flux factor for the design basis case is 1.12 for gamma-rays, assumed to vary linearly with fuel burnup. The flux factors for neutrons have been raised to the fourth power to account for the variation of neutron sources with fuel burnup. Differences between PWR fuel designs, including the locations of the grid spacers and associated hardware, is accounted for by applying the maximum peaking factor of 1.12 across the entire middle section of the active fuel region. The flux factor data used in this analysis is shown in Table 5.4-1. Note that because the length-averaged flux factor shown in Table 5.4-1 is greater than 1.0, the total source present in the in-core region is greater than that discussed in Section 5.2.

Table 5.4-1

PWR Fuel Assembly Axial Flux Distribution

Midpoint of Fuel Segment (in)	Average Gamma Factor in Fuel Segment[1]	Average Neutron Factor in Segment	Product of Segment Length and γ Flux Factor (in)
0.43	0.50	0.06	0.22
1.15	0.54	0.09	0.39
2.40	0.60	0.13	0.75
4.00	0.65	0.18	1.04
5.10	0.68	0.21	0.75
6.10	0.70	0.24	0.70
6.75	0.74	0.30	0.48
7.87	0.79	0.39	0.89
9.50	0.84	0.50	1.37
10.62	0.88	0.60	0.99
11.32	0.90	0.66	0.63
12.94	0.94	0.78	1.53
15.00	0.96	0.85	1.97
16.55	0.98	0.92	1.52
18.92	1.01	1.04	2.40
21.00	1.03	1.13	2.14
23.15	1.05	1.22	2.26
25.02	1.06	1.26	1.99
26.12	1.07	1.31	1.18
27.50	1.10	1.46	1.51
29.37	1.11	1.52	2.08
71.79	1.12	1.57	91.94
114.15	1.11	1.52	2.91
115.00	1.10	1.46	0.94
117.75	1.08	1.36	2.97
120.37	1.05	1.22	2.76
121.50	1.03	1.13	1.16
124.75	0.99	0.96	3.22
128.00	0.94	0.78	3.06
130.20	0.90	0.66	1.98
132.82	0.82	0.45	2.15
134.50	0.76	0.33	1.27
135.80	0.72	0.27	0.94
137.09	0.65	0.18	0.84
138.80	0.60	0.13	1.02
140.50	0.58	0.11	0.99
141.26	0.56	0.10	0.43
141.60	0.55	0.09	0.18
	Total ➔		145.58

(1) The length-average flux factor for gammas is (145.58/141.80)=1.027.

5.4.1.3 Model Geometry

The package geometry shown in Figure 5.3-2 through Figure 5.3-5 is used in the DORT-PC computer models. The package is modeled in cylindrical (R-Z) coordinates and one model is used for both radial and axial dose rates. A total of 46 zones are defined by a mesh of 86 intervals in the radial direction and 193 intervals in the axial direction. A reflective boundary condition is placed on the central axis of the cask (left boundary). The boundary conditions on the remaining boundaries are voids.

A total of twelve DORT-PC runs were made to calculate the normal operation (for both FO-DSCs and FC-DSCs) and hypothetical accident (for FC-DSCs only) dose rates around the package. The first two runs for each case include the in-core region gamma and neutron sources, respectively. The third run for each case includes only the top nozzle source. The final run includes only the bottom nozzle source. Each run includes the full cask geometry. The normal operation case materials are as shown in Figure 5.3-6 and the hypothetical accident case materials are as shown in Figure 5.3-7.

5.4.1.4 Cross Section Data

The cross section data used in this analysis is taken from the CASK-81 22 neutron, 18 gamma-ray energy group, coupled cross-section library [5.4]. CASK-81 is an industry standard cross section library compiled for the purpose of performing calculations of spent fuel shipping casks and is distributed by ORNL/RSIC. The cross section data allows coupled neutron/gamma-ray runs to be made that account for secondary gamma radiation (n,γ).

Microscopic P_3 cross sections were taken from the CASK-81 library and mixed using the GIP-PC computer program distributed with DORT-PC [5.9] to provide macroscopic cross sections for the materials in the cask model. The GIP input file is reproduced in Section 5.5.4. The material compositions used in the GIP input file are listed in Table 5.3-1.

An additional element and material, "fluxdosium," is included in the cross section data and mixing table in the GIP input file. Fluxdosium is used to provide flux-to-dose rate conversion factors as described below for use in activity calculations. The presence of fluxdosium in the cross-section data does not impact the actual flux calculations.

5.4.1.5 Flux-to-Dose Rate Conversion Factors

The flux distribution calculated by the DORT-PC code is converted to dose rates using the flux-to-dose rate conversion factors provided in ANSI/ANS-6.1.1-1977 [5.11]. The gamma-ray and neutron flux-to-dose rate conversion factors for the CASK–81 energy groups are shown in Table 5.4-2 and Table 5.4-3 respectively.

The dose rate at each node in the DORT-PC model is calculated using the activity calculation feature of DORT-PC. The "cross section" data for one material in the input file contains only flux-to-dose rate conversion factors. This material, "fluxdosium," is then specified for activity calculations which determines the gamma and neutron dose rate at each node.

Table 5.4-2

Gamma-Ray Flux-to-Dose Rate Factors

Energy Group	E_{Lower} (MeV)	E_{Upper} (MeV)	Flux-to Dose Factor (mRem/hr)/(g/s/cm^2)
23	8.00e+00	1.00e+01	8.7716
24	6.50e+00	8.00e+00	7.4785
25	5.00e+00	6.50e+00	6.3748
26	4.00e+00	5.00e+00	5.4136
27	3.00e+00	4.00e+00	4.6221
28	2.50e+00	3.00e+00	3.9596
29	2.00e+00	2.50e+00	3.4686
30	1.66e+00	2.00e+00	3.0192
31	1.33e+00	1.66e+00	2.6276
32	1.00e+00	1.33e+00	2.2051
33	8.00e-01	1.00e+00	1.8326
34	6.00e-01	8.00e-01	1.5228
35	4.00e-01	6.00e-01	1.1725
36	3.00e-01	4.00e-01	0.87594
37	2.00e-01	3.00e-01	0.63061
38	1.00e-01	2.00e-01	0.38338
39	5.00e-02	1.00e-01	0.26693
40	1.00e-02	5.00e-02	0.93477

Table 5.4-3

Neutron Flux-to-Dose Rate Factors

Energy Group	E_{Lower} (MeV)	E_{Upper} (MeV)	Flux-to Dose Factor (mRem/hr)/(n/s/cm^2)
1	12.2e+01	1.49e+01	194.49
2	1.00e+01	1.22e+01	159.71
3	8.18e+00	1.00e+01	147.06
4	6.36e+00	8.18e+00	147.73
5	4.96e+00	6.36e+00	153.39
6	4.06e+00	4.96e+00	150.62
7	3.01e+00	4.06e+00	138.92
8	2.46e+00	3.01e+00	128.43
9	2.35e+00	2.46e+00	125.27
10	1.83e+00	2.35e+00	126.32
11	1.11e+00	1.83e+00	128.94
12	5.50e-01	1.11e+00	116.85
13	1.11e-01	5.50e-01	65.209
14	3.35e-03	1.11e-01	9.1878
15	5.83e-04	3.35e-03	3.7134
16	1.01e-04	5.83e-04	4.0086
17	2.90e-05	1.01e-04	4.2946
18	1.07e-05	2.90e-05	4.4761
19	3.06e-06	1.01e-05	4.5673
20	1.12e-06	3.06e-06	4.5355
21	4.14e-07	1.12e-06	4.3701
22	1.00e-08	4.14e-07	3.7142

5.4.1.6 Quadrature Data

The DORT-PC runs use a 402 direction radially biased set based on the half-symmetric S_{10} set and the 210 direction upward biased set discussed in Reference 5.12. In two-dimensional systems such as that which is used to describe the package, the discrete ordinates method can lead to solutions with flux distortions. This is particularly true in poorly scattering media (such as air and the impact limiter materials) that contain isolated sources. Because the cask structural shell directly adjacent to the top and bottom end fittings exhibits localized high dose rates, flux oscillations could be observed at the one and two meter distances required for this evaluation. The potential for flux oscillations is reduced by using a more detailed, radially biased quadrature set in the top and bottom nozzle source runs. The quadrature data is provided in the DORT-PC input files listed in Section 5.5.4.

5.4.1.7 DORT-PC Input Files

The DORT-PC input files are included in Section 5.5.4. The DORT-PC input parameters are discussed in the preceding sections for the twelve normal operation and hypothetical accident runs. DORT-PC is run using the quadrature sets described above and a P_3 order of scattering.

5.4.1.8 Evaluation of Cask Penetrations

Several penetrations exist through the NUHOMS®-MP187 Cask shielding. These include the upper and lower trunnions, the shear key, the test ports, and the drain and vent ports. An evaluation of the impact of these penetrations on the shielding effectiveness of the cask is provided in this section.

5.4.1.8.1 Upper Trunnions

The NUHOMS®-MP187 cask upper trunnion sleeve extends through the neutron shield and partially into the lead gamma shield as shown in Figure 5.4-2. The trunnion sleeve contains a plug during transportation that provides gamma and neutron shielding. The effect of the trunnion on the cask shielding analysis is assessed as described below.

The computer program ANISN-ORNL [5.13] is used to calculate the dose rate on the surface of the cask neutron shield panel in the center of the in-core region. ANISN is run using the same cross-section and flux-to-dose data as was used in the DORT-PC runs. The ANISN results are used as a "base case" for the evaluations and to provide information regarding the angular distribution of the neutrons and gamma-rays as they exit the cask surface.

Two additional ANISN-ORNL runs are made to estimate the dose rates on the face of the trunnion. The geometries used in these runs are shown in Figure 5.4-2. Models have been generated for both the trunnion sleeve and the trunnion plug. Although the skid is present during all normal operating transport conditions, no credit has been taken for shielding of the trunnions by the skid. Table 5.4-4 summarizes the results of the ANISN runs.

Table 5.4-4

ANISN Results for Trunnion Models

Case	Neutron (mrem/hr)	Gamma (mrem/hr)
Base	18.32	24.24
Sleeve	95.20	3.406
Plug	15.42	11.31

The dose rates on the surface of the trunnion are calculated for both the FC-DSC and FO-DSC in the following manner: (1) The neutron and gamma dose rates on the cask surface at each interval are taken from the DORT results; (2) These dose rates are scaled by the ratio of the ANISN results (see Table 5.4-4) for the case evaluated to the results from the base case; (3) The neutron and gamma dose rates are summed to calculate the total surface dose rate; and (4) Manual calculations are performed as described below to calculate dose rates on the transport vehicle outer surface and 2 meters from that surface. Because the surface dose rate is calculated at each interval in the trunnion region, axial variations in both source and geometry have been considered.

Table 5.4-5 shows the neutron and gamma dose rates calculated at the surface of the trunnions for the FC-DSC payload. The "interval" and "midpoint" refer to the axial location of the interval in the DORT model of the cask. For both neutrons and gammas, the DORT calculated dose rate on the package surface is listed. The sleeve and plug dose rates are calculated by multiplying the

DORT dose by the result from the appropriate ANISN run (Table 5.4-4) and dividing by the base case dose. The maximum surface dose rate on the trunnion is 160.2 mrem/hr at interval 128. Similar results for the FO-DSC are shown in Table 5.4-6 (FO-DSC peak is 237.1 mrem/hr).

Table 5.4-5

FC-DSC Trunnion Surface Dose Rates

	Midpoint	Neutron (mrem/hr)			Gamma (mrem/hr)		
Interval	(cm)	DORT	Sleeve	Plug	DORT	Sleeve	Plug
117	381.96	16.820	87.383		13.442	1.889	
118	387.03	15.982	83.031		12.585	1.769	
119	393.70	15.155	78.732	12.754	11.807	1.659	5.508
120	398.47	14.769	76.729	12.430	11.281	1.585	5.263
121	401.96	14.666	76.194	12.343	10.731	1.508	5.006
122	405.45	14.784	76.807	12.442	10.162	1.428	4.741
123	409.58	15.075	78.318	12.687	9.556	1.343	4.458
124	413.71	15.614	81.119	13.141	9.098	1.279	4.245
125	416.16	16.185	84.084	13.621	8.696	1.222	4.057
126	418.06	17.338	90.074	14.591	8.294	1.166	3.869
127	420.69	20.889	108.524		7.465	1.049	
128	423.86	30.688	159.434		5.790	0.814	

Table 5.4-6

FO-DSC Trunnion Surface Dose Rates

	Midpoint	Neutron (mrem/hr)			Gamma (mrem/hr)		
Interval	(cm)	DORT	Sleeve	Plug	DORT	Sleeve	Plug
116	380.69	20.026	104.039		6.317	0.888	
117	388.94	18.829	97.820		5.907	0.830	
118	394.53	18.003	93.531	15.151	5.534	0.778	2.582
119	401.20	17.510	90.971	14.737	5.254	0.738	2.451
120	405.45	17.494	90.886	14.723	5.146	0.723	2.401
121	408.75	17.656	91.725	14.859	5.043	0.709	2.353
122	412.05	17.914	93.070	15.077	4.965	0.698	2.316
123	416.37	19.502	101.319	16.413	4.788	0.673	2.234
124	420.69	24.111	125.261		4.449	0.625	
125	422.64	29.001	150.666		4.118	0.579	
126	423.50	32.775	170.273		3.776	0.531	
127	424.37	38.613	200.606		3.387	0.476	
128	425.09	45.555	236.671		3.002	0.422	

To calculate the contributions from the trunnions to the vehicle surface and 2 meter dose rates, cosine power functions, $Cos^n(\theta)$, are fit to the neutron and gamma ray angular data. As shown in Figure 5.4-3, the neutron angular flux distribution can be approximated by a $Cos(\theta)$ function and the gamma-ray angular flux distribution can be approximated by a $Cos^6(\theta)$ function. Note that the $Cos(\theta)$ fit for the neutron distribution is more sharply peaked than the data. This will result in a conservative estimate of the neutron dose rate two meters from the vehicle surface.

The neutron and gamma surface "delta dose" (the difference between the DORT calculated dose and the trunnion sleeve/plug dose at a radius of 46.25 in) is calculated for each trunnion interval. Negative delta doses result from DORT model results which exceed those of the trunnion sleeves and plugs. A point kernel approximation is used to calculate the delta dose at the vehicle surface and 2 meters from the vehicle surface. For a $Cos(\theta)$ angular distribution, the dose rate at a distance R from a source point is given by,

$$S = \frac{S_O \cdot Cos(\theta) \cdot A}{\pi R^2}$$

Where S_O is the surface delta dose, θ is the angle to the detector relative to the surface normal, and A is the area assigned to the source point. The corresponding equation for a $Cos^6(\theta)$ distribution is,

$$S = \frac{7S_O \cdot Cos^6(\theta) \cdot A}{2\pi R^2}$$

The trunnion sleeves are divided into rectangular regions corresponding to the DORT intervals as shown in Figure 5.4-4, which also shows the location of the trunnions relative to the active fuel region. The height of each region is equal to the difference in height between the sleeve radius (10 inches) and the plug radius (6 inches) at the midpoint of the interval. The contribution from each rectangular region to each trunnion interval (as reported in Table 5.4-5 and Table 5.4-6 for the FC-DSC and FO-DSC, respectively) at the vehicle surface and at a distance of 2 meters from the vehicle surface is calculated using the above equations and summed. Note that because the plug surface doses are less than those on the surface of the neutron shield, the plugs have been neglected from this calculation.

For each trunnion interval in the FC-DSC model, Table 5.4-7 shows the calculated vehicle surface dose rates, the delta dose due to the presence of the trunnions, and the total dose rate including both the DORT results and the trunnion contribution. Corresponding results for the 2-meter dose rates are provided in Table 5.4-8. The package surface, vehicle surface, and 2-meter dose rates, including the trunnion contributions, are included in the results presented in Section 5.4.2.

Table 5.4-7

Trunnion Dose Calculations on the Vehicle Surface

FC-DSC Results:

Interval	Midpoint (cm)	Neutron (mrem/hr) DORT	Neutron Trunnion Δ	Neutron Total	Gamma (mrem/hr) DORT	Gamma Trunnion Δ	Gamma Total
117	381.96	17.237	9.779	27.016	7.528	-2.893	4.635
118	387.03	17.455	10.625	28.080	7.233	-3.226	4.007
119	393.70	18.524	11.461	29.985	6.770	-3.338	3.432
120	398.47	19.685	11.840	31.525	6.360	-3.232	3.128
121	401.96	19.994	11.997	31.991	6.050	-3.099	2.951
122	405.45	20.159	12.052	32.211	5.865	-2.942	2.923
123	409.58	20.289	11.980	32.269	5.637	-2.743	2.894
124	413.71	20.648	11.754	32.402	5.326	-2.527	2.799
125	416.16	20.324	11.545	31.869	4.939	-2.388	2.551
126	418.06	20.504	11.344	31.848	4.677	-2.273	2.404
127	420.69	20.590	11.013	31.603	4.499	-2.103	2.396
128	423.86	19.374	10.535	29.909	4.295	-1.879	2.416

FO-DSC Results:

Interval	Midpoint (cm)	Neutron (mrem/hr) DORT	Neutron Trunnion Δ	Neutron Total	Gamma (mrem/hr) DORT	Gamma Trunnion Δ	Gamma Total
116	380.69	18.418	12.379	30.797	3.566	-1.620	1.946
117	388.94	19.406	13.757	33.163	3.450	-1.767	1.683
118	394.53	20.832	14.327	35.159	3.319	-1.723	1.596
119	401.20	21.885	14.625	36.510	3.092	-1.598	1.494
120	405.45	21.619	14.604	36.223	2.963	-1.510	1.453
121	408.75	22.189	14.473	36.662	2.988	-1.441	1.547
122	412.05	22.822	14.237	37.059	2.941	-1.369	1.572
123	416.37	22.377	13.765	36.142	2.673	-1.262	1.411
124	420.69	22.581	13.105	35.686	2.457	-1.131	1.326
125	422.64	21.824	12.750	34.574	2.405	-1.064	1.341
126	423.50	21.115	12.583	33.698	2.368	-1.033	1.335
127	424.37	20.897	12.407	33.304	2.328	-1.001	1.327
128	425.09	19.788	12.257	32.045	2.257	-0.973	1.284

Table 5.4-8

Trunnion Dose Calculations 2 Meters from the Vehicle Surface

FC-DSC Results:

Interval	Midpoint (cm)	Neutron (mrem/hr) DORT	Neutron Trunnion Δ	Neutron Total	Gamma (mrem/hr) DORT	Gamma Trunnion Δ	Gamma Total
117	381.96	4.867	0.476	5.343	2.299	-0.198	2.101
118	387.03	4.939	0.478	5.417	2.235	-0.200	2.035
119	393.70	5.051	0.480	5.531	2.159	-0.201	1.958
120	398.47	5.095	0.481	5.576	2.109	-0.202	1.907
121	401.96	5.023	0.482	5.505	2.082	-0.202	1.880
122	405.45	4.877	0.482	5.359	2.065	-0.201	1.864
123	409.58	4.741	0.482	5.223	2.038	-0.200	1.838
124	413.71	4.678	0.481	5.159	2.005	-0.199	1.806
125	416.16	4.664	0.480	5.144	1.982	-0.198	1.784
126	418.06	4.632	0.480	5.112	1.962	-0.197	1.765
127	420.69	4.542	0.477	5.019	1.932	-0.196	1.736
128	423.86	4.441	0.477	4.918	1.899	-0.194	1.705

FO-DSC Results:

Interval	Midpoint (cm)	Neutron (mrem/hr) DORT	Neutron Trunnion Δ	Neutron Total	Gamma (mrem/hr) DORT	Gamma Trunnion Δ	Gamma Total
116	380.69	4.921	0.588	5.509	1.060	-0.106	0.954
117	388.94	5.064	0.592	5.656	1.020	-0.107	0.913
118	394.53	5.148	0.594	5.742	0.993	-0.108	0.885
119	401.20	5.085	0.595	5.680	0.973	-0.108	0.865
120	405.45	4.916	0.595	5.511	0.966	-0.108	0.858
121	408.75	4.804	0.595	5.399	0.960	-0.107	0.853
122	412.05	4.761	0.594	5.355	0.955	-0.107	0.848
123	416.37	4.681	0.592	5.273	0.939	-0.106	0.833
124	420.69	4.543	0.590	5.133	0.917	-0.105	0.812
125	422.64	4.469	0.589	5.058	0.905	-0.104	0.801
126	423.50	4.448	0.589	5.037	0.899	-0.104	0.795
127	424.37	4.431	0.588	5.019	0.894	-0.104	0.790
128	425.09	4.410	0.588	4.998	0.891	-0.103	0.788

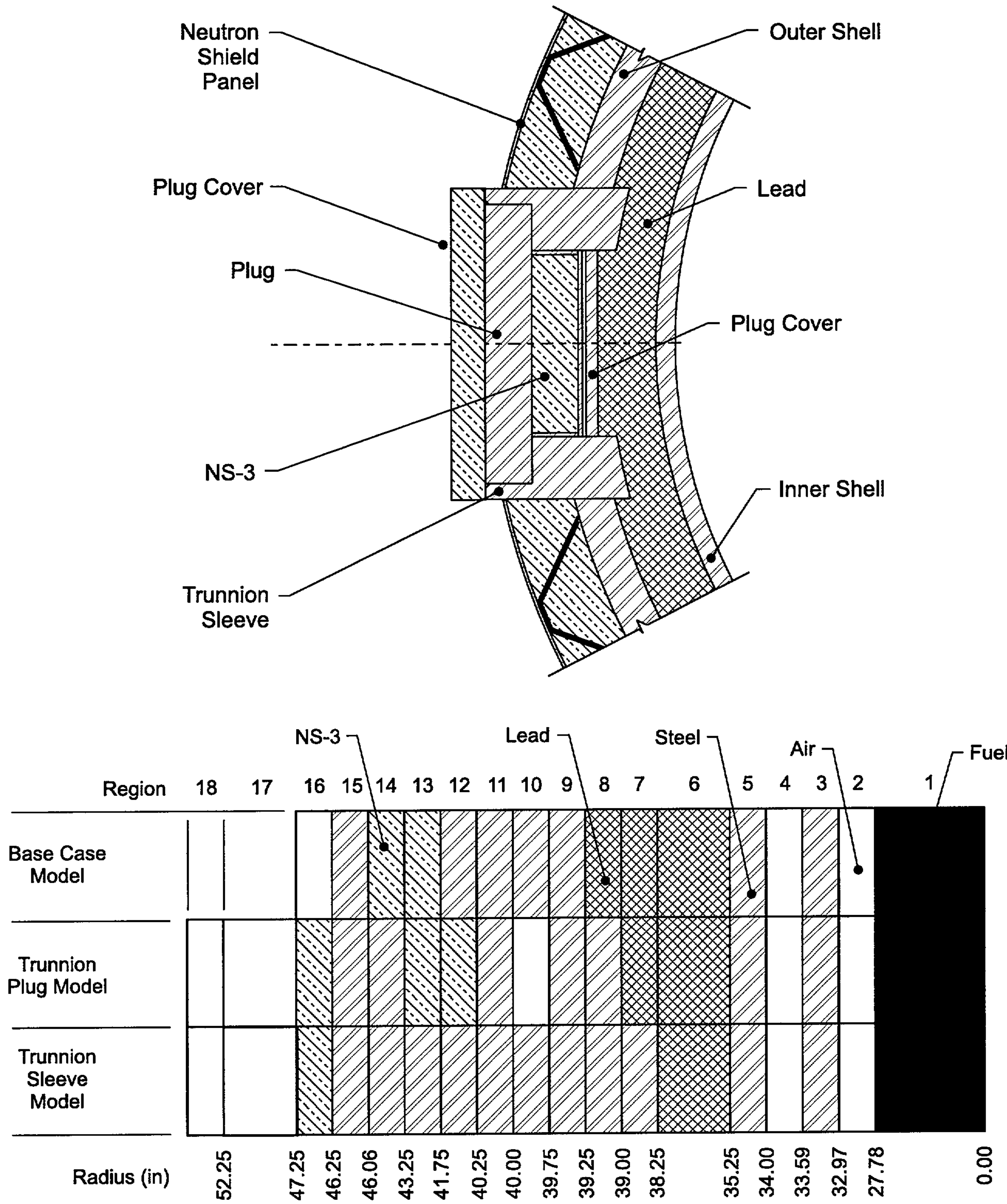

Figure 5.4-2

NUHOMS®-MP187 Cask Upper Trunnion Geometry

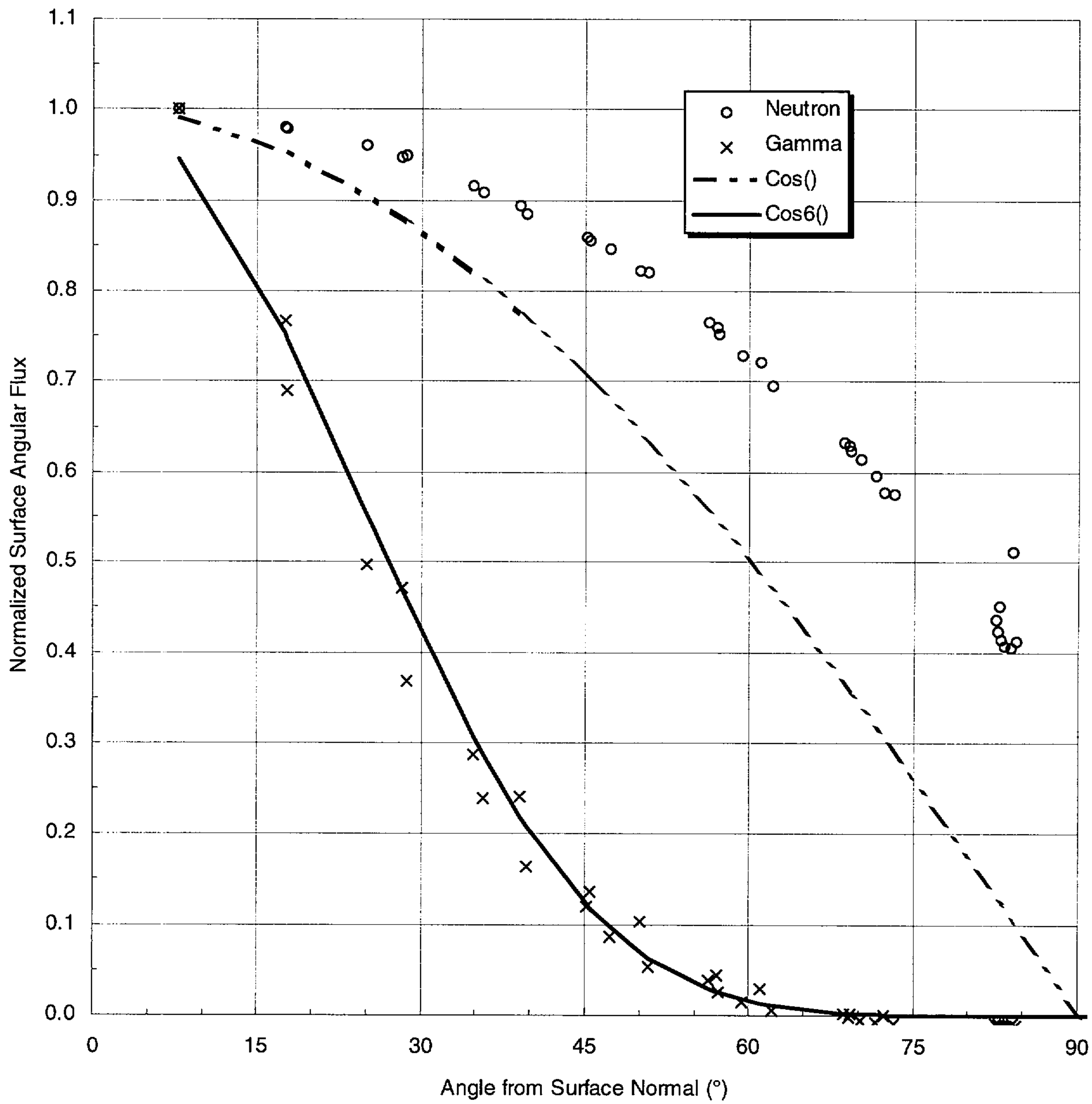

Figure 5.4-3

Neutron and Gamma-Ray Angular Distributions on the Cask Surface

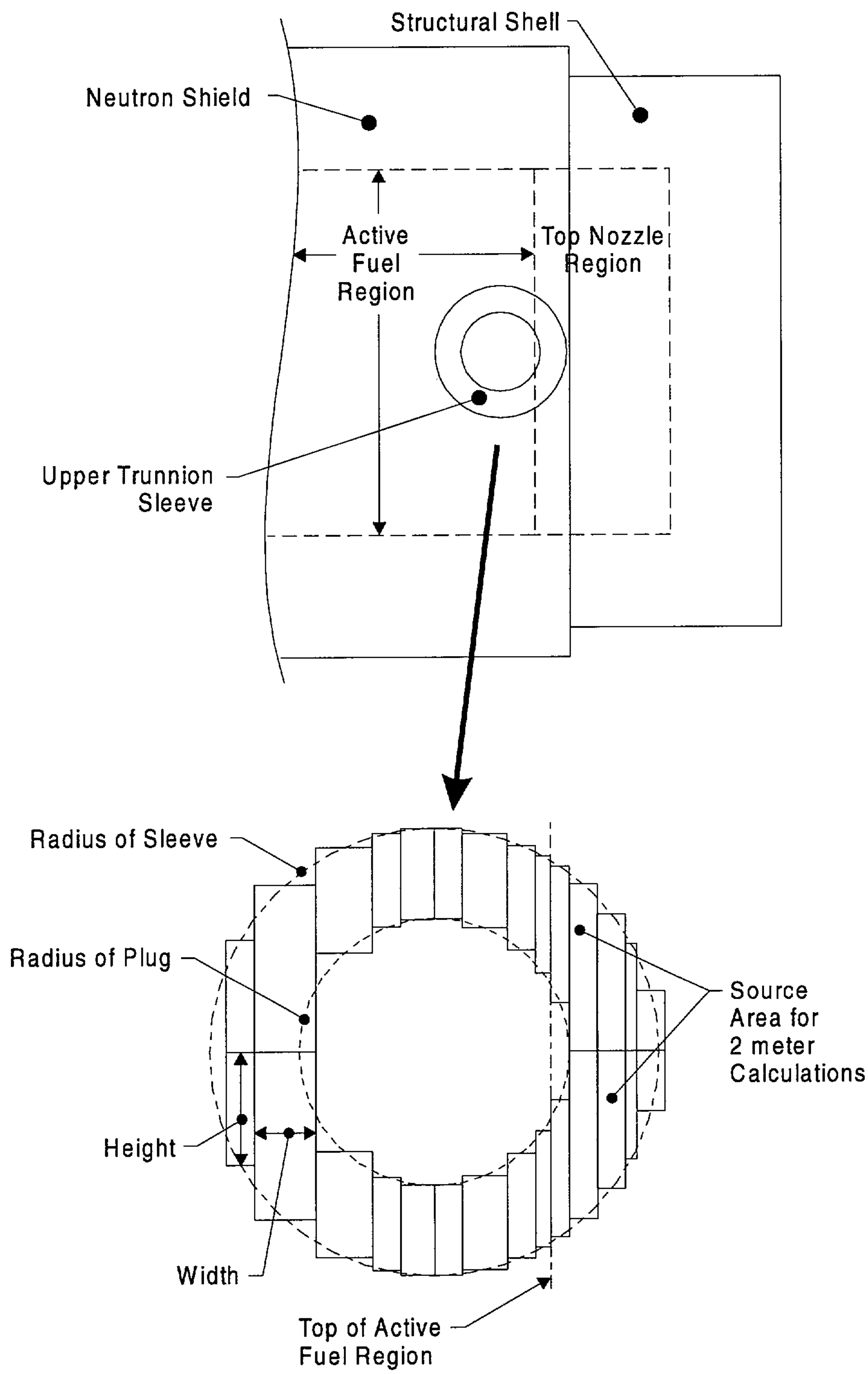

Figure 5.4-4

Source Geometry Used in Trunnion Manual Dose Calculations

5.4.1.8.2 Lower Trunnions

The lower trunnions are located below the cask neutron shield and displace only the impact limiter honeycomb. Because the lower trunnions provide shielding superior to that of the honeycomb, the lower trunnions serve to reduce the package dose rates.

5.4.1.8.3 Shear Key

The cask shear key opening extends through the cask neutron shield. The shear key opening is underneath the cask during transportation and is shielded by the shear key itself, the cask support skid, and the railcar. Although the dose rate on the underside of the vehicle is expected to be well below the applicable limits, an analysis similar to that performed for the upper trunnions is provided below to demonstrate compliance with the 200 mrem/hr limit of 10CFR71.47(b)(2).

The ANISN-ORNL [5.13] code is used to estimate the dose rates in the vicinity of the shear key. The models and assumptions are similar to those described in Section 5.4.1.8.1. The geometry in the region of the shear key, including the cask, skid, and shear key is shown in Figure 5.4-5. The base case model from Section 5.4.1.8.1 is used for comparison to the cask dose rates calculated in the DORT runs described in Section 5.4.1. Three additional ANISN runs, using the geometries shown in Figure 5.4-5, are used to estimate one-dimensional dose rates through the 1.5 inch thick plate, through the shear key sleeve, and through the shear key itself.

The ANISN models assume that the skid is directly adjacent to the neutron shield panels. The skid is composed of two plates, 1.5 inches thick, assembled as shown in Figure 5.4-5 with a total box thickness of 18 inches. The shear key fills the cask shear key opening with the exception of a 0.25 inch thick gap at the top. The shear key is located with its centerline 100.75 inches from the cask bottom and its axial thickness is six inches. No credit is taken for the railcar deck or structures.

The dose rates at the bottom of the skid in the vicinity of the shear key are calculated for each of the three models in the following manner: (1) The maximum neutron and gamma dose rates on the cask surface at the axial location of the shear key are taken from the DORT results; (2) These dose rates are scaled by the ratio of the ANISN results for the case evaluated to those from the base case; and (3) The neutron and gamma dose rates are summed to calculate the total dose rate. This calculation, therefore, accounts for axial variations in both source and geometry.

The results of the shear key analysis are shown in Table 5.4-9. The peak calculated dose rate, due to streaming through the shear key sleeve, is 190.3 mrem/hr, about 5% less than the limit of 200 mrem/hr. Note that there are several significant conservatisms in this calculation. The ANISN models are one-dimensional, assuming that the modeled geometry exists over 360° of the cask surface. The shear key sleeve is actually only three inches wide and as shown in Table 5.4-9, the dose rates on either side of the sleeve are only about 20 mrem/hr. The railcar is completely neglected in this calculation and the space between the cask and the skid has been ignored.

Table 5.4-9

Shear Key Dose Rate Results

	DORT Result (D) (mrem/hr)		Base Case (B) (mrem/hr)		ANISN Result (A) (mrem/hr)		Total (D*A/B) (mrem/hr)
Location	Neutron	Gamma	Neutron	Gamma	Neutron	Gamma	
Plate	28.85	18.26	18.32	24.24	13.46	0.58	21.63
Sleeve	28.85	18.26	18.32	24.24	120.6	0.51	190.3
Shear Key	28.85	18.26	18.32	24.24	10.48	0.058	16.55

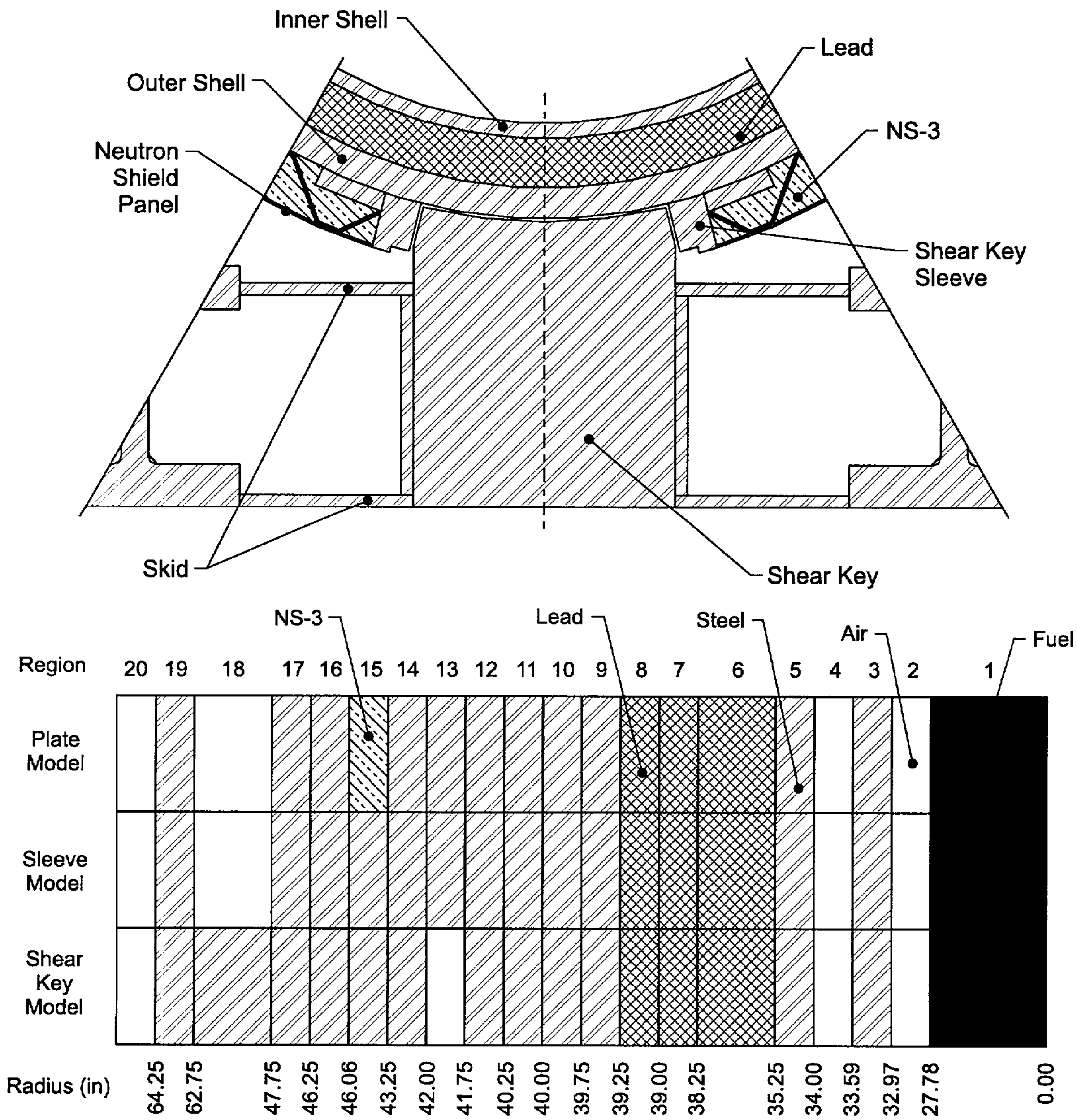

Figure 5.4-5

NUHOMS®-MP187 Cask Shear Key Geometry and ANISN Models

5.4.1.8.4 Cask Test and Drain/Vent Ports

The cask test, drain, and vent ports extend through the steel top and bottom covers and bottom forging. Because these ports are shielded by steel plugs that effectively fill the ports during shipment, no further analysis is required.

5.4.1.8.5 DSC Shield Plug Geometry

The geometry of the FC-DSC shield plug used in the shielding models differs from that shown on the drawings in Chapter 1. The differences include the thickness of the lead shielding, the steel plate thicknesses, and the addition of steel stiffeners in the lead. The FC-DSC DORT models described in Section 5.4.1.3 have been modified as described below to conservatively model these changes to the shield plug in order to demonstrate that the analysis presented in this Chapter remains bounding for the MP187 Package.

A comparison of the modeled geometry versus that shown on the drawings is provided in Table 5.4-10. The total thickness of both shield plugs is identical in the models and on the drawings. The total steel thickness in the bottom shield plug has been reduced from 2.50 inches to 2.25 inches, with a corresponding increase in the lead thickness of 0.25 inches. Similarly, the total steel thickness in the top shield plug has been reduced 0.12 inches with a 0.12 inch increase in the lead thickness. In both cases, however, stiffeners have been provided which extend through the lead shielding. As shown on the drawings, the stiffeners have been angled to eliminate direct shine paths through the plug but still represent a reduction in the effective lead thickness.

The FC-DSC DORT models have been modified to incorporate the thicknesses shown on the drawings. Additionally, a one inch thick portion of the lead shielding has been replaced with steel to account for the presence of the stiffeners (the actual axial thickness of the stiffeners is 0.86 inches) and a steel annulus representing the grappling ring has been included in the bottom shield plug. A sample modified DORT input file is provided in Section 5.5.4. Note that the DORT model conservatively assumes that the reduction in lead thickness occurs over the entire radius of the shield plug. The actual geometry of the stiffeners will limit this reduction to a few localized areas.

Table 5.4-10

FC-DSC Shield Plug Geometry Comparison

Parameter	Modeled Geometry (Section 5.4.1.3)	Drawing Geometry (Chapter 1)
DSC Bottom End		
Outer Cover Thickness	1.75 in	0.75 in
Lead Thickness	3.50 in	3.75 in
Inner Cover Thickness	0.75 in	1.50 in
Stiffeners	not modeled	included
Grapple Ring	not modeled	penetrates lead
DSC Top End		
Plug Bottom Casing	0.75 in	0.50 in
Lead Thickness	4.00 in	4.12 in
Plug Top Casing	0.25 in	0.38 in
Stiffeners	not modeled	included

The dose rates calculated by the modified DORT input files show an increase in the peak gamma dose rates on the cask ends, as is expected due to the reduction in lead shielding. The greatest increase occurs on the cask bottom surface in the grapple ring region. The gamma dose rate at this location increased from 0.64 mrem/hr to 0.75 mrem/hr. However, the peak total (neutron plus gamma) dose rates for the Package side, top, and bottom remain below those calculated using the geometry described in Section 5.4.1.3.

This result is consistent with expectations because: (1) The peak side dose rates are unaffected by changes in the shield plug design provided the total thickness is unchanged; (2) The neutron dose rate, which is the primary contributor to the peak top and bottom dose rates, is reduced by replacing lead with steel; and (3) The peak top and bottom dose rates occur outside the cask body radius and are due primarily to contributions from the cask side which are shielded only by the impact limiters. Because the peak dose rates on all Package surfaces are unchanged, the model described in Section 5.4.1.3 calculates dose rates which bound those for the shield plug design shown on the drawings. The average lead thickness specified on the drawing notes has been selected to correspond to the shielding analysis described in Section 5.4.1.3.

5.4.1.8.6 Shielding Uncertainty Evaluation

The purpose of this calculation is to evaluate the impact of several uncertainties present in the shielding calculations presented in this Chapter. This evaluation demonstrates that the overall impact of these uncertainties will not affect the conclusions of the shielding analysis presented in Section 5.4.2.

As stated in Section 5.3.1, the MP187 shielding calculations are based on nominal cask dimensions. This represents a potential non-conservatism in that shielding thicknesses less than those used in the analysis may exist in fabricated packages while still complying with the tolerances shown on the drawings. The 1-D discrete-ordinates computer code ANISN [5.13] is used to calculate the potential dose rate increase associated with assuming each shielding layer is at its minimum acceptable material thicknesses. This calculation is performed on the cask side surface during normal operations which is the location and configuration associated with the bounding dose rates for the MP187 cask.

There are also several conservatisms in the MP187 shielding calculations which are listed in Section 5.1. These include an overprediction of the quantity of ^{154}Eu present in the fuel assemblies, neglecting the shielding of control components by the fuel assemblies, and neglecting half of the boron in the neutron shield. The value of each of these conservatisms will be quantified by making modifications to the computer runs provided in the Appendices. By summing the effects of these conservatisms and the tolerance calculation, this evaluation shows that the analyses provided in this Chapter fully support the design, including tolerances, of the NUHOMS®-MP187 cask. Additional conservatisms in the shielding models remain and are listed below as well.

This calculation determines correction factors for both neutron and gamma-ray dose rates based on a 1-D radial slice through the cask midplane. These correction factors are assumed to apply to the neutron and gamma, package surface, vehicle surface and two meter, side doses reported in Section 5.4.2. The cask ends are not evaluated because the dose rates at these locations are at least an order of magnitude less than the applicable limit. Because the peak accident dose rates result from gaps in the lead due to drop loads (lead slump), the cask tolerances (particularly the lead tolerance) will not significantly affect the accident dose rates.

(A) Tolerances

The effect of tolerances (i.e. minimum allowed shielding thicknesses) on the MP187 dose rates has been determined by performing a 1-D, radial shielding analysis through the cask neutron shield. This location was selected because the bounding dose rates (those closest to the 10CFR71.47 limits) occur on the cask side and because this cask section includes each of the cask layers. The base ANISN computer model described in Section 5.4.1.8.1 was modified to include the minimum material thicknesses as shown on the drawings provided in Chapter 1.

The modified ANISN computer run, provided in Section 5.5.5, calculates maximum MP187 dose rates based on the minimum dimensions allowed by the drawings. The neutron and gamma dose rates on the surface of the cask calculated by this run are shown in Table 5.4-11, as are the corresponding results from the base run and the fractional dose rate increases due to the minimum shielding dimensions.

Table 5.4-11

Tolerance Evaluation Results

	ANISN Base	ANISN Tolerance	Fractional Change (tol/base)
Neutron	18.32	18.85	1.029
Gamma	24.24	31.94	1.318

As shown below, there is sufficient margin in the FO-DSC calculations to support this potential increase with no additional analysis:

Package Surface: $(0.42\gamma)(1.318) + (236.7n)(1.029) = 244.1$ mrem/hr is less than 1000

Vehicle Surface: $(2.24\gamma)(1.318) + (40.2n)(1.029) = 44.3$ mrem/hr is less than 200

2 Meter: $(1.31\gamma)(1.318) + (6.34n)(1.029) = 8.3$ mrem/hr is less than 10

However, because there is little margin in the existing FC-DSC results, additional evaluations have been performed as described below to demonstrate that existing conservatisms in the calculations fully offset the increase in dose rates related to minimum material thicknesses.

(B) Photon Source Term

As described in Section 5.2, the ORIGEN2 code [5.3] was used to calculate all neutron and gamma source terms for the MP187 shielding analysis. The ORIGEN2 cross section libraries are based primarily on ENDF/B-IV data. More recent cross-section data (ENDF/B-VI) has significantly revised the production rate of ^{154}Eu - an important contributor to the gamma-ray dose rates. Several references have documented this overprediction of the ^{154}Eu inventory. Reference [5.16], Section 5.4 states (TNW clarifications in brackets) , "the percentage difference for isobar 154 (^{154}Sm+^{154}Eu+^{154}Gd) is 30.8% using ENDF/B-V Eu data [similar to the ORIGEN2 data for Eu] and -2.1% using ENDF/B-VI data. This change is due to comparable [relative to a similar change for isobar 155] structural variations [the addition of resonances in ENDF/B-VI that result in greater depletion of Eu during operation]in the ^{154}Eu data in the two libraries."

Reference [5.17], Section 5 states, "These Eu isotopes are important for both spent fuel source terms and burnup credit applications, and major updates were made in the ENDF/B-VI evaluation. The effect of these cross-section changes was enhanced ^{154}Eu capture and, hence, decreases of some 30 to 40% in the ^{154}Eu inventories in the spent fuel." To address the impact of this ^{154}Eu overprediction, an additional 1-D ANISN run was made, using a source term which reduces the contribution due to ^{154}Eu by 30%.

Table 5.4-12 lists the design basis (FO) in-core source term as well as the ^{154}Eu contribution to that source. The ^{154}Eu contribution is taken directly from the fission product photon data in the ORIGEN2 output. Following the methodology described in Section 5.2.1, the design basis control component source is added to the revised FO source and the result is converted to a volumetric source, in the CASK-81 format required by the ANISN model.

Table 5.4-12

Calculation of Corrected Assembly Source Term

ORIGEN Group	Mean Energy (MeV)	In-Core (γ/sec/assy)	^{154}Eu (γ/sec/assy)	30% ^{154}Eu (γ/sec/assy)	Revised In-Core (γ/sec/assy)
1	0.010	8.441E+14	1.227E+13	3.681E+12	8.404E+14
2	0.025	1.703E+14	1.810E+12	5.430E+11	1.697E+14
3	0.038	2.167E+14	1.669E+13	5.007E+12	2.117E+14
4	0.058	1.770E+14	4.478E+12	1.343E+12	1.756E+14
5	0.085	9.495E+13	0.000E+00	0.000E+00	9.495E+13
6	0.125	8.705E+13	2.728E+13	8.184E+12	7.887E+13
7	0.225	7.949E+13	5.637E+12	1.691E+12	7.779E+13
8	0.375	3.371E+13	8.982E+11	2.695E+11	3.344E+13
9	0.575	1.459E+15	0.000E+00	0.000E+00	1.459E+15
10	0.850	4.841E+13	3.191E+13	9.573E+12	3.883E+13
11	1.250	6.239E+13	3.533E+13	1.060E+13	5.179E+13
12	1.750	1.186E+12	1.059E+12	3.177E+11	8.684E+11
13	2.250	3.839E+08	0.000E+00	0.000E+00	3.839E+08
14	2.750	3.094E+08	0.000E+00	0.000E+00	3.094E+08
15	3.500	2.136E+07	0.000E+00	0.000E+00	2.136E+07
16	5.000	7.839E+06	0.000E+00	0.000E+00	7.839E+06
17	7.000	9.037E+05	0.000E+00	0.000E+00	9.037E+05
18	9.500	1.038E+05	0.000E+00	0.000E+00	1.038E+05
	Total	3.274E+15	1.374E+14	4.121E+13	3.233E+15

The modified ANISN computer run, provided in Section 5.5.5, calculates maximum MP187 dose rates based on the corrected source term provided in Table 5.4-12. The neutron and gamma dose rates on the surface of the cask calculated by this run are shown in Table 5.4-13, as are the corresponding results from the base run and the fractional dose rate decreases due to the corrected source term.

Table 5.4-13

Photon Source Evaluation Results

	ANISN Base	ANISN ^{154}Eu	Fractional Change (Eu/base)
Neutron	18.32	18.32	1.000
Gamma	24.24	22.89	0.944

(C) FC-DSC Source Self-Shielding

The shielding analysis described in Section 5.4 assumes a uniform, "smeared" source. This uniform source includes both the fuel assemblies as well as the control components stored within the assemblies. However, because the control components are stored inside the assemblies, the activated control component rods are shielded by two or more rows of fuel pins. The uniform source model, therefore, underpredicts the shielding of the control components by the fuel assemblies.

As shown in Section 5.4.2, the calculated peak surface gamma dose rate for the FC-DSC exceeds that of the FO-DSC by a factor of 2.15 (both peaks occur near the center of the active fuel region). The only difference between these two calculations is the inclusion of the control component source terms and number densities in the FC-DSC model. The large increase in dose rate for the FC-DSC is due primarily to the large control component source at 1.25 MeV, which is the photon energy group that contributes the greatest amount to the cask dose rates. The fuel source at 1.25 MeV is 6.24×10^{13} γ/s/assy while the gray APSRA source is 1.44×10^{14} γ/s/assy. The actual increase in dose rate due to the presence of control components is calculated below by modifying the MCNP [5.7] model described in Section 5.4.1.2.

One MCNP run is made to calculate the gamma dose rate on the surface of the DSC (the DSC is used rather than the cask surface to improve the monte-carlo statistics - this same technique was used in Section 5.4.1.2) using only the fuel pin source in each fuel assembly. A second run was made using only the control component source. This pin-by-pin model places the 16 control component rods in the appropriate locations in the 15x15 assembly array (for each assembly) to correctly calculate the dose rate contribution from the control components. These runs are provided in Section 5.5.3 and the model geometry is shown in Figure 5.4-6.

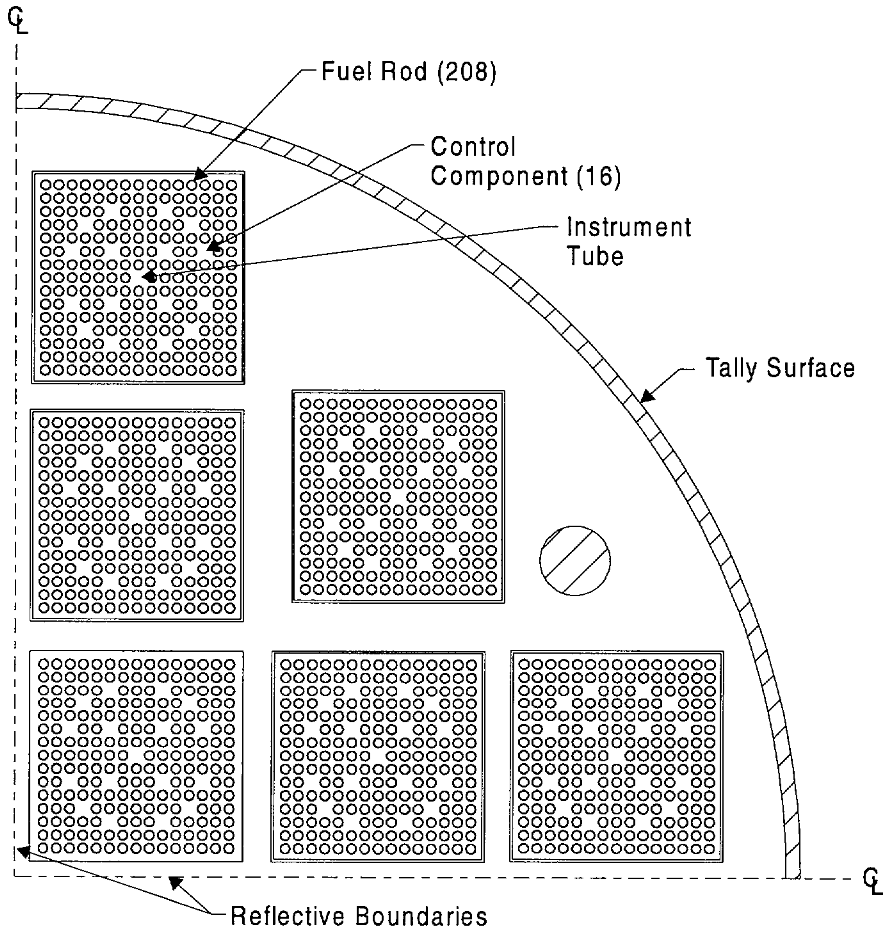

Figure 5.4-6

Source Self-Shielding Geometry

The calculated fuel-only dose rate on the surface of the DSC shell is 4.067×10^6 mrem/hr and the control component only dose rate on the surface of the DSC shell is 1.216×10^6 mrem/hr. The total (fuel plus APSRA) dose rate on the DSC shell is then:

$$4.067 \times 10^6 + 1.216 \times 10^6 = 5.283 \times 10^6 \text{ mrem/hr}$$

The FC-DSC gamma dose rate is, therefore, expected to exceed the FO-DSC gamma dose rate by a factor of $(5.283 \times 10^6)/(4.067 \times 10^6) = 1.299$. The gamma dose rates on the side of the MP187 cask, as calculated by DORT using a homogenized source, can be factored by $1.299/2.15 = 0.604$ to account for shielding of the control components by the fuel rods. Note that the FC-DSC control component analysis is based on gray axial power shaping rods. Although the analysis assumes 24 such components, B&W plants typically only have eight onsite.

(D) Neutron Shield Materials

As discussed in Section 5.3.2, the MP187 shielding calculations take credit for only 50% of the minimum acceptable boron concentration specified for the neutron shield. NRC practice for criticality analyses, which have a greater safety impact than shielding calculations, has been to allow 75% credit for boron in fixed neutron absorbers. This 75% value has been used for the absorber sheets in the MP187 criticality analysis as well. An additional ANISN run has been made to quantify the conservatism associated with using 50% of the boron loading rather than 75%.

The modified ANISN computer run, provided in Section 5.5.5, calculates maximum MP187 dose rates based on increasing the neutron shield boron loading by a factor of 1.5 (75%/50%) relative to the base model. The revised boron atom density is 1.070×10^{-3} atoms/b·cm. The neutron and gamma dose rates on the surface of the cask calculated by this run are shown in Table 5.4-14, as are the corresponding results from the base run and the fractional dose rate decreases due to the additional boron. These decreases will only be applied to dose rates adjacent to the neutron shield. Note that this result takes credit for only 75% of the boron in the neutron shield and only 90% of the hydrogen, providing additional conservatism.

Table 5.4-14

Neutron Shield Material Evaluation Results

	ANISN Base	ANISN Boron	Fractional Change (boron/base)
Neutron	18.32	18.01	0.983
Gamma	24.24	24.08	0.993

(E) Results and Conclusions

Using the correction factors described above, the revised package surface dose rates for the MP187 package containing an FC-DSC are (neutron and gamma doses at the location representing the peak surface dose rate from the DORT shielding models):

Neutron	(192.95)(1.029) =	198.55 mrem/hr
Gamma	(4.74)(1.318)(0.944)(0.604) =	3.56 mrem/hr
Total		202.11 mrem/hr < 1000 mrem/hr

The revised vehicle surface dose rates are:

Neutron	(51.26)(1.029) =	52.75 mrem/hr
Gamma	(4.30)(1.318)(0.944)(0.604) =	3.23 mrem/hr
Total		55.98 mrem/hr < 200 mrem/hr

The revised vehicle lower external surface dose rates are:

Neutron	(189.92)(1.029) =	195.43 mrem/hr
Gamma	(0.38)(1.318)(0.944)(0.604) =	0.29 mrem/hr
Total		195.72 mrem/hr < 200 mrem/hr

The revised two meter dose rates are:

Neutron	(6.94)(1.029)(0.983) =	7.02 mrem/hr
Gamma	(3.0)(1.318)(0.944)(0.604)(0.993) =	2.24 mrem/hr
Total		9.26 mrem/hr < 10 mrem/hr

As shown above, the package surface and vehicle surface dose rates increase slightly (<3%) while the peak 2 meter dose rate slightly decreases based on the evaluations performed herein. In both cases, the peak dose rate remains within the 10CFR71.47 acceptance criteria. Therefore, because the potential increase in dose rates due to components with below nominal thicknesses is sufficiently offset by the conservatisms in the shielding calculations to maintain dose rates within allowable levels, the MP187 shielding analysis fully supports the cask dimensions, including tolerances.

Additional conservatisms remain in the analysis, including minimum impact limiter thicknesses, minimum initial enrichments used to calculate neutron sources, conservative neutron shield material parameters, and a design basis source which corresponds to a cask heat of 14.3 kW (compared to a limit of 13.5 kW). Also, as discussed in References [5.15] and [5.17], the shielding calculations performed for this cask are expected to be conservative, particularly along the cask side, by 40% to 200% relative to measured doses.

5.4.2 NUHOMS®-MP187 Package Dose Rate Results

The DORT-PC computer run dose rate results are included in Section 5.5.5. The results of each of the four runs are summed node-by-node for both the normal operations and hypothetical accident cases. The dose rates calculated in Section 5.4.1.8.1 are then added, as appropriate, to the maximum normal operation, radial dose rates. The maximum gamma, neutron, and total dose rates at the package side, top, and bottom for the normal operations case are listed in Table 5.4-15. As shown in Table 5.4-15, with the exception of the surface dose rate, the cask dose rates with the FC-DSC bound those with the FO-DSC. Because the FO-DSC surface dose rate peak is due to the penetration of the neutron shield by the trunnion, and because the neutron shield is neglected in the hypothetical accident analysis, the FC-DSC is used in the hypothetical accident calculations as described below. Note that at some locations the sum of the maximum gamma-ray and neutron dose rates does not equal the maximum total dose rate. This implies that the maximum gamma, neutron, and total dose rates occur at different locations around the package. As shown in Table 5.4-15, the 10 CFR Part 71.47 [5.1] limits at the surface of the package, at the surface of the vehicle, and at a distance of two meters from the surface of the vehicle are not exceeded. The limit for occupied locations in the vehicle is met as well because the package top and bottom surface dose rates are less than the two mrem/hr requirement. The packaging therefore provides suitable shielding during normal operating conditions to ship 24 PWR fuel assemblies with sources bounded by those discussed in Section 5.2 in accordance with 10 CFR Part 71.

Table 5.4-15

Summary of Maximum Normal Operation Dose Rates

Package Surface	FC-DSC			FO-DSC		
	Side (mrem/hr)	Top (mrem/hr)	Bottom (mrem/hr)	Side (mrem/hr)	Top (mrem/hr)	Bottom (mrem/hr)
Normal Conditions						
Gamma	1.87E+1	2.18E-1	6.40E-1	8.71E+0	1.31E-1	2.82E-1
Neutron	1.93E+2	6.79E-1	1.31E+0	2.37E+2	6.60E-1	1.01E+0
Total	1.98E+2	8.47E-1	1.62E+0	2.37E+2	7.57E-1	1.18E+0
10 CFR 71 Limit	1.00E+3	1.00E+3	1.00E+3	1.00E+3	1.00E+3	1.00E+3
Vehicle Outer Surface	FC-DSC			FO-DSC		
	Side (mrem/hr)	Top (mrem/hr)	Bottom (mrem/hr)	Side (mrem/hr)	Top (mrem/hr)	Bottom (mrem/hr)
Normal Conditions						
Gamma	1.07E+1	2.18E-1	6.40E-1	4.86E+0	1.31E-1	2.82E-1
Neutron	5.13E+1	6.79E-1	1.31E+0	4.02E+1	6.60E-1	1.01E+0
Total	5.56E+1	8.47E-1	1.62E+0	4.24E+1	7.57E-1	1.18E+0
10 CFR 71 Limit	2.00E+2	2.00E+2	2.00E+2	2.00E+2	2.00E+2	2.00E+2
2 Meters from Vehicle Outer Surface	FC-DSC			FO-DSC		
	Side (mrem/hr)	Top (mrem/hr)	Bottom (mrem/hr)	Side (mrem/hr)	Top (mrem/hr)	Bottom (mrem/hr)
Normal Conditions						
Gamma	3.14E+0	6.46E-2	2.16E-1	1.35E+0	4.20E-2	9.76E-2
Neutron	7.04E+0	3.02E-1	5.39E-1	6.34E+0	2.94E-1	4.28E-1
Total	9.94E+0	3.37E-1	6.72E-1	7.65E+0	3.19E-1	4.97E-1
10 CFR 71 Limit	1.00E+1	1.00E+1	1.00E+1	1.00E+1	1.00E+1	1.00E+1

Note: Peak dose rate on the lower external surface of the vehicle is 190.3 mrem/hr located adjacent to the shear key. Applicable 10CFR71.47 limit is 200 mrem/hr.

The maximum gamma, neutron, and total dose rates at the package side, top, and bottom for the hypothetical accident case are listed in Table 5.4-16. As shown in Table 5.4-16, the 10 CFR Part 71.51 [5.1] limit at a distance of one meter from the surface of the package is not exceeded. The packaging therefore provides suitable shielding during the hypothetical accident conditions to ship 24 PWR fuel assemblies with sources bounded by that discussed in Section 5.2 in accordance with 10 CFR Part 71. Because the hypothetical accident dose rates are less than 50% of the limit while the maximum normal operation dose rates are at the allowable, the normal operation case is bounding for the NUHOMS®-MP187. Because the dose rates are surveyed prior to transport and verified to meet the 10CFR71 and 49CFR173 limits for normal operation, the package will meet all applicable dose limits under both normal and accident conditions.

Table 5.4-16

Summary of Maximum Hypothetical Accident Dose Rates

	Package Surface			1 Meter from Surface of Package		
	Side (mrem/hr)	Top (mrem/hr)	Bottom (mrem/hr)	Side (mrem/hr)	Top (mrem/hr)	Bottom (mrem/hr)
Accident Conditions						
Gamma	1.7E+3	1.2E+1	5.3E+0	1.8E+2	1.7E+0	1.8E+0
Neutron	1.0E+3	8.5E+1	1.6E+2	4.4E+2	3.6E+1	5.8E+1
Total	1.8E+3	8.6E+1	1.6E+2	4.8E+2	3.6E+1	5.9E+1
10 CFR Part 71 Limit	-	-	-	1.0E+3	1.0E+3	1.0E+3

Figure 5.4-7 and Figure 5.4-8 show the total dose rate along the length of the package for normal operations for the FC-DSC and FO-DSC, respectively. Neutron, gamma, and total dose rates are shown at the package surface and at a distance of two meters from the vehicle surface. The total dose rate is also shown along the vehicle surface. The peak dose rates are seen to occur just above and below the neutron shield during normal operations. Peaks which are due to the presence of the trunnions are visible at a height of 200 inches to 210 inches. The package surface dose rate peak for the FC-DSC occurs at the bottom end of the neutron shield, while the peak for the FO-DSC occurs at the upper trunnion. This difference is due to the fact that the active fuel region (neutron source) is closer to the trunnion with the FO-DSC than it is for the FC-DSC.

The dose rates in the vicinity of the shear key are not shown since they exist underneath the transport vehicle. The hypothetical accident dose rates are shown in Figure 5.4-9. The peak dose rates during the hypothetical accident occur due to streaming through the postulated gaps in the lead shielding.

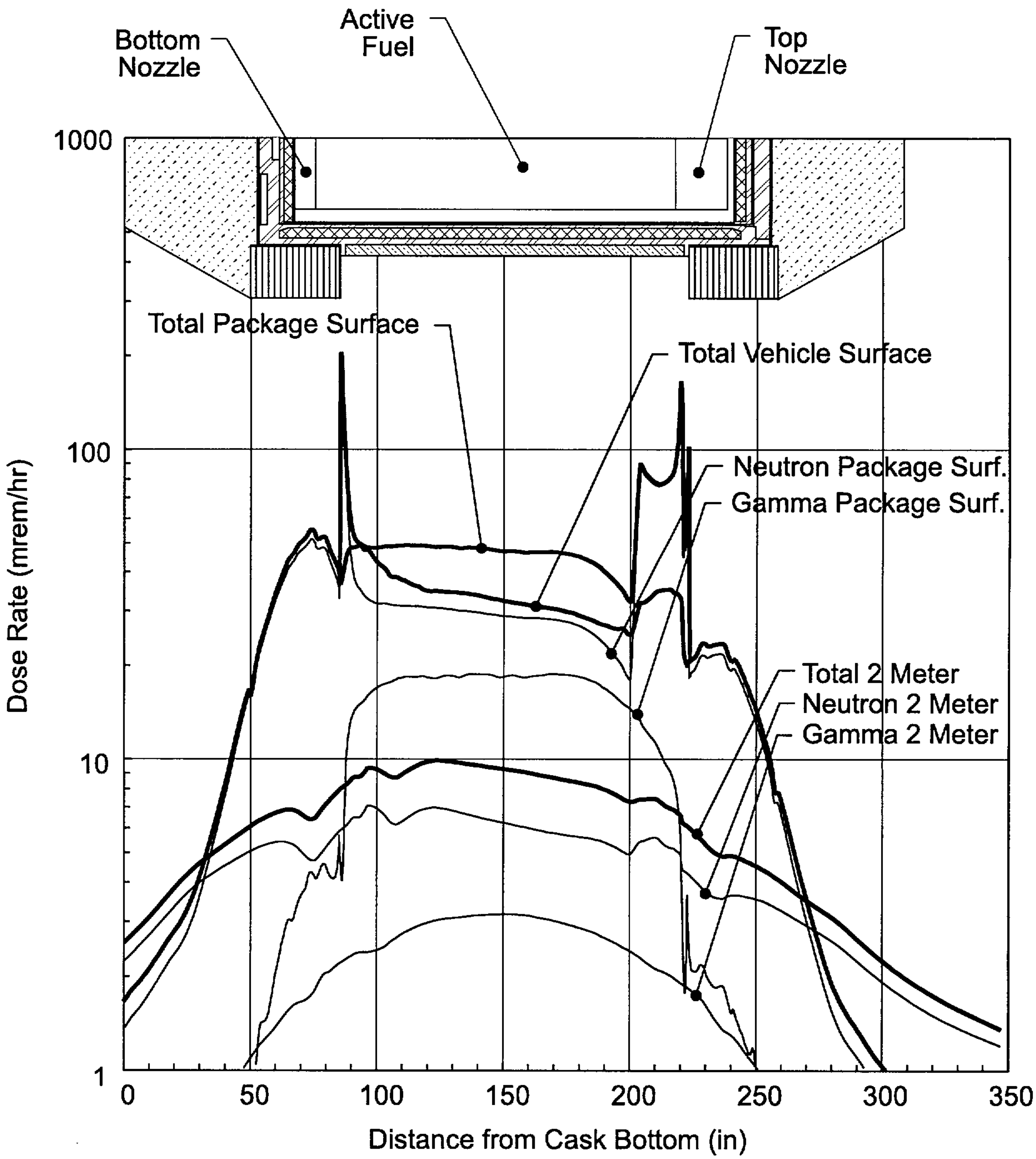

Figure 5.4-7

NUHOMS®-MP187 FC-DSC Normal Operation Dose Rate Distribution

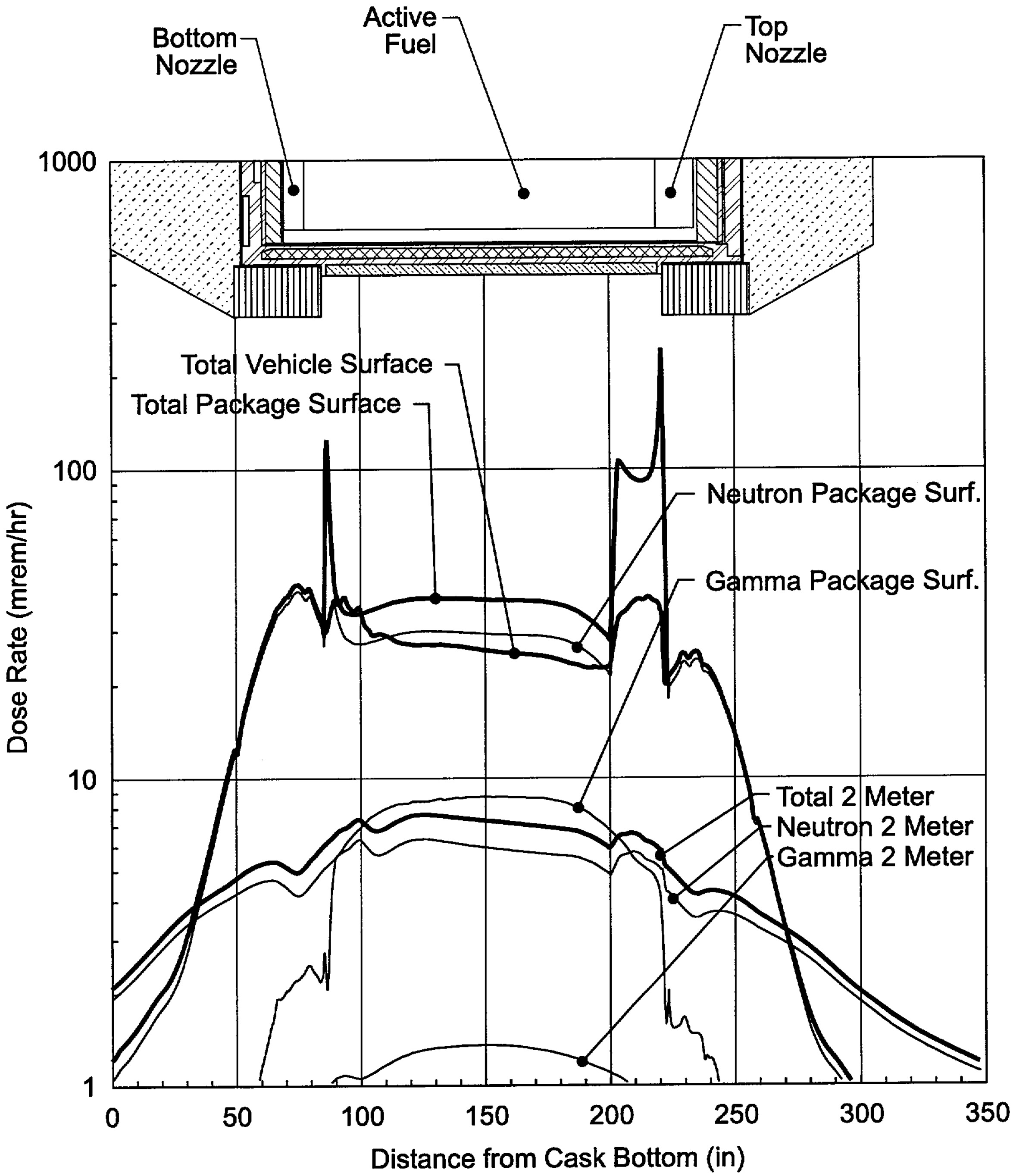

Figure 5.4-8

NUHOMS®-MP187 FO-DSC Normal Operation Dose Rate Distribution

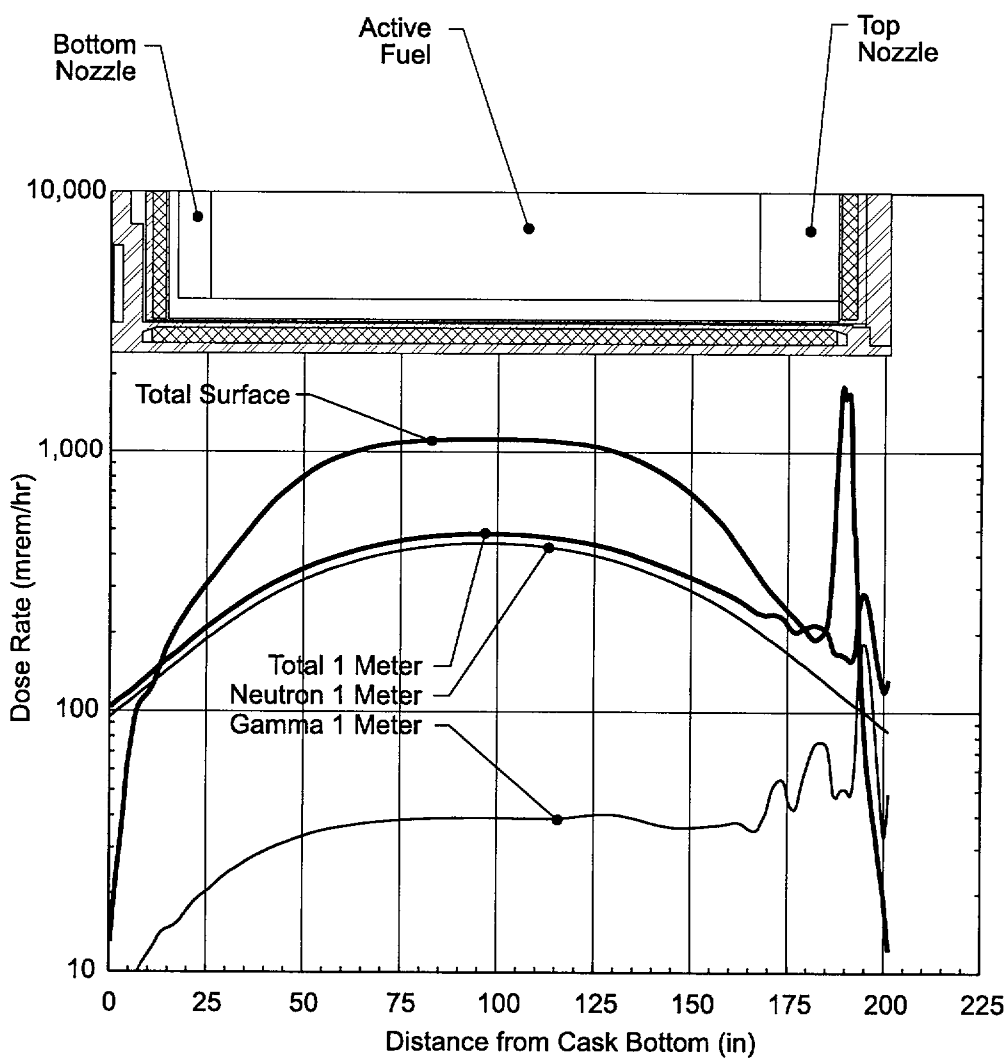

Figure 5.4-9

NUHOMS®-MP187 Hypothetical Accident Dose Rate Distribution

5.5 Appendix

5.5.1 References

5.1 U.S. Government, "Packaging and Transportation of Radioactive Material," Title 10 Code of Federal Regulations, Part 71, Office of the Federal Registrar, Washington DC.

5.2 U.S. Government, "Shippers – General Requirements for Shipments and Packagings," Title 49 Code of Federal Regulations, Part 173, Section 441, Office of the Federal Registrar, Washington DC.

5.3 "ORIGEN2.1 - Isotope Generation and Depletion Code - Matrix Exponential Method", CCC-371, Oak Ridge National Laboratory, RSIC Computer Code Collection, August 1991.

5.4 "CASK-81 - 22 Neutron, 18 Gamma-Ray Group, P_3, Cross Sections for Shipping Cask Analysis", DLC-23, Oak Ridge National Laboratory, RSIC Data Library Collection, June 1987.

5.5 Luksic, A., "Spent Fuel Assembly Hardware: Characterization and 10CFR61 Classification for Waste Disposal," Volume 1, Pacific Northwest Laboratory, PNL-6906, June 1989.

5.6 "Characteristics of Potential Repository Wastes", DOE/RW-0184-R1, Office of Civilian Radioactive Waste Management, July 1992.

5.7 "MCNP 4 - Monte Carlo Neutron and Photon Transport Code System", CCC-200A/B, Oak Ridge National Laboratory, RSIC Computer Code Collection, October 1991.

5.8 "Moderate Temperature (250°F) Weight Loss of NS-3," Technical Report No. NS-3-029, Bisco Products, Inc., Park Ridge, Illinois, Revision 0, April 1985 (Appendix 5.5.6).

5.9 "DORT-PC - Two-Dimensional Discrete Ordinates Transport Code System", CCC-532, Oak Ridge National Laboratory, RSIC Computer Code Collection, October 1991.

5.10 Watt, B. E., "Energy Spectrum of Neutrons and Thermal Fission of U^{235}," Phys. Rev 87, 1037 (1952).

5.11 "American National Standard Neutron and Gamma-Ray Flux-to-Dose-Rate Factors", ANSI/ANS-6.1.1-1977, American Nuclear Society, La Grange Park, Illinois, March 1977.

5.12 Jenal, J. P., P. J. Erickson, W. A. Rhoades, D. B. Simpson, and M. L. Williams, "The Generation of a Computer Library for Discrete Ordinates Quadrature Sets", ORNL/TM-6023, Oak Ridge National Laboratory, October 1977.

5.13 "ANISN-ORNL - One-Dimensional Discrete Ordinates Transport Code System with Anisotropic Scattering", CCC-254, Oak Ridge National Laboratory, RSIC Computer Code Collection, April 1991.

5.14 "Topical Report on Actinide-Only Burnup Credit for PWR Spent Nuclear Fuel Packages," DOE/RW-0472, Office of Civilian Radioactive Waste Management, Revision 0, May 1995.

5.15 Jones, K.B., and B.D. Thomas, "Dry Fuel Storage Cask Shielding Benchmarks," Proceedings of the Sixth Annual International High Level Radioactive Waste Management Conference, Las Vegas, Nevada, May 1995.

5.16 Hermann, O. W., and S. M. Bowman, M. C. Brady, and C. V. Parks, "Validation of the Scale System for PWR Spent Fuel Isotopic Composition Analysis," ORNL/TM-12667, Oak Ridge National Laboratory, March 1995.

5.17 "Evaluation of Shielding Analysis Methods in Spent Fuel Cask Environments", EPRI TR-104329, Electric Power Research Institute, May 1995.

5.5.2 ORIGEN2 Input Files

THIS SECTION CONTAINS
PROPRIETARY INFORMATION

5.5.3 MCNP Input Files

THIS SECTION CONTAINS
PROPRIETARY INFORMATION

5.5.4 DORT-PC and GIP Input Files

THIS SECTION CONTAINS
PROPRIETARY INFORMATION

5.5.5 ANISN Input Files

THIS SECTION CONTAINS
PROPRIETARY INFORMATION

5.5.6 Moderate Temperature Weight Loss of NS-3

This Appendix contains Bisco Products, Inc. Report NS-3-029, "Moderate Temperature (250°F) Weight Loss of NS-3," Revision 0, April 1995 (8 pages).

bisco

TECHNICAL REPORT

Number: NS-3-029

Subject: Moderate Temperature Weight Loss of NS-3

bisco products, inc.
1125 howard st.
elk grove village, illinois 60007
(312) 640-1840

Date: April 10, 1985

By: Michael L. McCullar
Michael L. McCullar
Research Chemist

PURPOSE:

To determine the rate of weight loss of NS-3 when exposed to 250° F for an extended period of time. Assuming that water loss is the primary reason for weight loss, the worst case hydrogen stability of NS-3 can then be determined.

CONCLUSIONS:

1. It takes about 2 months at 250° F before the NS-3 weight reaches a stab point.

2. The NS-3 loses about 4.2% weight during this time frame.

3. Under these conditions (250° F), the % hydrogen in NS-3 decreases from 5.1% to 4.6%.

PROCEDURE:

BISCO Procedure NS-3-03 Rev. 1 was followed (appendix).

RESULTS AND DISCUSSION:

A one inch thick slab of NS-3 was made with laboratory raw materials and cured in accordance with standard BISCO procedures. Two 1 inch cubes were cut from the slab for this test.

Table 1 contains the raw weight data for each cube, average weight loss, ar average percent weight loss for each time period. Graph 1 is a plot of average % weight loss versus time.

RESULTS AND DISCUSSION (cont.):

The justification for each conclusion is discussed:

1. The weight of both NS-3 cubes decreased steadily from day 1 to day 54. From day 54 to day 59, no change in weight was observed. Based on this data, it takes about 2 months for the NS-3 to stop losing weight.

2. The average percent weight loss at day 59 was 4.226%. See the data in Table 1.

3. The % hydrogen in properly formulated and cured NS-3 is 5.1%. The average % weight loss of the NS-3 was 4.226%. It is reasonable to assume that all of the weight loss was in the form of water since no other volatile materials are present in NS-3. Since water consists of 11.19% hydrogen (as H), the overall hydrogen loss = 11.19% times 4.226% = 0.473% Given the starting NS-3 hydrogen content (theoretical) of 5.1%, the worst case hydrogen stability at 250° F is 5.1% - 0.473% = 4.627%.

No visual changes were apparent in the heat treated NS-3 cubes, other than some minor darkening.

TABLE 1

NP-03

Raw Data For NS-3 Cubes Heated at 250° F

Time Frame	Cube #13 Weight (gms)	Cube #14 Weight (gms)	Average Weight Loss (gms)	Average % Weight Loss
Start	21.9182	24.2544	0	
1 day	21.1194	23.4523	.8005	3.467
3 days	21.0863	23.4152	.8356	3.619
4 days	21.0762	23.4038	.8463	3.666
5 days	21.0698	23.3972	.8528	3.694
6 days	21.0670	23.3944	.8556	3.706
7 days	21.0672	23.3942	.8556	3.706
10 days	21.0471	23.3721	.8767	3.797
11 days	21.0479	23.3734	.8757	3.793
12 days	21.0454	23.3702	.8785	3.805
13 days	21.0462	23.3710	.8779	3.802
14 days	21.0438	23.3687	.8801	3.812
1[illegible] ays	21.0344	23.3587	.8898	3.854
18 days	21.0319	23.3556	.8926	3.866
19 days	21.0331	23.3568	.8914	3.861
20 days	21.0297	23.3529	.8950	3.877
21 days	21.0288	23.3520	.8959	3.881
24 days	21.0252	23.3485	.8995	3.896
25 days	21.0251	23.3480	.8998	3.897
27 days	21.0192	23.3413	.9061	3.925
31 days	21.0140	23.3359	.9114	3.948
35 days	21.0125	23.3328	.9137	3.958
38 days	20.9873	23.3032	.9411	4.076
39 days	20.9840	23.3022	.9432	4.086
40 days	20.9815	23.3000	.9456	4.096
42 days	20.9806	23.2982	.9469	4.102

TABLE 1

Time Frame	Cube #13 Weight (gms)	Cube #14 Weight (gms)	Average Weight Loss (gms)	Average Weight Loss
46 days	20.9649	23.2786	.9646	4.178
48 days	20.9558	23.2715	.9727	4.213
52 days	20.9659	23.2805	.9631	4.172
53 days	20.9557	23.2697	.9736	4.217
54 days	20.9530	23.2671	.9763	4.229
56 days	20.9540	23.2679	.9754	4.225
59 days	20.9537	23.2678	.9756	4.226

Moderature Temperature Weight Loss of N at 250°F in Percent

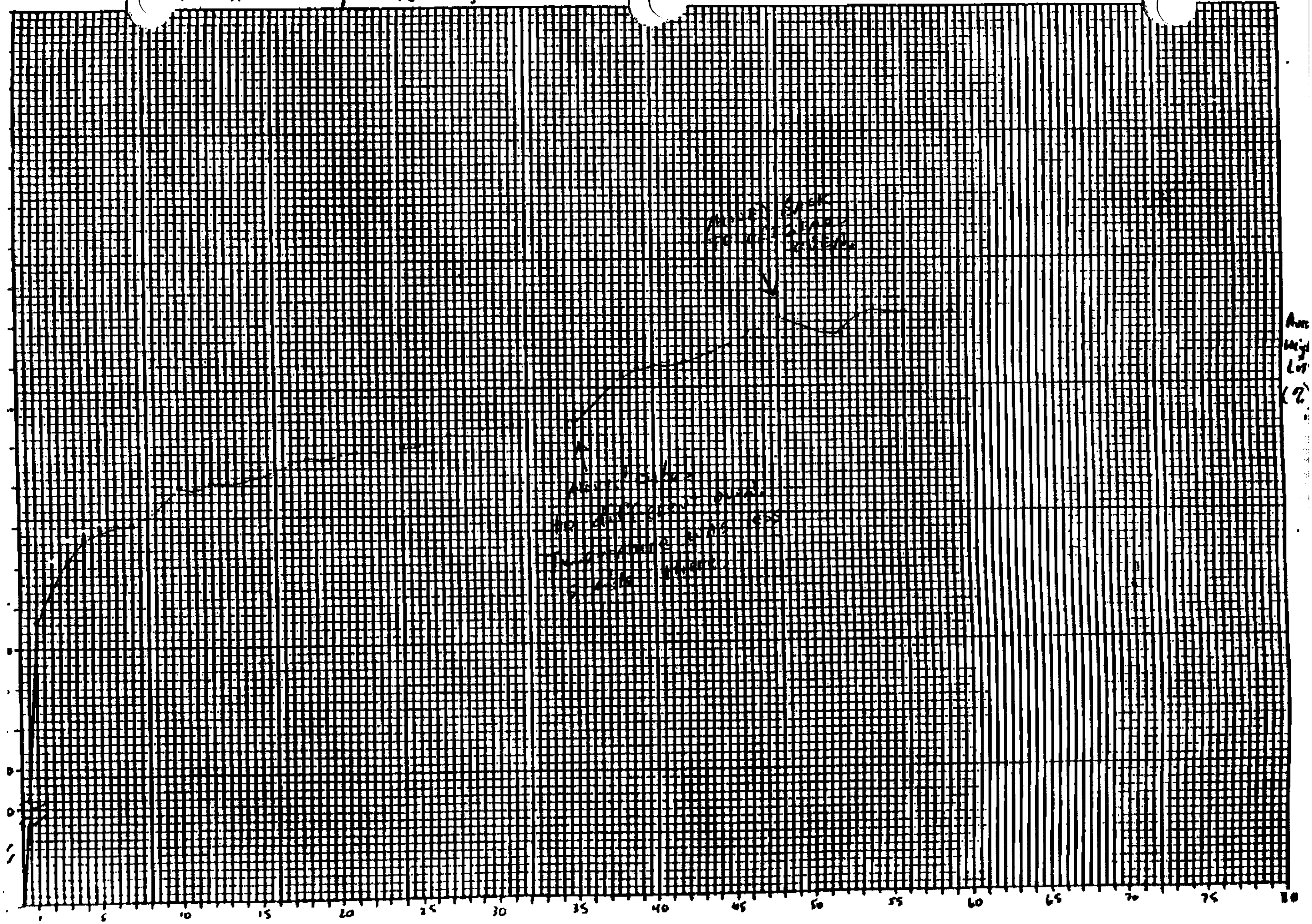

bisco

PROCEDURE

Procedure No. NS3-03

Project

Title: MODERATE TEMPERATURE WEIGHT LOSS OF NS-3

REV.	DATE	AUTHOR	TECH. REVIEW	Q.A. REVIEW	CORP. APPROVAL	SCOPE OF REVISION
0	5/15/84					Initial issue
1	1/20/85	MLM	[signature]	4/17/85 [signature]	[signature]	Change from weighing cube in glassware to weighing cube a… change min. cube size to 20mm
2						
3						
4						
5						
6						

DESCRIPTION

This test procedure describes the method to determine the weight loss of NS-3 when exposed to 250° F for an extended period of time. Data obtained from this test may be used to establish the worst case hydrogen stability of NS-3 at 250° F by considering that all weight loss is in the form of water and calculating the hydrogen equivalent loss as a fraction of total hydrogen.

MATERIALS

The test described is performed on NS-3 without additives, formulated and cured in accordance with standard BISCO procedures. The tests are performed in a static air oven with a temperature accuracy of ±5F. The samples are set in standard pyrex glassware while in the oven.

PROCEDURE

Two samples of NS-3, each sample not smaller than 20mm cubed, nor larger than 100mm cubed, shall be prepared, with each side of the cube machined smooth to prevent loose powder loss during the test. Each sample shall be wiped with a dry cloth and weighed to an accuracy obtainable on a Mettler type balance, then set in a clean dry glass container. The sample configuration shall be such that five sides of each sample are completely exposed. The container, with the cover removed, shall be placed in the oven and exposed to 250° F for a period of 24 hours. At the end of the exposure period gently remove each cube from the container using tongs, then weigh each cube within 15 minutes of removal. Following re-weighing, place the cubes back into the container and replace into the oven for further exposure. The cycle is to be repeated until the data indicates no further weight change is anticipated. The interval between weighings may be increased as deemed suitable by the shape of the weight loss curve.

REPORT

Following a completion of the test, a report shall be issued containing at least the following information:

1. A description of the samples including batch identification.
2. A summary of the data obtained.
3. An evaluation of worst case hydrogen stability as identified under "Description".
4. A list of observations.
5. A curve of showing the average weight loss of the samples as a function of time.
6. An appendix containing the test procedure and all data obtained.

End of Procedure

5.5.7 Fuel Assembly Axial Burnup Profiles

This Appendix contains portions of "Topical Report on Actinide-Only Burnup Credit for PWR Spent Nuclear Fuel Packages," DOE/RW-0472, Revision 0, May 1995 (3 pages). Note that Revision 1 of this report is scheduled to be issued in the near future. Transnuclear West has reviewed the current draft of Revision 1 and verified that the axial burnup profiles used in the MP187 shielding analysis bound those provided in the revised report (maximum factor of 1.12 used herein, 1.108 used in Revision 1 of DOE/RW-0472).

Burnup credit analyses must consider the effects of moderator density from 0 to 1.0 g/cc within the spent fuel package. The moderator density effects must be evaluated with zero burnup at low enrichments (the maximum fresh fuel enrichment limit for the SNF package) and at high enrichments (the highest enrichment evaluated for the package) with the associated burnup from the burnup credit loading curve. If these evaluations indicate that a reactivity maximum exists at any density but 1.0 g/cc, then an optimum moderator density search is required at all enrichments evaluated for the burnup credit loading curve.

4.2.2 Axial Burnup Profile

The axial power peaking effect caused by neutron leakage from the ends of the finite-length fuel assembly produces an axial profile in the burnup. The effect of the burnup profile is to have less burnup in the fuel assembly ends than the average for the assembly, resulting in a local reactivity increase at the fuel ends and a decrease in the central region compared to the reactivity that would have existed if the assembly were uniformly burned to the average value. The axial burnup effect can be incorporated into burnup credit criticality safety analyses by dividing the assembly length into a number of zones of varying burnup. An evaluation was performed to determine the number of zones necessary to accurately model the reactivity effect of the axial burnup profile for two cases: 1) burned PWR fuel whose composition includes only the actinide isotopes validated in Chapter 2 of this topical report, and 2) burned fuel with a composition that also includes fission products. The fission product cases are provided as a basis of comparison for the end-effects with actinide-only credit.

4.2.2.1 Modeling of Fuel Ends

An example of the axial profile of spent fuel is illustrated by the measurement of Cs-137 as shown in Figure 4-3.[4-2] The shape of the burnup profile is a flattened cosine, with a peak from 1.1 to 1.2 times the average value of the burnup, and a burnup at the fuel rod ends that equals from 50 to 60% of the average value. Details of the calculational modeling approach used for the end effects are discussed below. The axial profile for each individual spent fuel assembly will vary somewhat from this profile depending on the specific power history of the assembly. Restrictions are placed upon the selection of candidate fuel assemblies in Section 6 to ensure that the profiles of assemblies loaded into an SNF package system with burnup credit do not differ significantly from the profile used as a basis for studies in this topical report, which are depicted in Figure 4-4.

A study was performed to evaluate the effect that the number of axial zones has upon the calculated reactivity of spent fuel.[4-1] The results of this evaluation are illustrated in Figure 4-5 (actinide plus fission product isotopes) and Figure 4-6 (actinide isotopes, without fission products). The results for actinide plus fission product isotopes showed that a higher k_{eff} results from incorporating the end effects for fuel that has attained the major portion of its burnup potential, as shown in Figure 4-5. For fuel that has a relatively low burnup (compared to the burnup that it could achieve in a PWR reactor if maintenance problems or fuel failures do not occur to cause the fuel to be prematurely discharged), a flat burnup profile (one uniform axial zone) results in a higher k_{eff}. Similar results were reported in independent studies of burnup credit.[4-3]

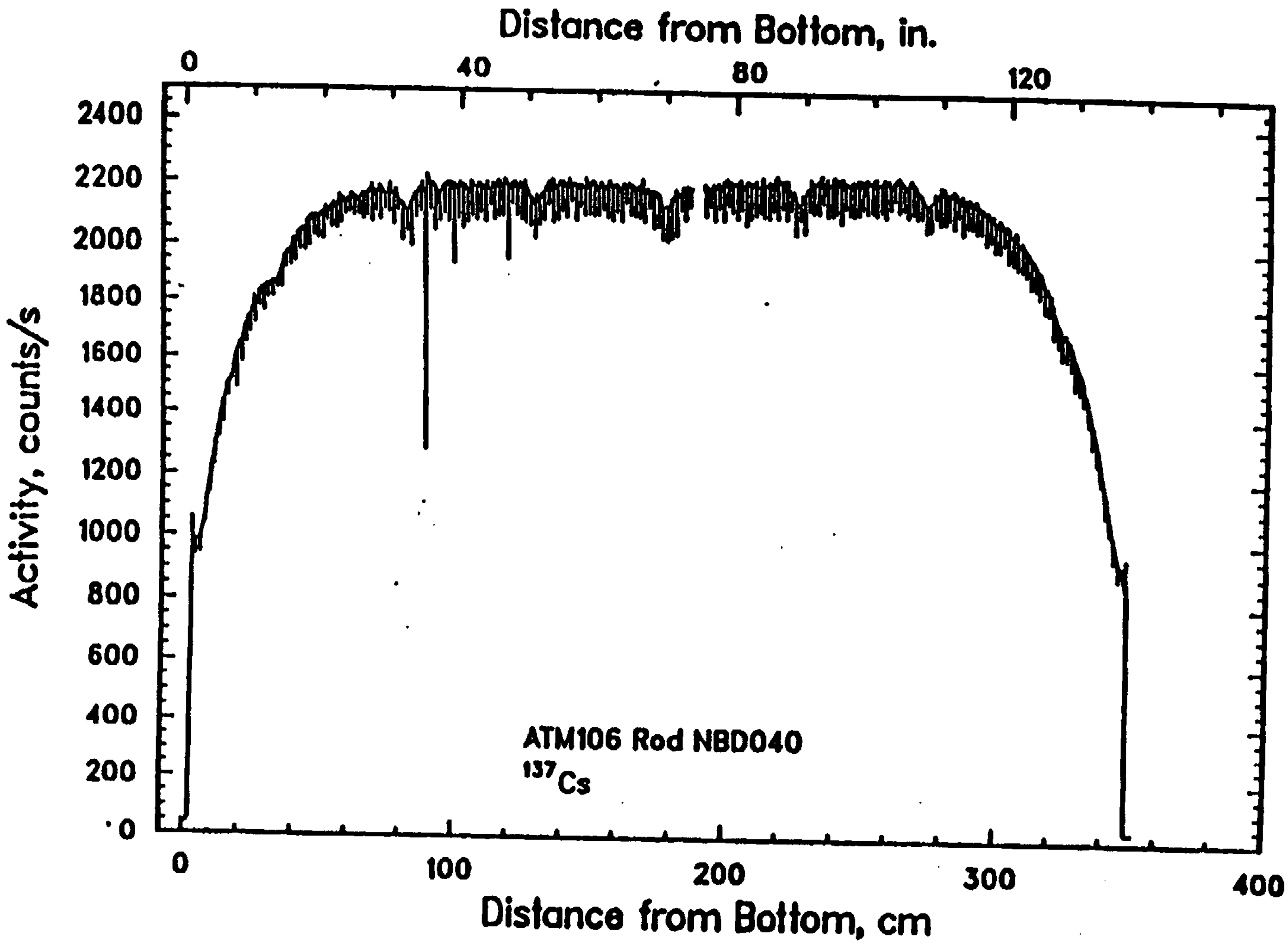

Figure 4-3. Burnup Profile Measurement by Gamma Scan

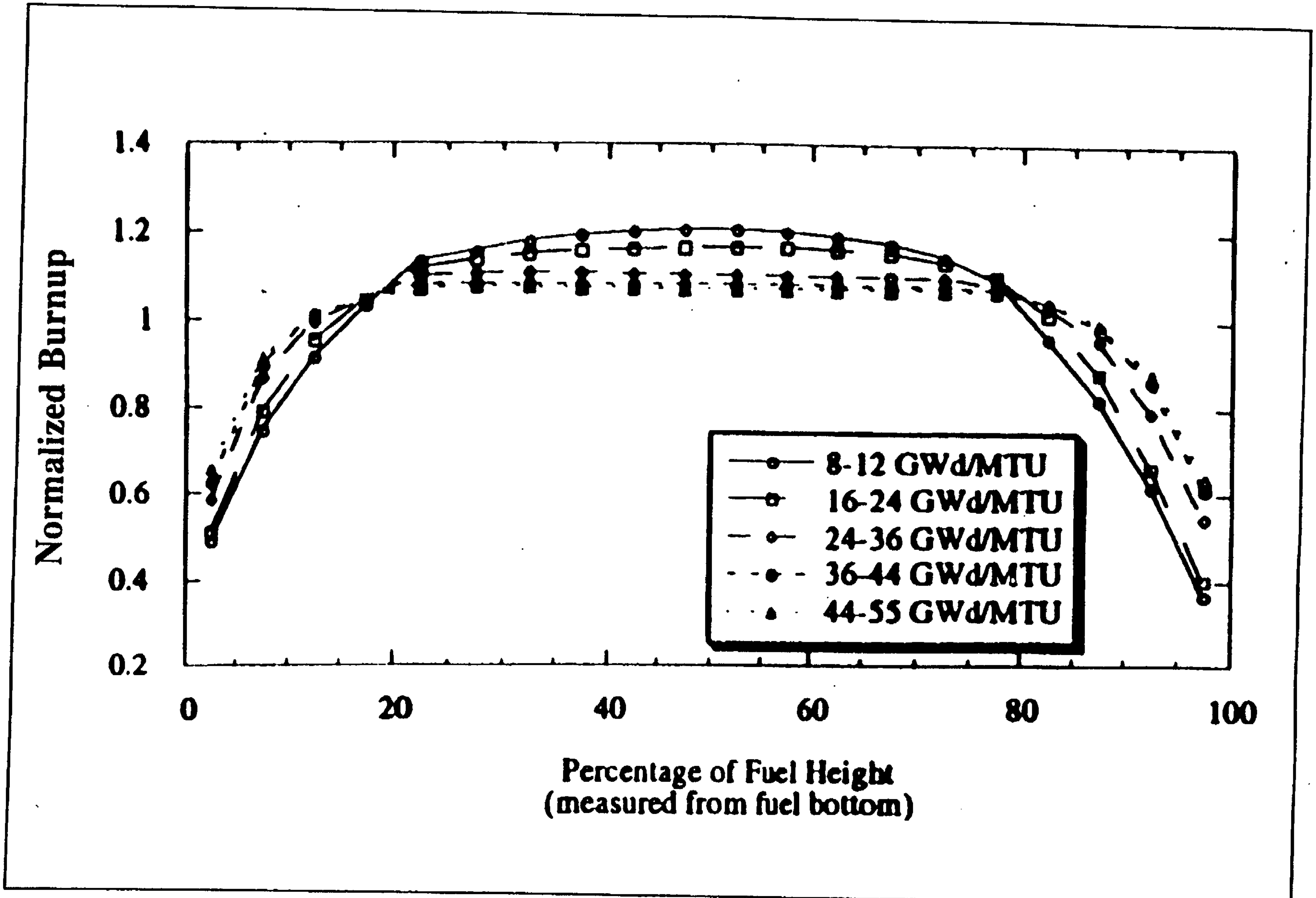

Figure 4-4. Normalized Axial Burnup Profiles

5.5.8 Alternate Fuel Parameters

This Appendix contains details of the analysis performed to generate the alternate fuel qualification criteria shown in Table 1.2-3. The intention of this table is to permit fuel assemblies with initial enrichments less than those permitted by Table 1.2-1 to be transported in the MP187 package, provided all other design criteria are satisfied. The fuel parameters shown in Table 1.2-3 are intended to supplement those in Table 1.2-1, and are not considered a replacement.

This is primarily a shielding evaluation, based on the fact that for a given burnup, the neutron source (and to a lesser extent the photon source) increases as the initial enrichment of the assembly decreases. The assembly decay heat also increases as the initial enrichment is decreased, but to a lesser extent than the radiological sources. Because only the maximum initial enrichment is important for criticality safety (limited to 3.43 w/o U-235), these low-enriched assemblies are bounded by the existing criticality analyses.

The low-enriched fuel assemblies will be qualified for loading in the MP187 cask in the following manner:

1. Three burnup/enrichment cases are modeled using the ORIGEN2 code [5.3]. The models are identical to those described in Section 5.2 to calculate the design basis MP187 source term. The ORIGEN2 code is used to calculate the decay heat, neutron source, photon source, and photon spectrum for each of the three cases.

2. The results of the three ORIGEN2 models are used to develop ANISN [5.13] source terms for each of the three cases, for both Type I and Type II fuel. The ANISN models are based on those described in Section 5.2.1.3 which determined the design basis fuel parameters. Source terms are developed using the same methodology as was used in the models described in Section 5.2.1.3.

3. The ANISN code calculates the neutron and gamma dose rates on the surface of the MP187 cask. These dose rates are multiplied by appropriate peaking factors and summed to calculate the total cask surface dose rate at the midpoint of the active fuel region. This duplicates the method used in Section 5.2.1.3 to determine the design bases burnup/enrichment case for the MP187 cask.

4. The DORT [5.9] code is used to calculate the dose rates at the package surface, vehicle outer surface, and two meters from the vehicle outer surface for the normal operating configuration. The DORT code is also used to calculate the dose rates one meter from the surface of the package for the hypothetical accident case. The DORT models duplicate those described in Section 5.4.1 of the SAR and include contributions from activated hardware in the end fittings, plenum, and control components.

5. Each of the three burnup/enrichment cases is qualified by demonstrating that:

   a) The total dose rate on the surface of the cask (as calculated by ANISN) for each case is bounded by that for the design basis case in the NUHOMS®-MP187 source term calculation (Section 5.2.1.3). For Type I assemblies the maximum dose rate is 61.5 mrem/hr and for Type II assemblies the maximum dose rate is 39.1 mrem/hr. This calculation ensures that both the Type I and Type II sources for each case are consistent with the criteria used to develop the MP187's design basis sources in Section 5.2.1.3.

   b) The maximum decay heat for a Type I assembly is limited to 0.764 kW and that for a Type II assembly is limited to 0.563 kW (Section 1.2.3).

   c) Because neutrons are the dominant contributor to the MP187 dose rates (at locations other than those modeled by ANISN), the neutron source term for each case must be bounded by the corresponding design basis neutron source term from Section 5.2.2. Because the primary neutron source for each case is the same (spontaneous fission of ^{244}Cm), the neutron spectrum for each case is the same and this provides assurance that all MP187 dose rates for the burnup/enrichment cases modeled herein will be bounded by those evaluated in Section 5.2.

d) The maximum total (neutron plus gamma for all assembly sources) dose rate on the package surface during normal operations is limited to 1000 mrem/hr per 10CFR71.47(b)(1). Compliance is demonstrated using the DORT models described above.

e) The maximum total (neutron plus gamma for all assembly sources) dose rate on the vehicle outer surface during normal operations is limited to 200 mrem/hr per 10CFR71.47(b)(2). Compliance is demonstrated using the DORT models described above.

f) The maximum total (neutron plus gamma for all assembly sources) dose rate two meters from the vehicle outer surface during normal operations is limited to 10 mrem/hr per 10CFR71.47(b)(3). Compliance is demonstrated using the DORT models described above.

g) The maximum total (neutron plus gamma for all assembly sources) dose rate one meter from the external surface of the package subsequent to the hypothetical accident conditions is limited to 1000 mrem/hr per 10CFR71.51(a)(2). Compliance is demonstrated using the DORT models described above.

h) Because the fuel design, maximum allowable initial enrichment, and uranium content are not being changed, no additional analyses are required for these parameters.

5.5.8.1 Calculations

5.5.8.1.1 Cases Addressed

The burnup/enrichment cases addressed in this calculation section are shown in Table 5.5.8-1 (DB refers to the design basis case from Section 5.2).

Table 5.5.8-1

Burnup/Enrichment Cases

Case	Enrichment (w/o U-235)	Burnup (MWd/MTU)
1	3.00	37,000
2	2.00	29,000
3	2.67	35,000
DB	3.19	40,000

5.5.8.1.2 Source Term Calculations

Source terms (neutron, photon, photon spectra, thermal) are calculated using the ORIGEN2 code with models based on those described in Section 5.2 (original ORIGEN2 models provided in Appendix 5.5.2). The alternate fuel source term models are described in the following sections.

(A) Case 1 - BW37-R0

The Case 1 ORIGEN2 model (37,000 MWd/MTU, 3 w/o U-235) is based on file BW40-R2A.INP from Appendix 5.5.2. All inputs are identical with the exception of: (1) The power irradiation was changed to account for the 37,000 MWd/MTU fuel burnup; (2) The decay times were changed as required for this calculation; and (3) The actinide composition was changed to account for the 3 w/o U-235 enrichment. The input cards which have been changed relative to those in Appendix 5.5.2 are shown below.

Specific Power: changed to 19.06 MW/assy which corresponds to a burnup of 37,000 MWd/MTU accumulated over 900 full power days (0.4636 MTU).

```
IRP      60.0  19.06  -6  1  4  2
IRP     120.0  19.06   1  1  4  0
IRP     180.0  19.06   1  1  4  0
IRP     240.0  19.06   1  1  4  0
IRP     300.0  19.06   1  1  4  0
DEC     380.0          1  1  4  0
IRP     440.0  19.06   1  1  4  0
IRP     500.0  19.06   1  1  4  0
IRP     560.0  19.06   1  1  4  0
IRP     620.0  19.06   1  1  4  0
IRP     680.0  19.06   1  1  4  0
DEC     760.0          1  1  4  0
IRP     820.0  19.06   1  1  4  0
IRP     880.0  19.06   1  1  4  0
```

```
IRP      940.0   19.06   1   1   4   0
IRP     1000.0   19.06   1   1   4   0
IRP     1060.0   19.06   1   1   4   0
```

Decay Time: Two decay times are addressed. Eight years cooling is assumed for Type I assemblies, and 14 years is assumed for Type II assemblies. The remainder of this Appendix will demonstrate that a 37,000 MWd/MTU, 3 w/o U-235 assembly cooled for these times satisfies the design criteria.

```
TIT      37,000 MWD/MTU AFTER 8.0 YEARS
DEC             8.000   -1        1         5         4
DEC             8.000   -2        2         5         4
DEC             8.000   -3        3         5         4
DEC             8.000   -4        4         5         4
HED             1 IN-CORE
HED             2 TOP
HED             3 PLENUM
HED             4 BOTTOM
OUT      -4    1    -1    0
TIT      37,000 MWD/MTU AFTER 14.0 YEARS
DEC             14.00   -1        1         5         4
DEC             14.00   -2        2         5         4
DEC             14.00   -3        3         5         4
DEC             14.00   -4        4         5         4
HED             1 IN-CORE
HED             2 TOP
HED             3 PLENUM
HED             4 BOTTOM
OUT      -4    1    -1    0
```

Actinide Composition: The U-235 mass (grams U-235 per MTU) has been changed to represent an initial enrichment of 3.0 w/o U-235. The U-238 mass has also been changed to maintain a total uranium weight of 1×10^6 grams per metric ton.

```
2    922340   240.00   922350   30000.00   922380   969760.00   0   0.0 FUEL
ACTINIDES
```

(B) Case 2 - BW29-R0

The Case 2 ORIGEN2 model (29,000 MWd/MTU, 2.0 w/o U-235) is based on that for 30,000 MWd/MTU fuel as described in Section 5.2.1.1. All inputs are identical with the exception of: (1) The power irradiation was changed to account for the 29,000 MWd/MTU fuel burnup; (2) The decay times were changed as required for this calculation; and (3) The actinide composition was changed to account for the 2 w/o U-235 enrichment. The input cards which have been changed relative to those in the original model are shown below.

Specific Power: changed to 14.94 MW/assy which corresponds to a burnup of 29,000 MWd/MTU accumulated over 900 full power days (0.4636 MTU).

```
IRP      60.0  14.94  -6  1  4  2
IRP     120.0  14.94   1  1  4  0
IRP     180.0  14.94   1  1  4  0
IRP     240.0  14.94   1  1  4  0
IRP     300.0  14.94   1  1  4  0
DEC     380.0          1  1  4  0
IRP     440.0  14.94   1  1  4  0
IRP     500.0  14.94   1  1  4  0
IRP     560.0  14.94   1  1  4  0
IRP     620.0  14.94   1  1  4  0
IRP     680.0  14.94   1  1  4  0
DEC     760.0          1  1  4  0
IRP     820.0  14.94   1  1  4  0
IRP     880.0  14.94   1  1  4  0
IRP     940.0  14.94   1  1  4  0
IRP    1000.0  14.94   1  1  4  0
IRP    1060.0  14.94   1  1  4  0
```

Decay Time: Two decay times are addressed. Six years cooling is assumed for Type I assemblies, and 10 years is assumed for Type II assemblies. The remainder of this Appendix will demonstrate that a 29,000 MWd/MTU, 2 w/o U-235 assembly cooled for these times satisfies the design criteria.

```
TIT      29,000 MWD/MTU AFTER  6.0 YEARS
DEC             6.00   -1       1        5        4
DEC             6.00   -2       2        5        4
DEC             6.00   -3       3        5        4
DEC             6.00   -4       4        5        4
HED            1 IN-CORE
HED            2 TOP
HED            3 PLENUM
HED            4 BOTTOM
OUT      -4   1   -1   0
TIT      29,000 MWD/MTU AFTER  10.0 YEARS
DEC            10.00   -1       1        5        4
DEC            10.00   -2       2        5        4
DEC            10.00   -3       3        5        4
DEC            10.00   -4       4        5        4
HED            1 IN-CORE
HED            2 TOP
HED            3 PLENUM
HED            4 BOTTOM
OUT      -4   1   -1   0
```

Actinide Composition: The U-235 mass (grams U-235 per MTU) has been changed to represent an initial enrichment of 2.0 w/o U-235. The U-238 mass has also been changed to maintain a total uranium weight of 1×10^6 grams per metric ton.

```
2      922340  240.00  922350 20000.0  922380  979760.00  0   0.0 FUEL
ACTINIDES
```

(C) Case 3 - BW35-R0

The Case 1 ORIGEN2 model (35,000 MWd/MTU, 2.67 w/o U-235) is based on file BW40-R2A.INP from Appendix 5.5.2. All inputs are identical with the exception of: (1) The power irradiation was changed to account for the 35,000 MWd/MTU fuel burnup; (2) The decay times were changed as required for this calculation; and (3) The actinide composition was changed to account for the 2.67 w/o U-235 enrichment. The input cards which have been changed relative to those in Appendix 5.5.2 are shown below.

Specific Power: changed to 18.03 MW/assy which corresponds to a burnup of 35,000 MWd/MTU accumulated over 900 full power days (0.4636 MTU).

```
IRP      60.0  18.03  -6  1  4  2
IRP     120.0  18.03   1  1  4  0
IRP     180.0  18.03   1  1  4  0
IRP     240.0  18.03   1  1  4  0
IRP     300.0  18.03   1  1  4  0
DEC     380.0          1  1  4  0
IRP     440.0  18.03   1  1  4  0
IRP     500.0  18.03   1  1  4  0
IRP     560.0  18.03   1  1  4  0
IRP     620.0  18.03   1  1  4  0
IRP     680.0  18.03   1  1  4  0
DEC     760.0          1  1  4  0
IRP     820.0  18.03   1  1  4  0
IRP     880.0  18.03   1  1  4  0
IRP     940.0  18.03   1  1  4  0
IRP    1000.0  18.03   1  1  4  0
IRP    1060.0  18.03   1  1  4  0
```

Decay Time: Two decay times are addressed. Seven years cooling is assumed for Type I assemblies, and 14 years is assumed for Type II assemblies. The remainder of this Appendix will demonstrate that a 2935,000 MWd/MTU, 2.67 w/o U-235 assembly cooled for these times satisfies the design criteria.

```
TIT      35,000 MWD/MTU AFTER 7.0 YEARS
DEC              7.00   -1         1        5        4
DEC              7.00   -2         2        5        4
DEC              7.00   -3         3        5        4
DEC              7.00   -4         4        5        4
HED            1 IN-CORE
HED            2 TOP
HED            3 PLENUM
HED            4 BOTTOM
```

```
OUT      -4   1    -1    0
TIT      35,000 MWD/MTU AFTER 14.0 YEARS
DEC             14.00    -1          1          5          4
DEC             14.00    -2          2          5          4
DEC             14.00    -3          3          5          4
DEC             14.00    -4          4          5          4
HED             1 IN-CORE
HED             2 TOP
HED             3 PLENUM
HED             4 BOTTOM
OUT      -4   1    -1    0
```

Actinide Composition: The U-235 mass (grams U-235 per MTU) has been changed to represent an initial enrichment of 2.67 w/o U-235. The U-238 mass has also been changed to maintain a total uranium weight of 1×10^6 grams per metric ton.

```
2    922340   240.00   922350   26700.00   922380   973060.00   0   0.0 FUEL
ACTINIDES
```

5.5.8.1.3 ORIGEN2 Results

The ORIGEN2 results for each case are summarized in Table 5.5.8-2. The values in the "Neutron" column are taken from the overall total portion of ORIGEN2's neutron table, summed across the four fuel assembly regions. The decay heat data shown in Table 5.5.8-2 is taken from the cumulative totals portion of ORIGEN2's thermal power table, again summed across the four assembly regions. The total gamma source for each assembly is equal to the sum of the source in each of ORIGEN2's 18 energy groups for the four assembly regions and three photon tables (activation products, actinides and daughters, and fission products). Data is provided in Table 5.5.8-2 for all three cases and for both Type I (shorter cooling) and Type II (longer cooling) fuel. The design basis data from Section 5.2 is provided as well (denoted "DB" and shown in italic). The values in Table 5.5.8-2 are all total source per assembly and include all contributions from the in-core region, top and bottom end fittings, and the gas plenum. Contributions from control components are not included in Table 5.5.8-2.

The results shown in Table 5.5.8-2 are suitable for determining compliance with the second and third acceptance criteria. The total decay heats for each case are below the decay heat limits for both Type I and Type II assemblies. Criterion (b) is, therefore, satisfied. The total neutron sources for each case, for both Type I and Type II assemblies, are less than those for the design basis case. Criterion (c) is, therefore, satisfied.

Table 5.5.8-2

ORIGEN2 Result Summary

Case	Enrichment (w/o U-235)	Burnup (MWd/MTU)	Type I Neutron (n/s/assy)	Type I Gamma (γ/s/assy)	Type II Neutron (n/s/assy)	Type II Gamma (γ/s/assy)	Decay Heat Type I (W/assy)	Decay Heat Type II (W/assy)
1	3.00	37,000	2.087E+08	4.658E+15	1.674E+08	3.344E+15	699.8	545.7
2	2.00	29,000	1.725E+08	4.544E+15	1.488E+08	3.071E+15	652.4	479.5
3	2.67	35,000	2.182E+08	4.872E+15	1.687E+08	3.138E+15	721.3	518.4
DB	*3.19*	*40,000*	*2.455E+08*	*4.672E+15*	*1.829E+08*	*3.280E+15*	*764.0*	*562.5*

The total in-core gamma source and spectrum is used to calculate the dose rates on the cask surface to determine compliance with acceptance criterion (a). This information is provided for each case in Table 5.5.8-3. The values in Table 5.5.8-3 are calculated by summing the activation product, actinide and daughter, and fission product source in the in-core region for each ORIGEN2 energy group and converting. Conversion of these spectra to an energy structure format useable in ANISN is (described in the next section and in Section 5.2.1.4). Contributions from the end fittings, gas plenum, and control components are not shown in Table 5.5.8-3.

Table 5.5.8-3

ORIGEN2 In-Core Gamma Results by Energy Group

		In-Core CASK Source (γ/s/assy)							
Cask Group	E_{upper} (MeV)	Case 1 Type I	Case 1 Type II	Case 2 Type I	Case 2 Type II	Case 3 Type I	Case 3 Type II	Design Basis Type I	Design Basis Type II
23	10.00	1.191E+05	9.507E+04	9.863E+04	8.485E+04	1.247E+05	9.584E+04	1.402E+05	1.038E+05
24	8.00	7.487E+05	5.975E+05	6.198E+05	5.333E+05	7.834E+05	6.024E+05	8.808E+05	6.525E+05
25	6.50	4.334E+06	3.460E+06	3.589E+06	3.088E+06	4.537E+06	3.489E+06	5.100E+06	3.779E+06
26	5.00	4.945E+06	3.948E+06	4.095E+06	3.523E+06	5.177E+06	3.980E+06	5.819E+06	4.311E+06
27	4.00	1.387E+09	3.884E+07	4.614E+09	3.100E+08	2.699E+09	3.865E+07	7.676E+08	2.136E+07
28	3.00	1.079E+10	4.176E+08	3.582E+10	2.429E+09	2.093E+10	3.978E+08	5.995E+09	3.094E+08
29	2.50	1.993E+11	1.993E+09	8.208E+11	3.223E+10	4.312E+11	1.934E+09	9.584E+10	3.839E+08
30	2.00	1.531E+12	8.690E+11	1.782E+12	9.254E+11	1.733E+12	8.276E+11	1.495E+12	7.686E+11
31	1.66	4.803E+13	2.380E+13	5.527E+13	3.248E+13	5.355E+13	2.313E+13	4.591E+13	1.895E+13
32	1.33	1.117E+14	5.523E+13	1.285E+14	7.569E+13	1.245E+14	5.369E+13	1.068E+14	4.386E+13
33	1.00	1.719E+14	4.334E+13	2.126E+14	7.202E+13	2.138E+14	4.091E+13	1.480E+14	3.030E+13
34	0.80	7.953E+14	5.405E+14	7.693E+14	5.139E+14	8.418E+14	5.111E+14	7.892E+14	5.274E+14
35	0.60	1.308E+15	9.702E+14	1.217E+15	8.886E+14	1.350E+15	9.174E+14	1.323E+15	9.598E+14
36	0.40	4.074E+13	2.515E+13	4.707E+13	2.504E+13	4.523E+13	2.332E+13	3.895E+13	2.393E+13
37	0.30	6.182E+13	4.688E+13	6.256E+13	4.054E+13	6.439E+13	4.336E+13	6.240E+13	4.650E+13
38	0.20	1.767E+14	1.249E+14	1.778E+14	1.142E+14	1.857E+14	1.165E+14	1.782E+14	1.200E+14
39	0.10	2.906E+14	2.294E+14	2.809E+14	1.946E+14	2.984E+14	2.137E+14	2.957E+14	2.298E+14
40	0.05	1.634E+15	1.276E+15	1.567E+15	1.100E+15	1.672E+15	1.186E+15	1.665E+15	1.273E+15
	Total	4.641E+15	3.336E+15	4.521E+15	3.058E+15	4.851E+15	3.130E+15	4.654E+15	3.274E+15

5.5.8.1.4 ANISN Source Term Generation

Derivation of source terms for use in the ANISN shielding models is performed in the following sections for neutrons and gammas. The ANISN models require volumetric source terms (particles per second per cubic centimeter) in the CASK-81 [5.4] energy group format. This calculation is performed in a manner identical to that described in Section 5.2.1.4.

The ANISN neutron source for each group is equal to the total neutron source per assembly (from Table 5.5.8-2) multiplied by 24 (the number of assemblies), divided by the active fuel volume (5,633,674 cm), and multiplied by the normalized group fraction. The results of these calculations for each case are shown in Table 5.5.8-4.

Table 5.5.8-4

Neutron Source Calculations

		CASK Grouped Volumetric Source (n/s/cm3)					
	^{244}Cm	Case 1		Case 2		Case 3	
Cask Group	Fraction	Type I	Type II	Type I	Type II	Type I	Type II
1	2.018E-04	1.794E-01	1.439E-01	1.483E-01	1.279E-01	1.876E-01	1.450E-01
2	1.146E-03	1.019E+00	8.173E-01	8.422E-01	7.265E-01	1.065E+00	8.236E-01
3	4.471E-03	3.975E+00	3.188E+00	3.286E+00	2.834E+00	4.156E+00	3.213E+00
4	1.768E-02	1.572E+01	1.261E+01	1.299E+01	1.121E+01	1.643E+01	1.271E+01
5	4.167E-02	3.705E+01	2.972E+01	3.062E+01	2.641E+01	3.873E+01	2.995E+01
6	5.641E-02	5.015E+01	4.023E+01	4.145E+01	3.576E+01	5.244E+01	4.054E+01
7	1.197E-01	1.064E+02	8.536E+01	8.796E+01	7.588E+01	1.113E+02	8.603E+01
8	9.616E-02	8.549E+01	6.858E+01	7.066E+01	6.096E+01	8.939E+01	6.911E+01
9	2.256E-02	2.006E+01	1.609E+01	1.658E+01	1.430E+01	2.097E+01	1.621E+01
10	1.227E-01	1.091E+02	8.750E+01	9.017E+01	7.778E+01	1.141E+02	8.818E+01
11	2.110E-01	1.876E+02	1.505E+02	1.551E+02	1.338E+02	1.961E+02	1.516E+02
12	1.794E-01	1.595E+02	1.279E+02	1.318E+02	1.137E+02	1.668E+02	1.289E+02
13	1.138E-01	1.012E+02	8.116E+01	8.363E+01	7.214E+01	1.058E+02	8.179E+01
14	1.301E-02	1.157E+01	9.278E+00	9.561E+00	8.247E+00	1.209E+01	9.350E+00
15	6.555E-05	5.828E-02	4.675E-02	4.817E-02	4.155E-02	6.093E-02	4.711E-02
16	4.765E-06	4.236E-03	3.398E-03	3.502E-03	3.021E-03	4.429E-03	3.425E-03
17	3.134E-07	2.786E-04	2.235E-04	2.303E-04	1.987E-04	2.913E-04	2.252E-04
18	4.527E-08	4.025E-05	3.228E-05	3.327E-05	2.870E-05	4.208E-05	3.253E-05
19	9.759E-09	8.677E-06	6.960E-06	7.172E-06	6.186E-06	9.072E-06	7.014E-06
20	1.521E-09	1.352E-06	1.085E-06	1.118E-06	9.642E-07	1.414E-06	1.093E-06
21	3.353E-10	2.981E-07	2.391E-07	2.464E-07	2.125E-07	3.117E-07	2.410E-07
22	9.683E-11	8.609E-08	6.905E-08	7.116E-08	6.138E-08	9.001E-08	6.959E-08
Total		8.891E+02	7.131E+02	7.349E+02	6.339E+02	9.295E+02	7.187E+02

Gamma source terms for use in ANISN are calculated using the same methodology as is described in Section 5.2.1.4. The gamma sources shown in Table 5.5.8-3 are converted to volumetric sources (multiplied by 24 and divided by the volume: 5,633,674 cm) and mapped into the CASK-81 energy structure. The mapping functions are shown in Table 5.2-10. The resulting in-core gamma source terms are shown in Table 5.5.8-5. The results in Table 5.5.8-5 include the in-core gamma source contribution for each case. Table 5.5.8-5 does not include contributions from end fittings or control components. Activated hardware sources are provided in Table 5.5.8-8.

Table 5.5.8-5

Gamma Source Calculations

Cask Group	CASK Grouped Volumetric Source (γ/s/cm3)					
	Case 1		Case 2		Case 3	
	Type I	Type II	Type I	Type II	Type I	Type II
23	5.074E-01	4.050E-01	4.202E-01	3.615E-01	5.312E-01	4.083E-01
24	3.190E+00	2.546E+00	2.641E+00	2.272E+00	3.337E+00	2.566E+00
25	1.846E+01	1.474E+01	1.529E+01	1.316E+01	1.933E+01	1.486E+01
26	2.107E+01	1.682E+01	1.744E+01	1.501E+01	2.206E+01	1.696E+01
27	5.909E+03	1.655E+02	1.966E+04	1.321E+03	1.150E+04	1.647E+02
28	4.595E+04	1.779E+03	1.526E+05	1.035E+04	8.917E+04	1.695E+03
29	8.492E+05	8.490E+03	3.497E+06	1.373E+05	1.837E+06	8.240E+03
30	6.521E+06	3.702E+06	7.592E+06	3.942E+06	7.382E+06	3.525E+06
31	2.046E+08	1.014E+08	2.354E+08	1.384E+08	2.281E+08	9.854E+07
32	4.759E+08	2.353E+08	5.475E+08	3.224E+08	5.305E+08	2.287E+08
33	7.325E+08	1.846E+08	9.058E+08	3.068E+08	9.106E+08	1.743E+08
34	3.388E+09	2.303E+09	3.277E+09	2.189E+09	3.586E+09	2.177E+09
35	5.574E+09	4.133E+09	5.186E+09	3.785E+09	5.753E+09	3.908E+09
36	1.736E+08	1.071E+08	2.005E+08	1.067E+08	1.927E+08	9.935E+07
37	2.634E+08	1.997E+08	2.665E+08	1.727E+08	2.743E+08	1.847E+08
38	7.526E+08	5.323E+08	7.576E+08	4.866E+08	7.911E+08	4.965E+08
39	1.238E+09	9.774E+08	1.196E+09	8.289E+08	1.271E+09	9.102E+08
40	6.960E+09	5.436E+09	6.677E+09	4.686E+09	7.121E+09	5.053E+09
Total	1.977E+10	1.421E+10	1.926E+10	1.303E+10	2.067E+10	1.333E+10

5.5.8.1.5 ANISN Dose Rate Calculations

The ANISN discrete-ordinates computer code is used to calculate the dose rate on the surface of the NUHOMS®-MP187 cask. Because the ANISN code is one-dimensional, the model is representative only of the dose rate along the neutron shield. These ANISN models are similar to those described in Section 5.2.1.3 (which are provided in Appendix 5.5.5), the only differences being the neutron and gamma source terms. These are taken directly from Table 5.5.8-4 (neutrons) and Table 5.5.8-5 (gammas).

Six ANISN runs are used to calculate the dose rate for each case, for both Type I and Type II assemblies. The neutron and gamma dose rates on the surface of the cask (interval 72) are shown in Table 5.5.8-6, as are the corresponding design basis dose rates from Figure 5.2-2 and Figure 5.2-3 (denoted "DB" and shown in italic).

The dose rates calculated by ANISN are based on assembly average enrichment and burnup. Peaking factors of 1.12 are applied to the gamma dose rates and 1.12^4 are applied to the neutron dose rates to calculate the total centerline dose rates. This is identical to the methodology used in Section 5.2.1.3. These totals are shown in Table 5.5.8-7. Table 5.5.8-7 demonstrates compliance with acceptance criterion (a) because the total dose rate for each case is bounded by the total dose rate for the design basis case.

Table 5.5.8-6

ANISN Dose Rate Results

	ANISN Results (mrem/hr)			
	Type I		Type II	
Case	Neutron	Gamma	Neutron	Gamma
DB	*2.46E+01*	*2.04E+01*	*1.83E+01*	*9.21E+00*
1	2.09E+01	2.12E+01	1.68E+01	1.09E+01
2	1.73E+01	2.53E+01	1.49E+01	1.40E+01
3	2.18E+01	2.41E+01	1.69E+01	1.06E+01

Table 5.5.8-7

Total Dose Rate Results

	Peaked Results (mrem/hr)					
	Type I			Type II		
Case	Neutron	Gamma	Total	Neutron	Gamma	Total
DB	*3.87E+01*	*2.29E+01*	*6.15E+01*	*2.88E+01*	*1.03E+01*	*3.91E+01*
1	3.29E+01	2.37E+01	5.66E+01	2.64E+01	1.22E+01	3.86E+01
2	2.72E+01	2.84E+01	5.55E+01	2.34E+01	1.56E+01	3.91E+01
3	3.44E+01	2.70E+01	6.13E+01	2.66E+01	1.19E+01	3.85E+01

5.5.8.1.6 DORT Model Generation

DORT models have been generated for each of the three cases to calculate dose rates on the package surface, vehicle outer surface, and 2-meters from the vehicle outer surface. These models are identical to the FC-DSC models described in Section 5.4.1, with the exception of the source terms. The FC-DSC, which includes control components, was selected for this evaluation because:

1. The FC-DSC produces the bounding total dose rates for all locations on the vehicle outer surface and at 2-meters from the vehicle outer surface. The FC-DSC 2-meter dose rate of 9.94 mrem/hr is the design basis value with the least margin relative to the regulatory limits.

2. The FC-DSC produces the larger gamma dose rate at all locations. The three cases evaluated herein have larger gamma source terms than the original design basis case. Utilizing the FC-DSC model will, therefore, calculate the largest gamma dose rates. All neutron source terms calculated herein are less than those used in the design basis analysis.

3. The peak dose rate on the package surface, calculated for the FO-DSC, is due completely to the streaming of neutrons through the trunnion sleeve. Because the neutron source terms for all three cases included in this section are less than those used for the design basis evaluation, the FO-DSC package surface dose rate at this location will decrease.

As discussed in Section 5.4.1.2, there are four DORT models required for each case: neutron, in-core gamma, top end fitting gamma, and bottom end-fitting gamma. The neutron source terms for the DORT models are identical to those used in the ANISN models, listed above in Table 5.5.8-4. The in-core gamma source term for each case is equal to the sum of the data in Table 5.5.8-5 and the control component source. These contributions are added group-by-group. The design basis (gray APSRA) control component sources (per assembly) are listed in Table 5.2-11. The total FC-DSC gamma source for the in-core region is shown in Table 5.5.8-8 for each case. Top and bottom sources are also shown in Table 5.5.8-8. These sources were calculated in the same manner as were the in-core sources. The top source includes contributions from the plenum, top end fitting, and control components. The bottom source includes only the bottom end fitting. As with the design basis analysis, all dose rates are calculated using the Type II assembly source and are multiplied by 1.03 to account for the presence of Type I fuel assemblies in the inner four fuel cells. This correction factor was determined in Section 5.4.1.2 and was selected to bound both neutrons and gammas. However, because the factor calculated for neutrons is greater than that for gammas, use of the 1.03 factor herein is conservative.

Table 5.5.8-8

FC-DSC Gamma Source Terms for DORT Calculations

Cask	Case 1 (γ/s/cm^3)			Case 2 (γ/s/cm^3)			Case 3 (γ/s/cm^3)		
Group	In-Core	Bottom	Top	In-Core	Bottom	Top	In-Core	Bottom	Top
23	4.050E-01	2.685E-11	3.779E-11	3.615E-01	2.377E-11	3.344E-11	4.083E-01	2.674E-11	3.764E-11
24	2.546E+00	1.701E-10	2.393E-10	2.272E+00	1.505E-10	2.117E-10	2.566E+00	1.695E-10	2.385E-10
25	1.474E+01	1.001E-09	1.409E-09	1.316E+01	8.843E-10	1.244E-09	1.486E+01	9.971E-10	1.403E-09
26	1.682E+01	1.143E-09	1.609E-09	1.501E+01	1.010E-09	1.421E-09	1.696E+01	1.139E-09	1.603E-09
27	1.655E+02	2.515E-07	3.540E-07	1.321E+03	3.444E-06	4.836E-06	1.647E+02	2.483E-07	3.492E-07
28	1.789E+03	4.477E+00	2.752E+00	1.036E+04	7.602E+00	4.034E+00	1.705E+03	4.458E+00	2.744E+00
29	1.174E+04	1.447E+03	8.892E+02	1.406E+05	2.457E+03	1.304E+03	1.149E+04	1.440E+03	8.867E+02
30	3.702E+06	3.188E-03	4.487E-03	3.942E+06	4.044E-03	5.690E-03	3.525E+06	3.174E-03	4.466E-03
31	2.836E+08	8.108E+07	4.983E+07	3.206E+08	1.377E+08	7.305E+07	2.807E+08	8.074E+07	4.969E+07
32	6.665E+08	1.919E+08	1.179E+08	7.537E+08	3.259E+08	1.729E+08	6.600E+08	1.911E+08	1.176E+08
33	1.855E+08	1.134E+05	1.255E+05	3.076E+08	1.621E+05	1.339E+05	1.751E+08	1.132E+05	1.254E+05
34	2.303E+09	1.586E+05	2.027E+05	2.190E+09	3.092E+05	3.785E+05	2.178E+09	1.579E+05	2.018E+05
35	4.133E+09	2.313E+05	3.226E+05	3.785E+09	5.388E+05	7.527E+05	3.908E+09	2.299E+05	3.206E+05
36	1.072E+08	1.514E+05	2.068E+05	1.067E+08	3.491E+05	4.795E+05	9.937E+07	1.505E+05	2.055E+05
37	1.998E+08	4.338E+04	4.244E+04	1.727E+08	8.637E+04	8.666E+04	1.848E+08	4.317E+04	4.223E+04
38	5.326E+08	1.554E+05	1.089E+05	4.869E+08	2.746E+05	1.804E+05	4.968E+08	1.548E+05	1.085E+05
39	9.795E+08	9.358E+05	5.782E+05	8.310E+08	1.591E+06	8.516E+05	9.123E+08	9.317E+05	5.765E+05
40	5.459E+09	1.024E+07	6.687E+06	4.708E+09	1.755E+07	1.037E+07	5.076E+09	1.020E+07	6.665E+06
Total	1.485E+10	2.850E+08	1.760E+08	1.367E+10	4.845E+08	2.592E+08	1.397E+10	2.838E+08	1.755E+08

(A) Case 1: 37,000 MWd/MTU

Four Case 1 DORT models were run to calculate the dose rates around the MP187 cask containing 37,000 MWd/MTU fuel assemblies. These runs are identical to those provided in Appendix 5.5.4, with the exception of the source terms. Source terms are given in Table 5.5.8-4 (neutron) and Table 5.5.8-8 (gamma).

The dose rate contributions from all of the models are summed node-by-node to calculate the total dose rate at each location around the cask. This was done in an identical manner to the DORT data reduction described in Section 5.4.2. Dose rates adjacent to the trunnions (DORT Jmeshes 117-128) include contributions from the trunnion streaming analysis provided in Section 5.4.1.8.1. Trunnion contributions are added to each of the affected nodes for the package surface dose rates (per Table 5.4-5), vehicle surface dose rates (per Table 5.4-7), and 2-meter dose rates (Table 5.4-8).

The trunnion dose rates are based on the design basis source terms evaluated in Section 5.4.1.8.1. The trunnion evaluation concluded that the presence of the trunnions increases the neutron dose rates while decreasing the gamma dose rates. Because the design basis neutron source bounds the neutron sources calculated for the three cases addressed herein, the trunnion dose rates calculated in Section 5.4.1.8.1 may conservatively be used in this calculation.

The maximum neutron, gamma, and total dose rates along the side, top, and bottom of the package are shown in Table 5.5.8-9. Comparisons between Table 5.5.8-9 and the results presented in Table 5.4-15 show while the gamma doses have increased, all of the "total" dose rates calculated for Case 1 are bounded by those of the design basis case. Acceptance criteria numbers (d), (e), and (f) are satisfied for Case 1.

It should also be noted that the dose rate on the lower external surface of the vehicle calculated in 5.4.1.8.3 remains bounding for all of the cases addressed herein. The calculated dose rate at this location was 190.3 mrem/hr, of which 189.9 mrem/hr (99.8%) was due to neutrons. Because the design basis neutron source bounds those of the three cases evaluated herein, the maximum shear key dose rate will be unaffected by this calculation.

Table 5.5.8-9

Case 1 Dose Rate Results

	Package Surface		
	Side (mrem/hr)	Top (mrem/hr)	Bottom (mrem/hr)
Normal Conditions			
Gamma	1.97E+1	2.07E-1	6.72E-1
Neutron	1.77E+2	6.21E-1	1.20E+0
Total	1.82E+2	8.01E-1	1.53E+0
10 CFR71 Limit	1.00E+3	1.00E+3	1.00E+3
	Vehicle Outer Surface		
	Side (mrem/hr)	Top (mrem/hr)	Bottom (mrem/hr)
Normal Conditions			
Gamma	1.13E+1	2.07E-1	6.72E-1
Neutron	4.69E+1	6.21E-1	1.20E+0
Total	5.20E+1	8.01E-1	1.53E+0
10 CFR71 Limit	2.00E+2	2.00E+2	2.00E+2
	2 Meters from Vehicle Outer Surface		
	Side (mrem/hr)	Top (mrem/hr)	Bottom (mrem/hr)
Normal Conditions			
Gamma	3.35E+0	5.91E-2	2.25E-1
Neutron	6.44E+0	2.77E-1	4.93E-1
Total	9.56E+0	3.09E-1	6.33E-1
10 CFR71 Limit	1.00E+1	1.00E+1	1.00E+1

(B) Case 2: 29,000 MWd/MTU

Four Case 2 DORT models were run to calculate the dose rates around the MP187 cask containing 29,000 MWd/MTU fuel assemblies. These runs are identical to those provided in Appendix 5.5.4, with the exception of the source terms. Source terms are given in Table 5.5.8-4 (neutron) and Table 5.5.8-8 (gamma).

The dose rate contributions from all of the models are combined in the same manner as was described above for Case 1. The maximum neutron, gamma, and total dose rates along the side, top, and bottom of the package are shown in Table 5.5.8-10. Comparisons between Table 5.5.8-10 and the results presented in Table 5.4-15 show while the gamma doses have increased, all of the "total" dose rates calculated for Case 2 are bounded by those of the design basis case. Acceptance criteria numbers (d), (e), and (f) are satisfied for Case 2.

Table 5.5.8-10

Case 2 Dose Rate Results

	Package Surface Side (mrem/hr)	Package Surface Top (mrem/hr)	Package Surface Bottom (mrem/hr)
Normal Conditions			
Gamma	2.16E+1	2.17E-1	7.87E-1
Neutron	1.57E+2	5.52E-1	1.06E+0
Total	1.63E+2	7.68E-1	1.46E+0
10 CFR71 Limit	1.00E+3	1.00E+3	1.00E+3
	Vehicle Outer Surface Side (mrem/hr)	Top (mrem/hr)	Bottom (mrem/hr)
Normal Conditions			
Gamma	1.25E+1	2.17E-1	7.87E-1
Neutron	4.17E+1	5.52E-1	1.06E+0
Total	4.85E+1	7.68E-1	1.46E+0
10 CFR71 Limit	2.00E+2	2.00E+2	2.00E+2
	2 Meters from Vehicle Outer Surface Side (mrem/hr)	Top (mrem/hr)	Bottom (mrem/hr)
Normal Conditions			
Gamma	3.75E+0	5.25E-2	2.61E-1
Neutron	5.73E+0	2.46E-1	4.38E-1
Total	9.26E+0	2.74E-1	6.01E-1
10 CFR71 Limit	1.00E+1	1.00E+1	1.00E+1

(C) Case 3: 35,000 MWd/MTU

Four Case 3 DORT models were run to calculate the dose rates around the MP187 cask containing 35,000 MWd/MTU fuel assemblies. These runs are identical to those provided in Appendix 5.5.4, with the exception of the source terms. Source terms are given in Table 5.5.8-4 (neutron) and Table 5.5.8-8 (gamma).

The dose rate contributions from all of the models are combined in the same manner as was described above for Case 1. The maximum neutron, gamma, and total dose rates along the side, top, and bottom of the package are shown in Table 5.5.8-11. Comparisons between Table 5.5.8-11 and the results presented in Table 5.4-15 show while the gamma doses have increased, all of the "total" dose rates calculated for Case 3 are bounded by those of the design basis case. Acceptance criteria numbers (d), (e), and (f) are satisfied for Case 3.

Table 5.5.8-11

Case 3 Dose Rate Results

	Package Surface		
	Side (mrem/hr)	Top (mrem/hr)	Bottom (mrem/hr)
Normal Conditions			
Gamma	1.95E+1	2.08E-1	6.73E-1
Neutron	1.78E+2	6.26E-1	1.21E+0
Total	1.83E+2	8.06E-1	1.54E+0
10 CFR71 Limit	1.00E+3	1.00E+3	1.00E+3
	Vehicle Outer Surface		
	Side (mrem/hr)	Top (mrem/hr)	Bottom (mrem/hr)
Normal Conditions			
Gamma	1.12E+1	2.08E-1	6.73E-1
Neutron	4.73E+1	6.26E-1	1.21E+0
Total	5.23E+1	8.06E-1	1.54E+0
10 CFR71 Limit	2.00E+2	2.00E+2	2.00E+2
	2 Meters from Vehicle Outer Surface		
	Side (mrem/hr)	Top (mrem/hr)	Bottom (mrem/hr)
Normal Conditions			
Gamma	3.32E+0	5.95E-2	2.26E-1
Neutron	6.49E+0	2.79E-1	4.97E-1
Total	9.58E+0	3.11E-1	6.37E-1
10 CFR71 Limit	1.00E+1	1.00E+1	1.00E+1

(D) Hypothetical Accident Conditions

The hypothetical accident condition DORT models provided in Appendix 5.5.4 have been revised to incorporate the Case 2 source terms defined above. Case 2 was selected because, as shown in Table 5.5.8-10, the Case 2 gamma dose rates bound those of Cases 1 and 3. The bounding gamma case was selected because a significant portion of the hypothetical accident dose rates is due to gamma streaming through the postulated lead-slump gap. Four hypothetical accident models were run to account for each of the source regions. The results of the runs were summed node-by-node and are summarized in Table 5.5.8-12.

Table 5.5.8-12

Hypothetical Accident Dose Rate Results

	Package Surface			1 Meter from Surface of Package		
Normal Conditions	Side (mrem/hr)	Top (mrem/hr)	Bottom (mrem/hr)	Side (mrem/hr)	Top (mrem/hr)	Bottom (mrem/hr)
Gamma (max)	3.01E+03	1.67E+01	9.99E+00	3.23E+02	2.28E+00	3.14E+00
Neutron (max)	8.53E+02	6.94E+01	1.29E+02	3.61E+02	2.91E+01	4.68E+01
Total (max)	3.10E+03	7.03E+01	1.38E+02	4.08E+02	2.99E+01	5.00E+01
10 CFR Part 71 Limit				1.00E+03	1.00E+03	1.00E+03

Comparisons between Table 5.5.8-12 and Table 5.4-16 show that while the gamma dose rates have nearly doubled for the Case 2 source, the total dose rates remain bounded by those calculated in Table 5.4-16. Acceptance criterion (g) is, therefore, satisfied.

5.5.8.1.7 Conclusions

As documented in Section 5.5.8.1.3, Table 5.5.8-2; and in Section 5.5.8.1.5, Table 5.5.8-7; and Section 5.5.8.1.6, Table 5.5.8-9, Table 5.5.8-10, Table 5.5.8-11, and Table 5.5.8-12, all of the acceptance criteria defined in Paragraph 5 of Section 5.5.8 have been satisfied for the three burnup/enrichment cases modeled herein. The following alternate fuel qualification table provided as Table 5.5.8-13 is, therefore, justified by this calculation. Table 5.5.8-14 provides a summary of the maximum calculated gamma, neutron, and total dose rates at the package surface, vehicle outer surface, two meters from the vehicle outer surface, and one meter from the surface of the package. This summary provides the bounding results from the design basis case and the three cases addressed in this Appendix.

Table 5.5.8-13

Alternate Cooling Times for Fuel Qualification

Maximum Burnup[1] (MWd/MTIHM)	Minimum Enrichment (w/o U-235)	Minimum Required Type I Cooling Time (years)	Minimum Required Type II Cooling Time (years)
29,000	2.00	6	10
35,000	2.67	7	14
37,000	3.00	8	14

(1) Actual fuel burnup shall be rounded up to the values shown in this column to determine applicable enrichment and cooling limits. For example, an assembly with a burnup of 29,300 MWd/MTIHM would have a minimum enrichment limit of 2.67 w/o U-235 and required cooling times of 7 years and 14 years for Type I and Type II, respectively.

Table 5.5.8-14

Summary of Maximum Package Dose Rates

	Package Surface		
	Side (mrem/hr)	Top (mrem/hr)	Bottom (mrem/hr)
Normal Conditions			
Gamma(1)	2.16E+1	2.18E-1	7.87E-1
Neutron(2)	1.93E+2	6.79E-1	1.31E+0
Total(2)	1.98E+2	8.47E-1	1.62E+0
10 CFR71 Limit	1.00E+3	1.00E+3	1.00E+3
	Vehicle Outer Surface		
	Side (mrem/hr)	Top (mrem/hr)	Bottom (mrem/hr)
Normal Conditions			
Gamma(1)	1.25E+1	2.18E-1	7.87E-1
Neutron(2)	5.13E+1	6.79E-1	1.31E+0
Total(2)	5.56E+1	8.47E-1	1.62E+0
10 CFR71 Limit	2.00E+2	2.00E+2	2.00E+2
	2 Meters from Vehicle Outer Surface		
	Side (mrem/hr)	Top (mrem/hr)	Bottom (mrem/hr)
Normal Conditions			
Gamma(1)	3.75E+0	6.46E-2	2.61E-1
Neutron(2)	7.04E+0	3.02E-1	5.39E-1
Total(2)	9.94E+0	3.37E-1	6.72E-1
10 CFR71 Limit	1.00E+1	1.00E+1	1.00E+1
	1 Meter from Surface of Package		
	Side (mrem/hr)	Top (mrem/hr)	Bottom (mrem/hr)
Hypothetical Accident Conditions			
Gamma(1)	3.23E+2	2.28E+0	3.14E+0
Neutron(3)	4.43E+2	3.57E+1	5.75E+1
Total(3)	4.83E+2	3.63E+1	5.93E+1
10 CFR71 Limit	1.00E+3	1.00E+3	1.00E+3

(1) Side and Bottom results taken from Case 2.
Top results per (2) and (3), below.
(2) Result taken from Table 5.4-15
(3) Result taken fromTable 5.4-16

6. CRITICALITY EVALUATION

This chapter describes the engineering/physics design elements of the NUHOMS®-MP187 Package which are important to safety and necessary to comply with the performance requirements specified in Sections 71.55 and 71.59 of 10 CFR Part 71 [6.1].

The results of detailed analyses are presented which demonstrate that the NUHOMS®-MP187 Package is critically safe, under normal and accident conditions, considering a variety of mechanical uncertainties. Sufficient detail has been included herein to permit reviewers to accomplish an independent evaluation of the criticality analyses. Much of this detail is available in the Appendix in which computer inputs have been provided for review.

6.1 Discussion and Results

6.1.1 NUHOMS®-MP187 Cask Design Features

The NUHOMS®-MP187 Package is designed to provide criticality control through a combination of mechanical and neutronic isolation of fuel assemblies. Unlike traditional spent fuel shipping packages, the NUHOMS®-MP187 Cask is designed to carry a payload of canisterized fuel. The dry shielded canisters (DSCs) are suitable for use in the NUHOMS®-24P dry storage system, and for transportation in the NUHOMS®-MP187 Cask. This SAR addresses three specific types of DSCs and one design basis fuel assembly type. Other fuel assembly types having varied characteristics will be licensed by amendment to the certificate of compliance for this package.

6.1.2 Fuel-Only (FO) DSC Design Features

The principal performance features of the NUHOMS®-MP187 Cask and FO-DSC as they relate to criticality control are:

A. The package is designed such that it would be subcritical if water were to leak into or out of the canister. No credit is taken for the containment capability of the canister to exclude moderator from the fuel matrix (10CFR71.55 b).

B. The criticality analyses have been performed with consideration for the most reactive credible configuration consistent with the chemical and physical form of the material (10CFR71.55b1), moderation by water to the most reactive credible extent (10CFR71.55b2), and close full reflection by water on all sides or such greater reflection of the containment system as may additionally be provided by the surrounding material of the packaging (10CFR71.55b3).

C. Any number of undamaged, or damaged (10CFR71.73) packages will remain subcritical in any arrangement with close full water reflection and optimum interspersed hydrogenous moderation. Therefore, the transport index for the package is zero (10CFR71.59b).

The FO-DSC support structure is composed of four axially oriented support rods and twenty-six spacer discs. This basket assembly provides positive location for twenty-four fuel assemblies under both normal operating condition (NOC) and post-hypothetical accident conditions (HAC). The basket assembly utilizes fixed neutron absorbers which isolate each fuel assembly. Guide sleeves are designed to permit unrestricted flooding and draining of fuel cells.

The absorber panel material was chosen due to its desirable neutron attenuation, low density, and minimal thickness. It has been used for applications and in environments comparable to those found in spent fuel storage and transportation since the early 1950s (the U.S. Atomic Energy Commission's AE-6 Water-Boiler Reactor). In the 1960s, it was used as a poison material to ship irradiated fuel rods from Canada's Chalk River laboratories to Savannah River. More than 12,000 British Nuclear Fuels, Ltd. (BNFL) flasks containing the material have been used to transport fuel to BNFL's reprocessing plant in Sellafield.

The neutron absorber panels are composed of boron carbide and 1100 alloy aluminum. Boron carbide provides the necessary content of the neutron absorbing B10 isotope in a chemically inert, heat resistant, highly crystalline and extremely hard form. Boron carbide contained in the panels does not react under these conditions. The boron carbide core is tightly held within an 1100 aluminum alloy matrix and further protected by solid 1100 aluminum alloy cladding plates. Although 1100 alloy aluminum is a chemically reactive material, it behaves much like an inert material when properly applied. Proper application includes due consideration to the formation of a highly protective aluminum oxide layer and allowance for creation of the reaction by-product hydrogen.

Aluminum reacts with water to produce hydrogen (H_2) and an impervious tightly adhering layer of hydrated aluminum oxide ($Al_2O_3 \bullet 3H_2O$) called bayerite which protects the surface from further attack.

$$2\ Al + 6\ H_2O \rightarrow Al_2O_3 \bullet 3H_2O + 6H^+ + 6\text{electrons}$$

Initially, the DSC basket will be submerged in the spent fuel pool. During this period, aluminum in the panels will react with water in the manner noted above to form a small amount of hydrogen gas and produce a stable bayerite layer on all surfaces of the panel. The bayerite layer formed on the panel during pool immersion persists through DSC drying, sealing, storage, and eventual shipping; preventing further corrosion or hydrogen production. A complete corrosion discussion for the package components is provided in Section 2.4.4.

Leaching of the boron carbide along the unsealed edges of the panels is expected to occur to an insignificant degree. There are three reasons why this is anticipated to be insignificant. First, the panel core is a sintered Al/B_4C material. Only the boron carbide particles exposed by saw cut are available for leaching. Second, the immersion environment is relatively benign and the time is brief (a few hours or days). The material has been commonly used in U.S. spent fuel racks for many years and, in fact, has gained a reputation for not leaching, as other neutron absorbing materials have done. And third, direct experimental observations of accelerated aging tests performed at the University of Michigan [6.10] showed no indications of boron degradation. The test specimens were exposed to high neutron and gamma irradiation in a reactor pool environment for over nine years. Subsequent neutron radiography showed no signs of reduced neutron attenuation anywhere on the test specimens.

6.1.3 Fuel-Control Components (FC) DSC Design Features

The FC-DSC is designed with a longer internal cavity length to accommodate fuel control components. No credit is taken for the presence of control hardware, thus the FC-DSC is identical to the FO-DSC for the purpose of criticality analysis. Further references to the FO-DSC apply to this canister design also.

6.1.4 Failed Fuel (FF) DSC Design Features

The FF-DSC is different from the FO-DSC in its capacity, function, and design. The FF-DSC's capacity is thirteen fuel assemblies. It is intended to package fuel with gross cladding defects which might be discovered during the plant defueling campaign. Fuel assemblies to be stored and/or transported are to be visually inspected to document that cladding damage is limited to no more than 15 fuel pins with known or suspected cladding damage greater than hairline cracks and pinhole leaks. The potential does exist, however, for individual pellets to escape the cladding during transportation. This material would still be confined by the 13 fuel cans. The fuel must not have damage that would preclude it from being handled in the ordinary manner. Each assembly is placed in a separate, removable can with a fixed mesh screen on the bottom and similarly screened lid on top. These cans have slightly larger interior dimensions than the FO-DSCs (9.00" vs. 8.90") to accommodate bowed or twisted fuel. Due to its smaller payload and the relatively massive nature of the FF-DSC cans, the FF-DSC does not require borated neutron absorbers. The fuel cans are designed to permit unrestricted flooding and draining of fuel cells.

The FF-DSC is analyzed using the same criteria as the FO-DSC, plus additional considerations arising from mechanical uncertainties of failed fuel after transport or hypothetical accident conditions.

6.1.5 Criticality Analysis Summary and Results

The calculated maximum k_{eff} for the NUHOMS®-MP187 Package is 0.94968 including all biases and uncertainties applicable to the calculational methodology and the design. The results are summarized in Table 6.1-1.

Table 6.1-1

Summary of Criticality Evaluation

	Required	Calculated
NORMAL CONDITIONS		
Number of undamaged packages calculated to be subcritical	∞	∞
Optimum interspersed hydrogenous moderation	yes	0.93740[(2)]
Closely and fully reflected by water	yes	yes
Package cavity size, cm^3	--	1.11E+07
ACCIDENT CONDITIONS		
Number of damaged packages calculated to be subcritical	∞	∞
Optimum interspersed hydrogenous moderation, optimum water reflection	yes	0.94968[(3)]
Package cavity size, cm^3	--	1.11E+07
Transport Index	--	0

Notes:

1 All K_{eff}s include 2σ uncertainty. See Section 6.4.3 for summary details.

2 Maximum of the "FONXF" studies (refer to Section 6.4.3).

3 Maximum of FF DSC analysis (refer to Section 6.4.3).

The criticality analysis was performed in accordance with the requirements of:

- ANSI/ANS-8.1-1983, "Nuclear Criticality Safety in Operations with Fissionable Materials Outside Reactors." [6.2]
- ANSI/ANS-8.17-1984, "Criticality Safety Criteria for the Handling, Storage, and Transportation of LWR Fuel Outside Reactors." [6.3]
- USNRC Regulatory Guide 3.41, "Validation of Calculational Methods for Nuclear Criticality Safety," Revision 1, May, 1977. [6.4]
- ANSI N16.9-1975, "Validation of Calculational Methods for Nuclear Criticality Safety." [6.5]

Guidance has been taken from USNRC Regulatory Guide 1.13, "Spent Fuel Storage Facility Design Basis," Proposed Revision 2, December 1981 [6.6], as it applies to the calculation of k_{eff} for a transportation cask.

6.2 Package Fuel Loading

The NUHOMS®-MP187 Cask is designed to accommodate one of the three DSCs as described above. The design basis fuel is B&W 15x15 Mark B fuel with a maximum fuel enrichment of 3.43 w/o U235. The fuel loading parameters as they relate to criticality are summarized in Table 6.2-1. Since no credit for burnup was assumed in the criticality calculations, unirradiated fuel is qualified for shipment. Other fuel assembly types having varied characteristics will be licensed by amendment to the certificate of compliance for this package.

Table 6.2-1

Maximum Fuel Loading Parameters

Parameter	Value
Number of Assemblies, FO/FC-DSCs	≤ 24
Number of Assemblies, FF-DSC	≤ 13
Enrichment, w/o U235	≤ 3.43%
Minimum Burnup	0
Design Basis Fuel	B&W 15x15
Maximum Number of Failed Rods (FF-DSC only)	15/assy

The design properties of the reference fuel are given in Table 6.2-2.

Table 6.2-2

Design Basis Fuel Parameters for Criticality Analysis

Parameter	Value
Fuel Pellet Outside Diameter	0.3686 in
Fuel Clad Thickness	0.0265 in
Fuel Clad Outside Diameter	0.43 in
Fuel Rod Pitch	0.568 in
Active Fuel Height	141.8 in
Enrichment, w/o U-235	3.43%
UO2 Density, %Theoretical Dens.	95.0%
Rod Array (NxN Rods)	15
Fueled Rod Locations	208

6.3 Model Specification

6.3.1 Description of Calculational Model

The criticality calculations were done using full-cask KENO5A [6.8] models. They are described in detail below and in the Appendices.

The safety requirements of ANSI/ANS-8.17 [6.3] prescribe that all applicable biases and uncertainties must be investigated and statistically attached to the nominal case k_{eff}. Rather than a statistical approach, this criticality analysis models the system with all the important parameters concurrently in their worst-case state:

- Maximum fabrication thickness and minimum boron content for all the neutron absorber plates (this combination is the worst case since aluminum displaces moderator and is not a strong absorber),
- Minimum fabrication width for all the neutron absorber plates,
- Minimum fabrication thickness for all steel guide tubes and steel absorber wrappers,
- Only 75% credit taken for the boron in neutron absorber plates,
- Worst-case fuel assembly position (includes DSC fabrication tolerances and an allowance for fuel assembly bow and twist),
- Maximum enrichment (3.43 w/o U235) B&W 15x15 Mark B fuel.

6.3.2 NUHOMS®-MP187 Cask/FO-DSC Model

The KENO models consist of 560 axial layers stacked into an array. The layers consist of partial spacer disc and partial moderator regions inside and outside of the active fuel region. The very top and bottom of the model are the DSC steel cylinder. The length of the active fuel layers is equivalent to the greatest common denominator of the spacer disc and moderator region axial lengths. For example, five 0.25" layers of the spacer disc are stacked to make an equivalent 1.25" spacer disc region. The center to center spacing of the spacer disc intervals varies over a range starting at 0.0 and ending at 6.75 inches. However, some of these intervals occur in non-fuel areas. This axially finite arrangement is shown in Figure 6.3-1. By specifying specular reflection on the $\pm x$ and $\pm y$ directions of these array layers, the model represents an infinite array of casks.

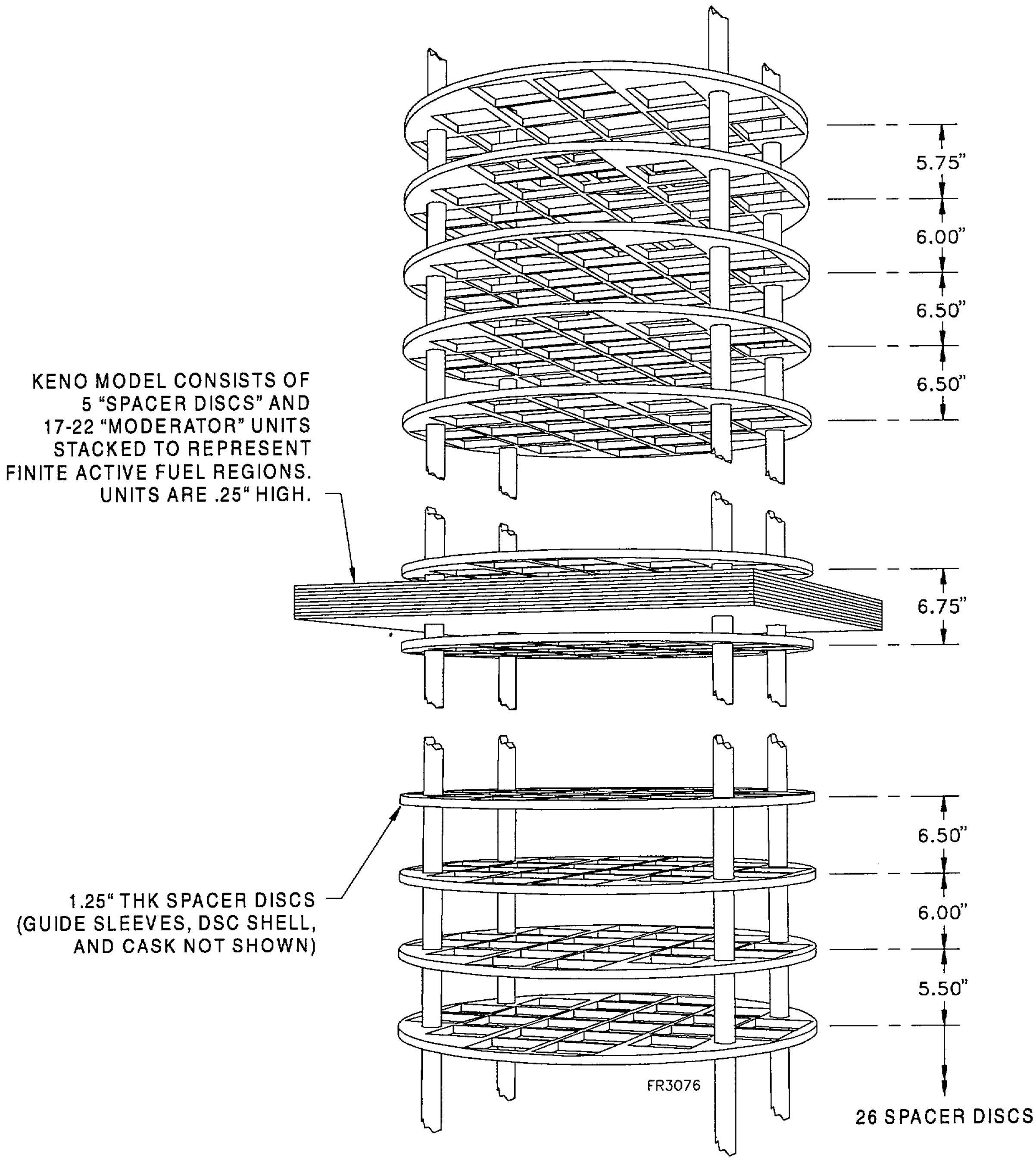

Figure 6.3-1

KENO Model and DSC Basket

Figure 6.3-2 shows the KENO model in an exploded view. UNIT 33 is a slice through the cask at the DSC spacer disc level. UNIT 34 is a similar slice, but in between the spacer discs.

Figure 6.3-3 shows the structure of UNITs 33 and 34: the cask slices. Note that the difference between the two UNITs is that UNIT 33 is a spacer disc (steel surrounding fuel assemblies) and UNIT 34 has steel support rods only (water surrounding fuel assemblies). Also, for the HAC cases, there is no guide sleeve deformation within the spacer disc (Unit 33) region. The fuel assemblies are identified in Figure 6.3-3 by the position numbers (1-24) used to refer to their unique locations. UNIT numbers 1-8 represent the active fuel assemblies in the spacer disc region and UNIT numbers 82-89 represent the active fuel assemblies in the moderator region. The fuel assemblies are inserted into the model using KENO5A's HOLE capability.

A detail of the guide sleeve assembly is shown in the enlarged section of Figure 6.3-3. These models include all major components of the guide sleeve assembly: the square tube, absorber sheets (4 per tube), and the over sleeves which hold the sheets in place. Note that the guide sleeves on the outer periphery of the basket (12 total) only have two absorber sheets per tube.

Figure 6.3-4 shows more closely the way in which UNITs 1-8 are constructed. Each HOLE is identified by UNIT number and its own particular coordinate origin.

UNIT 32 is a cross section of the design basis B&W 15x15 Mark B fuel assembly. It is illustrated in Figure 6.3-5 , which also shows the locations of the fuel assembly guide tubes, instrumentation tube, and the UNIT origin for insertion as a HOLE. The theoretical half width of the fuel (fifteen times half the rod pitch) is 4.26" (10.8204 cm).

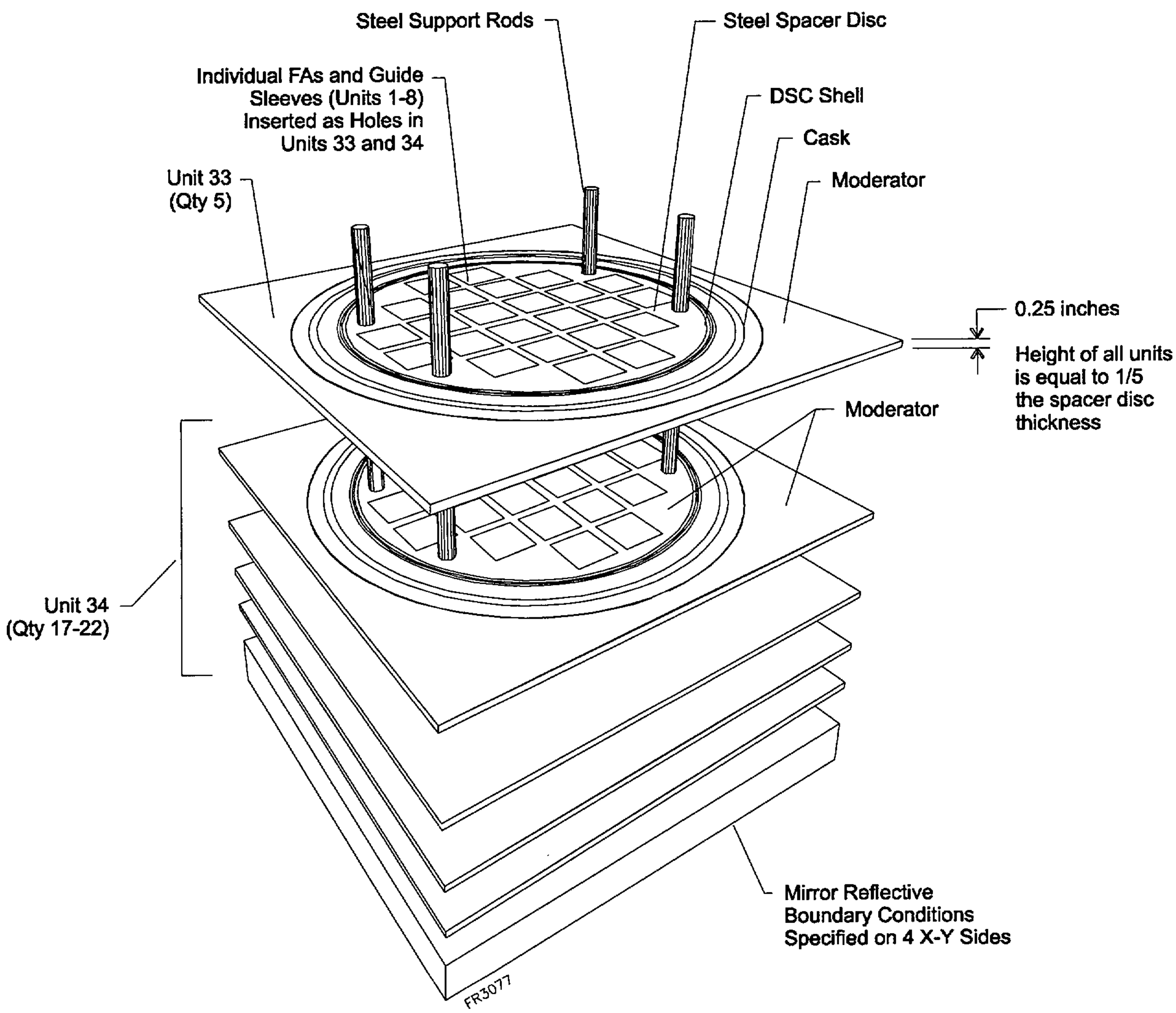

Figure 6.3-2

Exploded View of KENO Model

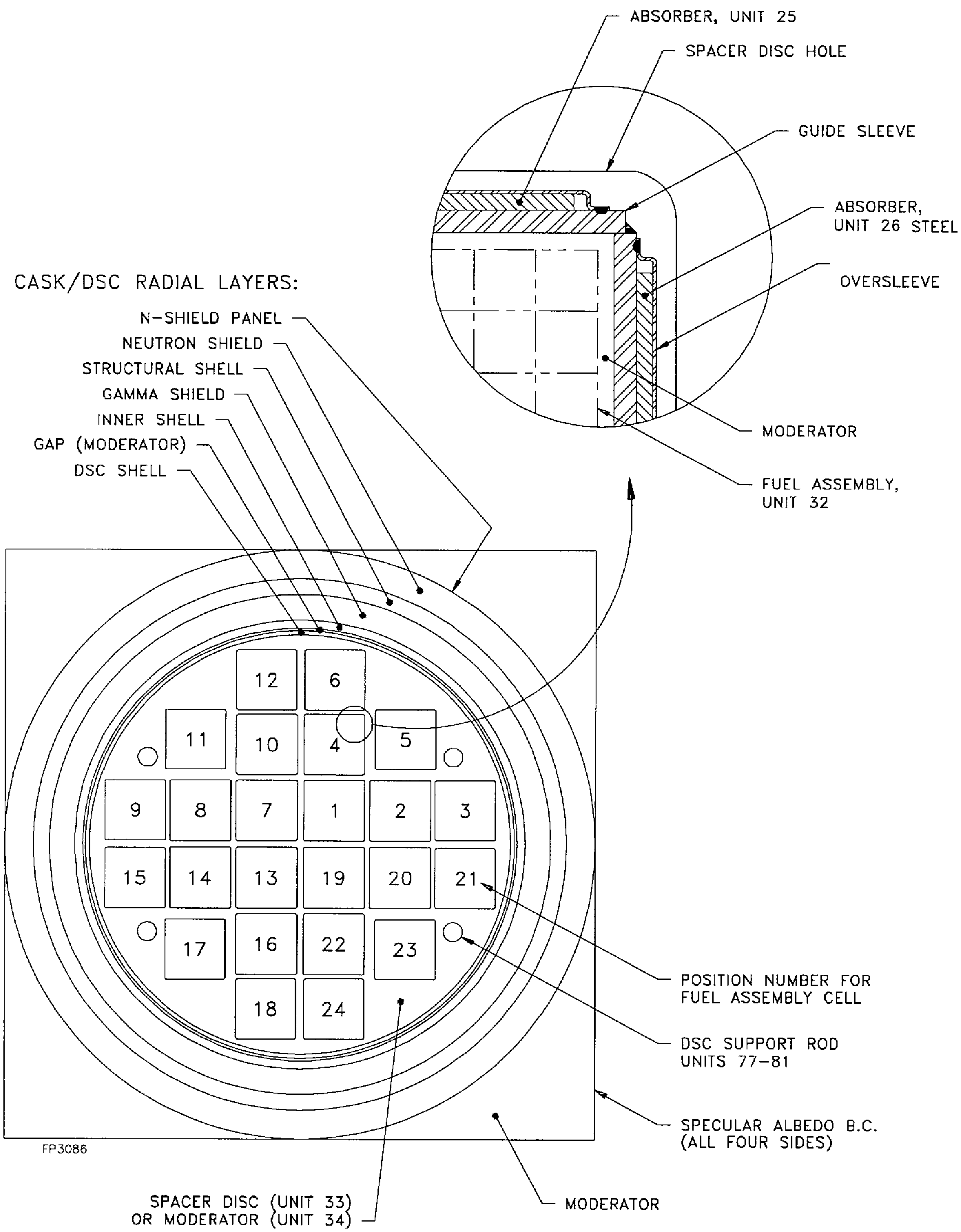

Figure 6.3-3

Structure of KENO Model UNITS 33 and 34

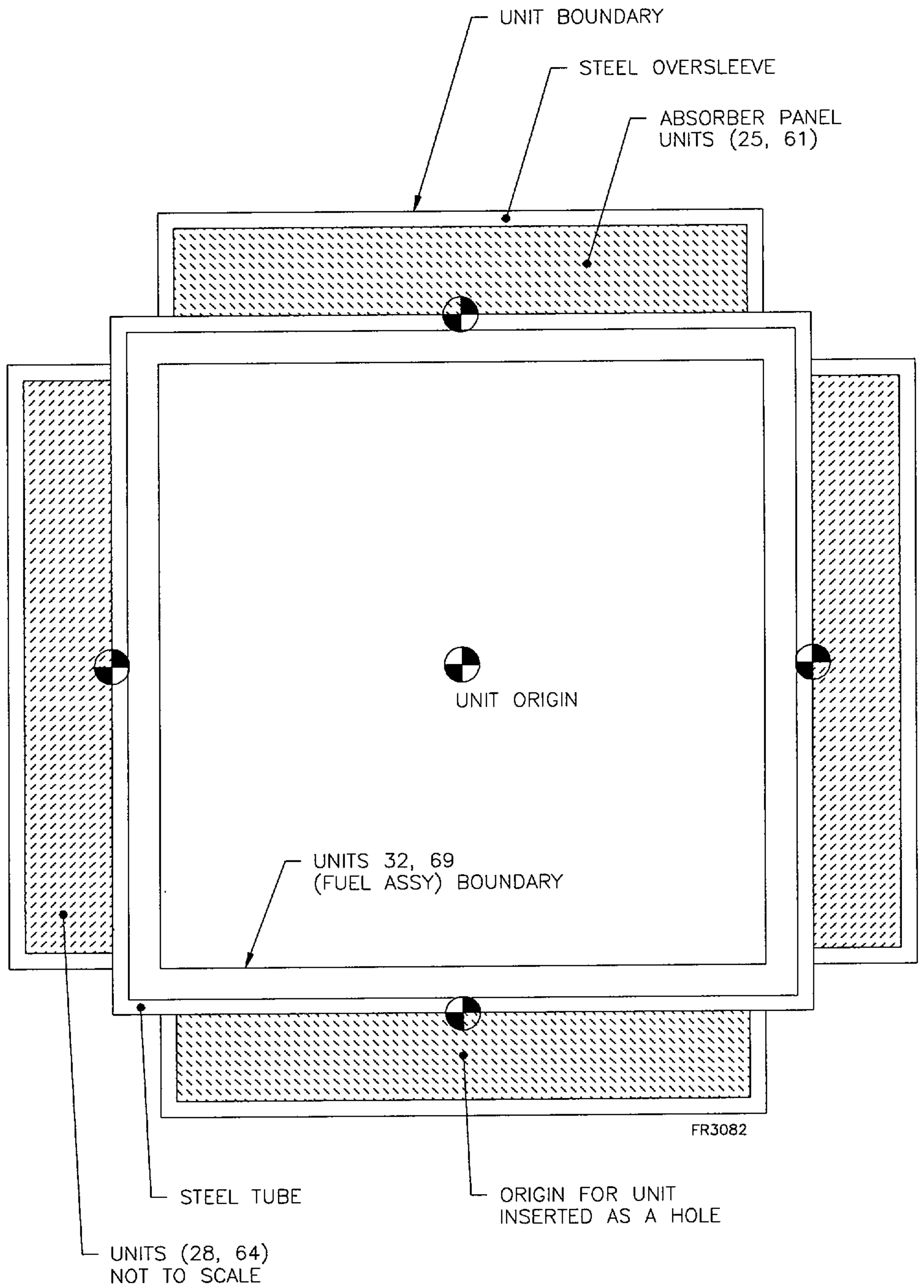

Figure 6.3-4

KENO Model UNITS 1-8, plus

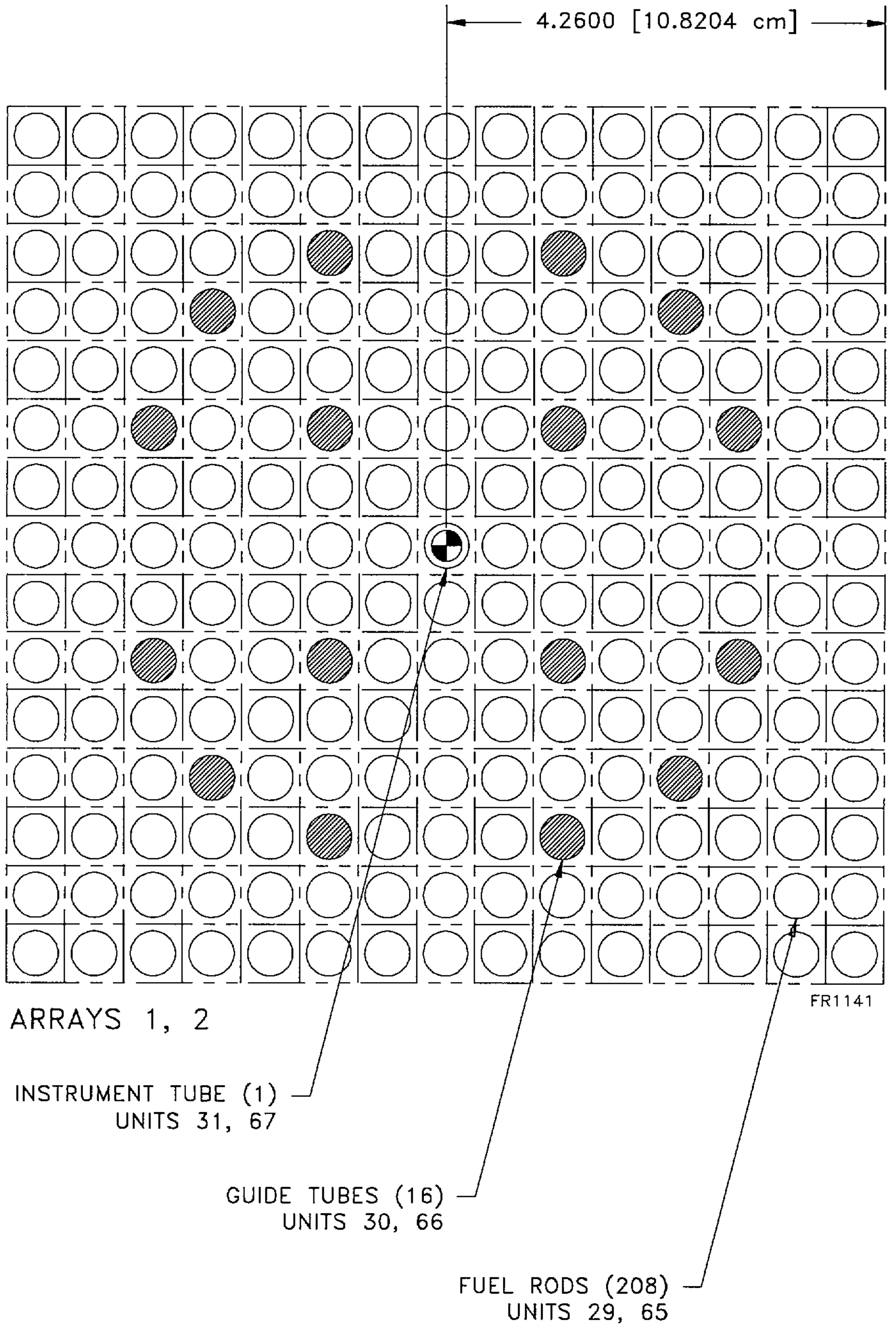

Figure 6.3-5

KENO Model of a Design Basis Fuel Assembly

6.3.3 NUHOMS®-MP187 Cask/FF-DSC Model

The NUHOMS®-MP187 Cask/FF-DSC KENO model is constructed in the same "slice of the cask" style as the MP187/FO-DSC model. The major differences are:

- 13 storage locations
- stainless steel fuel cans, no absorber panels/guide tubes
- different spacer disc pitch
- different support rod orientation (note that the support plates are modeled as an equivalent cylinder)

6.3.4 Package Regional Densities

Table 6.3-1 and Table 6.3-2 summarize the calculated atom densities used in the KENO models. Note that, when using the Hansen-Roach working library, resonance nuclides are specified by their σ_{peff}, thus the U235 and U238 atom density specifications in Table 6.3-1 are unique to each moderator state.

Table 6.3-1

KENO Model Atom Densities

Fuel Pellet			**Aluminum**		
Element	H-R ID No.	atom/b-cm	Element	H-R ID No.	atom/b-cm
Oxygen	8100	4.6540E-02	Aluminum	13100	6.0552E-02
U235	(run-unique)	8.0802E-04			
U238	(run-unique)	2.2462E-02			
Zircaloy-4			**Absorber Plate**		
Element	H-R ID No.	atom/b-cm	Element	H-R ID No.	atom/b-cm
Chromium	24100	7.5166E-05	Aluminum	13100	3.9268E-02
Iron	26100	1.4696E-04	Boron	5100	2.4879E-02
Nickel	28100	2.3299E-06	Carbon	6100	7.6705E-03
Zirconium	40100	4.2711E-02			
C-Steel			**Lead**		
Element	H-R ID No.	atom/b-cm	Element	H-R ID No.	atom/b-cm
Iron	26100	8.3801E-02	Lead	82100	3.2960E-02
Manganese	25100	8.6048E-04			
S_Steel			**NS-3**		
Element	H-R ID No.	atom/b-cm	Element	H-R ID No.	atom/b-cm
Chromium	24100	1.7274E-02	Aluminum	13100	7.0275E-03
Iron	26100	5.9042E-02	Calcium	20100	1.4835E-03
Manganese	25100	1.7210E-03	Carbon	6100	8.2505E-03
Nickel	28100	7.4481E-03	Hydrogen	1101	5.0996E-02
			Iron	26100	1.0628E-04
			Oxygen	8100	3.7793E-02
			Silicon	14100	1.2680E-03

Table 6.3-2

KENO Model Moderator Atom Densities

Density (g/cc)	Scaling Factor	Hydrogen (at/b-cm)	Oxygen (at/b-cm)
1.00000	1.00177	6.68544e-02	3.34272e-02
0.99823	1.00000	6.67361e-02	3.33680e-02
0.90000	0.90160	6.01690e-02	3.00845e-02
0.80000	0.80142	5.34835e-02	2.67418e-02
0.70000	0.70124	4.67981e-02	2.33990e-02
0.60000	0.60106	4.01126e-02	2.00563e-02
050000	0.50089	3.34272e-02	1.67136e-02
0.40000	0.40071	2.67418e-02	1.33709e-02
0.30000	0.30053	2.00563e-02	1.00282e-02
0.20000	0.20035	1.33709e-02	6.68544e-03
0.10000	0.10018	6.68544e-03	3.34272e-03
0.0500	0.05009	3.34272e-03	1.67136e-03
0.00000	0.00000	0.00000e-00	0.00000e-00

6.4 Criticality Calculation

6.4.1 Calculational Method

Criticality calculations for the NUHOMS®-MP187 Package are performed using the microcomputer application KENO5A [6.8] and the Hansen-Roach 16-group (HR-16) cross section working library. In order to use the HR-16 library, σ_{peff}, the effective resonance cross section, must be calculated for each resonance nuclide of interest (for this work, U235 and U238). σ_{peff} includes both resonance self shielding and heterogeneous effects. The proper working library nuclide, or more generally nuclides, must be selected from the HR-16 library based on σ_{peff}.

Corrections for resonance and heterogeneous effects are performed using the Transnuclear West proprietary program PN-HET. PN-HET was developed during TNW's validation of KENO5A as a means to streamline and unify the analytical approach used to calculate σ_{peff}. The calculational procedure is to:

A. Calculate σ_{peff} for U235 and U238 in the fuel rods.

B. Select H-R library nuclides with σ_{peff} above and below the calculated value.

C. Perform a weighted average to accurately represent the resonance nuclide using a mixture of the two selected nuclides.

The major assumptions made in the KENO modeling are:

A. Unirradiated fuel - no credit taken for fissile depletion or fission product poisoning.

B. No credit taken for fuel control components (applies to FC-DSC only).

C. Fuel is intact with no gross damage or missing rods (applies to FO/FC-DSCs only).

D. The fuel enrichment is modeled as uniform throughout the assembly. The maximum pellet enrichment is assumed to exist everywhere.

E. Fuel and cask are modeled as having finite length (water reflection is specified top and bottom) in all models.

F. Only 75% credit is taken for boron in neutron absorber panels.

G. All fuel rods are assumed to be filled with 100% moderator in the fuel cladding gap.

6.4.2 Fuel Loading Optimization

The NUHOMS®-MP187 Package criticality analysis is performed for 3.43 w/o enriched B&W 15x15 Mark B PWR fuel. This fuel design has been demonstrated to be the most reactive PWR fuel design [6.7]. In order to assure that the requirements of 10CFR71, Sections 71.55 and 71.59, are satisfied, the KENO models were specified with either 100% specular albedo, or infinite water conditions on all four sides. All void regions of the package have been modeled with optimum moderation, including the fuel pellet-clad gaps. Further discussion regarding the models can be found in Section 6.3.2 and in the Appendices.

6.4.2.1 Fuel Loading Optimization - Failed Fuel Considerations

THIS SECTION CONTAINS PROPRIETARY INFORMATION

THIS PAGE CONTAINS
PROPRIETARY INFORMATION

6.4.3 Criticality Results

THIS SECTION CONTAINS
PROPRIETARY INFORMATION

THIS SECTION CONTAINS
PROPRIETARY INFORMATION

Table 6.4-1

Summary of KENO Parametric Studies

Study	DSC Moderator Density	Ex-Cask Moderator Density	Neutron Shield	Radial Boundary Condition	Addresses
FONIF	Varies	1.0	Intact	Specular	§71.55(b)
FONXF	1.0	Varies	Intact	Specular	§71.59(a1)
FOHIF	Varies	1.0	None	Specular	§71.55(e)
FOHXF	1.0	Varies	None	Specular	§71.59(a2)
GSDEF*	1.0	0.70	None	Specular	§71.55(e)
FOCL	1.0	0.70	Varies	Specular	§71.55(b-3)
IFNCI	Varies	1.0	Intact	Water	§71.55(b)
IFNCX	1.0	Varies	Intact	Specular	§71.59(a2)
FFDSI	Varies	1.0	Intact	Water	§71.55(b)
FFDSX	1.0	Varies	Intact	Specular	§71.59(a2)

*This parametric study only applies to the FO Can.

The results of the studies are shown in graphic and tabular form at the end of this Section.

6.4.3.1 NUHOMS®–MP187 Cask/FO-DSC Summary

The highest calculated k_{eff} was for the Hypothetical Accident Condition, Cask Layer Removal Study (cask structural shell vanished) with 0.70 g/cc moderator interspersed between an infinite array of packages. The reactivity was 0.94015 ± 0.00148. With a 95% confidence (2σ), the maximum k_{eff} is 0.94311. The KENO5A/HR-16/PN-HET calculational bias is zero.

6.4.3.2 NUHOMS®–MP187 Cask/FF-DSC Summary

The highest calculated k_{eff} was for the Hypothetical Accident Condition (neutron shield vanished) with double-ended shear, one row of half length rods failed, 1.0 g/cc internal moderator, 0.80 g/cc external moderator in a single package with specular reflection at all boundaries. The hypothetical accident calculations were performed assuming the fuel will be in the most reactive credible post-drop condition as described above. The reactivity was

0.94598 ± 0.00185. With a 95% confidence (2σ), the maximum k_{eff} is 0.94968. The KENO5A/HR-16/PN-HET calculational bias is zero.

Table 6.4-2

MP187/FO-DSC KENO Results (Guide Sleeve Deformation)

Model	k_{eff}	+/-	1 s	$k_{eff} + 2\sigma$
gsdef00.ko	0.93271	+/-	0.00152	0.93575
gsdef025.ko	0.93097	+/-	0.00149	0.93395
gsdef05.ko	0.93197	+/-	0.00143	0.93483
gsdef08.ko	0.93093	+/-	0.00157	0.93407
gsdef10.ko	0.93337	+/-	0.00154	0.93645
gsdef11.ko	0.93221	+/-	0.00157	0.93535
gsdef12.ko	0.93610	+/-	0.00152	0.93914
gsdef14.ko	0.93672	+/-	0.00142	0.93956
gsdef16.ko	0.93723	+/-	0.00162	0.94047
gsdef18.ko	0.93966	+/-	0.00157	0.94280

A graphical representation of the results for Table 6.4-2 is shown in Figure 6.4-1.

Table 6.4-3

MP187/FO-DSC KENO Results (Cask Layer Removal)

Model	k_{eff}	+/-	1 s	$k_{eff} + 2\sigma$
FOCLA.KO	0.93818	+/-	0.00158	0.94134
FOCLB.KO	0.93758	+/-	0.00155	0.94068
FOCLC.KO	0.93966	+/-	0.00157	0.94280
FOCLD.KO	0.94015	+/-	0.00148	0.94311
FOCLE.KO	0.93513	+/-	0.00157	0.93827
FOCLF.KO	0.93859	+/-	0.00155	0.94169

Table 6.4-4

MP187/FO-DSC KENO Results

Model	keff	+/-	1 σ	Model	keff	+/-	1 σ
FONIF00.KO	0.33984	+/-	0.00095	FOHIF00.KO	0.34009	+/-	0.00100
FONIF05.KO	0.37054	+/-	0.00084	FOHIF05.KO	0.37023	+/-	0.00085
FONIF10.KO	0.53723	+/-	0.00110	FOHIF10.KO	0.53972	+/-	0.00112
FONIF20.KO	0.60799	+/-	0.00110	FOHIF20.KO	0.61329	+/-	0.00120
FONIF30.KO	0.66953	+/-	0.00126	FOHIF30.KO	0.67393	+/-	0.00123
FONIF40.KO	0.71959	+/-	0.00136	FOHIF40.KO	0.72584	+/-	0.00140
FONIF50.KO	0.76679	+/-	0.00141	FOHIF50.KO	0.76799	+/-	0.00134
FONIF60.KO	0.80562	+/-	0.00145	FOHIF60.KO	0.81102	+/-	0.00146
FONIF70.KO	0.84433	+/-	0.00149	FOHIF70.KO	0.84750	+/-	0.00156
FONIF80.KO	0.87400	+/-	0.00156	FOHIF80.KO	0.88223	+/-	0.00144
FONIF90.KO	0.90667	+/-	0.00167	FOHIF90.KO	0.91096	+/-	0.00158
FONIF100.KO	0.93159	+/-	0.00158	FOHIF100.KO	0.93389	+/-	0.00151

Model	keff	+/-	1 σ	Model	keff	+/-	1 σ
FONXF00.KO	0.93436	+/-	0.00152	FOHXF00.KO	0.93548	+/-	0.00156
FONXF05.KO	0.93290	+/-	0.00158	FOHXF05.KO	0.93524	+/-	0.00153
FONXF10.KO	0.93030	+/-	0.00151	FOHXF10.KO	0.93899	+/-	0.00153
FONXF20.KO	0.93116	+/-	0.00149	FOHXF20.KO	0.93712	+/-	0.00158
FONXF30.KO	0.93397	+/-	0.00147	FOHXF30.KO	0.93950	+/-	0.00156
FONXF40.KO	0.93330	+/-	0.00159	FOHXF40.KO	0.93607	+/-	0.00152
FONXF50.KO	0.93269	+/-	0.00148	FOHXF50.KO	0.93604	+/-	0.00152
FONXF60.KO	0.93100	+/-	0.00149	FOHXF60.KO	0.93885	+/-	0.00147
FONXF70.KO	0.93331	+/-	0.00153	FOHXF70.KO	0.93966	+/-	0.00157
FONXF80.KO	0.93052	+/-	0.00161	FOHXF80.KO	0.93600	+/-	0.00156
FONXF90.KO	0.93074	+/-	0.00153	FOHXF90.KO	0.93734	+/-	0.00158
FONXF100.KO	0.93159	+/-	0.00158	FOHXF100.KO	0.93389	+/-	0.00151

Table 6.4-5

MP187/FF-DSC KENO Results

Model	keff	+/-	1 σ	Model	keff	+/-	1 σ
IFNCI000.KO	0.26349	+/-	0.00070	FFDSI000.KO	0.25584	+/-	0.00081
IFNCI005.KO	0.37248	+/-	0.00098	FFDSI005.KO	0.36074	+/-	0.00098
IFNCI010.KO	0.60350	+/-	0.00143	FFDSI010.KO	0.59256	+/-	0.00143
IFNCI020.KO	0.67650	+/-	0.00158	FFDSI020.KO	0.67131	+/-	0.00159
IFNCI030.KO	0.72586	+/-	0.00173	FFDSI030.KO	0.72868	+/-	0.00172
IFNCI040.KO	0.76875	+/-	0.00186	FFDSI040.KO	0.77097	+/-	0.00183
IFNCI050.KO	0.80214	+/-	0.00186	FFDSI050.KO	0.80398	+/-	0.00176
IFNCI060.KO	0.83485	+/-	0.00184	FFDSI060.KO	0.83614	+/-	0.00186
IFNCI070.KO	0.86550	+/-	0.00195	FFDSI070.KO	0.87030	+/-	0.00184
IFNCI080.KO	0.88686	+/-	0.00184	FFDSI080.KO	0.89273	+/-	0.00185
IFNCI090.KO	0.90846	+/-	0.00184	FFDSI090.KO	0.91861	+/-	0.00184
IFNCI100.KO	0.93493	+/-	0.00205	FFDSI100.KO	0.94382	+/-	0.00192

Model	keff	+/-	1 σ	Model	keff	+/-	1 σ
IFNCX000.KO	0.93065	+/-	0.00195	FFDSX000.KO	0.94015	+/-	0.00182
IFNCX005.KO	0.93402	+/-	0.00186	FFDSX005.KO	0.94498	+/-	0.00183
IFNCX010.KO	0.93828	+/-	0.00198	FFDSX010.KO	0.94164	+/-	0.00188
IFNCX020.KO	0.93636	+/-	0.00184	FFDSX020.KO	0.94164	+/-	0.00194
IFNCX030.KO	0.94004	+/-	0.00186	FFDSX030.KO	0.93913	+/-	0.00196
IFNCX040.KO	0.93472	+/-	0.00186	FFDSX040.KO	0.94024	+/-	0.00190
IFNCX050.KO	0.93430	+/-	0.00194	FFDSX050.KO	0.94159	+/-	0.00198
IFNCX060.KO	0.93829	+/-	0.00189	FFDSX060.KO	0.94471	+/-	0.00193
IFNCX070.KO	0.93336	+/-	0.00189	FFDSX070.KO	0.94150	+/-	0.00189
IFNCX080.KO	0.93152	+/-	0.00186	FFDSX080.KO	0.94598	+/-	0.00185
IFNCX090.KO	0.92930	+/-	0.00187	FFDSX090.KO	0.94417	+/-	0.00189
IFNCX100.KO	0.93405	+/-	0.00192	FFDSX100.KO	0.94015	+/-	0.00189

Single-ended Shear

Model	keff	+/-	1 σ	Model	keff	+/-	1 σ
FFSS010.KO	0.92971	+/-	0.00209	FFSS020.KO	0.93198	+/-	0.00195
FFSS030.KO	0.93866	+/-	0.00190	FFSS040.KO	0.93735	+/-	0.00194
FFSS048.KO	0.93920	+/-	0.00183				

Table 6.4-6

MP187/FF-DSC KENO Results (Cask Layer Removal)

File	Cask Layer	K_{eff}	+/-	1σ	K_{eff} + 2σ
FFCL80A.KO	Nominal	0.94248	+/-	0.00194	0.94636
FFCL80B.KO	N Shield Panel	0.94008	+/-	0.00180	0.94368
FFCL80C.KO	N Shield	0.94598	+/-	0.00185	0.94968
FFCL80D.KO	Cask Structural Shell	0.94336	+/-	0.00184	0.94704
FFCL80E.KO	Gamma Shield	0.93934	+/-	0.00189	0.94312
FFCL80F.KO	Cask Inner Shell	0.94492	+/-	0.00191	0.94874

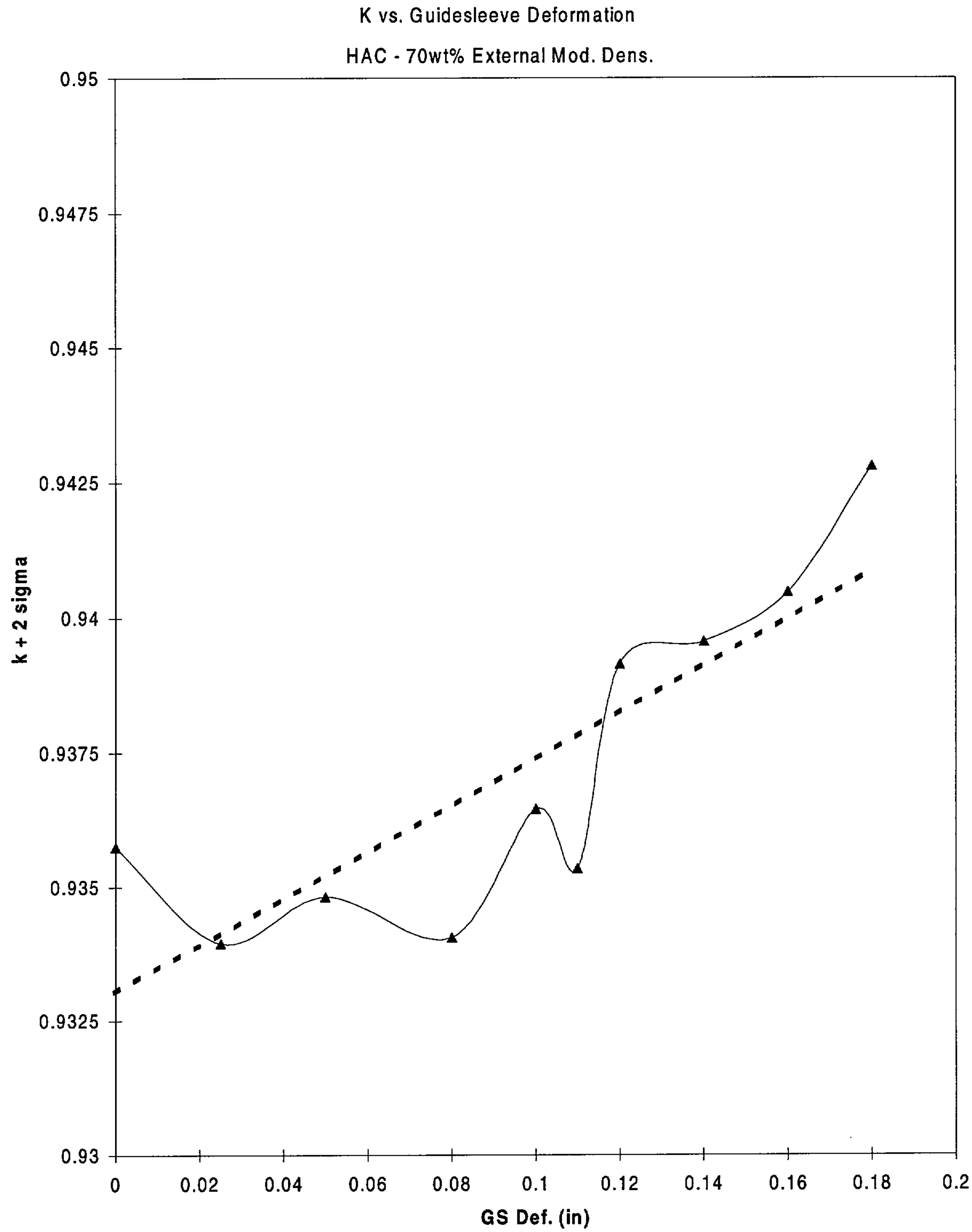

Figure 6.4-1

K vs. Guide Sleeve Deformation

THIS FIGURE CONTAINS
PROPRIETARY INFORMATION

Figure 6.4-2

FF-DSC Broken Fuel Rod Models

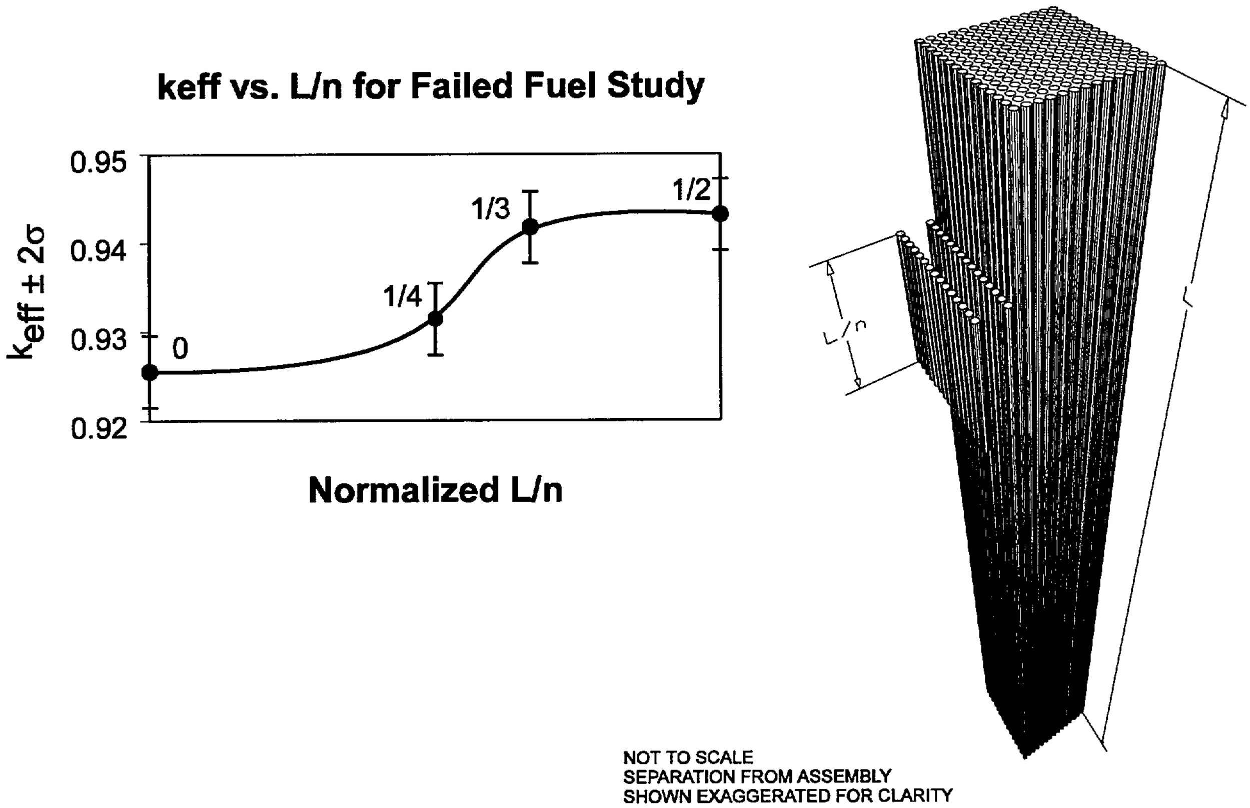

Figure 6.4-3

FF-DSC Double-Ended Rod Break Models

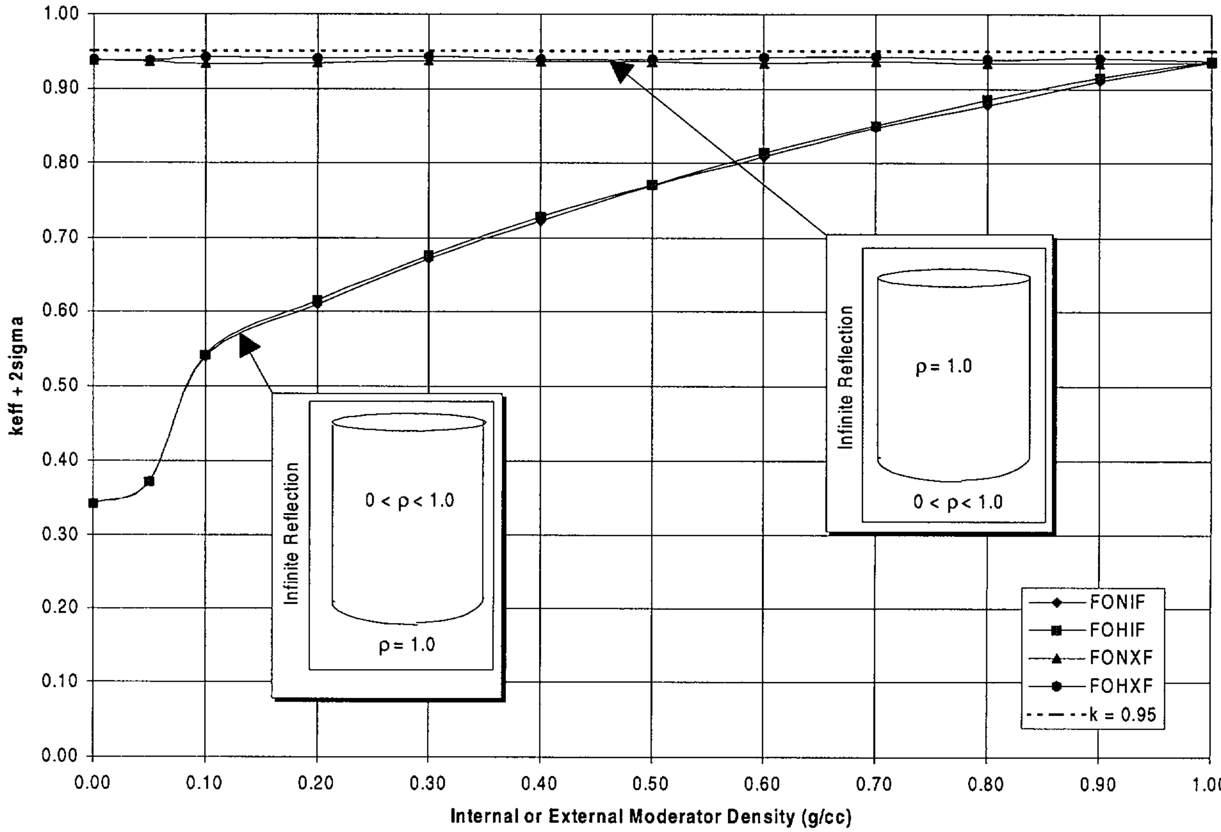

± 2σ error bars omitted for clarity

Figure 6.4-4

NUHOMS®-MP187 Cask/FO-DSC Criticality Results

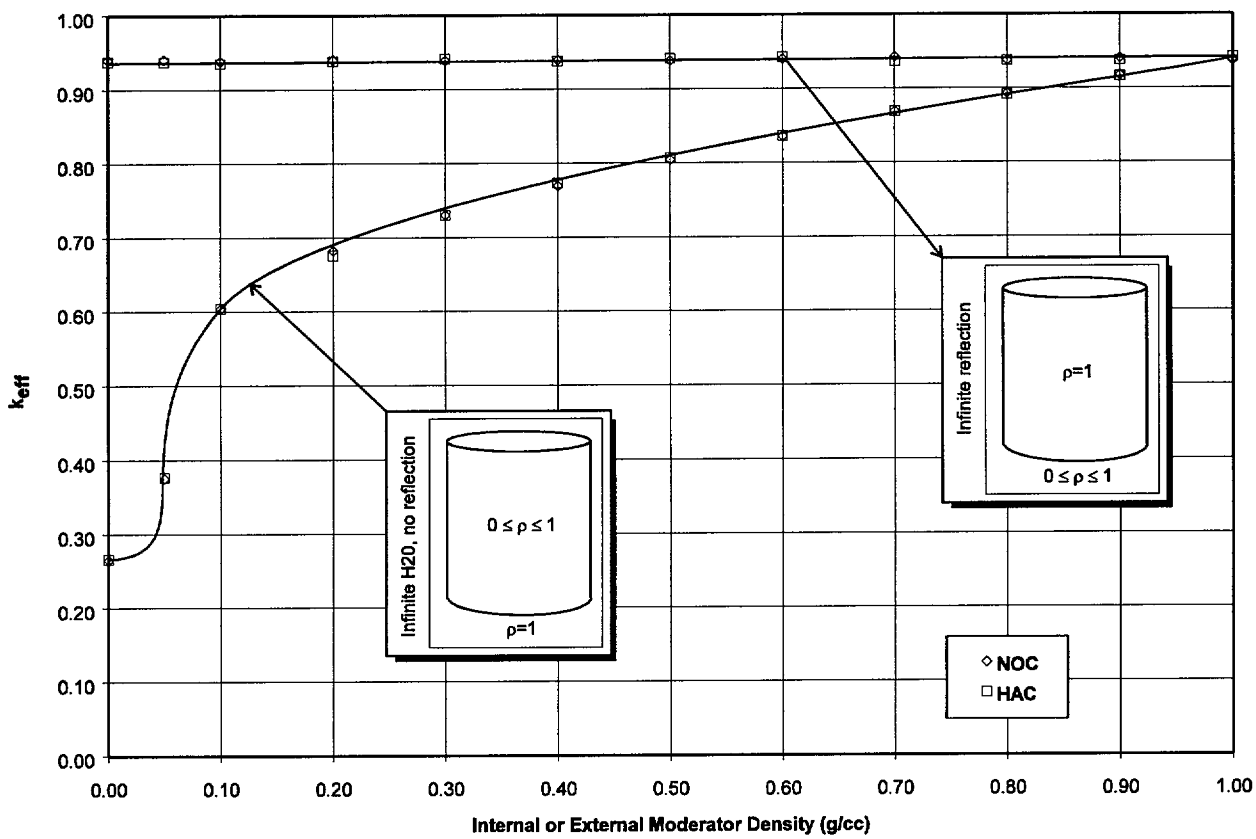

± 2σ error bars omitted for clarity

Figure 6.4-5

NUHOMS®-MP187 Cask/FF-DSC Criticality Results

6.5 Critical Benchmark Experiments

6.5.1 Benchmark Experiments and Applicability

A suite of 150 critical and subcritical LWR fuel benchmark cases was run by Transnuclear West to validate KENO5A, the Hansen-Roach 16 group working cross section library, and PN-HET [6.9] (a TNW proprietary code for performing nuclear resonance/heterogeneous effects calculations). The large number of cases was necessary to evaluate parameter dependencies, such as fuel enrichment, fuel rod pitch, absorber material, absorber thickness, absorber to cluster distance, reflector material, reflector to cluster distance, and critical cluster separation.

The benchmark problems are representative of critical or subcritical arrays of commercial light water reactor (LWR) fuels with the following characteristics:

A. water moderation

B. neutron absorbers:

- no special neutron absorbers,
- neutron absorption by fixed sheets,
- neutron absorption by aqueous solutions

C. unirradiated light water reactor type fuel (no fission products or "burnup credit") near room temperature (vs. reactor operating temperature)

D. close reflection:

- no specific reflector,
- steel,
- lead, and
- depleted uranium

A statistical analysis of the largest statistical population of benchmark cases was performed to determine if the KENO-Va/HR-16/PN-HET methodology produces any bias due to fuel enrichment, fuel rod pitch, absorber material, absorber thickness, absorber to cluster distance, reflector material, reflector to cluster distance, critical cluster separation, or other parameters. This population consisted of 134 benchmark experiments performed on critical arrays of fuel rods, References [6.11] through [6.14]. Of the 150 cases originally run by Transnuclear West, 14 B&W critical experiments (Reference 6.15) and two subcritical experiments (Reference 6.16) were not included with the 134 cases because they contained experimental or empirical uncertainties not related to the benchmark bias.

A subset of the 134 cases was chosen to be most representative of the NUHOMS®–MP187 Package design for the purpose of establishing a calculational bias. The criterion used to select the subset of cases was the neutron absorber material since that parameter most strongly influences the behavior of the system. From the set of 134 cases, those with cadmium, copper, copper/cadmium, unborated aluminum, Zircaloy, Boroflex, and no neutron absorbers were discarded. There were six benchmark cases with borated absorber panels (similar to the FO- and FC-DSC absorber panels) and 13 cases with stainless steel neutron absorbing panels (thick stainless steel guide tubes are used in the FF-DSC design, thin stainless sheets are used for guide tubes in the FO- and FC-DSCs).

6.5.2 Details of Benchmark Calculations

The KENO5A code and HR-16 library were used to model the critical configurations. The modeling technique incorporated a rod-by-rod representation of the fuel assemblies with explicit models of the material interspersed between assemblies. The cross section library identifiers for resonance materials were selected using PN-HET. All pertinent data for each critical configuration are documented in References [6.11] through [6.16] to permit use of these data for validating calculational methods in accordance with ANSI N16.9-1976 [6.5].

6.5.3 Results of Benchmark Calculations

Statistical analysis of the 134 critical benchmark cases showed that there are no systematic biases for fuel enrichment, fuel rod pitch, absorber material, absorber thickness, absorber to cluster distance, reflector material, reflector to cluster distance, and critical cluster separation. One dependency was noted on reflector to cluster distance for depleted uranium (DU) reflected benchmarks. The source of this bias could not be determined, but since the MP187 cask does not use a DU shielding, no corrections were made to the criticality results and the DU criticals were not used to calculate the final calculational bias for the KENO-Va/HR-16/PN-HET methodology. Figure 6.5-1 shows the results of the benchmark calculations.

Once the conclusion was drawn that the KENO-Va/HR-16/PN-HET methodology produces no systematic biases that would affect the MP187 calculations, a subset of cases most like the MP187 system were chosen as described above for the purpose of calculating the final calculational bias. The results of the nineteen most applicable benchmark critical cases are shown in bold face type in Table 6.5-1. The results are summarized below:

	Absorber Plates	
	Borated	Stainless
Cases	6	13
Maximum k_{eff}	1.01064	1.01405
Average k_{eff}	1.00819	1.00897
Minimum k_{eff}	1.00499	1.00254
Standard Deviation	0.00197	0.00372

The calculational bias is the maximum difference between any applicable calculated critical benchmark k_{eff} and unity, excluding any cases where the calculated k_{eff} was greater than unity. The calculated k_{eff}, without its associated uncertainty, is used for determining the bias. The group of applicable critical benchmark experiments is the nineteen cases described above.

Since all cases had a calculated k_{eff} greater than unity, the calculational bias is zero.

Table 6.5-1

Benchmark Calculation Results

THIS TABLE CONTAINS PROPRIETARY INFORMATION

Table 6.5-1

Benchmark Calculation Results

(continued)

THIS TABLE CONTAINS PROPRIETARY INFORMATION

Table 6.5-1

Benchmark Calculation Results

(continued)

THIS TABLE CONTAINS PROPRIETARY INFORMATION

Table 6.5-1

Benchmark Calculation Results

(continued)

THIS TABLE CONTAINS PROPRIETARY INFORMATION

Table 6.5-1

Benchmark Calculation Results

(concluded)

THIS TABLE CONTAINS
PROPRIETARY INFORMATION

THIS FIGURE CONTAINS
PROPRIETARY INFORMATION

Figure 6.5-1

Critical Benchmark Results

6.6 Appendix

6.6.1 References

6.1 Code of Federal Regulations, Title 10, Part 71, "Packaging and Transportation of Radioactive Material."

6.2 ANSI/ANS-8.1-1983, "Nuclear Criticality Safety in Operations with Fissionable Materials Outside Reactors."

6.3 ANSI/ANS-8.17-1984, "Criticality Safety Criteria for the Handling, Storage, and Transportation of LWR Fuel Outside Reactors."

6.4 USNRC Regulatory Guide 3.41, "Validation of Calculational Methods for Nuclear Criticality Safety," Revision 1, May, 1977.

6.5 ANSI N16.9-1975, "Validation of Calculational Methods for Nuclear Criticality Safety."

6.6 USNRC Regulatory Guide 1.13, "Spent Fuel Storage Facility Design Basis," Proposed Revision 2, December 1981 (for guidance only).

6.7 "Safety Analysis Report for the Standardized NUHOMS® Horizontal Modular Storage System for Irradiated Nuclear Fuel," NUH-003, Revision 4A, TNW, June 1996.

6.8 "KENO5A-PC, Monte Carlo Criticality Program with Supergrouping," CCC-548, Oak Ridge National Laboratory, June, 1990.

6.9 Thomas, B. D., "QA Category 2 Computer Code Verification Document - KENO5A," Pacific Nuclear Version 1.2.0," Revision 2, TNW Proprietary.

6.10 Burn, Reed R., "Boral Accelerated Radiation Aging Tests," Nuclear Reactor Laboratory, University of Michigan, Ann Arbor, Michigan, May 9, 1990.

6.11 Bierman, S.R., et al., "Criticality Experiments with Subcritical Clusters of 2.35 Wt% and 4.31 Wt% ^{235}U Enriched UO_2 Rods in Water With Steel Reflecting Walls," Battelle Pacific Northwest Laboratories, NUREG/CR-1784, April, 1981.

6.12 Bierman, S.R., et al., "Critical Separation Between Subcritical Clusters of 4.29 Wt% ^{235}U Enriched UO_2 Rods in Water With Fixed Neutron Poisons," Battelle Pacific Northwest Laboratories, NUREG/CR-0073, May 1978.

6.13 Bierman, S.R., et al., "Criticality Experiments with Subcritical Clusters of 2.35 Wt% and 4.31 Wt% ^{235}U Enriched UO_2 Rods in Water With Uranium or Lead Reflecting Walls," Battelle Pacific Northwest Laboratories, NUREG/CR-0796, August, 1981.

6.14 Bierman, S.R., et al., "Critical Separation Between Subcritical Clusters of 2.35 Wt% ^{235}U Enriched UO_2 Rods in Water with Fixed Neutron Poisons," Battelle Pacific Northwest Laboratories, PNL-2438, October, 1977.

6.15 Baldwin, M.N., et al., "Critical Experiments Supporting Close Proximity Water Storage of Power Reactor Fuel," BAW-1484-7, Babcock & Wilcox Company, Lynchburg, Virginia, July, 1979.

6.16 Bierman, S.R., "Reactivity Measurements on an Experimental Assembly of 4.31 Wt% ^{235}U Enriched UO_2 Fuel Rods Arranged in a Shipping Cask Geometry," Battelle Pacific Northwest Laboratories, PNL-6838, October, 1989.

6.6.2 KENO Input Files

THIS SECTION CONTAINS
PROPRIETARY INFORMATION

7. OPERATING PROCEDURES

7.1 Procedures for Loading the Package

The NUHOMS®-MP187 Cask can be used (1) to transport fuel offsite; (2) to transfer fuel to horizontal storage modules (HSMs) in an onsite storage facility; or (3) an onsite storage container. Each of these modes of use requires (1) preparation of the cask for use; (2) verification that the fuel assemblies to be loaded meet the criteria set forth in this document; and (3) installation of a DSC and fuel assemblies into the cask.

Onsite storage involves transfer of the DSC to the storage facility where it is either inserted into an HSM, or left inside the cask for storage. Offsite transport involves (1) preparation of the cask for transport; (2) assembly verification leakage-rate testing of the package containment boundary; (3) placement of the cask onto a transportation vehicle; and (4) installation of the impact limiters.

During shipment, the packaging contains up to 24 spent fuel assemblies in the FO-DSC or FC-DSC, or up to 13 spent fuel assemblies in the FF-DSC. Procedures are provided in this section for three different handling/storage schemes, as shown in Figure 7.1-1. These include transport of the cask/DSC directly from the plant fuel pool, transport after storage in a NUHOMS® Horizontal Storage Module (HSM), and transport after onsite storage in the NUHOMS®-MP187 cask. Additional procedures are provided for handling a DSC which has leaked during storage in an HSM. A glossary of terms used in this section is provided in Section 7.1.9.

7.1.1 Preparation of the NUHOMS®-MP187 Cask for Use

Procedures for preparing the cask for use after receipt at the site are provided in this section.

a. Remove the impact limiter attachment bolts from each impact limiter and remove the impact limiters from the cask.

b. Anytime prior to removing the lid, sample the cask cavity atmosphere through the vent port. Flush the cask interior gases to the site radwaste systems if necessary.

c. Remove the transportation skid closure assembly.

d. Take contamination smears on the outside surfaces of the cask. If necessary, decontaminate the cask until smearable contamination is at an acceptable level.

e. Inspect the cask hardware (including closure plates, rupture discs, and vent/drain/test ports) for damage which may have occurred during transportation. Repair or replace as required. Metallic O-ring seals shall be discarded after each use.

f. Place suitable slings around the cask top and bottom ends, lift cask and place on suitable cribbing.

g. Remove the cask trunnion plugs. Inspect the trunnion sockets as discussed in Section 8.2.3.4, and install the upper and lower trunnions. Torque the trunnion attachment screws for each of the four trunnions in accordance with the drawings in Appendix 1.3.2.

h. Using slings, lift the cask and place it onto the onsite transfer trailer.

i. Remove the slings from the cask.

j. Install the onsite support skid pillow block covers.

7.1.2 Wet Loading the NUHOMS®-MP187 Cask and DSC

The procedure for wet loading the cask and DSC is summarized in this section. This procedure is intended to describe the type and quality of work performed to load and seal a DSC. Actual DSC loading procedures may vary slightly from tasks described below. The cask/DSC wet loading procedure is shown in Figure 7.1-2. The NUHOMS®-MP187 Cask is designed to transport one FO-DSC or FC-DSC containing twenty-four PWR fuel assemblies or one FF-DSC containing 13 PWR fuel assemblies. Fuel assemblies with missing fuel pins shall not be shipped in the FO-DSC or FC-DSC unless dummy fuel pins that displace an equal amount of water have been installed in the fuel assembly. All fuel assembly locations are to be loaded with design basis fuel assemblies or dummy assemblies of the same weight. Verification that the burnup, enrichment, and cooling time of the assemblies are all within acceptable ranges will be performed by site personnel, prior to shipment, as discussed below.

a. Verify that the fuel assemblies to be placed in the DSC meet the maximum burnup, maximum initial enrichment, minimum cooling time, and maximum decay heat limits for Type I or Type II fuel assemblies as specified in Section 1.2.3 of this document.

   Note: All damaged fuel assemblies to be loaded into the FF-DSC must meet the criteria in Section 1.2.3 for damaged fuel, having no more than 15 known or suspected damaged fuel rods.

   The potential of fuel misloading is essentially eliminated through the implementation of multiple procedural and administrative barriers. The controls instituted to ensure that fuel assemblies are loaded into a known cell location within a DSC will typically take the following form:

   - A cask/DSC loading plan is developed to compare various parameters including decay heat values to guarantee that Type I fuel assemblies are identified to be placed only in the four innermost cells of the DSC. This loading plan is the same procedure that verifies the fuel assemblies to be placed in the DSC meet the maximum burnup, maximum initial enrichment, and minimum cooling time requirements.

- The loading plan is independently verified and approved.

- A fuel movement schedule is then written, verified and approved based upon the loading plan. All fuel movements from any rack location are performed under strict verbatim compliance of the fuel movement schedule.

- All fuel assemblies are videotaped and independently verified by ID number to match the movement schedule prior to the placement of the shield plug.

- A third verification is performed by the Special Nuclear Materials Manager in preparation for the DOE reporting requirements. This third verification independently verifies that fuel in the DSC is placed per the original cask loading plan.

b. Using a suitable prime mover, position the cask and onsite transfer trailer below the plant crane.

c. Remove the ram closure plate, inspect the sealing surfaces, and re-install the ram closure plate. If the cask is to be used for transportation offsite, new metallic seals shall be installed with the ram closure plate. If the cask is to be used for onsite transfer of the DSC, a single, elastomeric seal may be installed in the ram closure in lieu of the dual metallic seals specified on the drawings. The purpose of this seal is only to protect the cask cavity from contamination. This seal is not intended to act as a containment boundary. Inspect the rupture discs for damage during prior operations. Repair or replace as necessary.

d. Remove the onsite support skid pillow block covers.

e. Engage the cask upper trunnions with the lifting yoke using the plant crane, rotate the cask to a vertical orientation, lift the cask from the onsite support skid, and place the cask in the plant decon area.

Note: The empty cask may be uprighted and lifted using the lifting yoke either with the top closure installed or removed.

f. If the cask top closure plate has not already been removed, remove the bolts from the cask top closure plate and lift the top closure plate and seals (if present) from the cask.

g. Discard the used metallic seals.

h. Install the cask shear key plug assembly.

i. Place an empty DSC in the cask. Align DSC to ensure proper positioning of DSC grapple ring key within cask bottom forging keyway.

j. Fill the DSC cavity and the cask/DSC annulus with clean, demineralized water and install the cask annulus seal.

Note: The DSC cavity may optionally be filled with borated spent fuel pool water if required by plant specific procedures.

k. Lower the cask and DSC into the fuel pool and load 24 PWR fuel assemblies into the DSC (13 assemblies for the FF-DSC). In accordance with Chapter 1, no more than four Type I assemblies shall be installed in the center fuel spaces. Location of Type I assemblies shall be verified to be the center four fuel spaces.

Note: Failed fuel assemblies may be placed into their removable cans directly in the FF-DSC and then the can lids installed, or loaded in a separate area and the loaded failed fuel can placed into the DSC.

l. Place the DSC top shield plug onto the DSC.

m. Lift the cask/canister/fuel from the fuel pool and place it in the plant decon area.

n. Remove surface water from the top of the DSC and the cask/DSC annulus seal.

o. Decontaminate the cask surfaces such that smearable surface contamination on the cask is less than 2200 dpm/100 cm^2 from beta and gamma emitting sources and 220 dpm/100 cm^2 from alpha emitting sources.

p. Install the DSC inner top cover plate and place the inner seal weld.

CAUTION: Monitor the hydrogen concentration in the DSC cavity during this step to ensure that it does not exceed 2.4%.

q. Drain the DSC and draw and hold a vacuum of three torr or less for a minimum of 30 minutes in the DSC cavity.

r. Backfill the DSC cavity with helium to 0 psig to 2.5 psig.

s. Install and seal weld the DSC vent and siphon port cover plates.

t. Install and seal weld the DSC outer top cover plate.

u. Remove the cask drain port screw and drain the cask/DSC annulus.

v. Install the drain port screw and tighten in accordance with the drawings in Appendix 1.3.2. Install and tighten the drain port plug to the torque specified in the Appendix 1.3.2 drawings.

7.1.3 Transferring the DSC to an Onsite Storage Facility

DSCs may be stored onsite in a 10 CFR Part 72 licensed facility prior to transportation. This section provides an outline of the procedure for transferring the DSC from the Auxiliary/Fuel building to an onsite ISFSI for storage either in the NUHOMS®-MP187 Cask or in an HSM. Note that the NUHOMS®-MP187 Cask or an alternate NRC approved onsite transfer cask may be used for onsite movements of the DSC. This procedure is described herein to provide a general description of 10 CFR 72 operations to be performed with the MP187 cask. These operations are governed by a 10 CFR 72 license. For onsite transfer operations, the DSC provides the fuel containment boundary and the cask is used for physical protection and shielding. The cask cavity, therefore, need not be sealed during onsite movements of the DSC.

a. Install the cask top closure and install a minimum of 12 top closure bolts snug tight. The top closure seals are not required to be installed.

b. Using the cask lifting yoke engage the upper trunnions, lift the cask from the decon area, and place the cask in the onsite support skid.

c. Install the onsite support skid pillow block covers.

d. Using a suitable prime mover, tow the onsite transfer trailer to the onsite storage facility.

7.1.4 Placing the DSC in an HSM for Storage

The procedure for loading a DSC into an HSM is summarized in this section. As noted above, either the NUHOMS®-MP187 Cask or an alternate onsite transfer cask may be used during HSM loading. This procedure is described herein to provide a general description of 10 CFR 72 operations to be performed with the MP187 cask. These operations are governed by a 10 CFR 72 license. This procedure is typical of NUHOMS® ISFSIs and some of the steps listed below may not be required and/or may be performed in a different order.

a. Position the onsite transfer trailer in front of the module face.

b. Remove the cask ram closure plate.

c. Install the ram trunnion support assembly.

d. Remove the HSM door.

e. Use the trailer skid positioning system and optical surveying transits to align the cask with the HSM.

f. Remove the cask top closure.

g. Dock the cask with the HSM and install the cask/HSM restraints.

h. Install and align the hydraulic ram cylinder in the ram trunnion support assembly.

i. Extend the ram hydraulic cylinder until the grapple contacts the DSC bottom cover.

j. Engage the DSC grapple ring with the ram grapple.

k. Extend the ram hydraulic cylinder until the DSC is fully inserted in the HSM.

l. Disengage the grapple from the DSC.

m. Remove the hydraulic ram from the cask.

n. Remove the cask from the HSM.

o. Install the HSM door and DSC seismic restraint.

7.1.5 Loading the DSC into the Cask from an HSM

The procedure for loading a DSC into the cask from a NUHOMS® Horizontal Storage Module (HSM) is summarized in this section. DSCs stored in HSMs have previously been loaded and sealed as described in Section 7.1.2 above. The cask/HSM loading procedure is shown in Figure 7.1-3. Depending on the most recent use of the cask, several of the initial steps listed below may not be necessary.

a. Using a suitable prime mover, bring the onsite transfer trailer (and cask) to the ISFSI site and back the trailer in front of the module face.

b. Remove the ram closure plate and the top closure plate.

c. Install the ram trunnion support assembly.

d. Remove the HSM door and the DSC seismic restraint assembly from the HSM.

e. Use the trailer skid positioning system and optical surveying transits to align and dock the cask with the HSM.

f. Install the cask/HSM restraints.

g. Install and align the hydraulic ram cylinder in the ram trunnion support assembly.

h. Extend the ram hydraulic cylinder until the grapple contacts the DSC bottom cover.

i. Engage the DSC grapple ring with the ram grapple.

j. Retract the ram hydraulic cylinder until the DSC is fully seated in the cask.

k. Disengage the grapple from the DSC.

l. Remove the hydraulic ram and ram trunnion support assembly from the cask.

m. Install the ram closure plate. If the DSC transfer is to result in long term storage or transportation, install a new set of metallic O-ring seals and perform the procedure described in Section 7.1.7. If the DSC is being moved to another HSM or the plant fuel pool, then a single O-ring (metallic or elastomeric) may be installed.

n. Remove the cask/HSM restraints.

o. Using the skid positioning system, move the cask to the transfer position and secure the onsite support skid to the onsite transfer trailer.

p. Install the cask toop closure. If the transfer is to result in long term storage or transportaion, install metallic O-ring seals and perform the procedure described in Section 7.1.7. If the DSC is being transferred on site, then install the cask top closure per Step "a" of Section 7.1.3.

7.1.6 Placing the DSC in Metal Cask Storage at an Onsite Facility

The procedure for placing the NUHOMS®-MP187 cask containing intact or failed DSCs into onsite storage is summarized in this section. This procedure is described herein to provide a general description of 10 CFR 72 operations to be performed with the MP187 cask. These operations are governed by a 10 CFR 72 license. DSCs to be stored have previously been loaded, sealed, and transferred to the facility as described in Sections 7.1.2 and 7.1.3 above.

a. If the DSC is stored in an HSM, retrieve the DSC as described in Section 7.1.5.

b. Install a new set of top closure seals.

c. If necessary, apply vacuum grease to the seals and the adjoining sealing surfaces on the cask top closure.

d. Install the cask top closure. Lubricate, install and preload the top closure bolts per the drawing requirements.

e. Install a new set of ram closure seals.

f. If necessary, apply vacuum grease to the seals and the adjoining sealing surfaces on the cask ram closure.

g. Install the cask ram closure plate. Lubricate, install, and preload the ram closure bolts per the drawing requirements.

h. Using a suitable vacuum pump, evacuate the cask cavity and backfill with helium.

i. Perform an assembly verification leak test as specified in Appendix 7.4.2.

j. Set the cask on the storage pad and if required install the shear key plug assembly and the cask weather shield/tip over impact limiter device.

7.1.7 Preparing the Cask for Transportation

Once a loaded DSC has been placed inside the NUHOMS®-MP187 Cask, the following tasks are performed to prepare the cask for transportation. The cask is assumed to be seated horizontally in the onsite support skid. Note that steps 7.1.7(a) through 7.1.7(e) have already been performed for DSCs stored in the cask and need not be repeated.

a. Verify that all metallic O-ring seals are new. Discard any seals that have previously been installed in the cask.

b. If necessary, apply vacuum grease to the seals and the adjoining sealing surfaces on the cask top closure.

c. Install the cask top closure plate. Lubricate, install and preload the top closure bolts per the drawing requirements.

d. If necessary, apply vacuum grease to the seals and the adjoining sealing surfaces on the cask ram closure.

e. Install the cask ram closure plate. Lubricate, install and preload the ram closure bolts per the drawing requirements.

f. If necessary, remove the shear key plug assembly from the cask.

g. Verify that the drain port screw is installed and torqued in accordance with the drawings in Appendix 1.3.2.

h. Verify that the fuel assemblies meet the burnup, initial enrichment, cooling time, and decay heat criteria set forth in Section 1.2.3.

i. Not used.

j. Verify that the cask surface removable contamination levels meet the requirements of 49 CFR 173.443 [7.2] and 10 CFR 71.87 [7.3].

k. Perform the assembly verification leakage rate testing specified in Appendix 7.4.2. This test must be performed within 12 months prior to the shipment. This test includes drawing a vacuum in the cavity between the cask and DSC, which ensures that any water has been removed.

7.1.8 Placing the Cask onto the Railcar

The procedure for placement of the cask on the railcar is given in this section and shown in Figure 7.1-4.

a. Using a suitable prime mover, bring the cask and onsite transfer trailer to the transportation railcar.

b. Remove the onsite support skid pillow block covers.

c. Install suitable slings around the cask top and bottom ends.

d. Lift the cask from the onsite transfer trailer.

e. Remove the cask upper and lower trunnions and install the trunnion plugs.

f. Place the cask onto the railcar transportation skid.

g. Remove the lifting slings from the cask.

h. Install the skid closure assembly and insert the locking wedges.

i. Install the impact limiters on the cask and torque the mounting bolts in accordance with the drawings in Appendix 1.3.2.

j. Install the cask tamperproof seals.

k. Monitor the cask radiation levels per 49 CFR 173.441 [7.2] and 10 CFR 71.47 [7.3] requirements.

Note: The procedure outlined above may also be used to transfer the cask directly from the fuel pool to a rail car, without using the transfer trailer, should appropriate facilities be available for such a transfer. The procedures outlined in Section 7.1.7 would also be applicable to such a scenario.

7.1.9 Glossary

The following terms, used in the above procedures, are defined below. See Table 1.0-1 for terms relating to the package.

a.	Horizontal Storage Module (HSM):	Concrete shielded structure used for onsite storage of DSCs.
b.	Onsite Transfer Trailer:	A hydraulically supported trailer used for onsite movements of the cask.
c.	Onsite Support Skid:	Skid present on the onsite transfer trailer used to support the cask during onsite movements.
d.	Cask/DSC Annulus Seal:	Pneumatic seal placed between the cask and DSC during operations in the fuel pool.
e.	Cask Lifting Yoke:	Passive, open hook lifting yoke used for vertical lifts of the cask.
f.	Ram Trunnion Support Assembly:	Frame attached to the cask bottom which provides an anchor for the hydraulic ram during DSC insertion and retrieval.
g.	Skid Positioning System:	Hydraulically operated alignment system that provides the interface between the onsite transfer trailer and the onsite support skid.
h.	Hydraulic Ram:	Hydraulic cylinder used to insert/withdraw DSCs to/from HSMs.
i.	Cask/HSM Restraints:	Provides the load path between the cask and HSM during DSC transfer operations.
j.	Cask Weather Shield/ Tip Over Impact Limiter Device:	Provides environmental protection of the cask top cover during storage and protects cask contents in event of cask tipover.

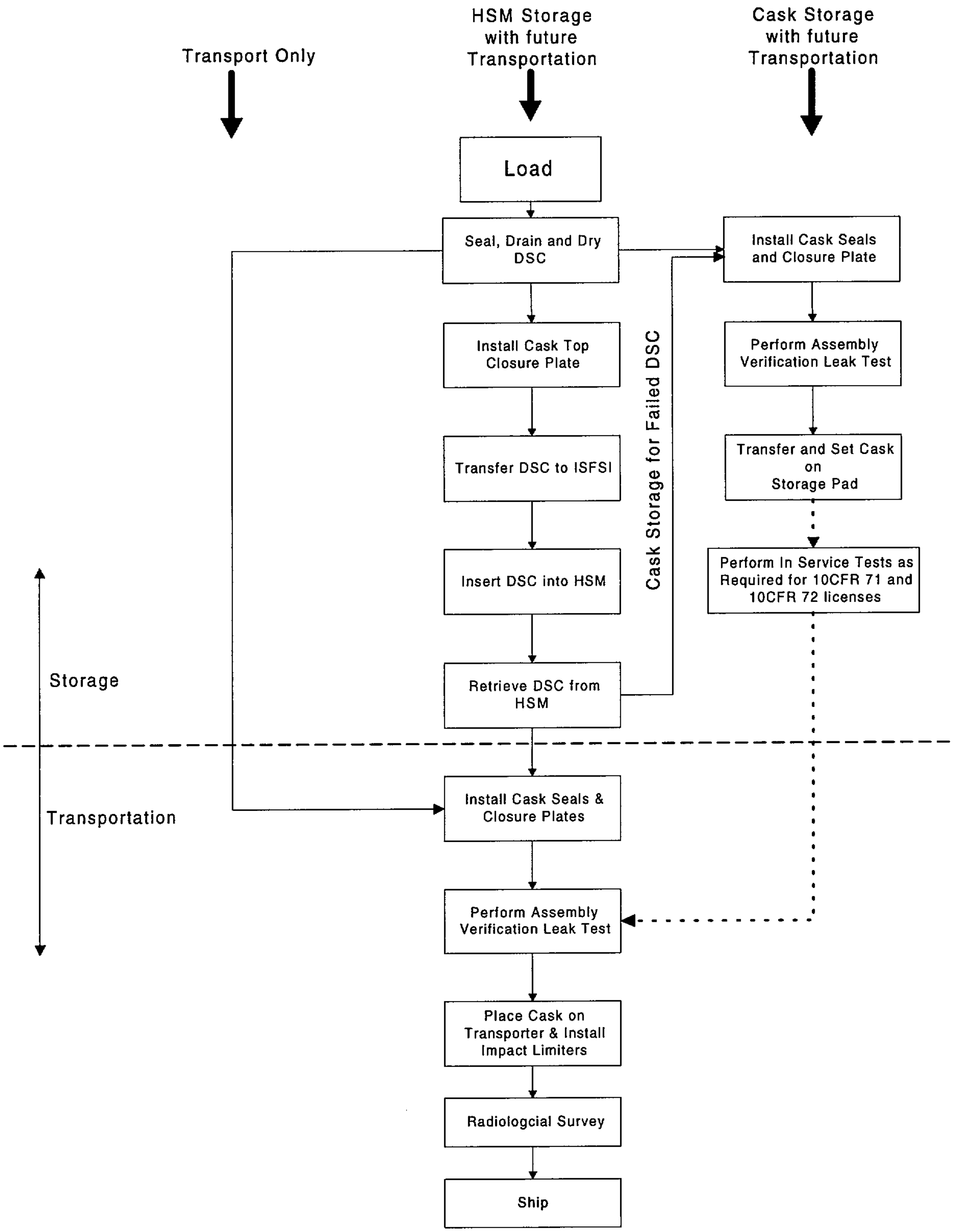

Figure 7.1-1

NUHOMS®-MP187 Cask Operating Procedures Flow Chart

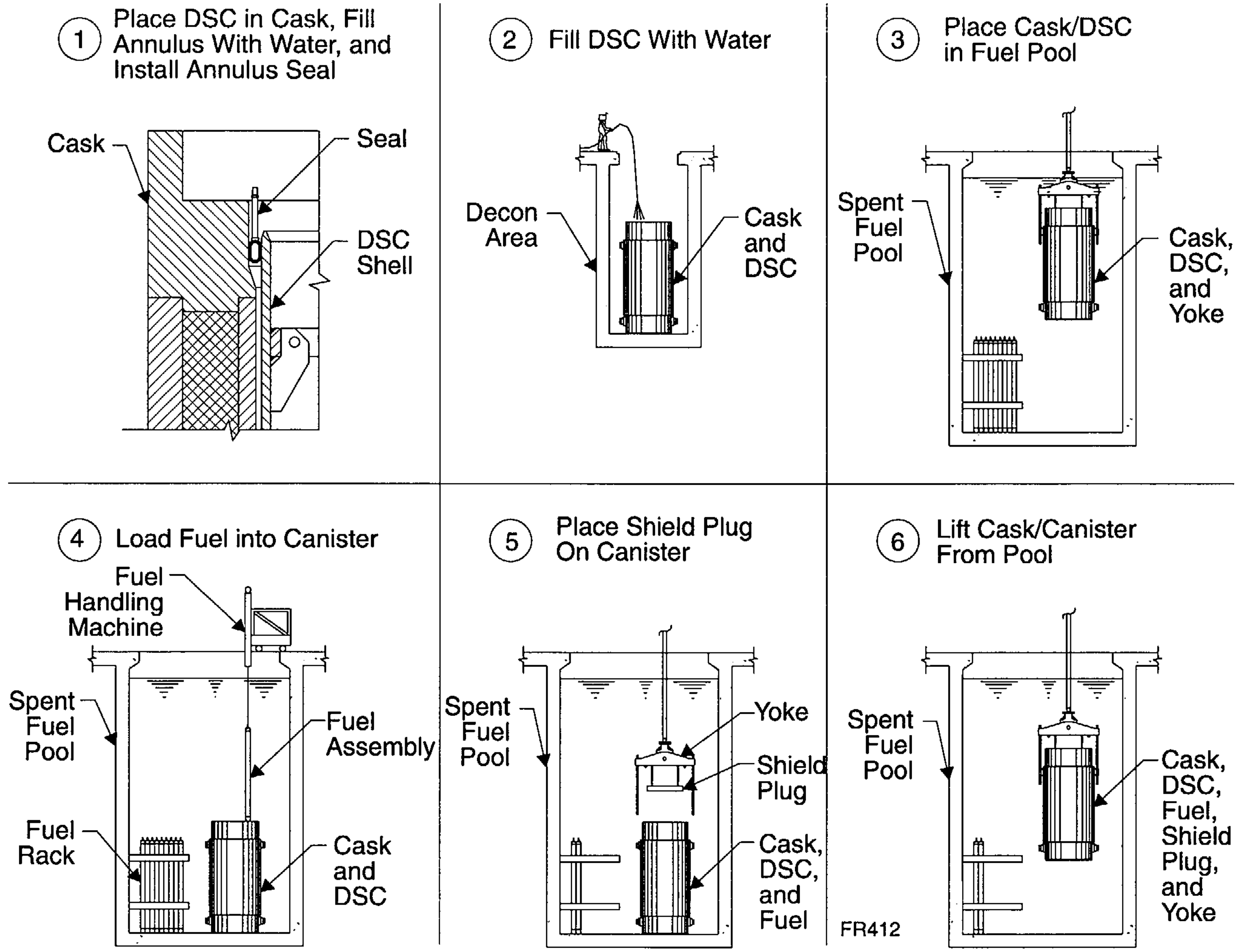

Figure 7.1-2
NUHOMS®-MP187 Wet Loading Procedure

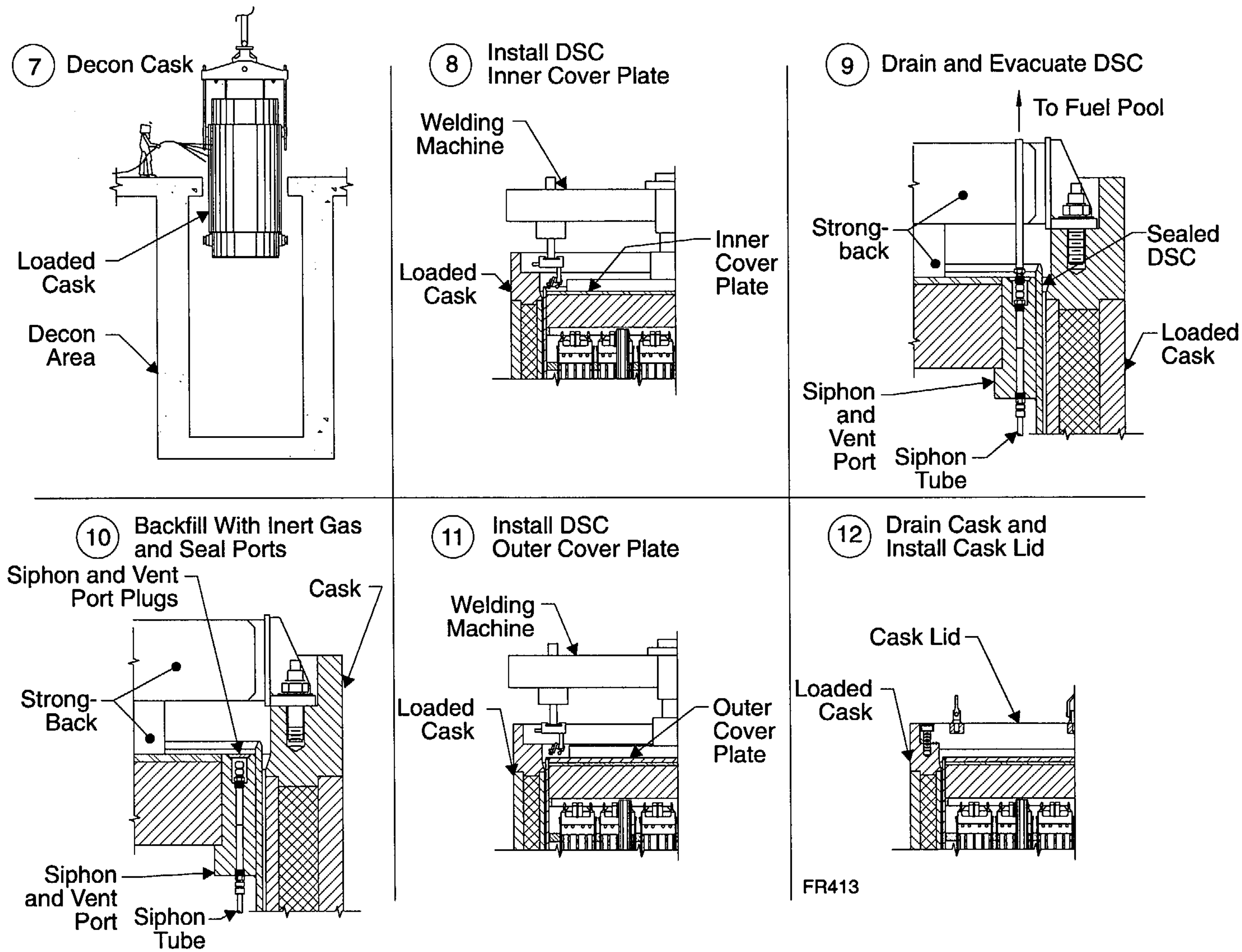

Figure 7.1-2
NUHOMS®-MP187 Wet Loading Procedure (concluded)

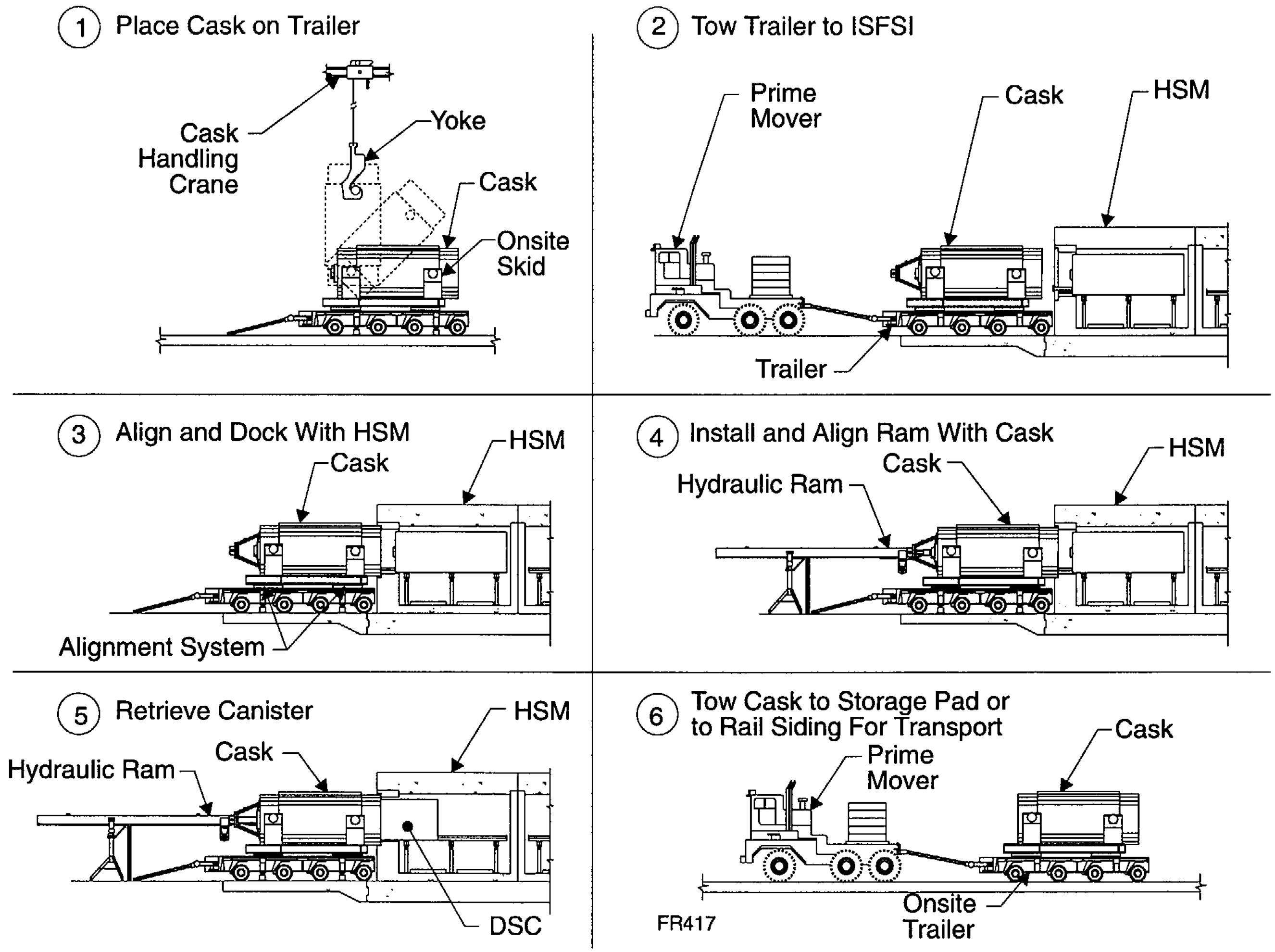

Figure 7.1-3
NUHOMS®-MP187 Dry Loading Procedure

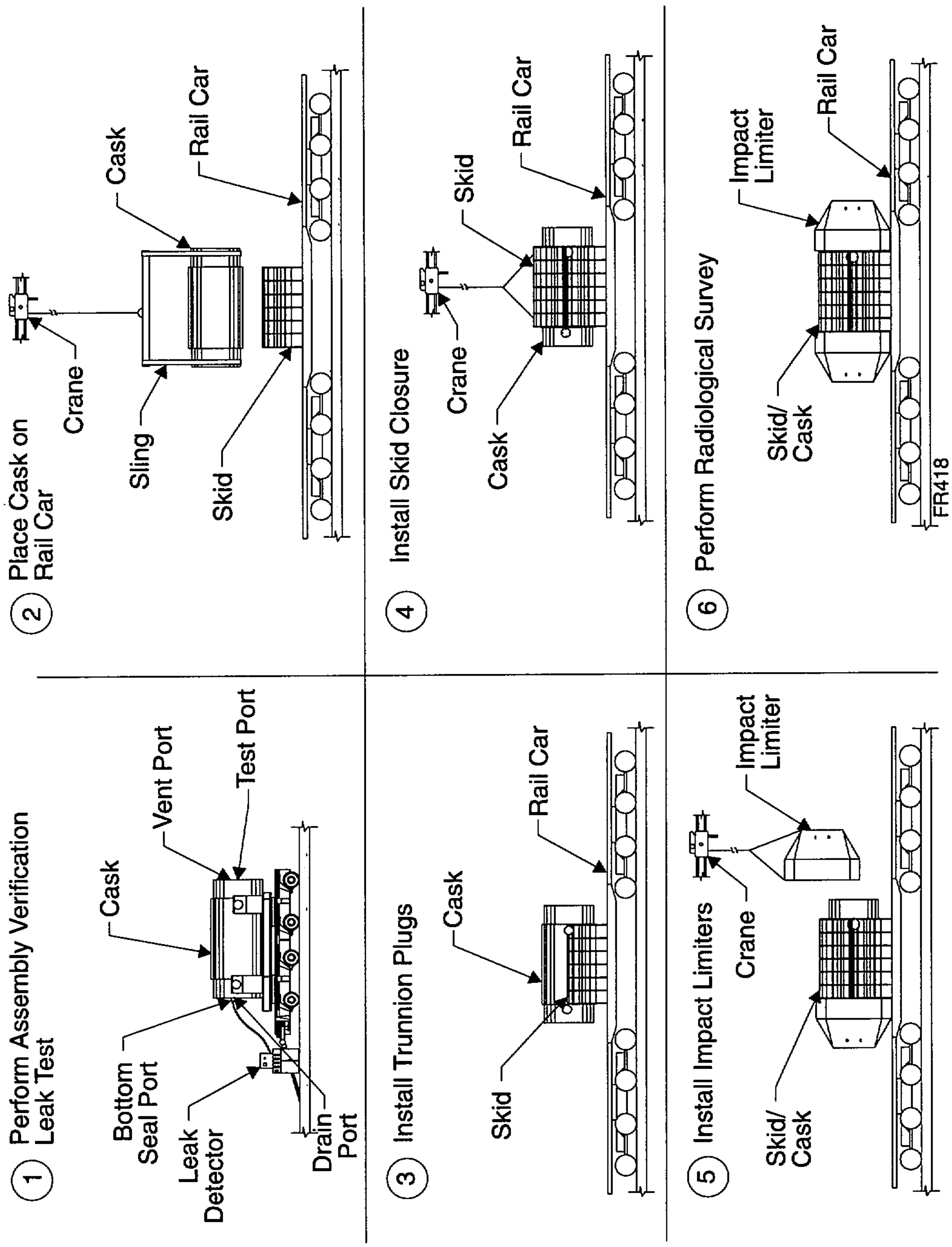

Figure 7.1-4

NUHOMS®-MP187 Preparation for Transportation

7.2 Procedures for Unloading the Cask

Unloading the NUHOMS®-MP187 Cask after transport involves removing the cask from the railcar and removing the canister from the cask. The cask is designed to allow the canister to be unloaded from the cask into a NUHOMS® staging module, or hot cell, and provisions exist to allow wet unloading into a fuel pool. The necessary procedures for these tasks are essentially the reverse of those described in Section 7.1.

7.2.1 Receipt of the Loaded NUHOMS®-MP187 Cask

Procedures for receiving the loaded cask after shipment are described in this section. Procedures for receiving an empty cask are provided in Section 7.1.1.

a. Verify that the tamperproof seals are intact.

b. Remove the tamperproof seals.

c. Remove the impact limiter attachment bolts from each impact limiter and remove the impact limiters from the cask.

d. Remove the transportation skid closure assembly.

e. Take contamination smears on the outside surfaces of the cask. If necessary, decontaminate the cask until smearable contamination is at an acceptable level.

f. Place suitable slings around the cask top and bottom ends.

g. Using a suitable crane, lift the cask from the railcar and remove the cask trunnion plugs. Inspect the trunnion sockets as discussed in Section 8.2.3.4 and install the upper and lower trunnions. Torque the trunnion attachment screws for each of the four trunnions in accordance with the drawings in Appendix 1.3.2. Place cask onto the onsite transfer trailer. Remove the slings from the cask.

h. Install the onsite support skid pillow block covers.

i. Transfer the cask to a staging module, fuel pool, or dry cell and unload using the procedures described in the following sections.

7.2.2 Unloading the NUHOMS®-MP187 Cask to a Staging Module

The procedure for unloading a DSC from the cask into an HSM is summarized in this section. This procedure is typical of NUHOMS® ISFSIs and some of the steps listed below may be performed in a different order.

a. Position the onsite transfer trailer in front of the module face.

b. Sample the cask cavity atmosphere through the vent port. Flush the cask interior gases to the site radwaste systems if necessary.

c. Remove the cask ram closure plate. Discard the metallic ram closure seals.

d. Install the ram trunnion support assembly.

e. Remove the HSM door.

f. Use the skid positioning system and optical surveying transits to align the cask with the HSM.

g. Remove the cask top closure. Discard the metallic top closure seals.

h. Dock the cask with the HSM and install the cask/HSM restraints.

i. Install and align the hydraulic ram cylinder in the ram trunnion support assembly.

j. Extend the ram hydraulic cylinder until the grapple contacts the DSC bottom cover.

k. Engage the DSC grapple ring with the ram grapple.

l. Extend the ram hydraulic cylinder until the DSC is fully inserted in the HSM.

m. Disengage the grapple from the DSC.

n. Remove the hydraulic ram from the cask.

o. Remove the cask from the HSM.

p. Install the HSM door and DSC seismic restraint.

q. Move the onsite transfer trailer and cask to a low-dose maintenance area.

r. Inspect the cask hardware (including covers and vent/drain/test ports) for damage that may have occurred during transportation. Repair or replace as necessary.

7.2.3 Unloading the NUHOMS®-MP187 Cask to a Fuel Pool

The procedure for unloading the cask and DSC into a fuel pool is summarized in this section. This procedure is intended to describe the type and quality of work performed to unload a DSC. Actual DSC unloading procedures may vary slightly from the tasks described below. Note that the NUHOMS®-MP187 cask or an alternate suitable cask may be used for onsite movements of the DSC.

a. Tow the onsite transfer trailer to the fuel receiving area.

b. Remove the onsite support skid pillow block covers.

c. Using the cask lifting yoke, engage the upper trunnions, rotate the cask to a vertical orientation, lift the cask from the onsite support skid, and place the cask in the decon pit.

d. Sample the cask cavity atmosphere through the vent port. Flush the cask interior gases to the site radwaste systems if necessary.

e. Remove the bolts from the cask top closure and lift the top closure plate from the cask.

f. Remove and discard the cask top closure seals.

g. Install the shear key plug assembly.

h. Locate the DSC siphon and vent ports using the indications on the DSC outer top cover plate.

i. Drill a hole in the DSC outer top cover plate and remove the siphon closure plug to expose the siphon port quick connect.

j. Drill a hole in the DSC outer top cover plate and remove the vent closure plug to expose the vent port quick connect.

k. Sample the DSC cavity atmosphere. If necessary, flush the DSC cavity gases to the site radwaste systems.

l. Fill the DSC with demineralized water through the siphon port with the vent port open and routed to the plant's off-gas system.

Note: The DSC cavity may optionally be filled with borated water.

m. Install a debris shield over the cask/DSC annulus.

n. Use plasma arc-gouging, a mechanical cutting system, or other suitable means remove the closure weld from the outer top cover plate.

CAUTION: Monitor the hydrogen concentration in the DSC cavity during this step to ensure that it does not exceed 2.4%.

o. Remove the DSC outer top cover plate.

p. Remove the closure weld from the DSC inner top cover plate.

q. Remove the DSC inner top cover plate.

r. Fill the cask/DSC annulus with demineralized water and install the cask/DSC annulus seal.

s. Remove excess material on the DSC inside shell surface which will interfere with top shield plug removal.

t. Clean the cask surface of dirt and debris that may have accumulated during transportation or weld removal.

u. Engage the cask lifting yoke to the upper trunnions and install the shield plug cables between the yoke and the DSC top shield plug.

v. Lower the cask into the fuel pool.

w. Disengage the lifting yoke from the cask trunnions and remove the top shield plug.

x. Remove the fuel assemblies (or fuel cans for the FF-DSC) from the DSC.

y. Engage the lifting yoke to the cask upper trunnions, remove the cask from the pool, and place it in the decon area.

z. Remove the water from the DSC cavityand DSC/Cask annulus.

aa. Remove the DSC from the cask and handle in accordance with low-level waste procedures.

bb. Decontaminate the cask inner and outer surfaces as necessary.

cc. Inspect the cask hardware (including covers and valves) for damage that may have occurred during transportation. Repair or replace as necessary.

7.2.4 Unloading the NUHOMS®-MP187 Cask to a Dry Cell

The procedure for handling a DSC in a dry cell is highly dependent on the design of the dry cell and on the intended future use of the DSC. The procedure described below is intended to show the type of operations that will be performed and is not intended to be limiting.

a. Tow the onsite transfer trailer to the hot cell area.

b. Remove the onsite support skid pillow block covers.

c. Using the cask lifting yoke, engage the upper trunnions, rotate the cask to a vertical orientation, lift the cask from the onsite support skid, and place the cask in the appropriate handling area.

d. Sample the cask cavity atmosphere through the vent port. Flush the cask interior gases to the site radwaste systems if necessary.

e. Remove the bolts from the cask top closure and lift the top closure plate from the cask.

f. Remove and discard the cask top closure seals.

g. Install the shear key plug assembly, if required.

h. Transfer the cask into the hot cell using suitable handling equipment.

i. Remove the DSC from the cask and handle according to appropriate procedures.

j. Remove the cask from the hot cell.

k. Decontaminate the cask inner and outer surfaces as necessary.

l. Inspect the cask hardware (including covers and vent/drain/test ports) for damage that may have occurred during transportation. Repair or replace as necessary.

7.3 Preparation of an Empty Cask for Transport

Previously used and empty NUHOMS®-MP187 casks shall be prepared for transport per the requirements of 49 CFR 173.427 [7.2].

7.4 Appendix

7.4.1 References

7.1 ANSI N14.5-1987, "American National Standard for Radioactive Materials - Leakage Tests on Packages for Shipment," American National Standards Institute, Inc., New York, 1987.

7.2 Title 49, Code of Federal Regulations, Part 173 (49 CFR 173), "Shippers - General Requirements for Shipments and Packaging."

7.3 Title 10, Code of Federal Regulations, Part 71 (10 CFR 71), "Packaging and Transportation of Radioactive Material."

7.4.2 Leakage Rate Testing of the Containment Boundary

The procedure for leak testing the cask containment boundary prior to shipment is given in this section. Assembly verification leak testing shall conform to the requirements of Section 6.5 and Section A3.5 of ANSI N14.5-1987, "American National Standard for Radioactive Materials - Leakage Tests on Packages for Shipment [7.1]". A flow chart of the assembly verification leak test is provided in Figure 7.4-1. The order in which the leak tests of the various seals are performed may vary. If more than one leak detector is available then more than one seal may be tested at a time.

a. Remove the cask vent port plug.

b. Install the cask port tool in the cask vent port. (The port tool is designed to replace the vent/drain and test prot plugs and provide a means for loosening the vent/drain and test port screw in a controlled volume. This volume can be isolated from the cask volume by an externally accessible valve to ensure personell protection during cask venting operations.)

c. Turn the cask port tool handle to open the cask vent port.

d. Attach a suitable vacuum pump to the cask port tool.

e. Reduce the cask cavity pressure to below 1.0 psia.

f. Attach a source of helium to the cask port tool.

g. Fill the cask cavity with helium to atmospheric pressure.

h. Close the vent port screw by turning the cask port tool handle. Tighten the vent port screw in accordance with the drawings in Appendix 1.3.2.

i. Remove the helium saturated cask port tool and install a clean (helium free) cask port tool.

j. Connect a mass spectrometer leak detector capable of detecting a leak of $5x10^{-8}$ standard cubic centimeters per second to the cask port tool.

k. Evacuate the vent port until the vacuum is sufficient to operate the leak detection equipment per the manufacturer's recommendations.

l. Perform the leak test. If the leakage rate is greater than $1x10^{-7}$ standard cubic centimeters per second repair or replace the vent port screw and/or seal as required and retest.

Note: Upon removing the vent port screw, it will be necessary to reduce the cask cavity pressure below 1.0 psia and refill with helium through the vent port.

m. Remove the leak detection equipment from the cask vent port.

n. Remove the cask port tool from the vent port and replace the vent port plug.

o. Remove the top test port plug.

p. Install the cask port tool in the top test port.

q. Turn the cask port tool handle to open the top test port.

r. Connect the vacuum pump to the cask port tool.

s. Connect the leak detector to the cask port tool.

t. Evacuate the top test port until the vacuum is sufficient to operate the leak detection equipment per the manufacturer's recommendations. Perform a pressure rise leak test to confirm leakage past the outer seal is less than $7x10^{-3}$ std-cc/sec of air.

u. Perform the helium leak test. If the leakage rate is greater than 1×10^{-7} standard cubic centimeters per second repair or replace the cask top closure or the cask top closure O-ring seals as required and retest.

Note: Upon removing and reinstalling the cask top closure, it will be necessary to reduce the cask cavity pressure below 1.0 psia and refill with helium through the vent port. The vent port assembly verification test must also be retested as described above.

v. Remove the leak detection equipment from the top test port.

w. Tighten the top test port screw in accordance with the drawings in Appendix 1.3.2. Remove the cask port tool from the top test port and replace the top test port plug.

x. Remove the cask drain port plug.

y. Install the cask port tool in the cask drain port.

z. Turn the cask port tool handle to verify that the cask drain port is closed.

aa. Connect the vacuum pump to the cask port tool.

bb. Connect the leak detector to the cask port tool.

cc. Evacuate the drain port until the vacuum is sufficient to operate the leak detection equipment per the manufacturer's recommendations.

dd. Perform the leak test. If the leakage rate is greater than 1×10^{-7} standard cubic centimeters per second repair or replace the drain port screw and/or seal as required and retest.

Note: Upon removing the drain port screw, it will be necessary to reduce the cask cavity pressure below 1.0 psia and refill with helium through the vent port. The vent port assembly verification test must also be retested as described above.

ee. Remove the leak detection equipment from the drain port.

ff. Tighten the drain port screw in accordance with the Drawings in Appendix 1.3.2. Remove the cask port tool from the cask drain port and replace the drain port plug.

gg. Remove the bottom test port plug.

hh. Install the cask port tool in the bottom test port.

ii. Turn the cask port tool handle to open the bottom test port.

jj. Connect the vacuum pump to the cask port tool.

kk. Connect the leak detector to the cask port tool.

ll. Evacuate the bottom test port until the vacuum is sufficient to operate the leak detection equipment per the manufacturer's recommendations. Perform a pressure rise leak test to confirm leakage past the outer seal is less than $7x10^{-3}$ std-cc/sec of air.

mm. Perform the helium leak test. If the leakage rate is greater than $1x10^{-7}$ standard cubic centimeters per second repair or replace the cask ram closure or the cask ram closure O-ring seals as required and retest.

Note: Upon removing the cask ram closure, it will be necessary to reduce the cask cavity pressure below 1.0 psia and refill with helium through the vent port. The vent port assembly verification test must also be retested as described above.

nn. Remove the leak detection equipment from the bottom test port.

oo. Tighten the bottom test port screw in accordance with the drawings in Appendix 1.3.2. Remove the cask port tool from the bottom test port and replace the bottom test port screw.

This concludes the assembly verification leak test procedure.

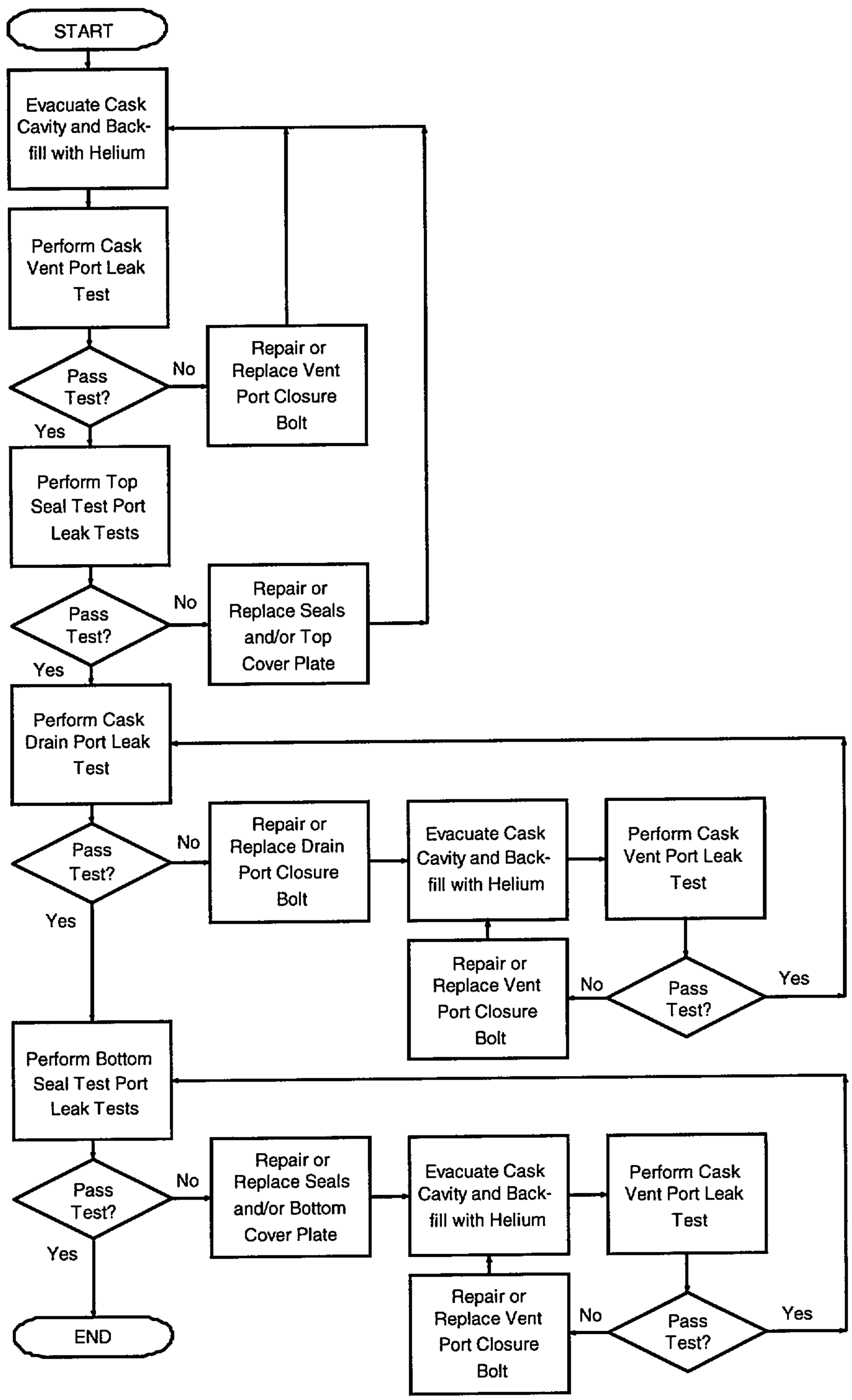

Figure 7.4-1

Assembly Verification Leak Test Flow Chart

8. ACCEPTANCE TESTS AND MAINTENANCE PROGRAM

8.1 Acceptance Tests

This section discusses the tests to be performed prior to first use of the package.

8.1.1 Visual Inspection

All NUHOMS®-MP187 Multi-Purpose Cask materials of construction and welds shall be examined in accordance with the specifications delineated on the Packaging General Arrangement Drawing in Appendix 1.3.2.

8.1.2 Structural and Pressure Tests

The maximum working load for each of the lifting trunnions (the two trunnions closest to the top of the cask) is one-half the weight of the NUHOMS®-MP187 cask, canister and fuel, without impact limiters and lids, and including the weight of the cask cavity full of water. Each of the lifting trunnions will be load tested to 150% of this maximum working load per ANSI N14.6 - 1986 [8.2], as specified in the design drawings provided in Appendix 1.3.2.

Per the drawings in Appendix 1.3.2, all welds and material in the lifting load path for the trunnions shall be visually inspected for plastic deformation or cracking, visually inspected and liquid penetrant inspected or magnetic particle inspected per ASME Boiler and Pressure Vessel Code [8.1], Section V, Article 6 and Section III, Division 1, Subsection NB, Article NB-5000 as called for in ANSI N14.6-1986 [8.2]. Any indication of cracking or distortion shall be recorded on a Nonconformance Report and dispositioned prior to final acceptance in accordance with the Transnuclear West Quality Assurance Program.

The cask containment boundary shall be pressure tested to 150% of the maximum normal operating pressure per the requirements of Reference 8.3, Paragraph 71.85(b) to verify structural integrity. The cask containment maximum design pressure is 50 psig which is greater than the maximum normal operating pressure calculated in Section 3.1.3 of 45.1 psia. The containment vessel will be tested to 75 psig which is 150% of the design pressure. Accessible weld and material inspections will be performed after the pressure test to verify maintenance of structural integrity and absence of any permanent deformations.

8.1.3 Leak Tests

The fabrication verification leak test will be performed after initial fabrication to verify package configuration and performance to design criteria in accordance with Reference 8.3, Paragraph 71.85(a) and ANSI 14.5 [8.4].

The fabrication verification leak test can be separated into the following five tests: 1) cask leakage integrity, 2) cask vent port closure bolt seal integrity, 3) cask drain port closure bolt seal integrity, 4) cask top closure plate seal integrity, and 5) ram closure plate seal integrity. The testing will be accomplished in accordance with the ANSI N14.5 [8.4]. Typical methodology for complying with ANSI N14.5 are presented below. These sections also include the typical rework steps in the event of test failure. The tests need not be performed concurrently or in the specific order provided herein.

All references to the vent, test and drain port closure bolts reflect the assembly which is made up of a slotted cap screw and a metallic O-ring.

8.1.3.1 Prerequisites

a. Obtain a helium mass spectrometer leak detector capable of detecting a leak of $5x10^{-8}$ standard cubic centimeters per second, or better.

b. Calibrate the leak detector according to the manufacturer's recommendations such that the leak detector sensitivity is $5x10^{-8}$ standard cubic centimeters per second, or better.

8.1.3.2 Testing the Cask Leakage Integrity

Prior to lead pour and final machining of the inner shell, the cylindrical portion of the containment boundary including the bottom end closure will be leak tested in accordance with the requirements of ANSI N14.5, using temporary closures and seals for the ram and top closure plates. Final machining of the inner shell I.D. may be performed after completion of the lead pour when the lead and structural shell will provide support to the inner shell during final machining. For this test the interior of the cask cavity will be flooded with a helium atmosphere while vacuum is drawn on the lead cavity to determine the leak rate. If a leak is discovered the source will be determined, repaired and the shells retested to ensure that the measured leak rate is less than 1×10^{-7} standard cubic centimeters per second.

A leak test at this interim stage of fabrication will ensure leak tightness of the containment shell. The test will be performed in conjunction with the non-destructive examination of the inner shell welds in accordance with ASME BPVC, Section III, Subsection NB, a PT examination of every weld layer in the shell to top forging closure weld, and a PT examination of all final machined surfaces of the inner shell per the ASME Code. These examinations combined with the fabrication leak test, plus a second helium leak test performed on the completed cask, will ensure that the containment is leak tight.

On the completed cask, the cask body integrity is tested as follows:

a. Clean and inspect O-ring top and ram closure plate seals. Sparingly apply new vacuum grease to the seals and adjoining seal areas if needed. Install O-ring seals into the O-ring grooves.

b. Remove the protective cover from the vent port, followed by the vent port closure bolt.

c. Install a vent port tool into the vent port.

d. Sparingly apply new vacuum grease to the seal area on the cask body. Inspect the cask top closure bolts for signs of damage or wear. Replace defective bolts. Install the cask top closure plate, tightening the thirty-six (36) 2 inch bolts in accordance with the preload requirements of the Packaging General Arrangement Drawings, Appendix 1.3.2.

e. Clean and inspect both ram closure port cover O-ring seals. Sparingly apply new vacuum grease to the seals and adjoining seal areas if needed. Install the O-ring seals into the O-ring grooves.

f. If needed, sparingly apply new vacuum grease to the seal area on the ram closure plate. Inspect the ram closure plate bolts for signs of damage or wear. Install the ram closure plate, tighten twelve (12) 1 inch bolts in accordance with the torque requirements found on the Packaging General Arrangement Drawings in Appendix 1.3.2.

g. Utilizing appropriate fittings, attach a leak detector and a source of helium gas, in parallel, to the vent port tool. Install valves on each of the lines to allow independent isolation of the leak detector and the source of the helium gas to the vent port tool. Close the valve to the helium gas source and open the valve to the leak detector.

h. Evacuate the system through the vent port tool until the vacuum is adequate to operate the leak detector per the manufacturer's instructions.

i. Provide a helium atmosphere about the exterior of the cask body, taking care to purge all other gases from any pockets or cavities adjacent to the cask body.

j. Determine the leak rate of the system using the leak detector manufacturer's recommendations, and so note.

k. If the leak rate of the system is determined to be greater than $1\text{x}10^{-7}$ standard cubic centimeters per second, release the vacuum, disassemble the system and utilize appropriate methods to locate/isolate the leak path. Repair the leak path and repeat Steps c. through m. to verify cask leakage integrity.

l. Remove the leak detector from the vent port tool.

8.1.3.3 Testing the Cask Vent Port Closure Bolt Seal Integrity

a. Open the isolation valve to the source of helium gas thereby allowing free passage of the gas into the evacuated cask cavity.

NOTE: The next step must be performed quickly to reduce the loss of helium gas from the cask cavity.

b. When the internal pressure of the system reaches atmospheric, remove the helium-saturated vent port tool and install the vent port closure bolt, pressure tight.

c. Install a clean (helium-free) vent port tool.

d. Rotate the handle on the vent port tool closed to verify the vent port closure bolt is properly seated. Torque the vent Port closure bolt in accordance with the requirements on the drawings in Appendix 1.3.2.

e. Utilizing appropriate fittings, attach the leak detector to the vent port tool.

f. Evacuate the system through the vent port tool until the vacuum is sufficient to operate the leak detector as per the manufacturer's recommendations. Note any adjustments made to the connecting fittings required to achieve sufficient vacuum.

g. Determine the leak rate of the system using the leak detector manufacturer's recommendations, and so note.

h. If the leak rate of the system is determined to be greater than $1x10^{-7}$ standard cubic centimeters per second, release the vacuum, remove the vent port closure bolt, and inspect the vent port closure bolt seal for cuts, tears, or abrasion, and the seal area for cleanliness and surface condition. If necessary, replace the seal and/or repair the seal area. Repeat Steps a through h. If, after repeated testing, it has been determined that the vent port closure bolt cannot be made to pass the test, utilize appropriate methods to locate and isolate the leak path. Repair the leak path and repeat Steps a through h to verify vent port closure bolt seal integrity.

NOTE: Upon removing and replacing the vent port closure bolt, it will be necessary to plug the vent port to reduce the loss of helium from the cask cavity prior to retesting.

i. Remove the vent port tool/leak detector assembly from the vent port and replace the vent port plug.

8.1.3.4 Testing the Cask Drain Port Closure Bolt Seal Integrity

a. Verify that the drain port closure bolt has been installed properly with the seal. The closure bolt should be torqued in accordance to the requirements on the drawings in Appendix 1.3.2.

b. Verify that the cask has been evacuated and filled with helium.

c. Install a clean (helium-free) port tool at the drain port.

d. Rotate the handle on the port tool closed to verify the drain port closure bolt is properly seated and tighten in accordance with the requirements of the drawings in Appendix 1.3.2.

e. Utilizing appropriate fittings, attach the leak detector to the port tool.

f. Evacuate the system through the port tool until the vacuum is sufficient to operate the leak detector as per the manufacturer's recommendations. Note any adjustments made to the connecting fittings required to achieve sufficient vacuum.

g. Determine the leak rate of the system using the leak detector manufacturer's recommendations, and so note.

h. If the leak rate of the system is determined to be greater than 1×10^{-7} standard cubic centimeters per second, release the vacuum, remove the drain port closure bolt, and inspect the drain port closure bolt seal for cuts, tears, or abrasion, and the seal area for cleanliness and surface condition. If necessary, replace the seal and/or repair the seal area. Repeat Steps a through h. If, after repeated testing, it has been determined that the drain port closure cannot be made to pass the test, utilize appropriate methods to locate/isolate the leak path. Repair the leak path and repeat Steps a through h to verify drain port closure bolt seal integrity.

NOTE: Upon removing and replacing the drain port closure bolt, it will be necessary to plug the drain port to reduce the loss of helium from the cask cavity prior to retesting.

i. Remove the vent port tool/leak detector assembly from the drain port and replace the drain port plug.

8.1.3.5 Testing the Cask Top Closure Plate Seal Integrity

a. Rotate the handle on the cask top closure plate test port tool to open the test port closure bolt. Continue to rotate the knurled handle until it stops.

b. Utilizing appropriate fittings, attach the leak detector to the lid test port tool.

c. Evacuate the system through the test port tool until the vacuum is sufficient to operate the leak detector per the manufacturer's recommendations. Note any adjustments made to the connecting fittings required to achieve sufficient vacuum. Determine the leak rate of the outer seal by performing a pressure rise test.

d. Determine the helium leak rate of the system using the leak detector manufacturer's recommendations, and so note.

e. If the leak rate of the system is determined to be greater than 3×10^{-3} std-cc/sec of air for the pressure rise test or greater than 1×10^{-7} standard cubic centimeters per second of helium, release the vacuum, remove the top closure plate, and inspect the O-ring seals for cuts, tears, or abrasion, and the seal areas for cleanliness and surface condition. If necessary, replace the seal(s) and/or repair the seal area(s). Repeat Steps a through e. If, after repeated testing, it has been determined that the cask top closure seals cannot be made to pass the test, utilize appropriate methods to locate/isolate the leak path. Repair the leak path and repeat Steps a through e to verify top closure seal integrity.

NOTE:: Upon removing and replacing the top closure, it will be necessary to reduce the cavity pressure below 1.0 psia and refill the cask cavity with helium through the vent port.

8.1.3.6 Testing the Ram closure Seal Integrity

a. Remove the protective cover from the ram closure test port and, in its place, install a test port tool.

b. Rotate the handle on the test port tool to open the test port closure bolt. Continue to rotate the handle until it stops.

c. Utilizing appropriate fittings, attach the leak detector to the test port tool.

d. Evacuate the system through the test port tool until the vacuum is sufficient to operate the leak detector as per the manufacturer's recommendations. Note any adjustments made to the connecting fittings required to achieve sufficient vacuum. Determine the leak rate of the outer seal by performing a pressure rise test.

e. Determine the helium leak rate of the system using the leak detector manufacturer's recommendations, and so note.

f. If the leak rate of the system is determined to be greater than $3x10^{-3}$ std-cc/sec of air for the pressure rise test or greater than $1x10^{-7}$ standard cubic centimeters per second of helium, release the vacuum, remove the ram closure plate, and inspect the O-ring seals for cuts, tears, or abrasion, and the seal areas for cleanliness and surface condition. If necessary, replace the seal(s) and/or repair the seal area(s). Repeat Steps a through f. If, after repeated testing, it has been determined that the ram closure seals cannot be made to pass the test, utilize appropriate methods to locate/isolate the leak path. Repair the leak path and repeat Steps a through f to verify ram closure seal integrity.

NOTE: Upon removing and replacing the ram closure plate, it will be necessary to reduce the cavity pressure below 1.0 psia and refill the cask cavity with helium through the vent port.

This concludes the fabrication verification leak test of the cask.

8.1.4 Component Tests -Impact Limiter - Energy Absorption Material

8.1.4.1 Polyurethane Foam

Foam will be installed within the NUHOMS®-MP187 Multi-Purpose Cask impact limiters and tested to ensure conformance with the required foam material properties. To ensure that the samples tested are representative of the installed foam, the foam will be installed according to the following:

The foam shall be polyurethane closed-cell material with a density of approximately 15 pounds per cubic foot. The shells shall be cleaned of scale, oils, grease and debris prior to waxing to prevent foam adhesion.

With the aluminum honeycomb type materials in place or equivalent dunnage to simulate the honeycomb material, the liquid foam material shall be poured directly into the cavity. Each pour shall be carefully controlled so that the liquid components will react to form the rigid foam, and rise in such a way that the entire volume of the foamed assembly will be filled with expanded foam with a density of approximately fifteen pounds per cubic foot (15 pcf). The direction of foam rise shall be parallel to the vertical (axial) axis of the impact limiters. The temperature of the mixed foam components shall be maintained at a minimum of 60°F. The surrounding walls of the impact limiter shall be maintained at a minimum of 55°F prior to the foam installation.

The foam shall be poured in small batches to ensure uniformity of the final foam assembly. The level of each batch pour shall be recorded.

Bracing and shoring of the surrounding impact limiter walls shall be provided as necessary to prevent distortion due to internal foam pressures. The method used for bracing must be adequate to maintain the required dimensions specified on the Packaging General Arrangement Drawings in Appendix 1.3.2. If a simulated honeycomb block was used as shoring to pour the foam, it shall be removed after the foam pour and replaced with the actual honeycomb assembly.

Production records for each foam pouring operation shall be compiled during the operation. At a minimum, the record shall include pour dates, operator name, shell part number and serial number, Quality Assurance acceptance, and material traceability identified by batch.

Upon completion of production, a certification referencing the production record data and all testing data pertaining to each impact limiter shall be issued by the foam supplier. Test data relevant to the pouring operation shall be included with the certification. All QA data submittals shall be dated and signed by the foam supplier's designated QA representative.

Each production pour, including its properties, shall be completely recorded. Test samples representing the production pour shall be formed using test boxes or containers with material from the actual production pour stream. Test specimens shall be taken from each sample box prepared during production. Test samples shall be tested prior to installation of the next pour.

The test specimens shall be tested for compressive strength within the parameters presented in Appendix 2.10.8, in accordance with the requirements of Reference 8.5. Stress-strain plots, similar to those shown in Appendix 2.10.8 shall be prepared for the parallel-to-rise orientation. The test data will be recorded and reviewed to ensure compliance with the foam structural acceptance criteria outlined in Appendix 2.10.8. The average compressive stress of the sample properties from each pour shall be within ±15% of the specified stress in the above referenced figures at foam strains of 10%, 40% and 70%. The average compressive stress of all pours into a single limiter shall be within ±10%.

At the time of polyurethane foam installation, test samples will be retained from each foam pour, as discussed above. Using these samples, each foam pour will be tested for flame retardancy in accordance with the requirements of Section 853(c) and Part I(d), Appendix F, of 14 CFR 25, Reference 8.6. In addition, foam samples shall be tested to verify leachable chloride levels below detectable levels.

8.1.4.2 Aluminum Honeycomb Type Material

The aluminum honeycomb type material utilized in the fabrication of the impact limiters shall be manufactured as a homogenous block of sufficient size to provide the joint configuration shown in the drawings in Appendix 1.3.2. Each block of material shall be tested to demonstrate that the static strength, density and dynamic strength at -20°F and at +200°F meet the specification in Appendix 2.10.8. The number of samples tested dynamically from each block, may be reduced, or deleted, if a reliable correlation between density and static and dynamic strengths is clearly established.

8.1.5 Tests for Shielding Integrity

8.1.5.1 Gamma Shield

The MP-187 cask body poured lead shielding integrity will be confirmed via gamma scanning prior to installation of the neutron shield. There are at least two different methods available to scan the cask body. The principal difference in the methods is the location of the source and the method of scanning. In the first method the source is placed at the cask centerline, on the bottom of the cask cavity, and the detector is rotated around the exterior of the cask body parallel to the source. After each rotation the source and detector are raised a predetermined distance, typically six inches, and the full circumference scan repeated, until the full height of the body has been scanned. An alternative method places the source and detector on a frame separated by a distance greater than the cask wall thickness. The frame is lowered to the bottom of the cask and the body is rotated through the full circumference. The frame/source is raised and the process repeated until the cask body has been fully scanned. The integrity of the FF and FC-DSC poured lead shield plugs will be checked using a similar gamma scan procedure to that described above, or other methods such as X-ray or UT measurement of lead thickness.

The outer cask surface is gridded and a chart is made to reflect the gridded surface. The gamma scan will be performed using a detector with a detection area enveloping the grid minimum area (e.g., for a 6" x 6" grid, the detector will encompass a 6" x 6" square). This data serves as the raw gamma scan results in milliroentgens per hour (mR/hr). The dose rates are evaluated by comparing them to predetermined dose rate values for the nominal (as designed) lead thickness and the nominal less 5% lead thickness. The acceptance criteria are determined by utilizing test blocks made up from nominal thicknesses for the lead and steel sheets. The source is placed behind the test block assembly and dose readings recorded. This test sequence is repeated on the nominal less 5% test block assembly and the dose rate established. Additional dose readings are taken in incremental thicknesses between and beyond the two base readings. The resultant data is then plotted on a chart of dose values versus lead thickness. The dose rate at the nominal less 5% lead thickness is used as the maximum acceptable dose reading for the inspected cask.

The probe time and source/detector distances used in the inspection shall be the same as that used in establishing the minimum dose rates in the mockup. Dose rates for minimum cask shell thickness shall be at least three times the background dose rate.

8.1.5.2 Neutron Shield

The cask annulus neutron shield and miscellaneous components are filled with NS-3 cementitious material with 2w/o B4C. As successfully demonstrated during the fabrication of the NuPac 125B cask [8.7] confirmation of acceptable placing of the NS-3 will be established using a combination of mockup testing, in-process production controls, and measurement of cask surface dose rates.

To account for potential stratification, a full scale mockup of a cask segment will be constructed with transparent panels in the face to permit monitoring of the pour process. The NS-3 material will be mixed and placed in accordance with the manufacturer's instructions. A sample of the NS-3 material will be retained from each pour for chemical testing to verify the elemental composition. The cured NS-3 mockup will be sectioned and chemical tests performed to establish the hydrogen and boron densities of each segment. A linear fit of the resultant densities will be performed to determine the direction and magnitude of any mockup stratification of boron or hydrogen. NS-3 test acceptance criteria will demonstrate that the densities of the boron and hydrogen meet the manufacturer's minimum specified values and exceed those assumed in the shielding analysis.

Production controls verified by the mockup test, and similar to those adopted for the fabrication of the NuPac 125B cask, will be used to ensure that the production placement will be performed in the same manner as the mockup test. This will include the use of a metered pump to ensure that the predetermined volume of material is poured into the neutron shield. Samples of each pour will be taken for chemical verification of the density, boron, and hydrogen concentrations to demonstrate compliance with the mockup test results and analytical requirements.

In addition to the controls described above, a confirmatory neutron scan may be performed either on the empty cask, or upon completion of the initial fuel load, but prior to placing the cask on the transportation skid. The empty cask test would be accomplished by inserting a known neutron source into the cask cavity and scanning the exterior surface with a neutron flux detector. The outer cask surface is gridded and a chart is made to reflect the gridded surface. The neutron scan will be performed using a detector with a detection area enveloping the grid minimum area (e.g., for a 6" x 6" grid, the detector will encompass a 6" x 6" square). This data serves as the raw neutron scan results in milliroentgens per hour (mR/hr). The measured dose rates will be evaluated by comparing them to predetermined dose rates developed from a calibration block equal to the nominal design thickness less 5%. The acceptance criteria are determined by utilizing test blocks made up from nominal thicknesses for the lead, NS3, and steel sheets. The source is placed behind the test block assembly and dose readings recorded. This test sequence is repeated on the nominal less 5% test block assembly and the dose rate established. Additional dose readings are taken in incremental thicknesses between and beyond the two base readings. The resultant data is then plotted on a chart of dose values versus NS3 thickness. The dose rate at the nominal less 5% NS3 thickness is used as the maximum acceptable dose reading for the inspected cask.

If the measurements are taken after the initial fuel load then the acceptance criteria will be developed based on the design limits ratioed by the fuel neutron source term to the design fuel basis source term.

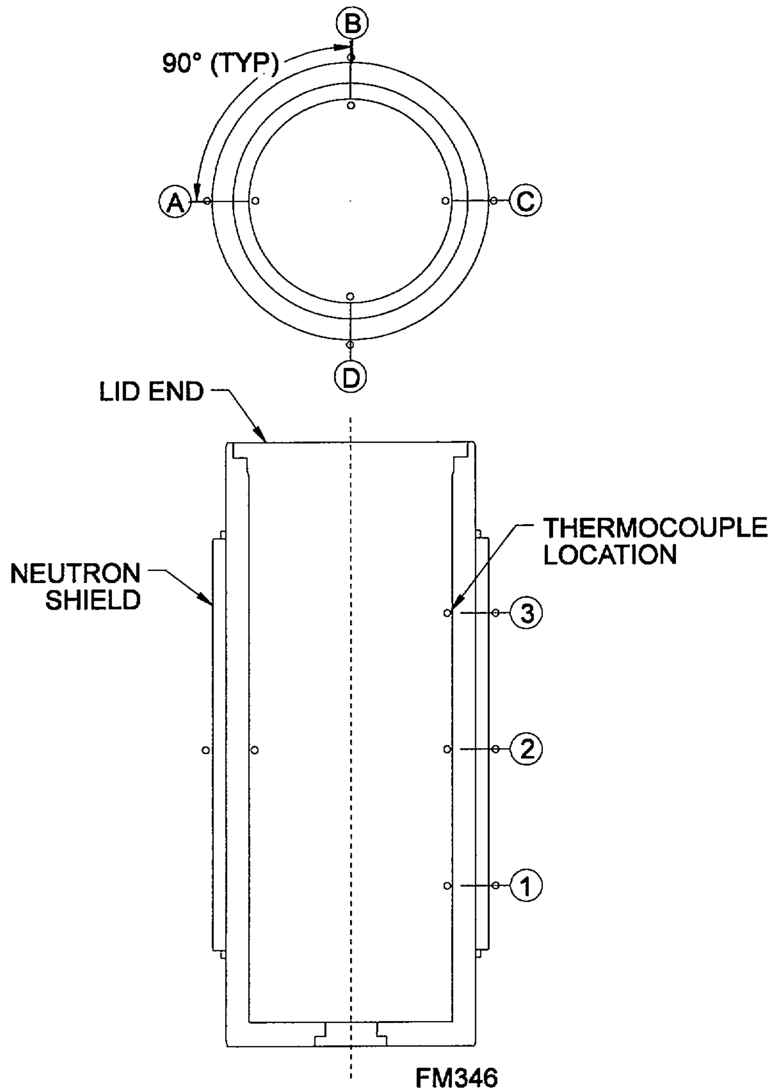

Figure 8.1-1

Thermocouple Locations for Thermal Acceptance Test

8.1.6 Thermal Acceptance Tests

8.1.6.1 Prior to First Use

Material properties established in Section 3.0 are conservative for the analyses performed. As such, acceptance tests for material thermal properties are not performed.

The complete cask shall be subjected to a thermal heat rejection test to demonstrate satisfactory operation of the as-built shells, top lid , and shielding materials but without the ram closure installed. This test is required for certification of the cask for transportation and will be performed following completion of fabrication and prior to first use as a transport cask. The cask shall be supported vertically with an internal heat source capable of producing a minimum of 4.5 kW suitably supported within the cask cavity. As shown in Figure 8.1-1, a minimum of six pairs of thermocouples will be attached on the containment shell and the neutron shield shell to record the thermal gradient between the cask cavity and the external surface. Power and instrumentation cables may exit the cask through the ram access port. A special temporary cover plate is not required. Power shall be applied to the heaters for sufficient time for the cask to reach thermal equilibrium with temperatures recorded at least every 30 minutes. The cask shall be held at equilibrium for a minimum of one hour then the power turned off and the cask allowed to cool without any mechanical cooling. The acceptance criteria shall be calculated for the change in temperature across the cask wall based on the specific internal heat and the exterior environmental conditions using the same analytical methods used to predict the cask performance for the normal and accident conditions.

8.1.6.2 Thermal Acceptance Test During Storage

When the MP187 cask is used in storage mode for time periods greater than 5 years, the thermal performance of the cask will be verified by performing a thermal acceptance test as follows. The test will be performed prior to shipment of the cask.

The cask is assumed to be in the vertical orientation on the storage pad at the ISFSI site. The total decay heat from the fuel assemblies in the cask will be calculated at the time of the thermal test. The steady state condition of the cask for the ambient conditions present will be verified prior to the start of the test. The temperature on the outside surface of the cask in the radial direction at four locations (90° from each other at the cask mid-plane) will be measured. Similarly, the temperature on the top surface of the cask top cover in the axial direction at four locations (90° from each other in line with the radial measurement locations) will be measured.

The acceptance criteria shall be calculated for the ratio of axial to radial temperature for the given heat load and ambient conditions using the same analytical methods used to predict the cask performance for the normal and accident conditions.

8.1.7 Lead Installation Tests

Testing during the lead installation process involves pre- and post-pour diameter and straightness measurements of the cask shells and close monitoring of the cask temperatures during the preheat, lead pour, and cool-down processes. A more detailed description of the lead installation and testing is presented in Section 8.3.2.

8.1.8 Neutron Absorber Plates

The neutron absorber plates are verified to have their minimum total B^{10} per unit area (areal density) of the sandwiched material as specified on the drawings in Appendix 1.3.2.

Samples from each sheet of the neutron absorber are retained for testing and record purposes. The minimum B^{10} content per unit area and the uniformity of dispersion within a panel are verified by wet chemical analysis and/or neutron attenuation testing. All material certifications, lot control records, and test records are maintained to assure material traceability.

Chemical (destructive) testing is the preferred method because the B^{10} areal density, which is the primary requirement for the material, can be directly measured. This is done by first taking two one inch square samples from each end of the rolled product. This one square inch sample size is small compared to the finished panel size, 1300 in^2, so that non-uniformities in B^{10} areal density would be readily apparent between the samples. The material on the ends of the rolled product is known to be thinner than the rest of the panel because of the rolling process. This characteristic of the finished product is confirmed by examination of thickness in four locations on 100% of the panels. The thinnest of these samples is used for destructive chemical determination of the amount of boron in the sample using written, approved procedures and standard laboratory processes and equipment. Using the measured thickness of the sample, the area of the sample, and the mass of boron in the sample, the areal boron density may be calculated. Once the areal boron density is known, the areal B^{10} density is calculated using the isotopic assay of the B_4C powder used to manufacture the product. The sample frequency is determined using standard statistical procedures to assure that minimum B^{10} areal densities are achieved with a 95/95 confidence level.

Neutron attenuation testing may be performed to augment or replace chemical (destructive) testing as required to demonstrate acceptable minimum areal B^{10} loading of the neutron absorber plates. Neutron transmission measurements may be performed on samples, or completed panels, using a neutron diffractometer. The neutron transmission measurements shall be performed using written, approved procedures in accordance with applicable portions of ASTM E94, "Recommended Practice for Radiographic Testing", ASTM E142, "Controlling Quality of Radiographic Testing", and ASTM E545, " Standard Method for Determining Image Quality in Thermal Radiographic Testing". Since this type of testing does not measure directly the B^{10} areal density of the panels, the results of neutron attenuation tests shall be demonstrated by calculation to show that the minimum specified B^{10} areal densities are achieved with a 95/95 confidence level.

8.2 Maintenance Program

This section describes the maintenance program used to ensure continued performance of the packaging.

8.2.1 Structural and Pressure Tests

Other than the tests required prior to first use, no structural or pressure tests are necessary to ensure continued performance of the packaging.

8.2.2 Leak Tests

The metallic containment seals are to be replaced after each use and shall be leak tested to show a leak rate less than $1x10^{-7}$ standard cubic centimeters per second of helium, (with a test sensitivity of at least $5x10^{-8}$ standard cubic centimeters per second). This test is to be performed for the inner seals, and a leak rate less than $7x10^{-3}$ std-cc/sec of air for the top closure and ram closure outer seals, (with a test sensitivity of at least $3.5x10^{-3}$ std-cc/sec), within the 12-month period prior to each shipment and after each seal replacement.

Appropriate sections of the maintenance verification leak test shall be performed during routine maintenance to verify cask configuration and performance to design criteria. Tests of the top closure, ram access and drain and vent port O-ring seals are to be performed upon replacement, but not necessarily at the same time (seals are to be replaced annually or when damaged). The maintenance verification leak test shall also be performed after the third use of the system per Section 6.5 of ANSI N14.5-1987 [8.4].

For the NUHOMS®-MP187 Multi-Purpose Cask the assembly verification leak test, the fabrication leak test for the seal integrity and the maintenance verification leak test all use the same methodology. Therefore, the maintenance verification leak test will be performed using the steps outlined for the assembly verification leak test in Appendix 7.4.2.

8.2.3 Subsystems Maintenance

This section describes the inspection and replacement schedule for packaging subsystems.

8.2.3.1 Fasteners

All threaded parts will be inspected after each use, and annually, for deformed or stripped threads. Damaged parts shall be evaluated for continued use and replaced as required. At a minimum, the replacement schedule for package fasteners is given below for the transportation mode. The replacement interval is initiated at the time of fastener torquing for package transportation. Pre-loading of bolts as part of a demonstration or training program would not initiate the five year interval. If the cask is used in a storage mode, the fasteners need not be inspected or replaced until after the first shipment if the replacement interval has been exceeded.

Component Fastener	Replacement Interval (years)
Vent/Test/Drain Ports	5
Impact Limiter Attachment	5
Cask Top Closure Plate	5
Ram closure Plate	5

8.2.3.2 Impact Limiters

A sound industrial maintenance program will be followed to assure the integrity of the impact limiters. The impact limiter attachment fastener and hole threads will be inspected after each use, and annually, when in use as a transportation cask for damaged or stripped threads. Damaged parts shall be evaluated for continued use and corrected as required. Additionally, plastic pipe plugs at the ends of the impact limiters shall be inspected for damage and replaced prior to further use if damage is present.

The impact limiters are sealed so that no water is expected to enter the internal cavity. The foam is a closed cell foam which in similar applications has not deteriorated or absorbed significant water in over 10 years of use. To ensure that no significant amount of water is absorbed in the impact limiter, the impact limiters shall be inspected within one year of use. The inspection shall consist of a visual inspection of the foam for water absorption or degradation by removing the plastic pipe plugs in the shell. Each impact limiter shall also be weighed at the time of inspection. The impact limiter shall be restricted from use if there is more than a 3% weight increase.

8.2.3.3 Seal Areas and Grooves

Sealing surfaces and O-ring grooves shall be inspected at the time of seal replacement, for potentially damaging burrs or scratches. Damaged parts shall be evaluated for continued use/repair and replaced as required (e.g., 400-600 grit emery cloth to polish the surface). More extensive damage may be repaired by the use of surface welding procedures and grinding to restore the original surface, or similar processes.

8.2.3.4 Trunnions Sockets

The trunnions sockets shall be inspected annually and before each use for excessive wear, galling, or distortion. Trunnions sockets exhibiting excessive wear, galling, or distortion shall be documented for proper QA disposition (e.g. use "as is" or repair).

8.2.4 Valves, Rupture Disks, and Gaskets

All containment O-ring seals and gaskets shall be replaced after each use per specifications as delineated on the Packaging General Arrangement Drawing in Appendix 1.3.2. Following seal replacement and prior to a loaded shipment, the seal(s) shall be leak tested to the requirements of Section 8.2.2.

There are no valves or rupture disks used on the NUHOMS®-MP187 cask that are in the containment boundary. The rupture disks in the lower neutron shield ring protect the neutron shield cavity from over-pressurization and require annual visual inspection to verify there is no evidence of damage when the cask is in use for transportation. The neutron shield rupture disks require no special maintenance.

8.2.5 Shielding

Other than the tests required prior to first use, no shielding tests are necessary to ensure continued performance of the package.

8.2.6 Thermal

The heat removal capacity of the cask shall be verified periodically by performing the applicable test described in section 8.1.6.1. The test shall be performed within five years of each use of the cask for transportation purposes. An increase of the temperature drop across the wall of more than 25°F from the previous test is unacceptable.

The test described in section 8.1.6.1 is to be performed if the cask is used in the storage mode for time periods greater than five years.

8.3 Appendix

8.3.1 References

8.1 American Society of Mechanical Engineers (ASME) Boiler and Pressure Vessel Code.

8.2 ANSI N14.6-1986, American National Standard for Radioactive Materials -Special Lifting Devices for Shipping Containers Weighing 10,000 Pounds (4,500 kg) or More.

8.3 Title 10, Code of Federal Regulations, Part 71 (10 CFR 71), Packaging and Transportation of Radioactive Materials.

8.4 ANSI N14.5-1987, American National Standard for Radioactive Materials - Leakage Tests on Packages for Shipment.

8.5 ASTM D1623-73, Method of Test for Tensile Properties of Rigid Cellular Plastics.

8.6 Title 14, Code of Federal Regulations, Part 25, (14 CFR 25), Airworthiness Standards: Transport Category Airplanes, July 21, 1986.

8.7 Pacific Nuclear, "Consolidated Safety Analysis Report for the NuPac 125-B Fuel Shipping Cask," NRC Docket No. 71-9200, April 1991.

8.3.2 Lead Installation Procedure

The following delineates a representative procedure for installation of poured lead into the NUHOMS®-MP187 Multi-Purpose Cask structural shell/inner shell cavity. The procedure presents pre-pour cask inner shell dimensional inspection requirements, lead pour, gamma scan or X-ray inspection of the lead shielding, and post-pour cask inner shell dimensional inspection requirements. Note: The neutron shield is attached after lead pour and cool down.

a. Record the cask, inner and outer shell diameter and straightness in accordance with the requirements of ASME Boiler and Pressure Vessel Code [8.1], Section III, Subsection NE, Article NE-4220. At a minimum, record the inside diameter at five locations approximately four equal spaces along the inside diameter length, and at 8 points 45° apart along the circumference at each of the five locations along the cask longitudinal axis as shown in Figure 8.3-1.

b. All cask inner and outer surfaces shall be supported or braced, as necessary, depending on the shell thickness and based upon shell buckling calculations for the anticipated loading during lead pour.

c. The lead shall be poured with the cask in the vertical position. The lead may be pumped from below the cask or poured from above the cask. The cask may be positioned with either the open end up or down.

   Stand pipes or equivalent shall be placed on the top of the cask to insure an excess head of liquid lead when the cask lead cavity is full (during cooling operation). This excess head shall be maintained during the cooling operation. Vent risers shall be provided to allow for escape of air and impurities.

d. The cask shall be instrumented with thermocouple wires at a minimum of twelve (12) locations on the inside and outside to monitor temperature differentials between the two shells as shown in Figure 8.3-1.

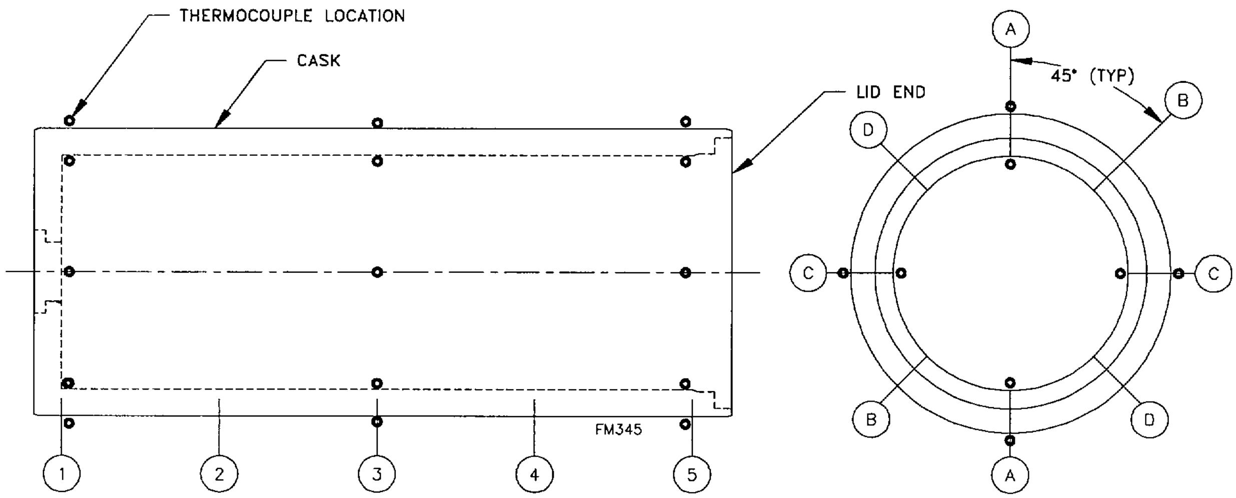

Figure 8.3-1

Thermocouple Locations for Lead Installation

e. All cask components (i.e., outer shell, inner shell, top end forging and bottom end closure) shall be uniformly preheated at a maximum heat up rate of 150 °F per hour to a temperature between 500°F and 725°F over the entire surface prior to lead pouring. No temperature deviation between any two points on the cask shell shall exceed 250°F. Maximum differential temperature between inner and outer shell shall not be greater than 100°F.

f. The temperature of the lead at the time of lead pour shall be above 625°F and less than 790°F.

g. The rate of lead flow shall be controlled to fill the cask lead cavity as rapidly and evenly as possible. The lead shall enter the cavity, and flow shall be controlled, in such a way as to minimize impingement on the cask shells.

h. Heat sources shall be controlled during the cool-down period so that the cask is cooled to insure that only one solidifying front exists in the lead. Cooling shall be initiated from the lowest portion of the cask as it is positioned for lead pour. Maximum cool-down rate shall not exceed 100°F per hour. No deviation between 2 points from top to bottom shall be more than 250°F.

i. Molten lead shall be added to the standpipes at a rate consistent with normal shrinkage.

j. After cool-down is complete, the thermocouples and any internal and/or external bracing shall be removed and the outer cask gamma scanned or X-ray examined in accordance with the tests delineated in Section 8.1.5.

k. Upon a successful gamma scan inspection, the cask shell diameter and straightness shall be measured. All measurements after lead pour must meet the requirements specified on the Packaging General Arrangement Drawing in Appendix 1.3.2.

l. Remove all fill, vent, and standpipes, or equivalent, clean the holes thoroughly of all lead, and install plugs of a material that is compatible with the base material.

8.3.3 NS-3 Specification

Specific Gravity	1.76
Hydrogen	5.14e+22 atom/cc
Thermal Aging:	
100 hrs. @ 150°F	Wt. loss=2.15%, H loss=4.68%
100 hrs. @ 200°F	Wt. loss=2.90%, H loss=6.33%
2 hrs. @ 340°F	Wt. loss=4.16%, H loss=8.90%
Radiation Exposure:	
Gamma	1.5e+10 Rads Gamma
Thermal Neutron (<.55eV)	1.5e+19 n/cm^2
Epithermal Neutron (.55eV-1keV)	9.3e+16 n/cm^2
Fast Neutron (> 1MeV)	1.6e+17 n/cm^2
Wt. Loss	7.17%
Hydrogen loss	13.4%
Thermal Conductivity	5.86 Btu-in/hr-ft^2-°F)
Coefficient of Thermal Expansion	7.81e-6 in/in/°F
Compressive Strength	4500 psi

Theoretical Elemental Composition:

Hydrogen 4.85 wt. %	Oxygen 57.05 wt. %	Iron 0.56 wt. %
Carbon 9.35 wt. %	Silicon 3.36 wt. %	Trace 1.33 wt. %
Calcium 5.61 wt. %	Aluminum 17.89 wt. %	

Maximum B_4C Loading 11.25 wt. %